

TURKISH JOURNAL OF PHARMACEUTICAL SCIENCES



TURKISH JOURNAL OF PHARMACEUTICAL SCIENCES



Editor-in-Chief

Feyyaz ONUR, Prof. Dr.

Lokman Hekim University, Ankara, Turkey,

E-mail: onur@pharmacy.ankara.edu.tr

ORCID ID: orcid.org/0000-0001-9172-1126

Vice Editor

Gülgün KILCIĞIL, Prof. Dr.

Ankara University, Ankara, Turkey

E-mail: Gulgun.A.Kilcigil@pharmacy.ankara.edu.tr

ORCID ID: orcid.org/0000-0001-5626-6922

Associate Editors

Rob VERPOORTE, Prof. Dr.

Leiden University, Leiden, Netherlands

E-mail: verpoort@chem.LeidenUniv.NL

Bezhan CHANKVETADZE, Prof. Dr.

Ivane Javakishvili Tbilisi State University,

Tbilisi, Georgia

E-mail: jpba_bezhan@yahoo.com

Ülkü ÜNDEĞER-BUCURGAT, Prof. Dr.

Hacettepe University, Ankara, Turkey

E-mail: uundeger@hacettepe.edu.tr

ORCID ID: orcid.org/0000-0002-6692-0366

Luciano SASO, Prof. Dr.

Sapienza University, Rome, Italy

E-mail: luciano.saso@uniroma1.it

Müge KILIÇARSLAN, Assoc. Prof. Dr.

Ankara University, Ankara, Turkey

E-mail: muge.kilicarслан@pharmacy.ankara.edu.tr

ORCID ID: orcid.org/0000-0003-3710-7445

Fernanda BORGES, Prof. Dr.

Porto University, Porto, Portugal

E-mail: fborges@fc.up.pt

Tayfun UZBAY, Prof. Dr.

Üsküdar University, İstanbul, Turkey

E-mail: uzbayt@yahoo.com

İpek SUNTAR, Assoc. Prof. Dr.

Gazi University, Ankara, Türkiye

E-mail: ipesin@gazi.edu.tr

ORCID ID: orcid.org/0000-0003-4201-1325

Advisory Board

Ali H. MERİÇLİ, Prof. Dr.

Near East University, Nicosia, Cypruss

Ahmet BAŞARAN, Prof. Dr.

Hacettepe University, Ankara, Turkey

Berrin ÖZÇELİK, Prof. Dr.

Gazi University, Ankara, Turkey

Betül DORTUNÇ, Prof. Dr.

Marmara University, İstanbul, Turkey

Christine LAFFORGUE, Prof. Dr.

Paris-Sud University, Paris, France

Cihat ŞAFAK, Prof. Dr.

Hacettepe University, Ankara, Turkey

Fethi ŞAHİN, Prof. Dr.

Eastern Mediterranean University, Famagusta,

Cyprus

Filiz ÖNER, Prof. Dr.

Hacettepe University, Ankara, Turkey

Gülten ÖTÜK, Prof. Dr.

İstanbul University, İstanbul, Turkey

Hermann BOLT, Prof. Dr.

Dortmund University, Dortmund, Germany

Hilbert WAGNER, Prof. Dr.

Ludwig-Maximilians University, Munich, Germany

Jean-Alain FEHRENTZ, Prof. Dr.

Montpellier University, Montpellier, France

Joerg KREUTER, Prof. Dr.

Johann Wolfgang Goethe University, Frankfurt, Germany

Makbule AŞIKOĞLU, Prof. Dr.

Ege University, İzmir, Turkey

Meral KEYER UYSAL, Prof. Dr.

Marmara University, İstanbul, Turkey

Meral TORUN, Prof. Dr.

Gazi University, Ankara, Turkey

Mümtaz İŞCAN, Prof. Dr.

Ankara University, Ankara, Turkey

Robert RAPOPORT, Prof. Dr.

Cincinnati University, Cincinnati, USA

Sema BURGAZ, Prof. Dr.

Gazi University, Ankara, Turkey

Uğur ATİK, Prof. Dr.

Mersin University, Mersin, Türkiye

Wolfgang SADEE, Prof. Dr.

Ohio State University, Ohio, USA

Yasemin YAZAN, Prof. Dr.

Anadolu University, Eskişehir, Turkey

Yılmaz ÇAPAN, Prof. Dr.

Hacettepe University, Ankara, Turkey

Yusuf ÖZTÜRK, Prof. Dr.

Anadolu University, Eskişehir, Turkey

Yücel KADIOĞLU, Prof. Dr.

Atatürk University, Erzurum, Turkey

Zühre ŞENTÜRK, Prof. Dr.

Yüzüncü Yıl University, Van, Turkey

TÜRK ECZACILIK BİLİMLERİ DERGİSİ



Baş Editör

Feyyaz ONUR, Prof. Dr.

Lokman Hekim Üniversitesi, Ankara, Türkiye

E-posta: onur@pharmacy.ankara.edu.tr

ORCID ID: orcid.org/0000-0001-9172-1126

İkinci Editör

Gülgün KILCIGİL, Prof. Dr.

Ankara Üniversitesi, Ankara, Türkiye

E-posta: kilcigil@pharmacy.ankara.edu.tr

ORCID ID: orcid.org/0000-0001-5626-6922

Yardımcı Editörler

Rob VERPOORTE, Prof. Dr.

Leiden Üniversitesi, Leiden, Amsterdam

E-posta: verpoort@chem.LeidenUniv.NL

Bezhan CHANKVETADZE, Prof. Dr.

Ivane Javakhishvili Tbilisi Devlet Üniversitesi, Tbilisi, Gürcistan

E-posta: jpba_bezhan@yahoo.com

Ükü ÜNDEĞER-BUCURGAT, Prof. Dr.

Hacettepe Üniversitesi, Ankara, Türkiye

E-posta: uundeger@hacettepe.edu.tr

ORCID ID: orcid.org/0000-0002-6692-0366

Luciano SASO, Prof. Dr.

Sapienze Üniversitesi, Roma, İtalya

E-posta: luciano.saso@uniroma1.it

Müge KILIÇARSLAN, Assoc. Prof. Dr.

Ankara Üniversitesi, Ankara, Türkiye

E-posta: muge.kilicarслан@pharmacy.ankara.edu.tr

ORCID ID: orcid.org/0000-0003-3710-7445

Fernanda BORGES, Prof. Dr.

Porto Üniversitesi, Porto, Portekiz

E-posta: fborges@fc.up.pt

Tayfun UZBAY, Prof. Dr.

Üsküdar Üniversitesi, İstanbul, Türkiye

E-posta: uzbayt@yahoo.com

İpek SUNTAR, Assoc. Prof. Dr.

Gazi Üniversitesi, Ankara, Türkiye

E-posta: ipesin@gazi.edu.tr

ORCID ID: orcid.org/0000-0003-4201-1325

Danışma Kurulu

Ali H. MERİÇLİ, Prof. Dr.

Near East Üniversitesi, Lefkoşa, Kıbrıs

Ahmet BAŞARAN, Prof. Dr.

Hacettepe Üniversitesi, Ankara, Türkiye

Berrin ÖZÇELİK, Prof. Dr.

Gazi Üniversitesi, Ankara, Türkiye

Betül DORTUNÇ, Prof. Dr.

Marmara Üniversitesi, İstanbul, Türkiye

Christine LAFFORGUE, Prof. Dr.

Paris-Sud Üniversitesi, Paris

Cihat ŞAFAK, Prof. Dr.

Hacettepe Üniversitesi, Ankara, Türkiye

Fethi ŞAHİN, Prof. Dr.

Doğu Akdeniz Üniversitesi, Gazimağusa, Kıbrıs

Filiz ÖNER, Prof. Dr.

Hacettepe Üniversitesi, Ankara, Türkiye

Gülten ÖTÜK, Prof. Dr.

İstanbul Üniversitesi, İstanbul, Türkiye

Hermann BOLT, Prof. Dr.

Dortmund Üniversitesi, Dortmund, Almanya

Hilbert WAGNER, Prof. Dr.

Ludwig-Maximilians Üniversitesi, Münih, Almanya

Jean-Alain FEHRENTZ, Prof. Dr.

Montpellier Üniversitesi, Montpellier, Fransa

Joerg KREUTER, Prof. Dr.

Johann Wolfgang Goethe Üniversitesi, Frankfurt, Almanya

Makbule AŞIKOĞLU, Prof. Dr.

Ege Üniversitesi, İzmir, Türkiye

Meral KEYER UYSAL, Prof. Dr.

Marmara Üniversitesi, İstanbul, Türkiye

Meral TORUN, Prof. Dr.

Gazi Üniversitesi, Ankara, Türkiye

Mümtaz İŞCAN, Prof. Dr.

Ankara Üniversitesi, Ankara, Türkiye

Robert RAPOPORT, Prof. Dr.

Cincinnati Üniversitesi, Cincinnati, Amerika

Sema BURGAZ, Prof. Dr.

Gazi Üniversitesi, Ankara, Türkiye

Uğur ATİK, Prof. Dr.

Mersin Üniversitesi, Mersin, Türkiye

Wolfgang SADEE, Prof. Dr.

Ohio State Üniversitesi, Ohio, Amerika

Yasemin YAZAN, Prof. Dr.

Anadolu Üniversitesi, Eskişehir, Türkiye

Yılmaz ÇAPAN, Prof. Dr.

Hacettepe Üniversitesi, Ankara, Türkiye

Yusuf ÖZTÜRK, Prof. Dr.

Anadolu Üniversitesi, Eskişehir, Türkiye

Yücel KADIOĞLU, Prof. Dr.

Atatürk Üniversitesi, Erzurum, Türkiye

Zühre ŞENTÜRK, Prof. Dr.

Yüzüncü Yıl Üniversitesi, Van, Türkiye

TURKISH JOURNAL OF PHARMACEUTICAL SCIENCES

AIMS AND SCOPE

The Turkish Journal of Pharmaceutical Sciences is the only scientific periodical publication of the Turkish Pharmacists' Association and has been published since April 2004.

Turkish Journal of Pharmaceutical Sciences is an independent international open access periodical journal based on double-blind peer-review principles. The journal is regularly published 3 times a year and the publication language is English. The issuing body of the journal is Galenos Yayınevi/Publishing House.

The aim of Turkish Journal of Pharmaceutical Sciences is to publish original research papers of the highest scientific and clinical value at an international level.

The target audience includes specialists and physicians in all fields of pharmaceutical sciences.

The editorial policies are based on the "Recommendations for the Conduct, Reporting, Editing, and Publication of Scholarly Work in Medical Journals (ICMJE Recommendations)" by the International Committee of Medical Journal Editors (2016, archived at <http://www.icmje.org/>) rules.

Editorial Independence

Turkish Journal of Pharmaceutical Sciences is an independent journal with independent editors and principles and has no commercial relationship with the commercial product, drug or pharmaceutical company regarding decisions and review processes upon articles.

ABSTRACTED/INDEXED IN

Web of Science-Emerging Sources Citation Index (ESCI)

SCOPUS SJR

Directory of Open Access Journals (DOAJ)

ProQuest

Chemical Abstracts Service (CAS)

EBSCO

EMBASE

Analytical Abstracts

International Pharmaceutical Abstracts (IPA)

Medicinal & Aromatic Plants Abstracts (MAPA)

TÜBİTAK/ULAKBİM TR Dizin

Türkiye Atıf Dizini

UDL-EDGE

OPEN ACCESS POLICY

This journal provides immediate open access to its content on the principle that making research freely available to the public supports a greater global exchange of knowledge.

Open Access Policy is based on the rules of the Budapest Open Access Initiative (BOAI) <http://www.budapestopenaccessinitiative.org/>. By "open access" to peer-reviewed research literature, we mean its free availability on the public internet, permitting any users to read, download, copy, distribute, print, search, or link to the full texts of these articles, crawl them for indexing, pass them as data to software, or use them for any other lawful purpose, without financial, legal, or technical barriers other than those inseparable from gaining access to the internet itself. The only constraint on reproduction and distribution, and the only role for copyright in this domain, should be to give authors control over the integrity of their work and the right to be properly acknowledged and cited.

CORRESPONDENCE ADDRESS

Editor-in-Chief, Feyyaz ONUR, Prof.Dr.

Address: Lokman Hekim University, Faculty of Pharmacy, Department of Analytical Chemistry, 06100 Tandoğan-Ankara, TURKEY

E-mail: onur@pharmacy.ankara.edu.tr

PERMISSION

Requests for permission to reproduce published material should be sent to the editorial office. Editor-in-Chief, Prof. Dr. Feyyaz ONUR

ISSUING BODY CORRESPONDING ADDRESS

Issuing Body : Galenos Yayınevi

Address: Molla Gürani Mah. Kaçamak Sk. No: 21/1, 34093 İstanbul, TURKEY

Phone: +90 212 621 99 25 Fax: +90 212 621 99 27

E-mail: info@galenos.com.tr

INSTRUCTIONS FOR AUTHORS

Instructions for authors are published in the journal and on the website <http://turkjps.org>

MATERIAL DISCLAIMER

The author(s) is (are) responsible for the articles published in the JOURNAL.

The editor, editorial board and publisher do not accept any responsibility for the articles.

This work is licensed under a Creative Commons Attribution-NonCommercial-NoDerivatives 4.0 International License.



Galenos Publishing House
Owner and Publisher
Erkan Mor

Publication Coordinator
Burak Sever

Web Coordinators
Soner Yıldırım
Turgay Akpınar

Graphics Department
Ayda Alaca
Çiğdem Birinci
Gülşah Özgül

Project Coordinators
Eda Kolküsa
Hatice Balta
Lütfiye Ayhan İrtem
Sedanur Sert
Zeynep Altındağ

Project Assistants
Gamze Aksoy
Nurcan Açarçağ

Finance Coordinator
Sevinç Çakmak

Research&Development
Kevser Arslantürk

Publisher Contact

Address: Molla Gürani Mah. Kaçamak Sk. No: 21/1
34093 İstanbul, Turkey

Phone: +90 (212) 621 99 25 Fax: +90 (212) 621 99 27

E-mail: info@galenos.com.tr/yayin@galenos.com.tr

Web: www.galenos.com.tr | Publisher Certificate Number: 14521

Printing at: Üniform Basım San. ve Turizm Ltd. Şti.

Matbaacılar Sanayi Sitesi 1. Cad. No: 114 34204 Bağcılar, İstanbul, Turkey

Phone: +90 (212) 429 10 00 | Certificate Number: 42419

Printing Date: January 2019

ISSN: 1304-530X

International scientific journal published quarterly.

TURKISH JOURNAL OF PHARMACEUTICAL SCIENCES

INSTRUCTIONS TO AUTHORS

Turkish Journal of Pharmaceutical Sciences is the official double peer-reviewed publication of The Turkish Pharmacists' Association. This journal is published every 4 months (3 issues per year; April, August, December) and publishes the following articles:

- Research articles
- Reviews (only upon the request or consent of the Editorial Board)
- Preliminary results/Short communications/Technical notes/Letters to the Editor in every field or pharmaceutical sciences.

The publication language of the journal is English.

The Turkish Journal of Pharmaceutical Sciences does not charge any article submission or processing charges.

A manuscript will be considered only with the understanding that it is an original contribution that has not been published elsewhere.

The Journal should be abbreviated as "Turk J Pharm Sci" when referenced.

The scientific and ethical liability of the manuscripts belongs to the authors and the copyright of the manuscripts belongs to the Journal. Authors are responsible for the contents of the manuscript and accuracy of the references. All manuscripts submitted for publication must be accompanied by the Copyright Transfer Form [copyright transfer]. Once this form, signed by all the authors, has been submitted, it is understood that neither the manuscript nor the data it contains have been submitted elsewhere or previously published and authors declare the statement of scientific contributions and responsibilities of all authors.

Experimental, clinical and drug studies requiring approval by an ethics committee must be submitted to the JOURNAL with an ethics committee approval report including approval number confirming that the study was conducted in accordance with international agreements and the Declaration of Helsinki (revised 2013) (<http://www.wma.net/en/30publications/10policies/b3/>). The approval of the ethics committee and the fact that informed consent was given by the patients should be indicated in the Materials and Methods section. In experimental animal studies, the authors should indicate that the procedures followed were in accordance with animal rights as per the Guide for the Care and Use of Laboratory Animals (<http://oacu.od.nih.gov/regs/guide/guide.pdf>) and they should obtain animal ethics committee approval.

Authors must provide disclosure/acknowledgment of financial or material support, if any was received, for the current study.

If the article includes any direct or indirect commercial links or if any institution provided material support to the study, authors must state in the cover letter that they have no relationship with the commercial product, drug, pharmaceutical company, etc. concerned; or specify the type of relationship (consultant, other agreements), if any.

Authors must provide a statement on the absence of conflicts of interest among the authors and provide authorship contributions.

All manuscripts submitted to the journal are screened for plagiarism using the 'iThenticate' software. Results indicating plagiarism may result in manuscripts being returned or rejected.

The Review Process

This is an independent international journal based on double-blind peer-review principles. The manuscript is assigned to the Editor-in-Chief, who reviews the manuscript and makes an initial decision based

on manuscript quality and editorial priorities. Manuscripts that pass initial evaluation are sent for external peer review, and the Editor-in-Chief assigns an Associate Editor. The Associate Editor sends the manuscript to at least two reviewers (internal and/or external reviewers). The reviewers must review the manuscript within 21 days. The Associate Editor recommends a decision based on the reviewers' recommendations and returns the manuscript to the Editor-in-Chief. The Editor-in-Chief makes a final decision based on editorial priorities, manuscript quality, and reviewer recommendations. If there are any conflicting recommendations from reviewers, the Editor-in-Chief can assign a new reviewer.

The scientific board guiding the selection of the papers to be published in the Journal consists of elected experts of the Journal and if necessary, selected from national and international authorities. The Editor-in-Chief, Associate Editors may make minor corrections to accepted manuscripts that do not change the main text of the paper.

In case of any suspicion or claim regarding scientific shortcomings or ethical infringement, the Journal reserves the right to submit the manuscript to the supporting institutions or other authorities for investigation. The Journal accepts the responsibility of initiating action but does not undertake any responsibility for an actual investigation or any power of decision.

The Editorial Policies and General Guidelines for manuscript preparation specified below are based on "Recommendations for the Conduct, Reporting, Editing, and Publication of Scholarly Work in Medical Journals (ICMJE Recommendations)" by the International Committee of Medical Journal Editors (2016, archived at <http://www.icmje.org/>).

Preparation of research articles, systematic reviews and meta-analyses must comply with study design guidelines:

CONSORT statement for randomized controlled trials (Moher D, Schultz KF, Altman D, for the CONSORT Group. The CONSORT statement revised recommendations for improving the quality of reports of parallel group randomized trials. *JAMA* 2001; 285: 1987-91) (<http://www.consort-statement.org/>);

PRISMA statement of preferred reporting items for systematic reviews and meta-analyses (Moher D, Liberati A, Tetzlaff J, Altman DG, The PRISMA Group. Preferred Reporting Items for Systematic Reviews and Meta-Analyses: The PRISMA Statement. *PLoS Med* 2009; 6(7): e1000097.) (<http://www.prisma-statement.org/>);

STARD checklist for the reporting of studies of diagnostic accuracy (Bossuyt PM, Reitsma JB, Bruns DE, Gatsonis CA, Glasziou PP, Irwig LM, et al., for the STARD Group. Towards complete and accurate reporting of studies of diagnostic accuracy: the STARD initiative. *Ann Intern Med* 2003;138:40-4.) (<http://www.stard-statement.org/>);

STROBE statement, a checklist of items that should be included in reports of observational studies (<http://www.strobe-statement.org/>);

MOOSE guidelines for meta-analysis and systemic reviews of observational studies (Stroup DF, Berlin JA, Morton SC, et al. Meta-analysis of observational studies in epidemiology: a proposal for reporting Meta-analysis of observational Studies in Epidemiology (MOOSE) group. *JAMA* 2000; 283: 2008-12).

Authorship

Each author should have participated sufficiently in the work to assume public responsibility for the content. Any portion of a manuscript that

TURKISH JOURNAL OF PHARMACEUTICAL SCIENCES

INSTRUCTIONS TO AUTHORS

is critical to its main conclusions must be the responsibility of at least 1 author.

GENERAL GUIDELINES

Manuscripts can only be submitted electronically through the Journal Agent website (<http://journalagent.com/tjps/>) after creating an account. This system allows online submission and review.

The manuscripts are archived according to ICMJE, Web of Science-Emerging Sources Citation Index (ESCI), SCOPUS, Chemical Abstracts, EBSCO, EMBASE, Analytical Abstracts, International Pharmaceutical Abstracts, MAPA (Medicinal & Aromatic Plants Abstracts), Tübitak/Ulakbim Turkish Medical Database, Türkiye Citation Index Rules.

Format: Manuscripts should be prepared using Microsoft Word, size A4 with 2.5 cm margins on all sides, 12 pt Arial font and 1.5 line spacing.

Abbreviations: Abbreviations should be defined at first mention and used consistently thereafter. Internationally accepted abbreviations should be used; refer to scientific writing guides as necessary.

Cover letter: The cover letter should include statements about manuscript type, single-Journal submission affirmation, conflict of interest statement, sources of outside funding, equipment (if applicable), for original research articles.

The ORCID (Open Researcher and Contributor ID) number of the all authors should be provided while sending the manuscript. A free registration can be done at <http://orcid.org>.

REFERENCES

Authors are solely responsible for the accuracy of all references.

In-text citations: References should be indicated as a superscript immediately after the period/full stop of the relevant sentence. If the author(s) of a reference is/are indicated at the beginning of the sentence, this reference should be written as a superscript immediately after the author's name. If relevant research has been conducted in Turkey or by Turkish investigators, these studies should be given priority while citing the literature.

Presentations presented in congresses, unpublished manuscripts, theses, Internet addresses, and personal interviews or experiences should not be indicated as references. If such references are used, they should be indicated in parentheses at the end of the relevant sentence in the text, without reference number and written in full, in order to clarify their nature.

References section: References should be numbered consecutively in the order in which they are first mentioned in the text. All authors should be listed regardless of number. The titles of Journals should be abbreviated according to the style used in the Index Medicus.

Reference Format

Journal: Last name(s) of the author(s) and initials, article title, publication title and its original abbreviation, publication date, volume, the inclusive page numbers. Example: Collin JR, Rathbun JE. Involuntal entropion: a review with evaluation of a procedure. Arch Ophthalmol. 1978;96:1058-1064.

Book: Last name(s) of the author(s) and initials, book title, edition, place of publication, date of publication and inclusive page numbers of the extract

cited.

Example: Herbert L. The Infectious Diseases (1st ed). Philadelphia; Mosby Harcourt; 1999:11;1-8.

Book Chapter: Last name(s) of the author(s) and initials, chapter title, book editors, book title, edition, place of publication, date of publication and inclusive page numbers of the cited piece.

Example: O'Brien TP, Green WR. Periocular Infections. In: Feigin RD, Cherry JD, eds. Textbook of Pediatric Infectious Diseases (4th ed). Philadelphia; W.B. Saunders Company; 1998:1273-1278.

Books in which the editor and author are the same person: Last name(s) of the author(s) and initials, chapter title, book editors, book title, edition, place of publication, date of publication and inclusive page numbers of the cited piece. Example: Solcia E, Capella C, Kloppel G. Tumors of the exocrine pancreas. In: Solcia E, Capella C, Kloppel G, eds. Tumors of the Pancreas. 2nd ed. Washington: Armed Forces Institute of Pathology; 1997:145-210.

TABLES, GRAPHICS, FIGURES, AND IMAGES

All visual materials together with their legends should be located on separate pages that follow the main text.

Images: Images (pictures) should be numbered and include a brief title. Permission to reproduce pictures that were published elsewhere must be included. All pictures should be of the highest quality possible, in JPEG format, and at a minimum resolution of 300 dpi.

Tables, Graphics, Figures: All tables, graphics or figures should be enumerated according to their sequence within the text and a brief descriptive caption should be written. Any abbreviations used should be defined in the accompanying legend. Tables in particular should be explanatory and facilitate readers' understanding of the manuscript, and should not repeat data presented in the main text.

MANUSCRIPT TYPES

Original Articles

Clinical research should comprise clinical observation, new techniques or laboratories studies. Original research articles should include title, structured abstract, key words relevant to the content of the article, introduction, materials and methods, results, discussion, study limitations, conclusion references, tables/figures/images and acknowledgement sections. Title, abstract and key words should be written in both Turkish and English. The manuscript should be formatted in accordance with the above-mentioned guidelines and should not exceed 16 A4 pages.

Title Page: This page should include the title of the manuscript, short title, name(s) of the authors and author information. The following descriptions should be stated in the given order:

1. Title of the manuscript (Turkish and English), as concise and explanatory as possible, including no abbreviations, up to 135 characters
2. Short title (Turkish and English), up to 60 characters
3. Name(s) and surname(s) of the author(s) (without abbreviations and academic titles) and affiliations
4. Name, address, e-mail, phone and fax number of the corresponding author
5. The place and date of scientific meeting in which the manuscript was

TURKISH

JOURNAL OF PHARMACEUTICAL SCIENCES

INSTRUCTIONS TO AUTHORS

presented and its abstract published in the abstract book, if applicable

Abstract: A summary of the manuscript should be written in both Turkish and English. References should not be cited in the abstract. Use of abbreviations should be avoided as much as possible; if any abbreviations are used, they must be taken into consideration independently of the abbreviations used in the text. For original articles, the structured abstract should include the following sub-headings:

Objectives: The aim of the study should be clearly stated.

Materials and Methods: The study and standard criteria used should be defined; it should also be indicated whether the study is randomized or not, whether it is retrospective or prospective, and the statistical methods applied should be indicated, if applicable.

Results: The detailed results of the study should be given and the statistical significance level should be indicated.

Conclusion: Should summarize the results of the study, the clinical applicability of the results should be defined, and the favorable and unfavorable aspects should be declared.

Keywords: A list of minimum 3, but no more than 5 key words must follow the abstract. Key words in English should be consistent with "Medical Subject Headings (MESH)" (www.nlm.nih.gov/mesh/MBrowser.html). Turkish key words should be direct translations of the terms in MESH.

Original research articles should have the following sections:

Introduction: Should consist of a brief explanation of the topic and indicate the objective of the study, supported by information from the literature.

Materials and Methods: The study plan should be clearly described, indicating whether the study is randomized or not, whether it is retrospective or prospective, the number of trials, the characteristics, and the statistical methods used.

Results: The results of the study should be stated, with tables/figures given in numerical order; the results should be evaluated according to the statistical analysis methods applied. See General Guidelines for details about the preparation of visual material.

Discussion: The study results should be discussed in terms of their favorable and unfavorable aspects and they should be compared with the literature. The conclusion of the study should be highlighted.

Study Limitations: Limitations of the study should be discussed. In addition, an evaluation of the implications of the obtained findings/results for future research should be outlined.

Conclusion: The conclusion of the study should be highlighted.

Acknowledgements: Any technical or financial support or editorial contributions (statistical analysis, English/Turkish evaluation) towards the study should appear at the end of the article.

References: Authors are responsible for the accuracy of the references. See General Guidelines for details about the usage and formatting required.

Review Articles

Review articles can address any aspect of clinical or laboratory pharmaceuticals. Review articles must provide critical analyses of contemporary evidence and provide directions of or future research. Most review articles are commissioned, but other review submissions are also welcome. Before sending a review, discussion with the editor is recommended.

Reviews articles analyze topics in depth, independently and objectively. The first chapter should include the title in Turkish and English, an unstructured summary and key words. Source of all citations should be indicated. The entire text should not exceed 25 pages (A4, formatted as specified above).

CORRESPONDENCE

All correspondence should be directed to the Turkish Journal of Pharmaceutical Sciences editorial board;

Post: Turkish Pharmacists' Association

Address: Willy Brandt Sok. No: 9 06690 Ankara, TURKEY

Phone: +90 312 409 8136

Fax: +90 312 409 8132

Web Page: <http://turkjps.org/home/>

E-mail: onur@pharmacy.ankara.edu.tr

TURKISH JOURNAL OF PHARMACEUTICAL SCIENCES

CONTENTS

- 1 Synthesis and Aldose Reductase Inhibitory Effect of Some New Hydrazinecarbothioamides and 4-Thiazolidinones Bearing an Imidazo[2,1-*b*]Thiazole Moiety
*İmidazo[2,1-*b*]Tiyazol Çekirdeği Taşıyan Bazı Yeni Hidrazinkarbotioamitler ve 4-Tiyazolidinonların Sentezi ve Aldoz Redüktaz İnhibitör Etkileri*
Nuray Ulusoy GÜZELDEMİRCİ, Selin CİMOK, Net DAŞ-EVCİMEN, Mutlu SARIKAYA
- 8 A Validated Reverse Phase-Ultra-Performance Liquid Chromatography Method for the Determination of Gemifloxacin Mesylate in Bulk and its Pharmaceutical Preparation
Gemifloksasin Mesilatın Bulk ve Farmasötik Preparatından Tayini için Valide Edilmiş Ters Faz-Ultra-Performans Sıvı Kromatografisi Metodu
Hebatallah A. WAGDY, Mohamed TAREK, Ahmed AMER, Menna GAMAL, Mohey ELMAZAR
- 14 Determination of Potential Drug-Drug Interactions Using Various Software Programs in a Community Pharmacy Setting
Serbest Eczanede Farklı Yazılım Programlarının Kullanılarak Olası İlaç-İlaç Etkileşimlerinin Saptanması
Mesut SANCAR, Aksa KAŞIK, Betül OKUYAN, Sevda BATUHAN, Fikret Vehbi İZZETTİN
- 20 Establishment and Escalation of an Amino Acid Stacked Reversible Release Embedded System Using Quality by Design
Tasarım Üzerinde Kaliteyi Kullanarak Amino Asit Yığılmış Bastırılabilir Salınan Gömülü Sistemin Kurulması ve Arttırılması
Vijay SHARMA, Lalit SINGH, Navneet VERMA
- 27 Preclinical Evaluation of the Haematinic Activity of an Oral Indiffusible Mixture of *Tamarindus indica* L. Leaf Extract
Tamarindus indica L. Yaprak Ekstresinden Hazırlanan Oral Dağılmayan Karışımın Hematinik Etkisinin Preklinik Değerlendirmesi
Sathiya RAMU, Shwetha Krishna MURTHY, Sukanya KRISHNA, Abhishek Lakkasandra SOMASHEKARAIHAH, Vani B. NANDIHALLI, Kanekal Mohammed MUZAMMIL
- 32 Quantification of Galantamine in *Sternbergia* Species by High Performance Liquid Chromatography
Sternbergia Türlerinde Yüksek Performanslı Sıvı Kromatografisi ile Galantamin Miktar Tayini
Özlem Bahadır ACIKARA, Betül Sever YILMAZ, Dilhun YAZGAN, Gülçin Saltan İŞCAN
- 37 Antiplasmodial Activity of the *n*-Hexane Extract from *Pleurotus ostreatus* (Jacq. ex. Fr) P. Kumm.
Pleurotus ostreatus (Jacq. ex. Fr) P. Kumm. *n*-Hekzan Ekstresinin Antiplazmodiyal Etkisi
Ozadheoghene Eriarie AFIEROHO, Xavier Siwe NOUNDOU, Chiazor P. ONYIA, Osamuyi H. FESTUS, Elizabeth C. CHUKWU, Olutayo M. ADEDOKUN, Michelle ISAACS, Heinrich C. HOPPE, Rui WM. KRAUSE, Kio A. ABO
- 43 Characterization of Gamma-Irradiated *Rosmarinus officinalis* L. (Rosemary)
Gama Işınlanmış Rosmarinus officinalis L. (Biberiye)
Reza REZANEJAD, Seyed Mahdi OJAGH, Marzieh HEIDARIEH, Mojtaba RAEISI, Gholamreza RAFIEE, Alireza ALISHAHI
- 48 Enhancement of Dissolution of Fenofibrate Using Complexation with Hydroxy Propyl β -Cyclodextrin
Hidroksi Propil β -Siklodekstrin ile Kompleksasyon Kullanılarak Fenofibratın Çözünmesinin Arttırılması
Sachin K. JAGDALE, Mohammad H. DEHGHAN, Nilesh S. PAUL
- 54 Effect of the Lipid Peroxidation Product 4-Hydroxynonenal on Neuroinflammation in Microglial Cells: Protective Role of Quercetin and Monochloropivaloylquercetin
Mikroglial Hücrelerde Lipid Peroksidasyon Ürünü 4-Hidroksinonenalin Nöroinflamasyon Üzerine Etkisi: Kersetin ve Monokloropivaloilkersetinin Koruyucu Rolü
Ahmet CUMAOĞLU, Aslı Özge AĞKAYA, Zehra ÖZKUL
- 62 Development of a Discriminative and Biorelevant Dissolution Test Method for Atorvastatin/Fenofibrate Combination with Appliance of Derivative Spectrophotometry
Türev Spektrofotometrik Yöntem ile Atorvastatin/Fenofibrat Kombinasyonunda Ayırıcı ve Biyoyoumlu Çözünme Testi Metodunun Geliştirilmesi
Panukumar Durga ANUMOLU, Sunitha GURRALA, Subrahmanyam Chavali VENKATA SATYA, Santoshi Vani POLISETTY, Anjana RAVINDRAN, Radhagayathri ACHANTA

TURKISH

JOURNAL OF PHARMACEUTICAL SCIENCES

CONTENTS

- 69 Comparison of the Essential Oils of *Ferula orientalis* L., *Ferulago sandrasica* Peşmen and Quézel, and *Hippomarathrum microcarpum* Petrov and Their Antimicrobial Activity
Ferula orientalis L., *Ferulago sandrasica* Peşmen ve Quézel ve *Hippomarathrum microcarpum* Petrov'un Uçucu Yağ ve Antimikrobiyal Etkilerinin Karşılaştırılması
Songül KARAKAYA, Gamze GÖGER, Fatmagül D. BOSTANLIK, Betül DEMİRCİ, Hayri DUMAN, Ceyda Sibel KILIÇ
- 76 Microanatomical and Physicochemical Characterization and Antioxidative Activity of Methanolic Extract of *Oudemansiella canarii* (Jungh.) Höhn
Oudemansiella canarii (Jungh.) Höhn Metanollü Ekstresinin Mikroanatomik ve Fizikokimyasal Karakterizasyonu ve Antioksidan Aktivitesi
Krishnendu ACHARYA, Sudeshna NANDI, Arun Kumar DUTTA
- 82 Degradation Kinetics, *In Vitro* Dissolution Studies, and Quantification of Praziquantel, Anchored in Emission Intensity by Spectrofluorimetry
Degradasyon Kinetiği, In Vitro Çözünme Çalışmaları ve Bağlanmış Prazikuantelin Emisyon Yoğunluklu Spektrofluorimetri ile Miktar Tayini
Panikumar D. ANUMOLU, Sunitha GURRALA, Ceema MATHEW, Vasavi PANCHAKATLA, Veda MADDALA
- 88 Subchronic Toxicity Assessment of Orally Administered Methanol (70%) Seed Extract of *Abrus precatorius* L. in Wistar Albino Rats
Wistar Albino Sıçanlarda Oral Olarak Uygulanmış Abrus precatorius L. Tohum Metanol (%70) Ekstraktının Subkronik Toksikite Değerlendirmesi
Shazia TABASUM, Swati KHARE, Kirti JAIN
- 96 Is There an Association Between Extreme Levels of Boron Exposure and Decrease in Y:X Sperm Ratio in Men? Results of an Epidemiological Study
Erkeklerde Y:X Sperm Oranındaki Azalma ile Aşırı Düzeyde Bor Maruziyeti Arasında Bir İlişki Var mıdır? Epidemiyolojik Çalışma Sonuçları
Can Özgür YALÇIN, Aylin ÜSTÜNDAĞ, Yalçın DUYDU
- 101 Histone Deacetylase Inhibitors: A Prospect in Drug Discovery
Histon Deasetilaz İnhibitörleri: İlaç Keşfinde Bir Aday
Rakesh YADAV, Pooja MISHRA, Divya YADAV
- 115 Two New Factors for the Evaluation of Scientific Performance: *U* and *U'*
Bilimsel Performansın Değerlendirilmesi İçin İki Yeni Faktör: U ve U'
Tayfun UZBAY

PUBLICATION NAME	Turkish Journal of Pharmaceutical Sciences
TYPE OF PUBLICATION	Vernacular Publication
PERIOD AND LANGUAGE	Quarterly- English
OWNER	Erdoğan ÇOLAK on behalf of the Turkish Pharmacists' Association
EDITOR-IN-CHIEF	Feyyaz ONUR
ADDRESS OF PUBLICATION	Cinnah Mah. Willy Brandt Sok. No: 9 Çankaya-Ankara/TURKEY

TURKISH JOURNAL OF PHARMACEUTICAL SCIENCES

Volume: 16, No: 1, Year: 2019

CONTENTS

Original articles

- Synthesis and Aldose Reductase Inhibitory Effect of Some New Hydrazinecarbothioamides and 4-Thiazolidinones Bearing an Imidazo[2,1-*b*]Thiazole Moiety
Nuray Ulusoy GÜZELDEMİRÇİ, Selin ÇİMOK, Net DAŞ-EVCİMEN, Mutlu SARIKAYA 1
- A Validated Reverse Phase-Ultra-Performance Liquid Chromatography Method for the Determination of Gemifloxacin Mesylate in Bulk and its Pharmaceutical Preparation
Hebatallah A. WAGDY, Mohamed TAREK, Ahmed AMER, Menna GAMAL, Mohey ELMAZAR 8
- Determination of Potential Drug-Drug Interactions Using Various Software Programs in a Community Pharmacy Setting
Mesut SANCAR, Aksa KAŞIK, Betül OKUYAN, Sevda BATUHAN, Fikret Vehbi İZZETTİN 14
- Establishment and Escalation of an Amino Acid Stacked Repressible Release Embedded System Using Quality by Design
Vijay SHARMA, Lalit SINGH, Navneet VERMA 20
- Preclinical Evaluation of the Haematinic Activity of an Oral Indiffusible Mixture of *Tamarindus indica* L. Leaf Extract
Sathiya RAMU, Shwetha Krishna MURTHY, Sukanya KRISHNA, Abhishek Lakkasandra SOMASHEKARAIHAH, Vani B. NANDIHALLI, Kanekal Mohammed MUZAMMIL 27
- Quantification of Galantamine in *Sternbergia* Species by High Performance Liquid Chromatography
Özlem Bahadır ACIKARA, Betül Sever YILMAZ, Dilhun YAZGAN, Gülçin Saltan İŞCAN 32
- Antiplasmodial Activity of the *n*-Hexane Extract from *Pleurotus ostreatus* (Jacq. ex. Fr) P. Kumm.
Ozadheoghene Eriarie AFIEROHO, Xavier Siwe NOUNDOU, Chiazor P. ONYIA, Osamuyi H. FESTUS, Elizabeth C. CHUKWU, Olutayo M. ADEDOKUN, Michelle ISAACS, Heinrich C. HOPPE, Rui WM. KRAUSE, Kio A. ABO 37
- Characterization of Gamma-Irradiated *Rosmarinus officinalis* L. (Rosemary)
Reza REZANEJAD, Seyed Mahdi OJAGH, Marzieh HEIDARIEH, Mojtaba RAEISI, Gholamreza RAFIEE, Alireza ALISHAHI 43
- Enhancement of Dissolution of Fenofibrate Using Complexation with Hydroxy Propyl β -Cyclodextrin
Sachin K. JAGDALE, Mohammad H. DEGHAN, Nilesh S. PAUL 48
- Effect of the Lipid Peroxidation Product 4-Hydroxynonenal on Neuroinflammation in Microglial Cells: Protective Role of Quercetin and Monochloropaloylquercetin
Ahmet CUMAOĞLU, Aslı Özge AĞKAYA, Zehra ÖZKUL 54
- Development of a Discriminative and Biorelevant Dissolution Test Method for Atorvastatin/Fenofibrate Combination with Appliense of Derivative Spectrophotometry
Panukumar Durga ANUMOLU, Sunitha GURRALA, Subrahmanyam Chavali VENKATA SATYA, Santoshi Vani POLISETTY, Anjana RAVINDRAN, Radhagayathri ACHANTA 62
- Comparison of the Essential Oils of *Ferula orientalis* L., *Ferulago sandrasica* Peşmen and Quézel, and *Hippomarathrum microcarpum* Petrov and Their Antimicrobial Activity
Songül KARAKAYA, Gamze GÖGER, Fatmagül D. BOSTANLIK, Betül DEMİRÇİ, Hayri DUMAN, Ceyda Sibel KILIÇ 69
- Microanatomical and Physicochemical Characterization and Antioxidative Activity of Methanolic Extract of *Oudemansiella canarii* (Jung.) Höhn
Krishnendu ACHARYA, Sudeshna NANDI, Arun Kumar DUTTA 76
- Degradation Kinetics, *In Vitro* Dissolution Studies, and Quantification of Praziquantel, Anchored in Emission Intensity by Spectrofluorimetry
Panikumar D. ANUMOLU, Sunitha GURRALA, Ceema MATHEW, Vasavi PANCHAKATLA, Veda MADDALA 82
- Subchronic Toxicity Assessment of Orally Administered Methanol (70%) Seed Extract of *Abrus precatorius* L. in Wistar Albino Rats
Shazia TABASUM, Swati KHARE, Kirti JAIN 88
- Is There an Association Between Extreme Levels of Boron Exposure and Decrease in Y:X Sperm Ratio in Men? Results of an Epidemiological Study
Can Özgür YALÇIN, Aylin ÜSTÜNDAĞ, Yalçın DUYDU 96

Reviews

- Histone Deacetylase Inhibitors: A Prospect in Drug Discovery
Rakesh YADAV, Pooja MISHRA, Divya YADAV 101
- Two New Factors for the Evaluation of Scientific Performance: U and U'
Tayfun UZBAY 115



Synthesis and Aldose Reductase Inhibitory Effect of Some New Hydrazinecarbothioamides and 4-Thiazolidinones Bearing an Imidazo[2,1-*b*]Thiazole Moiety

İmidazo[2,1-*b*]Tiyazol Çekirdeği Taşıyan Bazı Yeni Hidrazinkarbotiyoamitler ve 4-Tiyazolidinonların Sentezi ve Aldoz Redüktaz İnhibitör Etkileri

© Nuray ULUSOY GÜZELDEMİRÇİ^{1*}, © Selin CİMOK¹, Net DAŞ-EVCİMEN², © Mutlu SARIKAYA²

¹Istanbul University, Faculty of Pharmacy, Department of Pharmaceutical Chemistry, İstanbul, Turkey

²Ankara University, Faculty of Pharmacy, Department of Biochemistry, Ankara, Turkey

ABSTRACT

Objectives: To synthesize and characterize 2-[[6-(4-bromophenyl)imidazo[2,1-*b*]thiazol-3-yl]acetyl]-*N*-alkyl/arylhydrazinecarbothioamide and 3-alkyl/aryl-2-[[6-(4-bromophenyl)imidazo[2,1-*b*]thiazol-3-yl]acetyl]hydrazono]-5-nonsubstituted/methyl-4-thiazolidinone derivatives and evaluate them for their aldose reductase (AR) inhibitory effect.

Materials and Methods: 2-[[6-(4-bromophenyl)imidazo[2,1-*b*]thiazol-3-yl]acetyl]-*N*-alkyl/arylhydrazinecarbothioamides (**3a-f**) and 3-alkyl/aryl-2-[[6-(4-bromophenyl)imidazo[2,1-*b*]thiazol-3-yl]acetyl]hydrazono]-5-nonsubstituted/methyl-4-thiazolidinones (**4a-j**) were synthesized from 2-[[6-(4-bromophenyl)imidazo[2,1-*b*]thiazole-3-yl]acetohydrazide (**2**). Their structures were elucidated by elemental analyses and spectroscopic data. The synthesized compounds were tested for their ability to inhibit rat kidney AR.

Results: Among the synthesized compounds, 2-[[6-(4-bromophenyl)imidazo[2,1-*b*]thiazol-3-yl]acetyl]-*N*-benzoylhydrazinecarbothioamide (**3d**) showed the best AR inhibitory activity.

Conclusion: The findings of this study indicate that the different derivatives of the compounds in this study may be considered interesting candidates for future research.

Key words: Hydrazinecarbothioamide, 4-thiazolidinone, imidazo[2,1-*b*]thiazole, aldose reductase inhibition

ÖZ

Amaç: Bu çalışmanın amacı, 2-[[6-(4-bromofenil)imidazo[2,1-*b*]tiyazol-3-il]asetil]-*N*-alkil/arihidrazinkarbotiyoamit ve 3-alkil/aryl-2-[[6-(4-bromofenil)imidazo[2,1-*b*]tiyazol-3-il]asetil]hidrazono]-5-nonsüstitüe/metil-4-tiyazolidinon türevlerini sentezlemek, yapılarını aydınlatmak ve aldoz redüktaz (AR) inhibitör etkilerini araştırmaktır.

Gereç ve Yöntemler: 2-[[6-(4-bromofenil)imidazo[2,1-*b*]tiyazol-3-il]asetohidrazitten (**2**) hareketle 2-[[6-(4-bromofenil)imidazo[2,1-*b*]tiyazol-3-il]asetil]-*N*-alkil/arihidrazinkarbotiyoamit (**3a-f**) ve 3-alkil/aryl-2-[[6-(4-bromofenil)imidazo[2,1-*b*]tiyazol-3-il]asetil]hidrazono]-5-nonsüstitüe/metil-4-tiyazolidinon türevleri (**4a-j**) sentezlenmiştir. Bileşiklerin yapıları elementel analiz ve spektroskopik bulgularla kanıtlanmıştır. Sentezlenen bileşikler sıçan böbrek AR enzimini inhibe etme özellikleri açısından test edilmiştir.

Bulgular: Sentezlenen bileşikler arasından, 2-[[6-(4-bromofenil)imidazo[2,1-*b*]tiyazol-3-il]asetil]-*N*-benzoilhidrazinkarbotiyoamit (**3d**) en iyi AR inhibitör etkiyi göstermiştir.

Sonuç: Bu çalışmanın bulguları, bu çalışmadaki bileşiklerin farklı türevlerinin gelecek araştırmalar için ilginç adaylar olarak görülebileceğini göstermektedir.

Anahtar kelimeler: Hidrazinkarbotiyoamit, 4-tiyazolidinon, imidazo[2,1-*b*]tiyazol, aldoz redüktaz inhibisyon

*Correspondence: E-mail: nulusoy@istanbul.edu.tr, Phone: +90 532 574 92 63 ORCID-ID: orcid.org/0000-0002-4495-4282

Received: 06.08.2017, Accepted: 30.11.2017

©Turk J Pharm Sci, Published by Galenos Publishing House.

INTRODUCTION

Diabetes mellitus (DM) is a chronic disease caused by deficient production of insulin by the pancreas and by resistance to insulin's effects, or in some cases both. According to the World Health Organization, more than 422 million people worldwide have diabetes and the number is expected to rise to almost double by 2030.¹ Furthermore, hyperglycemia is the major risk factor responsible for the broad range of complications that are the main cause of mortality and morbidity in people with DM. There are two forms of complications: acute and chronic, including nephropathy, neuropathy and retinopathy.² Various biochemical pathways have been proposed to explain the pathological mechanisms of diabetic complications. These include increased polyol pathway flux, activation of the protein kinase C pathway, oxidative stress, and accelerated advanced glycation end-product formation.^{2,3}

Aldose reductase (AR) (AR; ALR2; EC 1.1.1.21) is the first enzyme in the polyol pathway and reduces glucose to sorbitol in the presence of nicotinamide adenine dinucleotide phosphate (NADPH). Sorbitol dehydrogenase, the second enzyme in the polyol pathway, oxidizes the intermediate sorbitol to fructose with NAD⁺ as cofactor (Figure 1).^{4,5} It has been reported that AR enzyme activity increases in diabetes.⁶ Total glucose utilization by AR-catalyzed reduction is less than 3% under normoglycemia (5.5 mM), whereas the rate is more than 30% under hyperglycemia (20 mM).⁶ Increased AR activity has been implicated in the pathogenesis of diabetic complications.^{6,7} Activated AR leads to cell damage through several mechanisms, including accumulation of sorbitol,^{8,9} NADPH depletion,^{10,11} increased NADH/NAD⁺ ratio,¹² and increased fructose levels.¹³ Inhibitors of AR thus seem to have the potential to prevent or treat diabetic complications. Even though a wide number of AR inhibitors (ARIs) have been obtained over the last 30 years, the clinical efficacy of these compounds is not completely satisfactory and several of them have shown undesirable side effects.¹⁴ Sorbinil, tolrestat, zopolrestat and ponalrestat were withdrawn from clinical trials because of their side effects.¹⁵ Various thiazolidinone derivatives are a newer class of antidiabetic drugs¹⁶⁻²⁰ that improve glycemic control in type 2 diabetes by increasing insulin action in skeletal muscles, the liver, and adipose tissue.^{21,22}

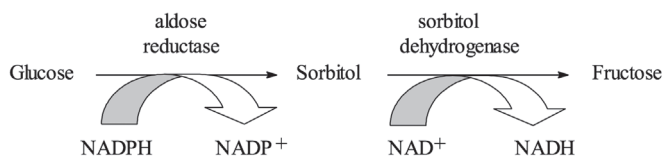


Figure 1. Polyol pathway

NADPH: Nicotinamide adenine dinucleotide phosphate

There has been considerable interest in the chemistry of 4-thiazolidinone ring systems, which are a core structure in various synthetic pharmaceuticals displaying a broad spectrum of biological activities such as antidiabetic,^{7,23-26} anticancer,²⁷⁻²⁹

antiviral/anti-HIV,³⁰ antibacterial and antifungal,^{31,32} antitubercular,³³ antiinflammatory, and analgesic³⁴ activities. Moreover, imidazo[2,1-*b*]thiazole³⁵ and thiosemicarbazide³⁶ moieties are also associated with various biological properties including antidiabetic activity.

As a continuation of our previous studies on 4-thiazolidinone derivatives with ARIs³⁷⁻⁴³ or different biological activities,⁴⁴⁻⁴⁸ we report the synthesis of some novel imidazo[2,1-*b*]thiazole derivatives incorporating two known bioactive nuclei such as hydrazinecarbothioamide or 4-thiazolidinone.

EXPERIMENTAL

Chemical methods

Melting points were determined using a Büchi B-540 melting point apparatus in open capillary tubes and are uncorrected. Elemental analyses were performed on a Thermo Finnigan Flash EA 1112 elemental analyzer. IR spectra were recorded on KBr discs, using a Shimadzu IR Affinity-1 FT-IR spectrophotometer. ¹H-NMR and ¹³C-NMR (APT) spectra were measured on a Varian UNITY INOVA (500 MHz) spectrometer using dimethyl sulfoxide (DMSO)-*d*₆. The starting materials were either commercially available or synthesized according to the references cited.

General procedure for the synthesis of 2-[[6-(4-bromophenyl)imidazo[2,1-*b*]thiazol-3-yl]acetyl]-*N*-cycloalkyl/aryl/hydrazinecarbothioamides (**3a-f**)

To a solution of 2-[6-(4-bromophenyl)imidazo[2,1-*b*]thiazol-3-yl]acetohydrazide (**2**) (0.005 mol) in ethanol (30 mL) was added the appropriate isothiocyanate (0.005 mol). The resulting mixture was heated under reflux for 3 h. After cooling, the precipitate was separated and purified by washing with hot ethanol.

2-[[6-(4-bromophenyl)imidazo[2,1-*b*]thiazol-3-yl]acetyl]-*N*-cyclohexylhydrazinecarbothioamide (**3a**)

Yield: 71%; m.p. 246°C; IR (KBr, cm⁻¹): 3207 (N-H), 1672 (C=O), 1195 (C=S); ¹H-NMR (500 MHz, DMSO-*d*₆): δ 10.09 (s, 1H, NH), 9.44; 9.18 (2s, 1H, NH), 8.27; 8.15 (2s, 1H, imidazothiazole C₅-H), 7.77-7.73 (m, 2H, 4-Brphenyl C_{2,6}-H), 7.66 (s, 1H, NH), 7.60-7.56 (m, 2H, 4-Brphenyl C_{3,5}-H), 7.10; 7.06 (2s, 1H, imidazothiazole C₂-H), 4.06 (s, 1H, cyclohexyl), 3.82 (s, 2H, CH₂CO), 1.77-1.03 (m, 10H, cyclohexyl). Anal. Calcd. for C₂₀H₂₂BrN₅OS₂: C, 48.78; H, 4.50; N, 14.22. Found: C, 48.25; H, 3.90; N, 13.97.

2-[[6-(4-bromophenyl)imidazo[2,1-*b*]thiazol-3-yl]acetyl]-*N*-benzylhydrazinecarbothioamide (**3b**)

Yield: 88%; m.p. 251-252°C; IR (KBr, cm⁻¹): 3217 (N-H), 1674 (C=O), 1195 (C=S); ¹H-NMR (500 MHz, DMSO-*d*₆): δ 10.24 (s, 1H, NH), 9.63; 9.45 (2s, 1H, NH), 8.68 (s, 1H, NH), 8.21 (s, 1H, imidazothiazole C₅-H), 7.72 (d, 2H, *J*=8.78 Hz, 4-Brphenyl C_{2,6}-H), 7.57 (d, 2H, *J*=8.78 Hz, 4-Brphenyl C_{3,5}-H), 7.30-7.20 (m, 5H, phenyl), 7.10 (s, 1H, imidazothiazole C₂-H), 4.78 (s, 2H, CH₂), 3.83 (s, 2H, CH₂CO). Anal. Calcd. for C₂₁H₁₈BrN₅OS₂: C, 50.40; H, 3.63; N, 13.99. Found: C, 50.20; H, 3.65; N, 13.46.

2-[[6-(4-bromophenyl)imidazo[2,1-b]thiazol-3-yl]acetyl]-N-phenethylhydrazinecarbothioamide (3c)

Yield: 89%; m.p. 251°C; IR (KBr, cm^{-1}): 3197 (N-H), 1672 (C=O), 1163 (C=S); $^1\text{H-NMR}$ (500 MHz, DMSO-d_6): δ 10.19 (s, 1H, NH), 9.55; 9.35 (2s, 1H, NH), 8.26 (s, 1H, NH), 8.21 (s, 1H, imidazothiazole C_5 -H), 7.77 (d, 2H, $J=9.27$ Hz, 4-Brphenyl $\text{C}_{2,6}$ -H), 7.58 (d, 2H, $J=8.78$ Hz, 4-Brphenyl $\text{C}_{3,5}$ -H), 7.31-7.28 (m, 2H, phenyl), 7.25-7.20 (m, 3H, phenyl), 7.11; 7.06 (2s, 1H, imidazothiazole C_2 -H), 3.83 (s, 2H, CH_2CO), 3.66 (q, 2H, $J=7.81$ Hz, N-CH_2), 2.82 (t, 2H, $J=7.07$ Hz, CH_2 -Ph). Anal. Calcd. for $\text{C}_{22}\text{H}_{20}\text{BrN}_5\text{OS}_2$: C, 51.36; H, 3.92; N, 13.61. Found: C, 51.33; H, 3.82; N, 13.60.

2-[[6-(4-bromophenyl)imidazo[2,1-b]thiazol-3-yl]acetyl]-N-benzoylhydrazinecarbothioamide (3d)

Yield: 73%; m.p. 215°C; IR (KBr, cm^{-1}): 3178 (N-H), 1666; 1645 (C=O), 1172 (C=S); $^1\text{H-NMR}$ (500 MHz, DMSO-d_6): δ 12.55 (s, 1H, NH), 11.77 (s, 1H, NH), 11.32 (s, 1H, NH), 8.35 (s, 1H, imidazothiazole C_5 -H), 7.95 (d, 2H, $J=8.78$ Hz, phenyl), 7.78 (d, 2H, $J=8.29$ Hz, 4-Brphenyl $\text{C}_{2,6}$ -H), 7.66-7.63 (m, 1H, phenyl), 7.60-7.57 (m, 2H, 4-Brphenyl $\text{C}_{3,5}$ -H), 7.54-7.50 (m, 2H, phenyl), 7.15 (s, 1H, imidazothiazole C_2 -H), 3.99 (s, 2H, CH_2CO). Anal. Calcd. for $\text{C}_{21}\text{H}_{16}\text{BrN}_5\text{O}_2\text{S}_2$: C, 49.03; H, 3.14; N, 13.61. Found: C, 48.97; H, 3.66; N, 12.89.

2-[[6-(4-bromophenyl)imidazo[2,1-b]thiazol-3-yl]acetyl]-N-(4-fluorophenyl)hydrazinecarbothioamide (3e)

Yield: 90%; m.p. 209-210°C; IR (KBr, cm^{-1}): 3134 (N-H), 1674 (C=O), 1213 (C=S); $^1\text{H-NMR}$ (500 MHz, DMSO-d_6): δ 10.40 (s, 1H, NH), 9.81 (s, 1H, NH), 9.73 (s, 1H, NH), 8.24 (s, 1H, imidazothiazole C_5 -H), 7.72 (d, 2H, $J=8.29$ Hz, 4-Brphenyl $\text{C}_{2,6}$ -H), 7.58 (d, 2H, $J=8.79$ Hz, 4-Brphenyl $\text{C}_{3,5}$ -H), 7.44-7.41 (m, 2H, phenyl), 7.20-7.17 (m, 2H, phenyl), 7.12 (s, 1H, imidazothiazole C_2 -H), 3.88 (s, 2H, CH_2CO). Anal. Calcd. for $\text{C}_{20}\text{H}_{15}\text{BrFN}_5\text{OS}_2$: C, 47.63; H, 3.00; N, 13.88. Found: C, 47.66; H, 3.19; N, 13.29.

2-[[6-(4-bromophenyl)imidazo[2,1-b]thiazol-3-yl]acetyl]-N-(4-methoxyphenyl)hydrazinecarbothioamide (3f)

Yield: 86%; m.p. 230°C; IR (KBr, cm^{-1}): 3296; 3134 (N-H), 1672 (C=O), 1236 (C=S); $^1\text{H-NMR}$ (500 MHz, DMSO-d_6): δ 10.36 (s, 1H, NH), 9.70 (s, 1H, NH), 9.59 (s, 1H, NH), 8.25 (s, 1H, imidazothiazole C_5 -H), 7.71 (d, 2H, $J=8.78$ Hz, 4-Brphenyl $\text{C}_{2,6}$ -H), 7.57 (d, 2H, $J=8.78$ Hz, 4-Brphenyl $\text{C}_{3,5}$ -H), 7.28 (d, 2H, $J=8.79$ Hz, phenyl), 7.12 (s, 1H, imidazothiazole C_2 -H), 6.91 (d, 2H, $J=8.79$ Hz, phenyl), 3.87 (s, 2H, CH_2CO), 3.76 (s, 3H, OCH_3). $^{13}\text{C-NMR}$ (APT) (500 MHz, DMSO-d_6): δ 181.50 (C=S), 162.20 (C=O), 157.59 (phenyl C_4), 149.53 (imidazothiazole C_{7a}), 145.47 (imidazothiazole C_6), 134.23 (4-Brphenyl C_1), 132.51 (phenyl C_1), 132.27 (4-Brphenyl $\text{C}_{3,5}$), 127.33 (phenyl $\text{C}_{2,6}$), 127.25 (4-Brphenyl $\text{C}_{2,6}$), 126.85 (imidazothiazole C_3), 120.50 (4-Brphenyl C_4), 114.10 (phenyl $\text{C}_{3,5}$), 111.46 (imidazothiazole C_2), 109.75 (imidazothiazole C_5), 55.92 (CH_3), 33.41 (CH_2). Anal. Calcd. for $\text{C}_{21}\text{H}_{18}\text{BrN}_5\text{O}_2\text{S}_2$: C, 48.84; H, 3.51; N, 13.56. Found: C, 49.05; H, 3.54; N, 13.71.

General procedure for the synthesis of 3-cycloalkyl/aralkyl/aryl-2-[[6-(4-bromophenyl)imidazo[2,1-b]thiazol-3-yl]acetyl]hydrazono]-5-nonsubstituted/methyl-4-thiazolidinones (4a-j)

To a suspension of 2-[[6-(4-bromophenyl)imidazo[2,1-b]thiazol-3-yl]acetyl]-N-alkyl/arylhydrazinecarbothioamides (0.005 mol) in

absolute ethanol (30 mL) were added anhydrous sodium acetate (0.02 mol) and ethyl bromoacetate/ethyl 2-bromopropionate (0.005 mol). The reaction mixture was refluxed for 20 h, then cooled, diluted with water, and allowed to stand overnight. The crystals were filtered, dried, and purified by crystallization from ethanol or ethanol/water.

3-Benzyl-2-[[6-(4-bromophenyl)imidazo[2,1-b]thiazol-3-yl]acetyl]hydrazono]-4-thiazolidinone (4a)

Yield: 96%; m.p. 232-233°C; IR (KBr, cm^{-1}): 3215 (N-H), 1720 (ring C=O), 1670 (C=O); $^1\text{H-NMR}$ (500 MHz, DMSO-d_6): δ (NH proton not observed), 8.32; 8.10 (2s, 1H, imidazothiazole C_5 -H), 7.76 (d, 2H, $J=8.30$ Hz, 4-Brphenyl $\text{C}_{2,6}$ -H), 7.58 (d, 2H, $J=7.32$ Hz, 4-Brphenyl $\text{C}_{3,5}$ -H), 7.38-7.19 (m, 5H, phenyl), 7.03; 6.84 (2s, 1H, imidazothiazole C_2 -H), 4.82 (s, 2H, NCH_2), 4.15-3.83 (m, 4H, CH_2CO and SCH_2). Anal. Calcd. for $\text{C}_{23}\text{H}_{18}\text{BrN}_5\text{O}_2\text{S}_2$: C, 51.11; H, 3.36; N, 12.96. Found: C, 50.74; H, 3.38; N, 13.10.

3-Phenethyl-2-[[6-(4-bromophenyl)imidazo[2,1-b]thiazol-3-yl]acetyl]hydrazono]-4-thiazolidinone (4b)

Yield: 88%; m.p. 134-135°C; IR (KBr, cm^{-1}): 3142 (N-H), 1716 (ring C=O), 1658 (C=O); $^1\text{H-NMR}$ (500 MHz, DMSO-d_6): δ 10.72; 10.55 (2s, 1H, NH), 8.28; 8.20 (2s, 1H, imidazothiazole C_5 -H), 7.78 (d, 2H, $J=8.78$ Hz, 4-Brphenyl $\text{C}_{2,6}$ -H), 7.59 (d, 2H, $J=8.30$ Hz, 4-Brphenyl $\text{C}_{3,5}$ -H), 7.28-7.23 (m, 2H, phenyl), 7.21-7.16 (m, 3H, phenyl), 7.08; 7.05 (2s, 1H, imidazothiazole C_2 -H), 4.08-3.82 (m, 6H, CH_2CO , SCH_2 and NCH_2), 2.89 (t, 2H, $J=7.32$ Hz, CH_2 -Ph). Anal. Calcd. for $\text{C}_{24}\text{H}_{20}\text{BrN}_5\text{O}_2\text{S}_2 \cdot 2\text{H}_2\text{O}$: C, 48.82; H, 4.10; N, 11.86. Found: C, 48.90; H, 3.51; N, 11.87.

3-Benzoyl-2-[[6-(4-bromophenyl)imidazo[2,1-b]thiazol-3-yl]acetyl]hydrazono]-4-thiazolidinone (4c)

Yield: 53%; m.p. 260°C; IR (KBr, cm^{-1}): 3197 (N-H), 1757 (ring C=O), 1681 (C=O); $^1\text{H-NMR}$ (500 MHz, DMSO-d_6): δ 11.48 (s, 1H, NH), 8.16 (s, 1H, imidazothiazole C_5 -H), 8.06 (d, 2H, $J=8.30$ Hz, phenyl), 7.65-7.56 (m, 3H, 4-Brphenyl $\text{C}_{2,6}$ -H and phenyl), 7.51-7.48 (m, 4H, 4-Brphenyl $\text{C}_{3,5}$ -H and phenyl), 7.20 (s, 1H, imidazothiazole C_2 -H), 4.28-4.12 (m, 4H, CH_2CO and SCH_2). Anal. Calcd. for $\text{C}_{23}\text{H}_{16}\text{BrN}_5\text{O}_3\text{S}_2$: C, 49.83; H, 2.91; N, 12.63. Found: C, 50.46; H, 2.97; N, 13.02.

3-(4-Fluorophenyl)-2-[[6-(4-bromophenyl)imidazo[2,1-b]thiazol-3-yl]acetyl]hydrazono]-4-thiazolidinone (4d)

Yield: 84%; m.p. 279-281°C; IR (KBr, cm^{-1}): 3122 (N-H), 1751 (ring C=O), 1705 (C=O); $^1\text{H-NMR}$ (500 MHz, DMSO-d_6): δ 11.33 (s, 1H, NH), 8.14 (s, 1H, imidazothiazole C_5 -H), 7.56 (d, 2H, $J=8.30$ Hz, 4-Brphenyl $\text{C}_{2,6}$ -H), 7.42 (d, 2H, $J=8.30$ Hz, 4-Brphenyl $\text{C}_{3,5}$ -H), 7.19-7.14 (m, 3H, phenyl and imidazothiazole C_2 -H), 6.91-6.88 (m, 2H, phenyl), 4.36-3.83 (m, 4H, CH_2CO and SCH_2). Anal. Calcd. for $\text{C}_{22}\text{H}_{15}\text{BrFN}_5\text{O}_2\text{S}_2$: C, 48.54; H, 2.78; N, 12.86. Found: C, 49.04; H, 2.99; N, 12.82.

3-(4-Methoxyphenyl)-2-[[6-(4-bromophenyl)imidazo[2,1-b]thiazol-3-yl]acetyl]hydrazono]-4-thiazolidinone (4e)

Yield: 98%; m.p. 277-279°C; IR (KBr, cm^{-1}): 3209 (N-H), 1732 (ring C=O), 1672 (C=O); $^1\text{H-NMR}$ (500 MHz, DMSO-d_6): δ (NH proton not observed), 8.14 (s, 1H, imidazothiazole C_5 -H), 7.53

(d, 2H, $J=6.35$ Hz, 4-Brphenyl C_{2,6}-H), 7.40 (d, 2H, $J=8.79$ Hz, 4-Brphenyl C_{3,5}-H), 7.15 (s, 1H, imidazothiazole C₂-H), 6.90 (d, 2H, $J=6.83$ Hz, phenyl), 6.82 (d, 2H, $J=8.79$ Hz, phenyl), 4.22-3.93 (m, 4H, CH₂CO and SCH₂), 3.80 (s, 3H, OCH₃). ¹³C-NMR (APT) (500 MHz, DMSO-d₆): δ 169.23 (thiazolidinone C=O), 166.69 (C=O), 156.99 (phenyl C₄), 152.44 (C=N), 149.60 (imidazothiazole C_{7a}), 145.54 (imidazothiazole C₆), 141.16 (phenyl C₁), 134.02 (4-Brphenyl C₁), 132.31 (4-Brphenyl C_{3,5}), 127.14 (4-Brphenyl C_{2,6}), 126.69 (imidazothiazole C₃), 122.55 (phenyl C_{2,6}), 120.34 (4-Brphenyl C₄), 115.32 (phenyl C_{3,5}), 111.61 (imidazothiazole C₂), 109.39 (imidazothiazole C₅), 55.90 (OCH₃), 33.24 (CH₂), 30.75 (thiazolidinone C₅). Anal. Calcd. for C₂₃H₁₇BrN₅O₃S₂: C, 49.65; H, 3.26; N, 12.59. Found: C, 49.84; H, 3.11; N, 12.40.

3-Benzyl-2-[[[(6-(4-bromophenyl)imidazo[2,1-b]thiazol-3-yl)acetyl]hydrazono]-5-methyl-4-thiazolidinone (4f)

Yield: 72%; m.p. 171-172°C; IR (KBr, cm⁻¹): 3186 (N-H), 1720 (ring C=O), 1668 (C=O); ¹H-NMR (500 MHz, DMSO-d₆): δ 10.68 (s, 1H, NH), 8.26; 8.11 (2s, 1H, imidazothiazole C₅-H), 7.77 (d, 2H, $J=8.29$ Hz, 4-Brphenyl C_{2,6}-H), 7.58 (d, 2H, $J=8.29$ Hz, 4-Brphenyl C_{3,5}-H), 7.34-7.23 (m, 5H, phenyl), 7.05; 6.87 (2s, 1H, imidazothiazole C₂-H), 4.87; 4.83 (2s, 2H, NCH₂), 4.52; 4.47 (2q, 1H, $J=7.33$; 7.32 Hz, SCH), 3.92; 3.85 (2s, 2H, CH₂CO), 1.58; 1.54 (2d, 3H, $J=7.32$ Hz, CH₃). Anal. Calcd. for C₂₄H₂₀BrN₅O₃S₂: C, 51.99; H, 3.64; N, 12.63. Found: C, 51.47; H, 3.11; N, 12.17.

3-Phenethyl-2-[[[(6-(4-bromophenyl)imidazo[2,1-b]thiazol-3-yl)acetyl]hydrazono]-5-methyl-4-thiazolidinone (4g)

Yield: 89%; m.p. 224-225°C; IR (KBr, cm⁻¹): 3169 (N-H), 1712 (ring C=O), 1666 (C=O); ¹H-NMR (500 MHz, DMSO-d₆): δ 10.71; 10.54 (2s, 1H, NH), 8.28; 8.20 (2s, 1H, imidazothiazole C₅-H), 7.78 (d, 2H, $J=8.78$ Hz, 4-Brphenyl C_{2,6}-H), 7.58 (d, 2H, $J=8.29$ Hz, 4-Brphenyl C_{3,5}-H), 7.27-7.23 (m, 2H, phenyl), 7.19-7.16 (m, 3H, phenyl), 7.08; 7.06 (2s, 1H, imidazothiazole C₂-H), 4.33; 4.27 (2q, 1H, $J=6.83$; 7.32 Hz, SCH), 4.10; 3.89 (2s, 2H, CH₂CO), 3.87-3.80 (m, 2H, NCH₂), 2.99-2.86 (m, 2H, CH₂-Ph), 1.44; 1.36 (2d, 3H, $J=7.32$ Hz, CH₃). Anal. Calcd. for C₂₅H₂₂BrN₅O₃S₂: C, 52.82; H, 3.90; N, 12.32. Found: C, 52.67; H, 3.75; N, 12.07.

3-Benzoyl-2-[[[(6-(4-bromophenyl)imidazo[2,1-b]thiazol-3-yl)acetyl]hydrazono]-5-methyl-4-thiazolidinone (4h)

Yield: 88%; m.p. 192-194°C; IR (KBr, cm⁻¹): 3219 (N-H), 1749 (ring C=O), 1697 (C=O); ¹H-NMR (500 MHz, DMSO-d₆): δ 11.52 (s, 1H, NH), 8.17; 8.15 (2s, 1H, imidazothiazole C₅-H), 8.07-8.03 (m, 2H, phenyl), 7.66-7.57 (m, 3H, 4-Brphenyl C_{2,6}-H and phenyl), 7.53-7.47 (m, 4H, 4-Brphenyl C_{3,5}-H and phenyl), 7.21; 7.20 (2s, 1H, imidazothiazole C₂-H), 4.52; 4.44 (2q, 1H, $J=7.32$ Hz, SCH), 4.23-4.11 (m, 2H, CH₂CO), 1.63; 1.56 (2d, 3H, $J=7.32$ Hz, CH₃). Anal. Calcd. for C₂₄H₁₈BrN₅O₃S₂: C, 50.71; H, 3.19; N, 12.32. Found: C, 50.72; H, 3.29; N, 12.39.

3-(4-Fluorophenyl)-2-[[[(6-(4-bromophenyl)imidazo[2,1-b]thiazol-3-yl)acetyl]hydrazono]-5-methyl-4-thiazolidinone (4i)

Yield: 90%; m.p. 194-196°C; IR (KBr, cm⁻¹): 3118 (N-H), 1747 (ring C=O), 1701 (C=O); ¹H-NMR (500 MHz, DMSO-d₆): δ 11.36 (s, 1H, NH), 8.22; 8.14 (2s, 1H, imidazothiazole C₅-H), 7.59-7.53 (m, 2H, 4-Brphenyl C_{2,6}-H), 7.45-7.42 (m, 2H, 4-Brphenyl C_{3,5}-H), 7.31-

7.14 (m, 2H, phenyl), 7.03 (s, 1H, imidazothiazole C₂-H), 6.92-6.87 (m, 2H, phenyl), 4.54; 4.50 (2q, 1H, $J=7.32$ Hz, SCH), 4.16-4.01 (m, 2H, CH₂CO), 1.58; 1.53 (2d, 3H, $J=7.32$ Hz, CH₃). Anal. Calcd. for C₂₃H₁₇BrFN₅O₃S₂: C, 49.47; H, 3.07; N, 12.54. Found: C, 49.68; H, 3.07; N, 12.51.

3-(4-Methoxyphenyl)-2-[[[(6-(4-bromophenyl)imidazo[2,1-b]thiazol-3-yl)acetyl]hydrazono]-5-methyl-4-thiazolidinone (4j)

Yield: 64%; m.p. 159-161°C; IR (KBr, cm⁻¹): 3163 (N-H), 1732 (ring C=O), 1672 (C=O); ¹H-NMR (500 MHz, DMSO-d₆): δ 11.34; 10.58 (2s, 1H, NH), 8.22; 8.12 (2s, 1H, imidazothiazole C₅-H), 7.77-7.71 (m, 2H, 4-Brphenyl C_{2,6}-H), 7.59-7.53 (m, 2H, 4-Brphenyl C_{3,5}-H), 7.42-6.80 (m, 5H, phenyl and imidazothiazole C₂-H), 4.51; 4.48 (2q, 1H, $J=7.32$ Hz, SCH), 3.83, 3.78 (2s, 2H, CH₂CO), 3.76 (s, 3H, OCH₃), 1.62; 1.53 (2d, 3H, $J=6.84$; 7.32 Hz, CH₃). ¹³C-NMR (APT) (500 MHz, DMSO-d₆): δ 175.00; 172.58 (thiazolidinone C=O), 166.44 (C=O), 159.84 (phenyl C₄), 151.40; 151.09 (C=N), 149.55 (imidazothiazole C_{7a}), 145.44 (imidazothiazole C₆), 140.98 (phenyl C₁), 134.20 (4-Brphenyl C₁), 132.30 (4-Brphenyl C_{3,5}), 127.29 (4-Brphenyl C_{2,6}), 126.28 (imidazothiazole C₃), 122.60 (phenyl C_{2,6}), 120.40 (4-Brphenyl C₄), 115.32 (phenyl C_{3,5}), 111.86 (imidazothiazole C₂), 109.60 (imidazothiazole C₅), 56.09 (OCH₃), 43.10; 40.49 (thiazolidinone C₅), 33.77 (CH₂), 19.90; 19.76 (thiazolidinone 5-CH₃). Anal. Calcd. for C₂₄H₂₀BrN₅O₃S₂: C, 49.60; H, 3.66; N, 12.23. Found: C, 49.17; H, 3.40; N, 12.54.

Biological methods

Isolation of aldose reductase enzyme

Kidneys obtained from Wistar albino rats were thawed on ice and homogenized with 3 volumes of distilled water. The homogenate were centrifuged at 10,000 × g for 20 min. Saturated ammonium sulfate was added to the supernatant for 40% saturation. The thick suspension was stirred for 15 min and then centrifuged at 10,000 × g for 20 min. The inert protein left in the supernatant was removed by increasing the ammonium sulfate concentration to 50% saturation followed by centrifuging the mixture at 10,000 × g for 20 min. The AR enzyme was precipitated from the 50% saturated solution by adding powdered ammonium sulfate to 75% saturation and was recovered by centrifugation at 10,000 × g for 20 min.⁴⁹ Protein concentration was measured as described by Bradford⁵⁰ using bovine serum albumin as a standard. The protein concentration was 5.13±0.09 mg/mL.

Determination of aldose reductase activity

AR activity of the freshly prepared supernatant was assayed spectrophotometrically by determining the decrease in NADPH concentration at 340 nm by a UV-1700 Visible spectrophotometer. DL-glyceraldehyde was used as a substrate. The enzyme was dissolved in 10 mL of 0.05 M NaCl solution. Then 25 µL of enzyme was added to the incubation medium, which contained 175 µL of phosphate buffer (0.067 M, pH: 6.2), 25 µL of NADPH (2×10⁻⁵ M final concentration), and 25 µL of inhibitor compound (10⁻⁴ M stock solution). The reaction was started by adding 25 µL of DL-glyceraldehyde (5×10⁻⁵ M final concentration) to the incubation medium and the decrease in NADPH concentration was recorded at 340 nm for 10 min at

37°C. Readings were taken at intervals in the periods when the changes in absorbance were linear.⁴⁹

The AR activity was calculated as,

$$\text{Activity} \left(\frac{\mu}{\text{mL}} \right) = \frac{(\Delta A \text{ Enzyme/min} - \Delta A \text{ Control/min})}{(6.22 \times \text{Volume of enzyme}) \cdot (\text{Total Volume})}$$

where 6.22 is the micromolar extinction coefficient of NADPH at 340 nm,

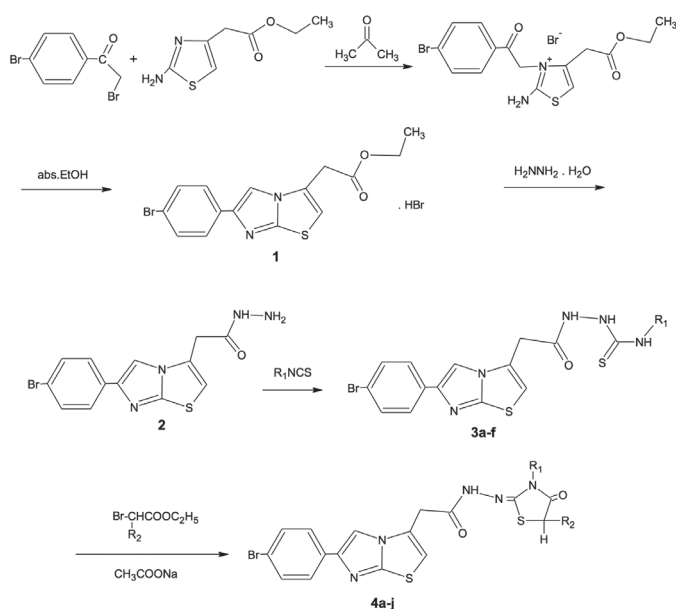
$$\text{Specific activity (U/mg protein)} = \frac{\text{Activity (U/mL)}}{\text{Protein Cont. (mg/mL)}}$$

The ARI activity of each sample was calculated using the formula.

$$\% \text{ Inhibition} = \left[1 - \frac{\Delta A \text{ Sample/min} - \Delta A \text{ Blank/min}}{\Delta A \text{ Control/min} - \Delta A \text{ Blank/min}} \right] \times 100$$

RESULTS AND DISCUSSION

The target compounds were prepared from 2-[6-(4-bromophenyl)imidazo[2,1-*b*]thiazole-3-yl]acetohydrazide (**2**)⁵¹ by a two-step synthesis as shown in Scheme 1. By heating ethyl (6-(4-bromophenyl)imidazo[2,1-*b*]thiazol-3-yl)acetate hydrobromide⁵² and hydrazine hydrate in ethanol, 2-[6-(4-bromophenyl)imidazo[2,1-*b*]thiazole-3-yl]acetohydrazide was obtained. Hydrazide and cycloalkyl/aralkyl/aryl isothiocyanates were heated in ethanol to yield 2-[[6-(4-bromophenyl)imidazo[2,1-*b*]thiazol-3-yl]acetyl]-*N*-cycloalkyl/aralkyl/aryl hydrazinecarbothioamides (**3a-f**). **3a-f** were then reacted with ethyl α -bromoacetate/ethyl 2-bromopropionate in the presence of anhydrous sodium



Scheme 1. Synthesis of title compounds **3a-f** and **4a-j**

acetate in absolute ethanol to yield 3-cycloalkyl/aralkyl/aryl-2-[[6-(4-bromophenyl)imidazo[2,1-*b*]thiazol-3-yl]acetyl]hydrazono]-5-nonsubstituted/methyl-4-thiazolidinones (**4a-j**).

The IR spectra of **3a-f** displayed bands at about 3296-3118 and 1674-1645 cm^{-1} associated with the N-H and C=O functions. Absorption bands at 1236-1163 cm^{-1} , which were attributed to the C=S stretching vibrations, were observed in the IR spectra of compounds **3a-f**. The three $^1\text{H-NMR}$ resonances located in the region of 12.55-7.66 ppm were assigned to the NH protons of the hydrazinecarbothioamides and supported the structures of **3a-f**.⁵³

New C=O bands (1757-1712 cm^{-1}) in the IR spectra of 4-thiazolidinones (**4a-j**) provided confirmatory evidence for ring closure.⁵⁴ $^1\text{H-NMR}$ and $^{13}\text{C-NMR}$ data were also in agreement with the formation of a 4-thiazolidinone ring. NH signals of **4b-d** and **4f-j** appeared at δ 11.52-10.54 ppm. In the $^1\text{H-NMR}$ spectra of compounds **4f-j**, CH-CH₃ protons appeared as a double quartet (1H) at δ 4.54-4.33 and δ 4.50-4.27 ppm and CH-CH₃ protons appeared as a double doublet (3H) at δ 1.63-1.44 and δ 1.56-1.36 ppm, indicating the presence of two isomers in unequal proportions in DMSO-*d*₆. This may be explained on the basis of the difference in the relative stability of the *E* and *Z* isomers formed due to the rotational restriction about the exocyclic N=C bond at position 2 of the 4-thiazolidinone ring.⁵⁴ In the $^{13}\text{C-NMR}$ (APT) spectra of **3f**, **4e**, and **4j** chosen as prototypes, all the carbons resonated in the expected regions.⁵⁵ For example, the protons resonated at δ 30.75, δ 152.44, and δ 169.23 ppm in the $^{13}\text{C-NMR}$ (APT) spectrum of the compound 3-(4-methoxyphenyl)-2-[[6-(4-bromophenyl)imidazo[2,1-*b*]thiazol-3-yl]acetyl]hydrazono]-4-thiazolidinone (**4e**) assigned for S-CH₂, C=N, and C=O moieties, confirming the carbon skeleton of the 4-thiazolidinone ring. Furthermore, $^{13}\text{C-NMR}$ resonances of the S-CH, C=N, and C=O carbons of the compound bearing 5-methyl substituted 4-thiazolidinone (**4j**) were observed at δ 43.10; 40.49, δ 151.40; 151.09 and δ 175.00; 172.58 ppm, respectively. The protons of the imidazo[2,1-*b*]thiazole nucleus and the other protons resonated in the expected regions.⁵⁵

The *in vitro* ARI activity of the synthesized compounds is listed in Table 1. The enzyme activity was assayed by spectrophotometrically monitoring the NADPH oxidation that accompanies the reduction of DL-glyceraldehyde, which is used as substrate. The inhibition study was performed merely by using a 10⁻⁴ M concentration of each drug. Depending upon the results the best ARI effect was found at the rate of 25.41% in compound **3d**. Among these inhibitors, in compound **3c**, which is the phenethyl substituted compound, 14.03% inhibition was observed, while in compounds **3e** and **3f**, which are 4-fluorophenyl and 4-methoxyphenyl substituted compounds, 21.31% and 13.73% inhibition were observed, respectively (Table 1). Compound **4g**, derived from compound **4b** as a result of methylation of the nitrogen atom on the thiazolidinone ring, showed 8.22% inhibition, while compound **4h**, obtained from compound **4c** by methylation of the nitrogen atom on the thiazolidinone ring, showed 5.93% inhibition (Table 1). Compounds **4i** and **4j**, obtained by methylation of compounds **4d** and **4e**, showed 9.31% and 1.42% inhibition, respectively. According to these results, 5-nonsubstituted thiazolidinone derivatives (**4a-e**) did not show inhibition but 5-methyl

substituted thiazolidinone derivatives (**4g-j**) showed significant inhibition in the range 1.42–9.31%. A positive influence was exerted by 5-methyl substitution at the thiazolidinone ring on activity. The most efficient compounds were hydrazinecarbothioamide derivatives (**3c-f**) with 25.41–13.73% (Table 1).

Table 1. Aldose reductase inhibition by compounds 3a-f and 4a-j*

Compounds	R ₁	R ₂	Inhibition ± SD (%)
3a	C ₆ H ₁₁	-	0.00±0.00
3b	CH ₂ -C ₆ H ₅	-	0.00±0.00
3c	CH ₂ -CH ₂ -C ₆ H ₅	-	14.03±1.07
3d	CO-C ₆ H ₅	-	25.41±0.12
3e	4-FC ₆ H ₄	-	21.31±1.07
3f	4-CH ₃ OC ₆ H ₄	-	13.73±0.49
4a	CH ₂ -C ₆ H ₅	H	0.00±0.00
4b	CH ₂ -CH ₂ -C ₆ H ₅	H	0.00±0.00
4c	CO-C ₆ H ₅	H	n.t.
4d	4-FC ₆ H ₄	H	0.00±0.00
4e	4-CH ₃ OC ₆ H ₄	H	0.00±0.00
4f	CH ₂ -C ₆ H ₅	CH ₃	0.00±0.00
4g	CH ₂ -CH ₂ -C ₆ H ₅	CH ₃	8.22±1.55
4h	CO-C ₆ H ₅	CH ₃	5.93±2.05
4i	4-FC ₆ H ₄	CH ₃	9.31±1.90
4j	4-CH ₃ OC ₆ H ₄	CH ₃	1.42±1.79

SD: Standard deviation, n.t.: Not tested, *Values represent the mean ± SD of three individual experiments

CONCLUSION

ARIs are one of quite a few types of drugs that have shown prevention of diabetic complications. It is still a challenge to develop a drug candidate molecule. We report the synthesis and ARI activity effects of hydrazinecarbothioamides (**3a-f**) and 4-thiazolidinones (**4a-j**) bearing an imidazo[2,1-*b*]thiazole moiety. On the basis of our preliminary ARI screening results on imidazo[2,1-*b*]thiazole derivatives, we embarked on the synthesis of more derivatives to discover more active molecules.

ACKNOWLEDGEMENTS

This work was supported by İstanbul University Scientific Research Project (Project Numbers: 40810, 52814 and 52534).

Conflict of Interest: No conflict of interest was declared by the authors.

REFERENCES

1. World Health Organization (WHO). WHO, Global report on diabetes, 2016.

- Forbes JM, Cooper ME. Mechanism of diabetic complications. *Physiol Rev.* 2013;93:137-188.
- Brownlee, M. The pathobiology of diabetic complications: a unifying mechanism. *Diabetes.* 2005;54:1615-1625.
- El-Kabbani O, Ruiz F, Darmanin C, Chung RP. Aldose reductase structures: implications for mechanism and inhibition. *Cell Mol Life Sci.* 2004;61:750-762.
- Hers HG. The mécanism of the transformation de glucose in fructose in the seminal vesicles. *Biochim Biophys Acta.* 1956;22:202-203.
- Srivastava SK, Ramana KV, Bhatnagar A. Role of aldose reductase and oxidative damage in diabetes and the consequent potential for therapeutic options. *Endocr Rev.* 2005;26:380-392.
- Alexiou P, Pegklidou K, Chatzopoulou M, Nicolaou I, Demopoulos VJ. Aldose reductase enzyme and its implication to major health problems of the 21(st) century. *Curr Med Chem.* 2009;16:734-752.
- Frank RN. Diabetic retinopathy. *N Engl J Med.* 2004;350:48-58.
- Sheetz MJ, King GL. Molecular understanding of hyperglycemia's adverse effects for diabetic complications. *JAMA.* 2002;288:2579-2588.
- Brownlee M. Biochemistry and molecular cell biology of diabetic complications. *Nature.* 2001;414:813-820.
- Yabe-Nishimura C. Aldose reductase in glucose toxicity: a potential target for the prevention of diabetic complications. *Pharmacol Rev.* 1998;50:21-33.
- Obrosova IG, Minchenko AG, Vasupuram R, White L, Abatan OI, Kumagai AK, Frank RN, Stevens MJ. Aldose reductase inhibitor fidarestat prevents retinal oxidative stress and vascular endothelial growth factor overexpression in streptozotocin-diabetic rats. *Diabetes.* 2003;52:864-871.
- Yan SF, Ramasamy R, Naka Y, Schmidt AM. Glycation, inflammation, and RAGE: a scaffold for the macrovascular complications of diabetes and beyond. *Circ Res.* 2003;93:1159-1169.
- Del-Corso A, Balestri F, Di Bugno E, Moschini R, Cappiello M, Sartini S, La-Motta C, Da-Settimo F, Mura U. A New Approach to Control the Enigmatic Activity of Aldose Reductase. *PLoS One.* 2013;8:74076.
- Kumar PA, Reddy GB. Focus on molecules: aldose reductase. *Exp Eye Res.* 2007;85:739-740.
- Nolan JJ, Ludvik B, Beerdsen P, Joyce M, Olefsky J. Improvement in glucose tolerance and insulin resistance in obese subjects treated with troglitazone. *N Engl J Med.* 1994;331:1188-1193.
- Suter SL, Nolan JJ, Wallace P, Gumbiner B, Olefsky JM. Metabolic effects of new oral hypoglycemic agent CS-045 in NIDDM subjects. *Diabetes Care.* 1992;15:193-203.
- Imran M, Ilyas B, Deepanjali and Khan SA. Recent thiazolidinones as antidiabetics. *Journal of Scientific and Industrial Research.* 2007;66:99-109.
- Arakawa K, Ishihara T, Aoto M, Inamasu M, Saito A, Ikezawa K. Actions of novel antidiabetic thiazolidinedione, T-174, in animal models of non-insulin-dependent diabetes mellitus (NIDDM) and in cultured muscle cells. *Br J Pharmacol.* 1998;125:429-436.
- Cantello BC, Cawthorne MA, Cottam GP, Duff PT, Haigh D, Hindley RM, Lister CA, Smith SA, Thurlby PL. [[omega-(Heterocyclylamino)alkoxy]benzyl]-2,4-thiazolidinediones as potent antihyperglycemic agents. *J Med Chem.* 1994;37:3977-3985.
- Zimmet P. Addressing the insulin resistance syndrome a role for the thiazolidinediones. *Trends Cardiovasc Med.* 2002;12:354-362.
- Lebovitz HE. Rationale for and role of thiazolidinediones in type 2 diabetes mellitus. *Am J Cardiol.* 2002;90:34-41.
- Bhosle MR, Mali JR, Pal S, Srivastava AK, Mane RA. Synthesis and antihyperglycemic evaluation of new 2-hydrazolyl-4-thiazolidinone-5-

- carboxylic acids having pyrazolyl pharmacophores. *Bioorg Med Chem Lett*. 2014;24:2651-2654.
24. Maccari R, Del Corso AD, Giglio M, Moschini R, Mura U, Ottanà R. *In vitro* evaluation of 5-arylidene-2-thioxo-4-thiazolidinones active as aldose reductase inhibitors. *Bioorg Med Chem Lett*. 2011;21:200-203.
 25. Ottanà R, Maccari R, Giglio M, Del Corso A, Cappiello M, Mura U, Cosconati S, Marinelli L, Novellino E, Sartini S, La Motta C, Da Settimo F. Identification of 5-arylidene-4-thiazolidinone derivatives endowed with dual activity as aldose reductase inhibitors and antioxidant agents for the treatment of diabetic complications. *Eur J Med Chem*. 2011;46:2797-2806.
 26. Calderone V, Rapposelli S, Martelli A, Digiacomo M, Testai L, Torri S, Marchetti P, Breschi MC, Balsamo A. NO-glibenclamide derivatives: Prototypes of a new class of nitric oxide-releasing anti-diabetic drugs. *Bioorg Med Chem*. 2009;17:5426-5432.
 27. Jackson JR, Patrick DR, Dar MM, Huang PS. Targeted anti-mitotic therapies: can we improve on tubulin agents? *Nat Rev Cancer*. 2007;7:107-117.
 28. Jiang N, Wang X, Yang Y, Dai W. Advances in mitotic inhibitors for cancer treatment. *Mini Rev Med Chem*. 2006;6:885-895.
 29. Schmidt M, Bastians H. Mitotic drug targets and the development of novel anti-mitotic anticancer drugs. *Drug Resist Updat*. 2007;10:162-181.
 30. Balzarini J, Orzeszko B, Maurin JK, Orzeszko A. Synthesis and anti-HIV studies of 2-adamantyl-substituted thiazolidin-4-ones. *Eur J Med Chem*. 2007;42:993-1003.
 31. Liesen AP, de Aquino TM, Carvalho CS, Lima VT, Araujo JM, de Lima JG, de Faria AR, de Melo EJ, Alves AJ, Alves EW, Alves AQ, Góes AJ. Synthesis and evaluation of anti-Toxoplasma gondii and antimicrobial activities of thiosemicarbazides, 4-thiazolidinones and 1,3,4-thiadiazoles. *Eur J Med Chem*. 2010;45:3685-3691.
 32. Omar K, Geronikaki A, Zoumpoulakis P, Camoutsis C, Sokovic M, Ciric A, Glamoclija J. Novel 4-thiazolidinone derivatives as potential antifungal and antibacterial drugs. *Bioorg Med Chem*. 2010;18:426-432.
 33. Küçükgülzel ŞG, Oruç EE, Rollas S, Sahin F, Ozbek A. Synthesis, characterisation and biological activity of novel 4-thiazolidinones, 1,3,4-oxadiazoles and some related compounds. *Eur J Med Chem*. 2002;37:197-206.
 34. Kumar A, Rajput CS, Bhati SK. Synthesis of 3-[4'-(p-chlorophenyl)-thiazol-2'-yl]-2-[(substituted azetidinone/thiazolidinone)-aminomethyl]-6-bromoquinazolin-4-ones as anti-inflammatory agent. *Bioorg Med Chem*. 2007;15:3089-3096.
 35. Vu CB, Bemis JE, Disch JS, Ng PY, Nunes JJ, Milne JC, Carney DP, Lynch AV, Smith JJ, Lavu S, Lambert PD, Gagne DJ, Jirousek MR, Schenk S, Olefsky JM, Perni RB. Discovery of imidazo[1,2-*b*]thiazole derivatives as novel SIRT1 activators. *J Med Chem*. 2009;52:1275-1283.
 36. Al-Abdullah ES, Al-Tuwaijri HM, Hassan HM, Al-Alshaikh MA, Habib EE, El-Emam AA. Synthesis, antimicrobial and hypoglycemic activities of novel *N*-(1-adamantyl)carbothioamide derivatives. *Molecules*. 2015;20:8125-8143.
 37. Daş-Evcimen N, Sarıkaya M, Gürkan-Alp AS, Bozdağ-Dündar O. Aldose Reductase Inhibitory Potential of Several Thiazolyl-thiazolidine-2,4-diones. *Lett Drug Des Discov*. 2013;10:415-419.
 38. Daş-Evcimen N, Sarıkaya M, Gürkök G, Süzen S. Evaluation of rat kidney aldose reductase inhibitory activity of some *N*-acetyl dehydroalanine derivatives. *Med Chem Res*. 2011;20:453-460.
 39. Bozdağ-Dündar O, Evranos B, Daş-Evcimen N, Sarıkaya M, Ertan R. Synthesis and aldose reductase inhibitory activity of some new chromonyl-2,4-thiazolidinediones. *Eur J Med Chem*. 2008;43:2412-2417.
 40. Bozdağ-Dündar O, Verspohl EJ, Daş-Evcimen N, Kaup RM, Bauer K, Sarıkaya M, Evranos B, Ertan R. Synthesis and biological activity of some new flavonyl-2,4-thiazolidinediones. *Bioorg Med Chem*. 2008;16:6747-6751.
 41. Süzen S, Daş-Evcimen N, Varol P, Sarıkaya M. Preliminary evaluation of rat kidney aldose reductase inhibitory activity of 2-phenylindole derivatives: affiliation to antioxidant activity. *Med Chem Res*. 2007;16:112-118.
 42. Şüküroğlu M, Çalışkan-Ergün B, Daş-Evcimen N, Sarıkaya M, Banoğlu E, Süzen S. Screening and evaluation of rat kidney aldose reductase inhibitory activity of some pyridazine derivatives. *Med Chem Res*. 2007;15:443-451.
 43. Bozdağ-Dündar O, Daş-Evcimen N, Ceylan-Ünlüsoy M, Ertan R, Sarıkaya M. Some new thiazolyl thiazolidinedione derivatives as aldose reductase inhibitors. *Med Chem Res*. 2007;16:39-47.
 44. Cihan-Üstündağ G, Gürsoy E, Naesens L, Ulusoy Güzeldemirci N, Çapan G. Synthesis and antiviral properties of novel indole-based thiosemicarbazides and 4-thiazolidinones. *Bioorg Med Chem*. 2016;24:240-246.
 45. Ulusoy Güzeldemirci N, İlhan E, Küçükbasmacı O, Satana D. Synthesis and antimicrobial evaluation of new 3-alkyl/aryl-2-[(alpha,alpha-diphenyl-alpha-hydroxy)acetyl]hydrazono]-5-methyl-4-thiazolidinones. *Arch Pharm Res*. 2010;33:17-24.
 46. Çapan G, Ulusoy N, Ergenç N, Kiraz M. New 6-phenylimidazo[2,1-*b*]thiazole derivatives: Synthesis and antifungal activity. *Monatsh Chem*. 1999;130:1399-1407.
 47. Ulusoy N, Ergenç N, Ekinci AC, Özer H. Synthesis and anticonvulsant activity of some new arylidenehydrazides and 4-thiazolidinones. *Monatsh Chem*. 1996;127:1197-1202.
 48. Çapan G, Ulusoy N, Ergenç N, Ekinci AC, Vidin A. Synthesis and anticonvulsant activity of new 3-[(2-furyl)carbonyl]amino-4-thiazolidinone and 2-[(2-furyl)carbonyl]hydrazono-4-thiazoline derivatives. *Farmaco*. 1996;51:729-732.
 49. Cerelli MJ, Curtis DL, Dun JP, Nelson PH, Peak TM, Waterbury LD. Antiinflammatory and aldose reductase inhibitory activity of some tricyclic arylacetic acids. *J Med Chem*. 1986;29:2347-2351.
 50. Bradford MM. A rapid and sensitive method for the quantitation of microgram quantities of protein utilizing the principle of protein-dye binding. *Anal Biochem*. 1976;72:248-254.
 51. Kühmstedt H, Kottke K, Knoke D, Robert JF, Panouse JJ. Synthesis of amides and heterocyclic acylhydrazides with potential immunomodulator properties. *Ann Pharm Fr*. 1983;40:425-429.
 52. Robert JF, Xicluna A, Panouse JJ. Advances in heterocyclic chemistry. *Eur J Med Chem Chim Ther*. 1975;10:59-64.
 53. Barbuceanu SF, Ilies DC, Saramet G, Uivarosi V, Draghici C, Radulescu V. Synthesis and antioxidant activity evaluation of new compounds from hydrazinecarbothioamide and 1,2,4-Triazole class containing diarylsulfone and 2,4-difluorophenyl moieties. *Int J Mol Sci*. 2014;15:10908-10925.
 54. Tatar E, Küçükgülzel ŞG, De Clercq E, Şahin F, Güllüce M. Synthesis, characterization and screening of antimicrobial, antituberculosis, antiviral and anticancer activity of novel 1,3-thiazolidine-4-ones derived from 1-[2-(benzoylamino)-4-(methylthio)butyryl]-4-alkyl/ arylalkyl thiosemicarbazides. *ARKIVOC*. 2008;14:191-210.
 55. Gürsoy E, Ulusoy Güzeldemirci N. Synthesis and primary cytotoxicity evaluation of new imidazo[2,1-*b*]thiazole derivatives, *Eur J Med Chem*. 2007;42:320-326.



A Validated Reverse Phase-Ultra-Performance Liquid Chromatography Method for the Determination of Gemifloxacin Mesylate in Bulk and its Pharmaceutical Preparation

Gemifloksasin Mesilatın Bulk ve Farmasötik Preparatından Tayini için Valide Edilmiş Ters Faz-Ultra-Performans Sıvı Kromatografisi Metodu

Hebatallah A. WAGDY^{1,2*}, Mohamed TAREK^{1,2}, Ahmed AMER², Menna GAMAL², Mohey ELMAZAR^{2,3}

¹The British University in Egypt, Faculty of Pharmacy, Department of Pharmaceutical Analytical Chemistry, Cairo, Egypt

²The British University in Egypt, Faculty of Pharmacy, The Center for Drug Research and Development, Cairo, Egypt

³The British University in Egypt, Faculty of Pharmacy, Department of Pharmacology and Toxicology, Cairo, Egypt

ABSTRACT

Objectives: Gemifloxacin Mesylate is a fourth generation fluoroquinolone antibacterial agent. A simple, accurate, and precise reversed phase (RP)-ultra performance liquid chromatography (UPLC) method was developed and validated for short time analysis of Gemifloxacin Mesylate in its bulk and pharmaceutical preparation.

Materials and Methods: The optimum separation was achieved at 0.5±0.03 min using an Acclaim™ RSLC 120 C18 column 2.2 µm (2.1×100 mm) at 30°C by isocratic mobile phase at pH 3.0 composed of acetonitrile:phosphate buffer (25 mM) in a ratio of 75:25 (v/v). The column effluents were monitored at 276 nm using a photodiode array detector at a flow rate of 0.5 mL/min. The method was validated according to International Conference on Harmonization guidelines.

Results: The linearity of the calibration curve ranged from 0.5 µg/mL to 10 µg/mL and the square of the regression coefficient (r^2) was 0.9991. The % relative standard deviation (RSD) of inter-day precision ranged from 0.081% to 1.233%, while for intra-day it ranged from 0.364% to 1.018%. The method was accurate with % recovery ranging from 93.71% to 100.29% and % RSD ranging from 1.054 to 2.722. The limit of detection and the limit of quantification were 0.066 and 0.2 µg/mL, respectively.

Conclusion: The validated method proved its ability for the assay of Gemifloxacin Mesylate in its bulk and dosage form in a short time (less than 1 min). To the best of our knowledge, this is the first RP-UPLC method for the determination of Gemifloxacin Mesylate.

Key words: Gemifloxacin Mesylate, ultra performance liquid chromatography, method validation

ÖZ

Amaç: Gemifloksasin Mesilat dördüncü jenerasyon fluorokinolon antibakteriyel ajandır. Basit, doğru ve hassas bir ters fazlı (RP)-ultra performanslı sıvı kromatografisi (UPLC) yöntemi, Gemifloksasin Mesilatın, bulk ve farmasötik preparatında kısa sürede analizi için geliştirilmiş ve valide edilmiştir.

Gereç ve Yöntemler: Optimum ayırma, Acclaim™ RSLC 120 C18, 2.2 µm (2.1×100 mm) kolonu kullanılarak, 30°C'de, 75:25 (h/h) asetonitril:fosfat tamponu (25 mM) içeren pH 3.0 izokratik hareketli faz ile 0.5±0.03 dk'da elde edildi. Kolon atığı 0.5 mL/dk'lık bir akış hızında fotodiyod detektörü kullanılarak 276 nm'de izlenmiştir. Yöntem Uluslararası Uyumlaştırma Konferansı kılavuzlarına göre valide edildi.

Bulgular: Kalibrasyon eğrisinin doğrusallığı 0.5 µg/mL ile 10 µg/mL arasındadır ve regresyon katsayısının karesi (r^2) 0.9991'dir. Gün içi kesinliğin % bağlı standart sapması (RSD) %0.081 ile %1.233 arasında değişirken, günler arası için %0.364 ile %1.018 arasında değişiyordu. Yöntem %93.71 ile %100.29 ve % RSD değeri 1.054 ile 2.722 arasında değişen % geri kazanım ile doğrudur. Saptama limiti ve tayin limiti sırasıyla 0.066 ve 0.2 µg/mL idi.

Sonuç: Valide edilmiş yöntem, Gemifloksasin Mesilatın bulk ve dozaj formundan tayininde kısa sürede (1 dakikadan az) tayinin olabileceğini kanıtlamıştır. Bildiğimiz kadarıyla, bu, Gemifloksasin Mesilatın belirlenmesi için ilk RP-UPLC yöntemidir.

Anahtar kelimeler: Gemifloksasin Mesilat, ultra performanslı sıvı kromatografisi, metod validasyonu

*Correspondence: E-mail: Hebatallah.wagdy@bue.edu.eg, Phone: +2 26890000 ORCID-ID: orcid.org/0000-0003-1975-7700

Received: 19.10.2017, Accepted: 30.11.2017

©Turk J Pharm Sci, Published by Galenos Publishing House.

INTRODUCTION

Gemifloxacin Mesylate (Figure 1) is a synthetic broad-spectrum antibacterial agent for oral administration. It is a member of the fourth generation fluoroquinolone antibiotics. Its mechanism of action is by inhibition of both topoisomerase IV and DNA gyrase, which are essential for bacterial cell replication. It is characterized by its broad spectrum of activity against both gram-positive and gram-negative bacteria. It is used in the treatment of respiratory tract and urinary tract infections.¹⁻⁴

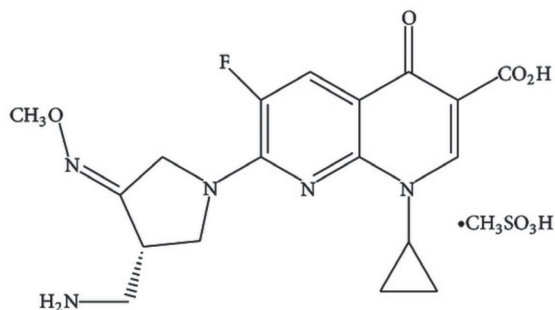


Figure 1. The chemical structure of Gemifloxacin Mesylate

The IUPAC name of Gemifloxacin Mesylate is 7-[(4Z)-3-(Aminomethyl)-4-methoxyiminopyrrolidin-1-yl]-1-cyclopropyl-6-fluoro-4-oxo-1,8 naphthyridine-3-carboxylic acid, methanesulfonic acid. Its molecular formula is $C_{18}H_{20}FN_5O_4 \cdot CH_4O_3S$; its molecular weight is 485.49 g/mol.

In the literature, different analytical methods have been reported for its determination, including spectrophotometry,⁵⁻⁷ spectrofluorimetry,⁸⁻¹⁰ high performance thin layer chromatography (HPTLC),¹¹⁻¹⁴ high performance layer chromatography (HPLC)-ultraviolet (UV),¹⁵⁻¹⁸ and liquid chromatography (LC)-mass spectrometry.^{19,20}

Ultra-performance liquid chromatography (UPLC), introduced in 2004, proved to be more efficient than HPLC in many aspects such as resolution, sensitivity, and consuming much smaller amounts of solvents.

The aim of the present research was the rapid and sensitive determination and quantification of Gemifloxacin Mesylate in its bulk and pharmaceutical preparation with lower consumption of solvents using reverse phase (RP)-UPLC-UV in addition to its validation with respect to International Conference on Harmonization (ICH) guidelines. To the best of our knowledge, this is the first RP-UPLC method for the determination of Gemifloxacin Mesylate.

MATERIALS AND METHODS

Instruments and software

The UPLC system employed was a Thermo Fisher UHPLC Dionex Ultimate 3000 (Germering, Germany). The pump was an ISO-3100SD, while the autosampler was a WPS 3000 SL, and the column thermostat was a TCC-3000 SD. The

detector was a diode array detector (3000 RS) (Germering, Germany). The software utilized for data acquisition was Chromeleon 6.8 (Germering, Germany). pH of the buffer was measured using a pH meter (Jenway pH-meter 3310, Dunmow, Essex, United Kingdom). Milli-Q water was produced in-house from an ultrapure water purification system (Thermo Scientific Barnstead Smart2Pure 3 UV, Hungary). The separation was carried out using an Acclaim™ RSLC 120 C18 column 2.2 μ m (2.1×100 mm), Thermo Fisher.

Chemicals and reagents

Acetonitrile (HPLC grade), monobasic potassium phosphate, and phosphoric acid (high grade) were purchased from Sigma-Aldrich, Germany. Gemifloxacin Mesylate standard was obtained from Sigma Pharmaceutical Company (Cairo, Egypt). Gemifloxacin Mesylate pharmaceutical preparations (Quinabiotic®, Utopia) were purchased from the Egyptian market.

Methods

Mobile phase preparation

The mobile phase was composed of acetonitrile and 25 mM phosphate buffer (pH 3.00) (75:25, v/v). The mobile phase was mixed and then degassed using an ultrasonicator.

The phosphate buffer was prepared by mixing monobasic potassium phosphate and phosphoric acid, and then the pH was measured by the pH meter and adjusted to 3.00.

Standard solution preparation and calibration curve plotting

The standard stock solution was prepared by dissolving 25 mg of Gemifloxacin Mesylate standard in 25 mL of deionized water, so that the final concentration was 1000 μ g/mL. After that, serial dilutions (0.5-10 μ g/mL) were accomplished to construct the calibration curve.

Sample preparation

Ten tablets of Quinabiotic® containing 320 mg of Gemifloxacin Mesylate equivalent to 320 mg of Gemifloxacin were accurately weighed and crushed into fine powder. A concentration of 1000 μ g/mL was prepared by taking an equivalent amount of 25 mg of Gemifloxacin Mesylate and dissolving it in 25 mL of deionized water. The solution was sonicated for 15 min and then filtered using a 0.22- μ m nylon syringe filter. After that a dilution equivalent to 1 μ g/mL was prepared and it was then injected into the UPLC system.

Chromatographic conditions

The mobile phase was a mixture of acetonitrile and phosphate buffer (75:25, v/v) at a flow rate 0.5 mL/min. The temperature of the column oven was adjusted to 30°C and the injection volume of the sample was 10 μ L. The photodiode array (PDA) detector was maintained at a wavelength of 276 nm.

Method validation

Validation was performed as stated in the ICH guidelines with reference to the following parameters: linearity, limit of

quantification and detection, precision (inter- and intra-day), and accuracy.²¹

Linearity is the ability of a method to get a response directly proportional to the sample concentration over a given range. The linearity of the analytical method was determined by preparing 7 serial dilutions ranging from 0.5 to 10 µg/mL. Each concentration was injected 3 times into the UPLC. After different peak areas were determined, the average peak area was obtained for each concentration. Hence, concentrations against the average peak area were plotted accordingly in a calibration curve. Using linear regression analysis, the regression equation was determined along with the correlation coefficient. Linearity was evaluated using the square of the regression coefficient (r^2).

For the limit of quantification (LOQ), it is equivalent to the concentration of the analyte in which S/N is equal to 10, while for the limit of detection (LOD), it is equivalent to the concentration of the analyte in which S/N is equal to 3.3.

Precision measures whether the method is able to generate reproducible results or not. The precision of the method was evaluated using intra-day (repeatability) and inter-day precision (intermediate precision). Intra-day precision was determined by injecting 4 different concentrations into the UPLC; each was injected three times on the same day. The average peak was obtained along with the standard deviation. The precision was evaluated with respect to % relative standard deviation (RSD). While inter-day precision was obtained by injecting four concentrations into the UPLC system, each concentration was injected 3 times on two consecutive days. The average peak between day one and day two was analyzed to calculate the standard deviation and, accordingly, % RSD was evaluated.

Accuracy is the closeness of the results obtained from a method to the true reference values. The accuracy of the method was determined by evaluating recovery studies on the pharmaceutical preparation. Three different solutions were prepared; each contained 1 µg/mL pharmaceutical preparation spiked with known concentrations of standard solution of 0.4 µg/mL, 0.8 µg/mL, and 1.2 µg/mL so that the final concentrations were 1.4 µg/mL, 1.8 µg/mL/mL, and 2.2 µg/mL, respectively. Each sample was injected three times on two consecutive days. Accuracy was evaluated by calculating percentage recovery and, accordingly, % RSD was determined.

The robustness of the method was assessed by the ability of the method to remain unaffected by small deliberate changes in the following parameters:²² wavelength, % acetonitrile, and pH of the buffer.

System suitability test

System suitability was tested by injecting a working solution of 1 µg/mL Gemifloxacin Mesylate under the optimum condition.

RESULTS AND DISCUSSION

Method development

In order to achieve the optimum condition, the analytical conditions, including temperature, mobile phase composition, wavelength, and flow rate, were optimized.

At the beginning, methanol was investigated as an organic solvent, instead of acetonitrile. Better peak shape and shorter retention time were achieved using acetonitrile.

Both the buffer strength and pH were also studied. Although a higher concentration of buffer gave a shorter retention time and better peak shape, it led to an increase in pump pressure; accordingly, 25 mM was selected as the optimum buffer strength. For pH, a value greater than 3.00 showed a broader peak and lower pH did not improve the peak shape. As a consequence, pH 3.00 was chosen as the optimum buffer pH. This could be explained by the fact that at pH 3.00 it was below the pKa of Gemifloxacin Mesylate ($pK_{a1}=5.53$, $pK_{a2}=9.53$).

While for the temperature, reaching T 30°C was enough to enhance the peak shape, higher temperature did not have a significant effect on the peak. For the flow rate, 0.5 mL/min was optimum to achieve a short analysis time without increasing the pump pressure.

The optimum wavelength for detecting Gemifloxacin Mesylate was 276 nm using the PDA detector as shown in the spectrum (Figure 2). The flow rate was set at 0.5 mL/min. The optimum temperature for analysis was 30°C and the pH for the phosphate buffer was 3.0. The mobile phase composition was acetonitrile: 25 mM phosphate buffer, pH 3.00 (75:25 v/v). Under this condition, the peak for Gemifloxacin Mesylate appeared at tR 0.5±0.03 min (Figure 3). To the best to our knowledge, this is the first UPLC-PDA method for the analysis of Gemifloxacin Mesylate reported in the literature. Accordingly, when compared to other HPLC-UV methods reported in the literature, it provided shorter analysis time and less consumption of solvents.

Next, the analytical method developed was evaluated and validated as per ICH guidelines.

Validation of the developed method

Linearity

The graphical representation calibration curve shows that the linearity ranged from 0.5 to 10 µg/mL. Using linear regression analysis, the slope, the intercept, and the regression coefficient

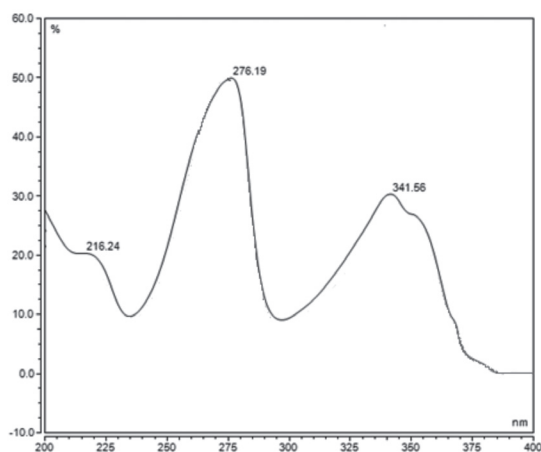


Figure 2. Ultraviolet spectrum of Gemifloxacin Mesylate

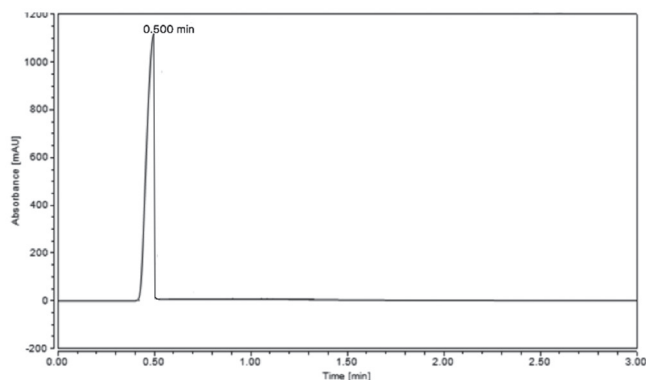


Figure 3. Chromatograms of 1 µg/mL Gemifloxacin Mesylate under the optimum condition, i.e., acetonitrile: 25 mM phosphate buffer, pH 3.00 (75:25; v/v), at a flow rate 0.5 mL/min and T 30°C

were determined from the regression equation $y = 396.69x - 6.8416$. The regression coefficient [R^2] was equal to 0.9991. The slope was 396.69 and the intercept was 6.8416.

The LOD was 0.066 µg/mL, while the LOQ was 0.2 µg/mL.

Precision

For the inter-day precision % RSD was determined and ranged from 0.0807% to 1.2326%, while for intra-day precision % RSD ranged from 0.1562% to 1.0176%.

The results of both inter- and intra-day precision are shown in Table 1.

Accuracy

Accuracy of the method was evaluated. % Recovery ranged from 93.71% to 100.29% while % RSD ranged from 1.054 to 2.721 as shown in Table 2.

Table 1. Inter-day and intra-day precision of Gemifloxacin Mesylate

Concentration (µg/mL)	Inter-day precision		Intra-day precision	
	Peak area*	% RSD	Peak area*	% RSD
1	76.458	1.233	75.791	0.156
2	145.734	0.653	145.061	1.018
4	230.634	0.368	230.035	0.364
8	306.400	0.081	306.575	0.653

RSD: Relative standard deviation, *Average of 3 times

Table 2. Accuracy of Gemifloxacin Mesylate

Theoretical concentration (µg/mL)	Actual concentration* (µg/mL)	% RSD	% Recovery*	% RSD
1.4	1.374	1.197	98.19	2.722
1.8	1.687	0.632	93.71	1.054
2.2	2.206	1.217	100.29	1.723

RSD: Relative standard deviation, *Average of 3 repetitions

Robustness

To evaluate the robustness of the method, minor changes were made to the parameters intentionally. Hence, the % RSD was calculated and the results were as follows: wavelength 276 ± 3 nm with % RSD 1.73%, the % acetonitrile $75 \pm 1\%$ with % RSD 2.35%, and pH of the buffer 3.00 ± 0.5 with % RSD 2.90%.

System suitability test

System suitability was tested to demonstrate the adequacy of the analysis system. In order to accomplish that, different parameters were verified. The column efficiency, which can be evaluated by the plate number, the asymmetric factor to evaluate the peak symmetry, and the reproducibility of the system were assessed by the % RSD of both the peak area and the retention time. The data are presented in Table 3.

Table 3. System suitability data of the suggested UPLC method

Parameters	Gemifloxacin Mesylate
Number of theoretical plates (N)	3300
Asymmetric factor (A_s)	1.05
Capacity factor	5.25
% RSD (retention time)*	0.35
% RSD (peak area)*	0.634

UPLC: Ultra-performance liquid chromatography, RSD: Relative standard deviation, *Average of 4 repetitions

Application on pharmaceutical preparation

To determine the suitability of the method for the determination of Gemifloxacin Mesylate in its pharmaceutical preparations, Quinabiotic® 320 mg was purchased from the local market. Next, 10 tablets were weighed and crushed. Hence an equivalent amount of 25 mg was dissolved in 25 mL of deionized water, followed by sonication and filtration. Then the filtrate was diluted with deionized water to have a concentration equivalent to 1 µg/mL. As presented in Figure 4, the tR of Gemifloxacin Mesylate was 0.500 min and tablet excipients did not interfere with the analysis. The % recovery was 99.496 with % RSD

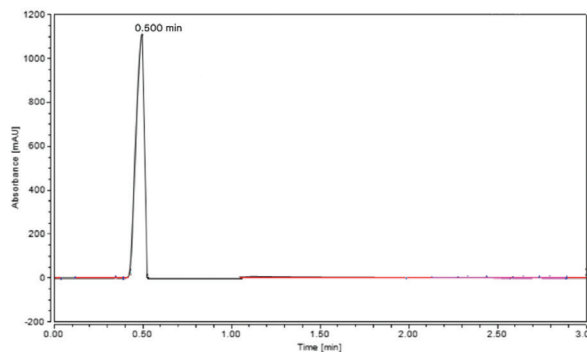


Figure 4. Chromatograms of 1 µg/mL Quinabiotic® under the optimum condition, i.e., acetonitrile: 25 mM phosphate buffer, pH 3.00 (75:25; v/v), at a flow rate 0.5 mL/min and T 30°C

1431. Accordingly, the method proved its ability to determine Gemifloxacin Mesylate in its pharmaceutical preparations.

Statistical analysis

To ensure the applicability of the newly suggested method, it was compared to a published reference method. It was investigated whether there are any significant differences between the two methods and to what extent this difference can affect the applicability of the new method rather than an already used one.

Comparing the obtained F- and t-values with the tabulated ones, it is clear that the obtained values were lower than the theoretical tabulated values, i.e., the methods suggested do not exhibit significant differences in comparison to those of the published methods, which reflects the accuracy and precision of the suggested UPLC method. The results are shown in Table 4.

Table 4. Statistical comparison between the proposed method and reference methods

	Proposed method	Reference method
Pure solution		
Mean \pm SD	100.06 \pm 0.76	99.38 \pm 0.51 ²³
n	7	6
Student's t-test (tabulated)	1.91 (2.18)	
F test (tabulated)	2.24 (4.95)	
Probability	<0.05	
Quinabiotic®		
Mean \pm SD	97.40 \pm 1.83	98.48 \pm 1.82 ¹¹
n	3	5
Student's t-test (tabulated)	0.81 (2.37)	
F test (tabulated)	1.01 (6.94)	
Probability	<0.05	

SD: Standard deviation

CONCLUSIONS

The newly developed RP-UPLC method for the short time analysis of Gemifloxacin Mesylate in its bulk and pharmaceutical preparation was rapid, simple, accurate, and precise. The method was validated as per ICH guidelines for linearity, accuracy, and precision. Linearity was determined at an acceptable range from 0.5 to 10 $\mu\text{g}/\text{mL}$. Finally, the method was accepted for the analytical evaluation of the drug in its pharmaceutical preparations with respect to the satisfactory results obtained and it showed a lower retention time in comparison to other HPLC methods reported in the literature.

Conflict of Interest: No conflict of interest was declared by the authors.

REFERENCES

1. Oh JI, Paek KS, Ahn MJ, Kim MY, Hong CY, Kim IC, Kwak JH. *In vitro* and

in vivo evaluations of LB20304, a new fluoronaphthyridone. *Antimicrob Agents Chemother.* 1996;40:1564-1568.

- Cormican MG, Jones RN. Antimicrobial activity and spectrum of LB20304, a novel fluoronaphthyridone. *Antimicrob Agents Chemother.* 1997;41:204-211.
- Hohl AF, Frei R, Pünter V, von Graevenitz A, Knapp C, Washington J, Johnson D, Jones RN. International multicenter investigation of LB20304, a new fluoronaphthyridone. *Clin microbiol infec.* 1998;4:280-284.
- Lomaestro BM. Gemifloxacin: A broad-spectrum oral quinolone for treatment of respiratory and urinary tract infections. *Formulary.* 2000;35:961-968.
- Tirupathi B, Venkateshwarlu G. Spectrophotometric determination of drugs using chloramine-T and rhodamine-B dye. *Int J Pharma Bio Sci.* 2015;6:218-226.
- Paim CS, Führ F, Miron DS, Steppe M, Schapoval EE. Highly Selective Colorimetric Method to Determine Gemifloxacin Mesylate in the Presence of a Synthetic Impurity. *J AOAC Inter.* 2014;97:94-98.
- Krishna MV, Sankar DG. Spectrophotometric determination of gemifloxacin mesylate in pharmaceutical formulations through ion-pair complex formation. *J Chem.* 2008;5:515-520.
- Al-Tamimi S, Al-Mohaimed AM, Alarfaj N, Aly F. Stability-indicating Spectrofluorimetric methods for determination of Gemifloxacin Mesylate in pharmaceutical dosage forms. *J Ind Chem Soc.* 2014;91:1247-1254.
- Moussa BA, Mahrouse MA, Hassan MA, Fawzy MG. Spectrofluorimetric determination of gemifloxacin mesylate and linezolid in pharmaceutical formulations: application of quinone-based fluorophores and enhanced native fluorescence. *Acta Pharm.* 2014;64:15-28.
- Kepekci Tekkeli SE, Önal A. Spectrofluorimetric methods for the determination of gemifloxacin in tablets and spiked plasma samples. *J fluoresc.* 2011;21:1001-1007.
- Mahmoud AM, Atia NN, El-Shabouri SR, El-Koussi WM. Development and Validation of Stability Indicating HPTLC Assay for Determination of Gemifloxacin Mesylate in Dosage Forms. *Am J Anal Chem.* 2015;6:85-97.
- El-Koussi WM, Atia NN, Mahmoud AM, El-Shabouri SR. HPTLC method for direct determination of gemifloxacin mesylate in human plasma. *J Chromatogr B Analyt Technol Biomed Life Sci.* 2014;967:98-101.
- Raja T, Atmakuri LO. Development and validation of HPTLC method for the simultaneous estimation of gemifloxacin mesylate and ambroxol hydrochloride in bulk and tablet dosage form. *Anal Chemi Lett.* 2012;2:152-158.
- Rote AR, Pingle SP. Reverse phase-HPLC and HPTLC methods for determination of gemifloxacin mesylate in human plasma. *J Chromatogr B Analyt Technol Biomed Life Sci* 2009;877:3719-3723.
- Baig MS, Dehghan MHG. Development and validation of in-vitro dissolution studies of Gemifloxacin Mesylate and Ambroxol Hydrochloride from its combined sustain release tablet dosage form with its combined sustain release tablet dosage form with respect to accelerated aging conditions by HPLC assay methods. *W J Pharm Pharm Sci.* 2015;4:1965-1981.
- Gumustas M, Ozkan SA. Simple, sensitive and reliable LC-DAD method of gemifloxacin determination in pharmaceutical dosage forms. *Turk J Pharm Sci.* 2012;9:161-170.
- Sultana N, Arayne MS, Shamim S, Akhtar M, Gul S. Validated method for the determination of Gemifloxacin in bulk, pharmaceutical formulations

- and human serum by RP-HPLC: *in vitro* applications. J Braz Chem Soci. 2011;22:987-992.
18. Mohammad Y, Kumar BP, Hussain A, Harish. Development and validation of RP-HPLC method for the estimation of gemifloxacin mesylate in bulk and pharmaceutical dosage forms. J Chem. 2010;7:1621-1627.
 19. Tammam MH. Photostability studies on gemifloxacin and lomefloxacin in bulk powder and dosage forms. Eur J Chem. 2014;5:73-80.
 20. Roy B, Das A, Bhaumik U, Sarkar AK, Bose A, Mukharjee J, Chakrabarty US, Das AK, Pal TK. Determination of gemifloxacin in different tissues of rat after oral dosing of gemifloxacin mesylate by LC-MS/MS and its application in drug tissue distribution study. J Pharm Biomed Anal. 2010;52:216-226.
 21. ICH Guideline Q2a (R1) Validation of analytical procedures: text and methodology. 2015: <https://www.fda.gov/Drugs/GuidanceComplianceRegulatoryInformation/Guidances/ucm265700.htm>
 22. Wagdy HA, Aboul-Enein HY. Analysis of Sitagliptin On Halogenated Reversed Phase Columns: A Comparative Study. J Pharm Anal. 2016;5:9-15.
 23. Al Mohaimeed AM, Al-Tamimi SA, Alarfaj NA, Aly FA. New coated wire sensors for potentiometric determination of gemifloxacin in pure form, pharmaceutical formulations and biological fluids. Int J Electrochem Sci. 2012;7:12518-12530.



Determination of Potential Drug–Drug Interactions Using Various Software Programs in a Community Pharmacy Setting

Serbest Eczanede Farklı Yazılım Programlarının Kullanılarak Olası İlaç-İlaç Etkileşimlerinin Saptanması

© Mesut SANCAR^{1*}, © Aksa KAŞIK¹, © Betül OKUYAN¹, © Sevda BATUHAN¹, © Fikret Vehbi İZZETTİN²

¹Marmara University, Faculty of Pharmacy, Department of Clinical Pharmacy, İstanbul, Turkey

²Bezmialem University, Faculty of Pharmacy, Department of Clinical Pharmacy, İstanbul, Turkey

ABSTRACT

Objectives: The aim of the present study was to compare various software programs in detecting potential drug–drug interactions in a community pharmacy setting.

Materials and Methods: Details of prescriptions were collected from 50 community pharmacies located in İstanbul in March and April 2015 (two days per week). From each pharmacy, the first 20 prescriptions that included more than one drug were collected to evaluate potential drug–drug interactions. The following software programs were utilized to detect potential drug–drug interactions: micromedexsolutions.com, medscape.com, and drugs.com. The number of potential interactions detected by the software programs was determined.

Results: At least one potential drug–drug interaction was detected in 39.2% of the 1000 prescriptions by one of the software programs. According to the rates of total drug–drug interactions gathered from various software programs, these programs gave the following results: medscape.com 33.3%, drugs.com 31.3%, and micromedexsolutions.com 21.2%.

Conclusion: After comparing different software programs, the potential drug–drug interactions found by the programs proved to be different. Therefore, we recommend that pharmacists confirm with a different program before making a decision when they detect clinically significant potential drug–drug interactions.

Key words: Drug–drug interactions, software programs, community pharmacy, pharmacist

ÖZ

Amaç: Çalışmada eczaneye gelen reçetelerdeki olası ilaç-ilaç etkileşimlerinin saptanması ve farklı yazılım programları kullanılarak belirlenen olası ilaç-ilaç etkileşim sonuçlarının karşılaştırılması amaçlanmıştır.

Gereç ve Yöntemler: Çalışma Mart ile Nisan 2015 (haftada iki gün) tarihleri arasında İstanbul’da yer alan 50 eczanede yürütülmüştür. Çalışmanın yürütüleceği eczanelerde en az 2 ilaç bulunan ardışık 20 reçetede olası ilaç-ilaç etkileşimleri incelenmiştir. Olası ilaç-ilaç etkileşimleri micromedexsolutions.com, medscape.com ve drugs.com programları kullanılarak karşılaştırılmıştır.

Bulgular: Çalışmamızda toplam 1000 elektronik reçete incelenmiş ve bu reçetelerin %39,2’sinde yazılım programların herhangi birine göre en az bir tane olası ilaç-ilaç etkileşimi tespit edilmiştir. Reçetelerde saptanan olası ilaç-ilaç etkileşimlerinin yazılımlar tarafından bulunma oranları, ‘micromedexsolutions.com’ için %21,2, ‘medscape.com’ için %33,3 ve ‘drugs.com’ için ise %31,3 olarak hesaplanmıştır.

Sonuç: Farklı yazılım programlarını karşılaştırdıktan sonra, yazılım programları tarafından bulunan potansiyel ilaç-ilaç etkileşimlerinin birbirlerinden farklı olduklarını kanıtlanmıştır. Bu nedenle, eczacıların, klinik olarak anlamlı ilaç-ilaç etkileşimi saptadıklarında, karar vermeden önce bu etkileşimleri farklı bir programla da teyit etmelerini önermekteyiz.

Anahtar kelimeler: İlaç-ilaç etkileşimleri, yazılım programları, serbest eczane, eczacı

*Correspondence: E-mail: sancarmesut@yahoo.com, Phone: +90 216 346 40 60 ORCID-ID: orcid.org/0000-0002-7445-3235

Received: 21.08.2017, Accepted: 30.11.2017

©Turk J Pharm Sci, Published by Galenos Publishing House.

INTRODUCTION

Drug–drug interactions (DDIs) are considered a drug-related problem that could result in severe consequences. Hospital admission, death, disability, organ failure, and congenital abnormalities can be caused by DDIs. Therefore, evaluation and determination of possible DDIs are essential.

It was determined that DDIs can result in risk according to results gathered from the reason for admission to emergency departments.¹ To eliminate the number of DDIs and their possible detriments, pharmacists should be aware of these possible interactions and must evaluate the clinical relevance of each. Pharmacists should be involved in optimizing medication treatment by preventing harmful DDIs and unsafe utilization of medication. However, pharmacists are exposed to countless warnings including many minor and moderate interactions while using software to detect possible DDIs. As a consequence, major DDIs might be ignored.²

The reliability of software programs commonly used to detect possible DDIs has been evaluated and the concordance rate between each has been investigated. The criterion for many DDIs has not been standardized for every software program. Therefore, some of the programs contained too much data. Hence, most of the time, it is difficult to distinguish clinically significant information.³

In one drug utilization review study retrospectively conducted with a high patient population, it was determined that the possible number of DDIs detected at baseline decreased 70.8% when more sophisticated filtration was applied and it was also observed that this number fell 80.6% after evaluation by a clinical pharmacist.⁴

Many studies highlighted a problem of inconsistency between these DDI software programs. These studies mostly examined DDI software programs that generally require subscription and paid membership, and in these studies researchers especially chose programs that they had institutional subscriptions to. Fewer evaluated some web sources that could be accessed freely.

Patient-oriented services including clinical pharmacy and pharmaceutical care have recently been developed in Turkey. In accordance with this development, it can be concluded that community pharmacists' skill to check possible DDIs is still progressing slowly.

Although there are many DDI checking programs in the literature and practical applications, Micromedex and Lexicomp are commonly used programs due to their providing strong and comprehensive evidence including onset, severity, scientific evidence, pharmacologic effects, mechanisms of action, and management of each DDI. In developing countries, Medscape Drug Interaction Checker and the Monthly Index of Medical Specialties Interaction Checker, which are accessible free of charge, are commonly used rather than Micromedex and Lexicomp.⁵

The aim of the present study was to compare Micromedex with two web-based programs freely accessible (medscape.com and drugs.com) to investigate whether one software program is sufficient to determine possible DDIs in the community pharmacy setting or not. The result of the present study will be important when establishing guidelines to determine DDIs in community pharmacies.

MATERIALS AND METHODS

Details of prescriptions were collected from 50 community pharmacies in İstanbul in March and April 2015 (two days per week). These pharmacies were chosen from among those where fifth-year pharmacy students went to complete their 'Pharmacy Practice' course. Oral and written consent was received from the pharmacist after he or she was given information regarding the aim and methods of the present study. Ethical approval was obtained from Marmara University, Institute of Health Science (Approval number: 26.01.2015-7).

Details of the first 20 prescriptions that included more than one drug were collected to evaluate potential DDIs from each pharmacy by students. If the prescription was for a patient under 18 years old, it was excluded from the study.

Patients' demographic information including age and sex were recorded. The prescriptions that included any drugs not covered by the software programs were excluded.

The following software programs were utilized to detect potential DDIs: micromedexsolutions.com, medscape.com, and drugs.com (Table 1). The possible DDIs were analyzed retrospectively. The interactions were reported as major or serious, moderate or significant, and minor or mild (Table 1).

Table 1. Characteristics of DDI software programs

Programs	Access/payment	Classification	Reference	Addition interactions
Micromedex	Required	0: None, 1: Minor, 2: Moderate, 3: Major, 4: Contraindicated	Yes, with quality of evidence	Yes, with alcohol, diseases, lab test, pregnancy, food
Medscape	Not required	None, Minor, Significant (monitor closely), Serious (use alternative), Contraindicated	No	No
Drugs.com	Not required, also with customer information	None, Minor, Moderate, Major	Yes	Yes, with food

Statistical analysis

Continuous variables were presented as mean ± standard deviation and ordinal and nominal data were shown as number (n) and percentage (%). The correlation between data was investigated using Spearman’s correlation test. The concordance between these online drug interaction programs according to the results of three severity levels of interaction was checked by evaluating each DDI using kappa analysis. The statistical analysis was done using SPSS for Windows 11.0. p<0.05 was defined as the level of statistical significance.

RESULTS

In each prescription, the mean number of medications was 3.01±1.19 (2-10). At least one potential DDI was detected in 39.2% of a total of 1000 prescriptions by using at least one software program. More than half (58.7%) of the prescriptions for which at least one potential DDI was detected were for female patients. Moreover, the mean of age of these patients was 54.63±17.20. The rates of total DDIs gathered from the various software programs were as follows: medscape.com 33.3%, drugs.com 31.3%, and micromedexsolutions.com 21.2%. The total numbers of DDIs detected by micromedexsolutions.com, medscape.com, and drugs.com were 389, 917, and 670, respectively. The rate of DDIs detected in prescriptions with all programs was 18%.

When considering the programs in two-pair comparisons, the concordance rate was high and kappa coefficients were of moderate level (Table 2).

The concordance rate of the three programs (which is defined as detecting the number of patients with or without DDI at the same time) was 78.9%, and this rate was lower than the concordance rates obtained in the two-pair comparison, which is shown in Table 2.

When considering two-pair correlations between the programs, Spearman’s r correlation values were 0.629, 0.711, and 0.688 (p<0.001), respectively. These results showed that the two-pair correlations were moderate.

To measure the severity rankings of the three DDI programs, the total number of DDIs without repetition (the number of DDIs

was considered as one if the same DDI was obtained for more than one patient or if the same DDI with different mechanisms was considered as more than one DDI) obtained in these three programs in 1000 patients was calculated. The total number of DDIs was calculated as 625 according to the above statement. The rate of these DDIs obtained in Micromedex 2.0® Software Drug Interactions, Medscape Drug Interaction Checker®, and drugs.com was 42.2%, 65.6%, and 74.1%, respectively. The severity ranking scored by three programs for these 625 DDIs was dissimilar (Table 3).

Table 3. Severity ranking of software programs according to 625 different DDIs

Programs	Severity ranking n (%)				
	0 (Not found)	1 (Minor)	2 (Moderate or significant)	3 (Major or serious)	4 (Contraindicated)
Micromedex	361 (57.8)	10 (1.6)	162 (25.9)	89 (14.2)	3 (0.5)
Medscape	215 (34.4)	74 (11.8)	302 (48.3)	32 (5.1)	2 (0.3)
Drugs.com	162 (25.9)	62 (9.9)	360 (57.6)	41 (6.6)	*

DDIs: Drug–drug interactions, *The severity classification of drugs.com did not contain 4, which was defined as contraindicated

When evaluating the two-pair concordances in programs according to the severity ranking none of them was higher than 50% (Table 4). It was determined that 82 (13.1%) of them were scored with the same severity level in all three programs among a total of 625 DDIs. Most of them (68) among these 82 DDIs were ranked as moderate DDIs. The major DDIs classified as major by Micromedex numbered 89 and only 12 of them were defined as major DDIs with the other two DDI programs used in the present study.

When considering two-pair correlations between the three programs according to the severity ranking, Spearman’s r correlation values were 0.222 (p<0.001), 0.366 (p<0.001), and 0.061 (p=0.125), respectively. These results showed that the two-pair correlations were moderate.

Table 2. Concordance rate obtained with two-pair comparison according to the number of DDIs gained in prescriptions in the three programs

Program	Concordance (%)	Kappa coefficient	Standard error	p
Micromedex - Medscape	83.9	0.601	0.027	<0.001
Micromedex - Drugs.com	87.6	0.686	0.025	<0.001
Medscape - Drugs.com	86.3	0.688	0.025	<0.001

DDIs: Drug–drug interactions

Table 4. Concordance rate obtained with two-pair comparisons according to the rate of severity ranking obtained among 625 DDIs in the three programs

Program	Concordance (%)	Kappa coefficient	Standard error	p
Micromedex - Medscape	38.9	0.083	0.027	0.001
Micromedex - Drugs.com	45.6	0.211	0.025	<0.001
Medscape - Drugs.com	35.9	-0.029	0.029	0.286

DDIs: Drug–drug interactions

DISCUSSION

In the literature, the studies that evaluated more than one DDI software program usually emphasized the difference between each program and they were compared especially in terms of their severity classifications. However, the three DDI software programs evaluated in the present study had similar classification systems when evaluating the clinical consequences of each possible DDI. Community pharmacists mostly prefer the freely accessible DDI software programs because of economic concerns. For that reason, two web-based DDI software programs were chosen in the present study. To compare these programs, Micromedex, which is utilized as a comprehensive drug information source, was selected. The researchers' university library had a subscription to Micromedex and in the present study, conducted during fifth year students' pharmacy courses, as a part their assignment during this course, all students could subscribe to Micromedex and could check possible DDIs in the prescriptions. The 1000 patient prescriptions were selected and analyzed by the researchers again in accordance with the purpose of the present study.

In the present study, which assessed possible DDIs in 1000 patient prescriptions in a community pharmacy setting with three DDI software programs, it was found that Micromedex detected possible DDIs in the fewer patients (21.2%) when compared with the other software programs. Moreover, comparison of the total number of possible DDIs in each program obtained showed that Micromedex detected half the number obtained by the other two DDI programs. Medscape DDI checker software evaluated separately each DDI with more than one mechanism attributed and scored with several severities. This discrepancy could be caused by the fact that in Medscape it was determined as a separate DDI in cases where more than one mechanism occurred. Moreover, the number of minor interactions found in Medscape is higher than that of the other programs. This could be reason for the higher total number of possible DDIs obtained in Medscape.

Similarly, Oshikoya et al.⁵ obtained a total of 596 potential DDIs in 280 patients with HIV and 84.6% of them were detected in Medscape and only 50.7% of them were obtained in USA MIMS (Monthly Index of Medical Specialties Interaction Checker). The rate of DDI was 46.1% and the correlation between severity scores was weak.

Olvey et al.⁶ compared Micromedex with two standard software programs: Drug-Reax and Drug Interactions: Analysis and Management by analyzing DDI lists at the US Department of Veterans Affairs (VA). According the result of that study, 13.7% of a total of 982 DDIs considered as critical by VA were detected in all three software programs and the concordance between programs was low. In the present study, the rate of DDIs detected in prescriptions with all programs was 18%. Binary concordance rates based on number of patient prescriptions obtained by the DDI software programs were approximately 84–88% and the kappa coefficient was between 0.6 and 0.7. On the other hand, when all of them were analyzed, the concordance

rate was under 80%. These results and correlation values showed that there was a moderate concordance between all three DDI software programs according the number of patient prescriptions. When compared with other studies, the concordance rate was higher in the present study. Vonbach et al.³ found a total of 157 DDIs by using Drug Interaction Facts, Drug-Reax, Lexi-Interact, and Pharmavista, and only 11% of them were detected by all of the DDI software programs. In that study, none of the DDI software programs could determine more than 50% of the total DDIs.

Bergk et al.⁷ determined that 33% of them were similar in all DDI programs when they compared clinically significant DDIs by utilizing German SmPC, DRUGDEX, Hansten/Horn's Drug Interaction Analysis and Management, and Stockley's Drug Interaction programs.

Chao and Maibach⁸ compared four DDI compendia (Mosby's GenRx, USP DI, AHFS Drug Information, and the Physicians' Desk Reference) most commonly utilized in the USA in their study by screening DDIs and the most prescribed four medications involved in dermatology services, and these programs were incompatible. The concordance rate was reduced when more than two software programs were compared. Only 8.9% of the total number of DDIs were found in all four DDI compendia. Therefore, Chao and Maibach⁸ suggested reassessment of these programs according to information in the literature and the clinical relevance of each DDI.

In another study that compared BNF with the programs Medicine Compendia (eMC) and DailyMed, it was found that BNF obtained two-fold more DDIs when compared with DailyMed and 63.9% of them were found with only one compendium and the rate of DDIs detected in all three compendia was 15.12%.⁹ A weak correlation coefficient (0.366) was measured between the three compendia. It was stated that this incompatibility was caused by the difference between drug classifications in the three systems and also the source of DDIs in the programs was not presented.⁹

The difference in the total number of possible DDIs did not cause this discordance between most of the various DDI programs and it was suggested that this could be caused because of differences in the severity classification in these programs.^{10–13}

The concordance between the DDI programs used in the present study was high in terms of the number of patients detected with possible DDI in each program when compared with previous studies mentioned above. Although the DDI programs used in the present study were quite similar to each other according to the severity classification of possible DDIs, the concordances regarding the rate of severity ranking were low. The rates of concordance in two-pair comparisons of the DDI programs were approximately less than 50% and the kappa coefficients were also relatively low in the present study. Only 13.1% of a total of 625 DDIs were scored with the same severity level in all three programs. The major DDIs classified as major by Micromedex numbered 89 and only 12 of them were defined as major DDIs by the two other DDI programs used in the present study.

Vitry¹⁴ found the rate of major interactions obtained by at least one program was between 14% and 44% when they compared four different programs and mentioned inconsistency between programs according to the grading of the severity and the quality of their supporting evidence. Vitry¹⁴ stated the reasons for this discordance between programs as various inclusion criteria, different information sources, and dissimilar therapeutic drug classifications in each program used, and also the severity classification based on the clinical relevance of each DDI was not common between the programs.

Ekstein et al.¹⁵ found more than 30% of interactions in at least one program when they compared three different DDI programs according to antiepileptic drugs in their study. In that study, the concordance rate was less than 30% even if severity levels were classified as high between programs. These discrepancies could be attributed to differences in definitions and terminology in each program, various clarifications of information in the literature, and different classifications of drugs used in various DDI programs.

It is well known that DDI programs should be more sensitive and specific for practical usage by pharmacists.^{16,17} Reis and Cassiani¹⁸ compared DDI programs by selecting one of them as the gold standard and calculated their sensitivity and specificity. In that study, the limitations of DDI programs were emphasized and evaluation of DDI programs chosen for detection of possible DDIs in a hospital setting was suggested.

Some of the possible DDIs were definitely different between programs in the present study. For example, some of the experts defined polypharmacy if two NSAIDs were present in the same prescription. Only Medscape warned of a moderate (significant) interaction for this situation when the DDI programs used in this study are considered. The other programs did not report any interaction between two NSAIDs if they were prescribed concurrently. Discordance between programs could be slightly attributed to this kind of interaction, which was obtained in 21 of 1000 patients in the present study. All these discrepancies raised the question of which DDI program should be selected as the gold standard when the sensitivity and specificity of DDI programs are evaluated.

Based on the result of the present study and other studies in the literature, DDI programs should be re-evaluated to improve concordance between them by assessing evidence-based outcomes and severity classifications. According to the report by the consensus panel where it was evaluated and evidence of DDIs in the process of clinical decision, the following statements were offered to obtain highly qualified information from DDI programs: consistent terminology should be constituted, the Drug Interaction Probability Scale should be utilized to assess case reports regarding possible DDIs, a new approach should be formed to evaluate evidence regarding DDIs, the assessment of FDA documents and drug leaflets should be performed with the same criterion like evidence reported, and when evidence is detected, this possible DDI should be classified according to therapeutic/pharmacology groups.¹⁹

The following suggestions would improve patient safety: well-designed studies should be conducted to determine the incidence, outcomes, and patient-related risk factors of DDIs; algorithms should be produced for defining systematic and clear processes of assessing evidence to evaluate the risk and severity of possible DDIs; and evidence of possible DDIs should be integrated into electronic systems.²⁰

Because of discordance between DDI programs, when pharmacists detect a major DDI and/or any DDI in clinically critical patients, they should confirm that using another DDI program. Although it seems time consuming, this could result in elevated patient safety. Therefore, it was suggested that health care providers should check possible DDIs with more than one DDI program in clinically critical patients such as those with HIV.⁵

Limitation of the study

In the present study, only three software programs were used, because the ones chosen had similar severity classification properties and the two web-based programs used are freely accessible worldwide including Turkey. One of the limitations of the present study was that Rx Media Pharma was not used, which is the most commonly utilized Turkish drug information sources. The number of the prescriptions analyzed in the present study was large. This allowed evaluation of different medications and diseases with a large number of them. Although this might seem to be advantage to assess possible DDIs comprehensively, some experts might consider it a limitation because of the lack of concordance demonstrated between special medication groups such as antiepileptics, antidepressants, and anticoagulants.

CONCLUSIONS

A high rate of potential DDIs was detected in a community pharmacy setting in the present study. After comparison of various software programs, it was found that potential DDIs reported in various software programs were different from each other. Therefore, we recommend that pharmacists confirm with a different DDI program before making a decision when they detect clinically significant potential drug-drug interactions.

ACKNOWLEDGEMENT

This study is supported by Marmara University Scientific Research Projects Committee (SAG-D-071015-0473).

Conflicts of Interest: No conflict of interest was declared by the authors.

REFERENCES

1. Raschetti R, Morgutti M, Menniti-Ippolito F, Belisari A, Rossignoli A, Longhini P, La Guidara C. Suspected adverse drug events requiring emergency department visits or hospital admissions. *Eur J Clin Pharmacol.* 1999;54:959-963.
2. Indermitte J, Beutler M, Bruppacher R, Meier CR, Hersberg KE. Management of drug-interaction alerts in community pharmacies. *J Clin Pharm Ther.* 2007;32:133-142.

3. Vonbach P, Dubied A, Krahenbühl S, Beer JH. Evaluation of frequently used drug interaction screening programs. *Pharm World Sci.* 2008;30:367-374.
4. Peng CC, Glassman PA, Marks IR, Fowler C, Castiglione B, Good CB. Retrospective drug utilization review: incidence of clinically relevant potential drug-drug interactions in a large ambulatory population. *J Manag Care Pharm.* 2003;9:513-522.
5. Oshikoya KA, Oreagba IA, Ogunleye OO, Lawal S, Senbanjo IO. Clinically significant interactions between antiretroviral and co-prescribed drugs for HIV-infected children: profiling and comparison of two drug databases. *Ther Clin Risk Manag.* 2013;9:215-221.
6. Olvey EL, Clauschee S, Malone DC. Comparison of Critical Drug-Drug Interaction Listings: The Department of Veterans Affairs Medical System and Standard Reference Compendia. *Clin Pharmacol Ther.* 2010;87:48-51.
7. Bergk V, Haefeli WE, Gasse C, Brenner H, Martin-Facklam M. Information deficits in the summary of product characteristics preclude an optimal management of drug interactions: a comparison with evidence from the literature. *Eur J Clin Pharmacol.* 2005;61:327-335.
8. Chao SD, Maibach HI. Lack of drug interaction conformity in commonly used drug compendia for selected at-risk dermatologic drugs. *Am J Clin Dermatol.* 2005;6:105-111.
9. Nikolic BS, Ilic MS. Assessment of the consistency among three drug compendia in listing and ranking of drug-drug interactions. *Bosn J Basic Med Sci.* 2013;13:253-258.
10. Abarca J, Malone DC, Armstrong EP, Grizzle AJ, Hansten PD, Van Bergen RC, Lipton RB. Concordance of severity ratings provided in four drug interaction compendia. *J Am Pharm Assoc (2003).* 2004;44:136-141.
11. Fulda TR, Valuck RJ, Vander Zanden JV, Parker S, Byrns PJ. Disagreement among drug compendia on inclusion and ratings of drug-drug interactions. *Current Therapeutic Research.* 2000;61:540-548.
12. Hines LE, Ceron-Cabrera D, Romero K, Anthony M, Woosley RL, Armstrong EP, Malone DC. Evaluation of Warfarin Drug Interaction Listings in US Product Information for Warfarin and Interacting Drugs. *Clin Ther.* 2011;33:36-45.
13. Martins MA, Carlos PP, Ribeiro DD, Nobre VA, César CC, Rocha MO, Ribeiro AL. Warfarin drug interactions: a comparative evaluation of the lists provided by five information sources. *Eur J Clin Pharmacol.* 2011;67:1301-1308.
14. Vitry AI. Comparative assessment of four drug interaction compendia. *Br J Clin Pharmacol.* 2007;63:709-714.
15. Ekstein D, Tirosh M, Eyal Y, Eyal S. Drug interactions involving antiepileptic drugs: Assessment of the consistency among three drug compendia and FDA-approved labels. *Epilepsy Behav* 2015;44:218-224.
16. Warholak TL, Hines LE, Saverno KR, Grizzle AJ, Malone DC. Assessment tool for pharmacy drug-drug interaction software. *J Am Pharm Assoc (2003).* 2011;51:418-424.
17. Sweidan M, Reeve JF, Brien JA, Jayasuriya P, Martin JH, Vernon GM. Quality of drug interaction alerts in prescribing and dispensing software. *Med J Aust.* 2009;190:251-254.
18. Reis AM, Cassiani SH. Evaluation of three brands of drug interaction software for use in intensive care units. *Pharm World Sci.* 2010;32:822-828.
19. Scheife RT, Hines LE, Boyce RD, Chung SP, Momper JD, Sommer CD, Abernethy DR, Horn JR, Sklar SJ, Wong SK, Jones G, Brown ML, Grizzle AJ, Comes S, Wilkins TL, Borst C, Wittie MA, Malone DC. Consensus Recommendations for Systematic Evaluation of Drug-Drug Interaction Evidence for Clinical Decision Support. *Drug Saf.* 2015;38:197-206.
20. Hines LE, Malone DC, Murphy JE. Recommendations for Generating, Evaluating, and Implementing Drug-Drug Interaction Evidence. *Pharmacotherapy.* 2012;32:304-313.



Establishment and Escalation of an Amino Acid Stacked Repressible Release Embedded System Using Quality by Design

Tasarım Üzerinde Kaliteyi Kullanarak Amino Asit Yığılmış Bastırılabilir Salınan Gömülü Sistemin Kurulması ve Arttırılması

© Vijay SHARMA^{1*}, © Lalit SINGH¹, © Navneet VERMA²

¹Shri Ram Murti Smarak College of Engineering, Technology and Research, Bareilly, India
²IFTM University, Faculty of Pharmacy, Moradabad, India

ABSTRACT

Objectives: The traditional approach of developing a new delivery system is an exhaustive task and requires a number of resources like manpower, money, material, and time. To overcome this problem Quality by Design (QbD) can be utilized to obtain pharmaceutical products of desired (best) quality with minimum use of the above resources as well as determination of the impact of one factor over the desired associated process. The present research is focused on establishing a design for formulating optimized gelatin microspheres using QbD.

Materials and Methods: Repressible released embedded microspheres of L-arginine were prepared by performing cross linking of gelatin using glutaraldehyde. Characterization of the formulated embedded microspheres was done based on infrared spectroscopy, scanning electron microscopy, percentage yield, microsphere size, drug entrapment efficiency, and drug release. The impact of concentrations of gelatin and ethyl cellulose was determined over dependent response like percentage yield, microsphere size, and drug entrapment efficiency.

Results: A response surface curve was obtained using a 3² central composite design and the optimized batch was obtained with percentage yield, microsphere size, and drug entrapment efficiency of 89.98, 333.32 mm, and 82.61%, respectively. Validation of the optimized batch was done by formulating four different batches with optimized values of independent response and a comparison of the observed responses with the predicted ones was set up and all these batches were found close to the predicted values and show the validity of the optimized data.

Conclusion: The QbD approach is quite efficient to get optimized drug delivery systems of L-arginine without exhaustive study.

Key words: L-arginine, gelatin, central composite design, microspheres, characterization of microspheres

ÖZ

Amaç: Yeni bir doğum sisteminin geliştirilmesine yönelik geleneksel yaklaşım, kapsamlı bir görevdir ve insan, para, malzeme ve zaman gibi birtakım kaynakları gerektirir. Bu sorunun üstesinden gelmek için Tasarım Üzerinde Kalite (QbD), istenen (en iyi) kalitenin farmasötik ürününün, yukarıda belirtilen kaynakların asgari kullanımı ile istenilen ilgili süreç üzerinde bir faktörün etkisinin belirlenmesi için kullanılmasını sağlar. Bu araştırma, QbD'yi kullanarak optimize edilmiş jelatin mikroküreleri formüle etmek için bir tasarım oluşturulmasına odaklanmıştır.

Gereç ve Yöntemler: Yeniden basılabilir serbestleştirilmiş L-argininin mikro-küreleri, glutaraldehit kullanılarak jelatinin çapraz bağlanmasıyla hazırlandı. Formüle edilmiş mikrosferlerin karakterize edilmesi kızıl ötesi spektroskopi, taramalı elektron mikroskobu, yüzde verimi, mikroskop boyutu, ilaç tutma verimi ve ilaç salınımı ile yapıldı. Jelatin ve etil selüloz konsantrasyonunun etkisi, yüzde verimi, mikro küre boyutu ve ilaç tutma verimi gibi bağımlı tepki üzerinde belirlenmiştir.

Bulgular: Yanıt merkezi eğrisi 3² merkezi kompozit dizayn kullanılarak elde edildi ve sırasıyla yüzde verim, mikro küre boyutu ve ilaç tutma verimi 89.98, 333.32 mm ve %82.61 olarak optimize edilmiş toplu elde edildi. Optimize edilmiş partinin geçerliliği, bağımsız yanıtın optimize edilmiş değerleri ile dört farklı parti formüle edildi ve gözlemlenen yanıtların öngörülen değerlerle karşılaştırılması ve tüm bu partilerin öngörülen değerlerin yakınında bulunduğu ve düzgünleştirilmiş verilerin geçerliliğini gösterdiği bulundu.

Sonuç: QbD yaklaşımı, aşırı etkili çalışma yapmadan L-argininin optimize edilmiş ilaç verme sistemlerini elde etmek için oldukça etkilidir.

Anahtar kelimeler: L-arginin, jelatin, merkezi kompozit tasarımı, mikrosferler, mikrosferlerin karakterizasyonu

*Correspondence: E-mail: vijaysrampur@gmail.com, Phone: +91945872561 ORCID-ID: orcid.org/0000-0003-1898-0476

Received: 02.08.2017, Accepted: 07.12.2017

©Turk J Pharm Sci, Published by Galenos Publishing House.

INTRODUCTION

Quality by Design (QbD) is a helpful tool for systemic development of drug formulations based on sound scientific principles; it refers to the successful achievement of predictable quality with desired predetermined specification and without doing exhaustive conventional study.¹ The QbD paradigm of drug regulation necessitates very good understanding of the product to overcome future product failures.² Design of experiment and response surface method help in finding the individual as well as combined effects of variables on a product.^{3,4}

Oral controlled release formulations are developed to lessen the problems associated with oral conventional dosage forms; for example, they can reduce side effects and improve therapeutic efficacy by delayed/prolonged drug release so that the frequency of drug administration can be reduced, thus assuring better patient compliance.^{5,6} Various techniques have been developed for controlled release formulations; they utilize the cross-linking ability of polyelectrolyte in the presence of counter ions to form a multiparticulate system. These delivery systems are spherical cross linked hydrophilic polymeric systems, which upon gelation and swelling in simulated biological fluids release the drug in a controlled manner. These developed microspheres can be loaded with high amounts of drug compared to the conventional delivery system.^{7,8}

Arginine, an ergogenic (i.e., performance enhancing) supplement, most notably in the nitric oxide (NO) class of supplements, is a semi-essential amino acid involved in multiple areas of human physiology and metabolism. NO produced from it improves outcomes in various diseases.⁹ L-arginine is readily available over the counter and is popular as a nutritional supplement to increase muscle mass. Recently, L-arginine has been tested as a potential therapeutic in numerous acute and chronic disease states, including sickle cell chest crisis, pulmonary artery hypertension, coronary heart disease, pre-eclampsia, and myocardial infarction, because of its bronchodilator and vasodilator actions.^{10,11}

MATERIALS AND METHODS

Materials

L-arginine was obtained from CDH Laboratory Chemicals and sodium alginate (low viscosity grade, 250 cp of 2% solution at 25°C) from Loba Chemie Pvt. Ltd (Mumbai). Gelatin, ethyl cellulose (EC), and Span 80 were purchased from Thermo Fisher Scientific India Pvt. Ltd. (Mumbai). Glutaraldehyde and light liquid paraffin were procured from Loba Chemie (Mumbai). All other chemicals used in the study were of analytical grade. high performance liquid chromatography (HPLC) grade water, methanol, and potassium dihydrogen orthophosphate were purchased from Qualigens Fine Chemicals (Gujrat).

Methods

Preparation of microspheres

Controlled release microspheres of L-arginine were prepared by cross linking of gelatin using glutaraldehyde. The required amount of gelatin was placed in a beaker; to this 8 mL of distilled

water was added and this mixture was heated at 40°C for 3-4 min to get a uniform polymer mixture. Different concentrations of EC were added as shown in Table 1. Then the specified amount of drug was dispersed thoroughly to the polymer solution. A mixture of light liquid paraffin (200 mL) and Span 80 (0.1 mL) was prepared. The mixture was maintained at 4°C with an ice bath and stirred at 200 rpm and to this mixture previously prepared polymeric drug solution was added through a syringe with a 22-gauge needle. After some time glutaraldehyde (2 mL) was added dropwise to it with continuous stirring for 2 h. The microspheres were filtered, washed with iso-propyl-alcohol to remove the liquid paraffin, and dried at room temperature. Then the dried microspheres were collected, weighed, and stored.^{12,13}

3² central composite design

A 3² central composite design (CCD) was adopted for the optimization study. The two independent variables investigated were functional excipients such as concentrations of gelatin (X) and EC (Y). The impact responses of these independent variables were investigated on the dependent responses such as percentage yield, microsphere size (MS), and drug entrapment efficiency (DEE). The experimental points used according to the design are shown in Table 1.

Polynomial equations were generated and used to express the function of independent variables. A common polynomial equation to observe the effect of an independent variable can be expressed as,

$$Y_1 = b_0 + b_1 X_1 + b_2 X_2 + b_3 X_1 X_2 + b_4 X_{12} + b_5 X_{22} + b_6 X_1 X_{22} + b_7 X_{12} X_2, \text{ eqn. (1)}$$

where Y_1 is the dependent variable and b_0 is the arithmetic mean response of 13 runs.

Table 1. Formulation design and their coded value

Batch code	Coded value		Actual value	
	Factor A gelatin (mg) (X)	Factor B EC (mg) (X)	Factor A gelatin (mg) (X)	Factor B EC (mg) (X)
B1	+1	-1	1000	50
B2	+1	0	1000	100
B3	+1	+1	1000	150
B4	0	-1	900	50
B5	0	0	900	100
B6	0	+1	900	150
B7	-1	-1	800	50
B8	-1	0	800	100
B9	-1	+1	800	150
B10	0	0	900	100
B11	0	0	900	100
B12	0	0	900	100
B13	0	0	900	100

EC: Ethyl cellulose

The main independent variables, that is, effects X_1 and X_2 , represent the average result of changing one factor at a time from its lower values to its higher values. The 3^2 CCD is the most efficient tool for estimating the influence of individual variables (main effects) and their interactions using minimum experimentation. In the present research, the 3^2 CCD was considered to be best as the values of the response surfaces were not known from the previous findings. Thus, this design was selected for optimization of the formulated microspheres.

Evaluation of prepared microspheres

Characterization of microspheres

Fourier-transform infrared (FTIR) spectra was obtained using a Jasco FTIR 6100 type A spectrometer (Japan), the sample was prepared in KBr disks, and the spectra were recorded over the wavenumber 4000–400 cm^{-1} . All three spectra were completely analyzed.¹⁴

Percentage yield

Microspheres dried at room temperature were weighed and the percentage yield of microspheres was calculated using the formula:¹⁴

$$\% \text{ yield} = \frac{\text{Amount of sphere prepared experimentally}}{\text{Theoretical amount of microspheres (mg)}} \times 100 \text{ eqn. (2)}$$

Morphological analysis

A scanning electron microscope (Zeiss, Supra 40, India) was used to characterize the surface topography of the microspheres. The microspheres were fixed on a brass support using thin adhesive tape and the samples were coated with thin layer gold under vacuum to render them electrically conductive (approximately 3000 Å). The surface picture was taken at 15 kV and 20 kV for the drug-loaded microspheres.

Particle size determination of microspheres

Particle size was analyzed by sieving. Microspheres were separated out in different size fractions by passing them through a set of sieves over 5 min. This set of sieves included standard sieves having nominal mesh apertures of 1.0 mm, 0.71 mm, and 0.5 mm (sieve no. 16, 22, and 30, respectively). The particle size distributions of the beads were determined and mean particle sizes of beads were calculated using the following formula:

$$\text{Mean particle size} = \frac{\sum (\text{Mean particle size of the fraction} \times \text{weight})}{\sum \text{Weight fraction}} \text{ eqn. (3)}$$

Swelling index

The gelatin microspheres were kept in double distilled water for swelling for 1 h to achieve maximum swelling. Volumetric measurements were made by determining the increase in volume in the swelling medium at specific time intervals. The swelling index was calculated as follows:¹⁵

$$\text{Swelling index} = \frac{\text{Volume of swollen particles}}{\text{Volume of dry particles}} \text{ eqn. (4)}$$

Drug entrapment efficiency

Accurately weighed drug-loaded microspheres equivalent to 100 mg of L-arginine were added to 0.1 N HCl and shaken on a mechanical shaker for 24 h. Then the solution was filtered and the drug content was estimated spectrophotometrically using HPLC (Younglin, ACME-9000, China). The drug entrapment efficiency was determined using the following formula:¹⁶

$$\text{Drug entrapment efficiency} = \frac{\text{Actual drug content}}{\text{Theoretical drug content}} \times 100 \text{ eqn. (5)}$$

In vitro drug release

In vitro release studies were carried out on L-arginine loaded microspheres using a USP XXIV dissolution test apparatus-I (Electrolab, TDT-06T, Maharashtra, India). Weighed quantities of microcarriers equivalent to 100 mg of L-arginine were introduced into a dissolution basket and the basket was placed in 900 mL of phosphate buffer solution (pH 7.4 for 8 h) at $37 \pm 0.5^\circ\text{C}$ (Ph. US 24th edn) and 50 rpm.¹⁷ Aliquots of 5 mL of solution were withdrawn at specific time intervals and replaced with fresh dissolution medium. The withdrawn samples were analyzed for drug content by HPLC (Younglin, ACME-9000, China) using a ultraviolet detector. The samples were studied at 210 nm to obtain the retention time of 2.2–2.4 min and AUC.¹⁸ The results of the *in vitro* release data were fitted into various release equations and kinetic models.^{19–21}

Optimization and data validation

Concentrations of gelatin were selected as 1000, 900, and 800 mg, whereas for EC they were 50, 100, and 150 mg. Thirteen formulations were developed by selecting nine possible combinations among which the center point was repeated four times and the mean value was taken for further study. The dependent responses were analyzed using Design Expert® 8.0.7.1 (trial version). The models were tested for significance and the optimized batch was selected with desired values of dependent responses. Four formulations (VCB1 to VCB4) along with the optimized batch were developed and validated by response surface methodology. The observed and predicted responses were critically compared. Linear correlation plots were constructed for the chosen check-point formulations. The residual graphs between predicted and observed responses were also constructed separately and the percent prediction error (% bias) was calculated with respect to the observed responses. The optimized batch was validated taking a total of four formulations selected as check-points.

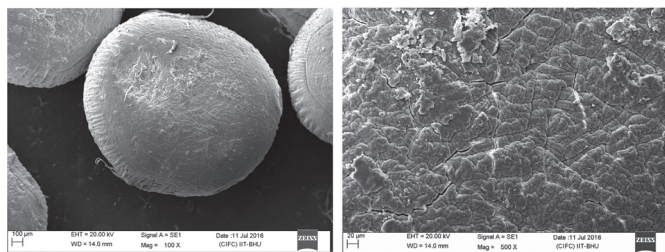
RESULTS

The FTIR profile of the formulated microspheres was obtained to identify the drug–polymer interaction. Hence the formulated microspheres were subjected to IR analysis to evaluate the possible interaction between drug and polymer. The infrared curve of pure drug and formulated microspheres shows similar peaks (Table 2, Figure 1), which confirms that there is no interaction between drug and polymer.

Table 2. IR interpretation of optimized L-arginine microspheres

IR frequencies (cm ⁻¹)	Assignments
3158.57	NH Str
2935.78	CH ₃ Str
1681.04	NH ₂ Bend
1576.87	CO Str
1517.08	OH Bend
1458.25	CH ₃ Asy Bend
1407.13	CH ₃ Sym Bend
1356.02	CH ₃ Sym Bend
1320.33	OH Bend
1176.56	Sym Str CCC Bond
899.46	NH ₂ Bend
521.77	CO Bend
447.50	NH ₂ Rock

IR: Infrared

**Figure 1.** Scanning electron micrograph of microspheres, a) single bead, b) enlarged surface view

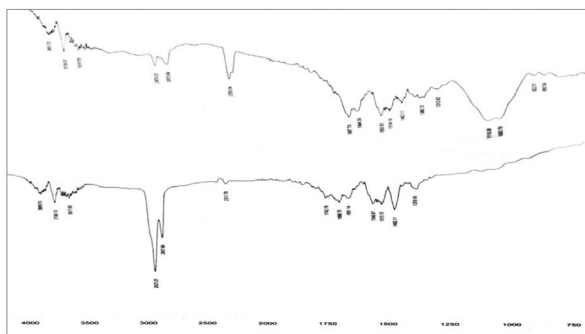
Surface topography

Scanning electron microscopy was used to investigate the surface topography of prepared microspheres and the result is shown in Figure 2.

The percentage yield and mean particle size of the formulation are given in Table 3.

Drug entrapment efficiency

DEE is an important variable used to assess the drug loading capacity of microspheres and their drug release profile. DEE

**Figure 2.** FTIR spectra of a) L-arginine and, b) formulated microspheres
FTIR: Fourier-transform infrared

depends upon various parameters such as the process used for preparation, physicochemical properties of the drug, and various formulation variables (Table 3).

Table 3. Evaluation of formulated batches of microspheres

Batch code	Yield%	Mean particle size (MS) (μm)	DEE (%)
B1	83.55	326.81	75.32±2.261
B2	86.36	329.38	78.0±2.458
B3	89.98	333.32	80.15±0.794
B4	77.98	315.98	73.59±1.744
B5	80.07	318.59	75.43±1.877
B6	83.44	321.53	78.76±1.572
B7	74.65	302.34	75.09±0.872
B8	75.45	307.08	78.15±0.519
B9	77.21	311.65	82.61±0.700
B10	81.07	317.73	75.87±0.519
B11	80.32	317.89	76.67±0.519
B12	80.54	316.52	77.05±0.519
B13	79.96	315.65	75.14±0.519

MS: Microsphere size, DEE: Drug entrapment efficiency

In vitro release behavior of drug

The *in vitro* drug release behavior of the formulated glutaraldehyde cross-linked gelatin microspheres is shown in Figure 3. All batches were studied for their drug release profile for up to 8 hits and it was observed that in all formulated systems the rate of release varied due to the use of different concentrations of dependent variables. It is clear that as the amount of EC increases from 50 to 150 mg the rate of drug release decreases, which indicates the hydrophobic nature of EC in the formulation; hence increasing amounts of EC lead to retardation in drug release. The cross linking property of glutaraldehyde leads to the formation of a rigid hydro gel to restrict leaching, thereby decreasing drug dissolution (Table 4, Figure 3).

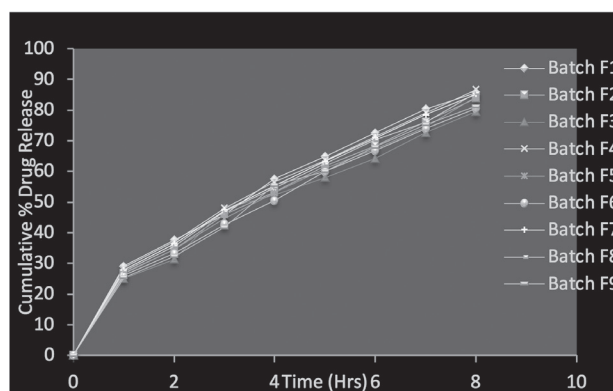
**Figure 3.** *In vitro* evaluation of L-arginine loaded gelatin microspheres

Table 4. Drug release kinetics study

Batch code	DR ₈	Korsmeyer R ²	Higuchi R ²	First-order R ²	Zero-order R ²	n
B1	85.754	0.9781	0.9953	0.9881	0.9122	0.4590
B2	83.963	0.9773	0.9935	0.9835	0.9325	0.4955
B3	79.508	0.9796	0.9917	0.9824	0.9474	0.4875
B4	86.693	0.9774	0.9955	0.9837	0.9263	0.4848
B5	84.323	0.9757	0.9920	0.983	0.9346	0.4826
B6	80.454	0.9778	0.9923	0.9869	0.9396	0.4905
B7	85.255	0.9633	0.9901	0.9830	0.9193	0.4861
B8	85.617	0.978	0.9892	0.9833	0.9268	0.4566
B9	81.194	0.972	0.9918	0.978	0.9351	0.4664

Data analysis and optimization

The drug release mechanism was investigated by fitting to models representing zero-order, first-order, Higuchi's square root of time, and Korsmeyer–Peppas models. Results of ANOVA for the response surface quadratic model for various dependent parameters were as follows:

$$\% \text{ yield} = +80.47 + 5.45A + 2.73B + 0.97AB + 0.51A^2 + 0.32B^2 - 0.48A^2B - 0.037AB^2, \text{ eqn. (7)}$$

$$MS = +317.64 + 11.15A + 2.77B - 0.62AB + 0.29A^2 + 0.82B^2 + 1.10A^2B + 0.31AB^2, \text{ eqn. (8)}$$

$$DEE = +76.38 - 0.075A + 2.39B - 0.67AB + 1.79A^2 + 0.082B^2 + 0.70A^2B - 0.48AB^2, \text{ eqn. (9)}$$

where A indicates the concentration of gelatin and B represents the concentration of EC.

Figure 4 shows response surface and contour plots for % yield, MS and DEE.

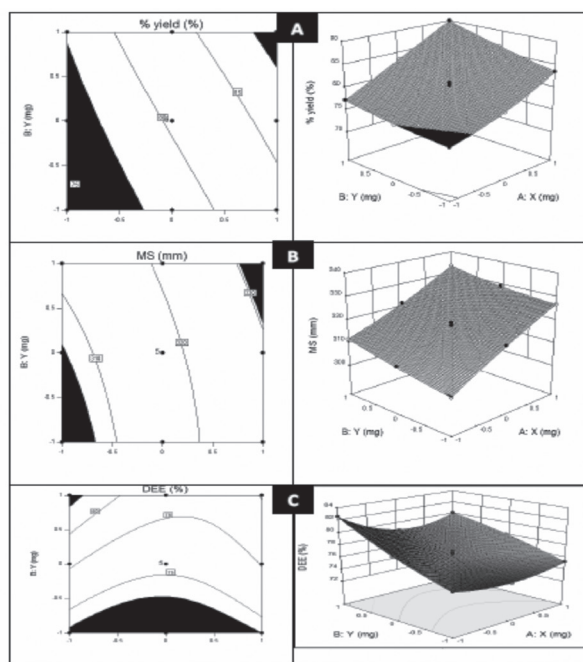


Figure 4. Response surface methodology and contour plots for a) percentage yield, b) microsphere size, c) drug entrapment efficiency

Validation of the statistical model

Validation of the optimized batch was done by formulating four different batches using an overlay plot (Figure 5) by utilizing the optimum value as found by statistical analysis, i.e., by considering the optimum value found (Table 5) and a comparative study was done between predicted values and observed values to determine the prediction error (Figure 6).

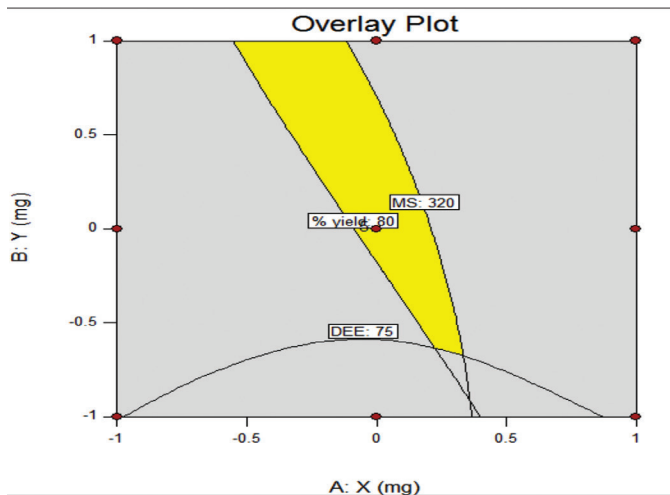


Figure 5. Overlay plot showing area for optimized product

Table 5. Validation checkpoint formulations and their results

Validation check batch	Response	Predicted value	Experimental value	Percent error
VCB1	yield%	79.91	79.97	-0.075
	MS	315.56%	315.50	0.019
	DEE	96.71%	96.67%	0.041
VCB2	yield%	82.15	82.11	0.048
	MS	319.94%	319.94	-0.990
	DEE	77.26%	77.19%	0.090
VCB3	yield%	81.45	81.47	-0.024
	MS	320.07%	320.27	-0.064
	DEE	76.14%	76.15%	-0.013
VCB4	yield%	80.69	80.67	0.024
	MS	319.96%	319.93	0.009
	DEE	75.29%	75.17%	0.159
Optimized batch	yield%	89.98	89.95	0.033
	MS	333.32%	333.30	0.006
	DEE	82.61%	82.98%	-0.447

MS: Microsphere size, DEE: Drug entrapment efficiency

DISCUSSION

FTIR spectra (Figure 1) of pure L-arginine and formulated microspheres of L-arginine shows the identical peaks as that of standard L-arginine which proves that excipients incorporated

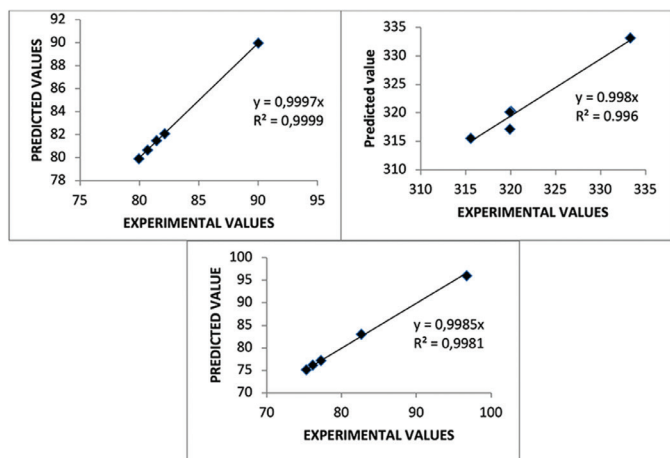


Figure 6. Regression coefficient between predicted and experimental response: a) % yield, b) microspheres size, c) drug entrapment efficiency

in formulated microspheres do not interact with L-arginine and all ingredients of beads are compatible with each other.

Scanning electron microscopy of microspheres of L-arginine shows well-rounded spheres with rough surface because of sudden cross linking of gelatin with glutaraldehyde. The particle size of the formulations was found to be between 320-351.11 μm . It was observed that the mean particle size of formulated microspheres were decreased with respect to the increased the amount of ethyl cellulose in the formulation (Figure 2).

Results for drug entrapment efficiency indicates that as the concentration of EC increases the DEE increase which is due practically insoluble nature of hydrophobic polymer i.e. EC. DEE was increased as the amount of EC was increased in the formulation because of practically insoluble nature of EC in water.

In vitro drug release study of microspheres of L-arginine was carried out in 900 mL of phosphate buffer solution (pH= 7.4 for 8 h) at $37 \pm 0.5^\circ\text{C}$. In the fasted state gel micro carriers exhibited a biphasic release profile as an initial rapid drug release phase due to burst which are loosely into or just beneath the surface of microspheres followed by a slower, gradually decreasing drug release phase after 1 hour extending up to 8 hours (Table 4, Figure 3).

Drug release mechanism was investigated for number of models i.e. zero-order, first order, Higuchi's square root of time model and Korsmeyer-Peppas model. Zero-order, first order, Higuchi's square root of time and Korsmeyer-Peppas model gave R^2 value 0.9101 to 0.9473, 0.9832-0.9889, 0.9901-0.9992 and 0.963-0.991 respectively, showing Fickian diffusion involving a combination of swelling, diffusion and/or erosion of matrices. Various response surface plots were also drawn to analyse impact of independent variables on dependent variables as discussed earlier.

Optimizations of formulated microspheres were done by using 32 CCD. The outcomes for response parameters, that is, % yield, MS and DEE were subjected to regression analysis and statistical models were found to be significant. Observed

dependent responses i.e. % yield, MS and DEE shows fair relation between the dependent and independent variables. Percentage yield for formulated batches were found in the range of 74.65-86.36% while particle size was found in range of 302.34-333.32 mm. Drug entrapment efficiency of all the formulation was found to be between 73.59 ± 1.744 to 82.61 ± 0.700 .

Figure 4a shows that values of % yield, increases with increase in concentration of gelatin and also increases with increasing EC concentration. Maximum % yield is observed at the highest levels of Gelatin and EC.

Figure 4b shows a nearly linear ascending pattern for MS, as the content of gelatin increased, this MS increase slowly with increasing gelatin. Value of MS achieves to its maximum value at the highest levels of gelatin and EC. Nonlinear pattern of contour lines indicates significant impact on gelatin and EC.

Figure 4c shows that the DEE increases almost linearly with increase in concentration of gelatin whereas it decreases very slowly and then increases with increase in EC concentration. Maximum value of DEE was observed at the highest gelatin and EC concentration.

Validation of optimized batch was done by setting up a comparison of the observed responses with the predicted ones (Table 5), the prediction error varied between -0.024 to 0.048, -0.990 to 0.090 and -0.013 to 0.159 for % yield, MS and DEE respectively. Validation of these data was also confirmed by overlay plot (Figure 5) obtained by design expert software (Dx8 trial version) The linear correlation plots drawn between the predicted and observed responses, forcing the line through the origin, demonstrated high values of R (0.996 to 0.999, Figure 6), indicating excellent goodness of fit ($p < 0.005$). The corresponding residual plots show nearly uniform and random scatter around the mean values of response variables.

CONCLUSIONS

Spherical amino acid loaded gelatin microspheres were prepared to achieve repressible release by cross-linking technique. An L-arginine stacked repressible release matrix delivery system was successfully established and escalation was achieved by using QbD applying a 3^2 central composite design. Hence it can be concluded that QbD is a powerful tool for the present research that helps in developing a desired formulation without wastage of time as well as manpower, money, and material.

Conflict of Interest: No conflict of interest was declared by the authors.

REFERENCES

- Verma S, Lan Y, Gokhale R, Burgess DJ. Quality by Design approach to understand the process of nano suspension preparation. *Int J Pharm.* 2009;377:185-198.
- Lionberger RA, Lee SL, Lee L, Raw A, Yu LX. Quality by Design: Concepts for ANDAs. *AAPS J.* 2008;10:268-276.

3. Singh, B, Pahuja S, Kapil R, Ahuja N. Formulation development of oral controlled release tablets of hydralazine: optimization of drug release and bioadhesive characteristics. *Acta Pharm.* 2009;59:1-13.
4. Singh L, Nanda A, Sharma S, Sharma V. Performance Optimization of Buoyant Beads of Anti-Diabetic Drug Using Quality by Design (QbD). *Lat Am J Pharm.* 2014;33:14-23.
5. Desai S, Bolton S. A floating controlled-release drug delivery system: *in vitro-in vivo* evaluation. *Pharm Res.* 1993;110:1321-1325.
6. Panos I, ACOSTA N, Heras A. New Drug delivery systems based on Chitosan. *Curr Drug Discov Technol.* 2008;5:333-341.
7. Patil JS, Kamalapur MV, Marapur SC, Kadam DV. Ionotropic gelation and polyelectrolyte complexation: the novel techniques to design hydrogel particulate sustained, modulated drug delivery system: a review. *Digest Journal of Nanomaterials and Biostructures.* 2010;5:241-248.
8. Suganeswari M, Senthil Kumar V, Anto SM. Formulation and evaluation of metoclopramide hydrochloride microbeads by ionotropic gelation method. *Int J Pharm Bio Arch.* 2011;2(Suppl 3):921-925.
9. Morris CR, Poljakovic M, Lavrisha L, Machado L, Kuypers FA, Morris SM Jr. Decreased arginine bioavailability and increased serum arginase activity in asthma. *Am J Respir Crit Care Med.* 2004;170:148-153.
10. Appleton J. Arginine: Clinical potential of a semi-essential amino acid. *Alt Med Rev.* 2002;7:512-522.
11. Sharma V, Singh L, Verma N, Kalra G. The nutraceutical amino acids-nature's fortification for robust health. *Br J Pharm Res.* 2016;11:1-20.
12. Esposito E, Cortesi R, Nastruzzi C. Gelatin microspheres: influence of preparation parameters and thermal treatment on chemico-physical and biopharmaceutical properties. *Biomaterials.* 1996;17:2009-2020.
13. Vandelli MA, Rivasi F, Guerra P, Forni F, Arletti R. Gelatin microspheres crosslinked with D,L-glyceraldehyde as a potential drug delivery system: Preparation, characterization, *in vitro* and *in vivo* studies. *Int J Pharm.* 2001;215:175-184.
14. Mishra B, Sahoo S, Biswal PK, Sahu SK, Behera BC, Jana GK. Formulation and Evaluation of Torsemide intragastric buoyant sustained release microspheres. 2010;3:742-746.
15. Wagner JG. Interpretation of percent dissolved-time plots derived from *in vitro* testing of conventional tablets and capsules. *J Pharm Sci.* 1969;58:1253-1257.
16. Sato Y, Kawaafaima Y, Takenchi H, Yamamoto H. *In vitro* and *in vivo* evaluation of riboflavin containing microballoons for floating controlled delivery system in healthy humans. *Int J Pharma.* 2004;275:75-82.
17. USP, (24th ed) (Rockville: United States Pharmacopeial Convention Inc; 2000;1941-1943.
18. Obreshkova D, Ivanov K. Quality Control of Aminoacids in Organic Foods and Food Supplements. *Int J Pharmacy Pharmaceutical Sciences.* 2012;4:404-409.
19. Ritger PL, Peppas NA. A simple equation for description of solute release II. Fickian and anomalous release from swellable devices. *J Controlled Release.* 1987;5:37-42.
20. Korsmeyer RW, Gurny R, Doelker E, Buri P, Peppas NA. Mechanisms of solute release from porous hydrophilic polymers. *Int J Pharmaceutics.* 1983;15:25-35.
21. Higuchi T. Mechanism of sustained-action medication: Theoretical analysis of rate of release of solid drugs dispersed in solid matrices. *J Pharm Sci.* 1963;52:1145-1149.



Preclinical Evaluation of the Haematinic Activity of an Oral Indiffusible Mixture of *Tamarindus indica* L. Leaf Extract

Tamarindus indica L. Yaprak Ekstresinden Hazırlanan Oral Dağılmayan Karışımın Hematinik Etkisinin Prelinik Değerlendirmesi

© Sathiya RAMU*, © Shwetha Krishna MURTHY, © Sukanya KRISHNA, © Abhishek Lakkasandra SOMASHEKARAIHAH, © Vani B. NANDIHALLI, © Kanekal Mohammed MUZAMMIL

M. S. Ramaiah University of Applied Sciences, Faculty of Pharmacy, Karnataka, India

ABSTRACT

Objectives: *Tamarindus indica* L. is known to be a multipurpose traditional plant in India. It is used to treat some bacterial infections, parasitic infestations, constipation, and inflammation. It is also used as a blood tonic and for wound healing. This study was designed to substantiate the traditional claim of haematinic activity for *T. indica*.

Materials and Methods: *T. indica* leaf extract was formulated into an oral indiffusible mixture (TIM) and evaluated for its haematinic activity in phenylhydrazine (single dose of 10 mg/kg *per oral* for 8 days) induced anaemia. Wistar rats were grouped into six (n=6). Groups I and II served as normal control and disease control groups, respectively. Group III received the standard drug (haematinic suspension 2 mL/kg). Groups IV, V, and VI received the formulated oral indiffusible mixture of *T. indica* at a dose of 100, 200, and 400 mg/kg, respectively.

Results: The TIM was formulated and pharmaceutically optimized. It produced significant increases in red blood cells, hemoglobin, and packed cell volume and a decrease in mean corpuscular volume.

Conclusion: The results showed that the treatment with TIM reversed phenylhydrazine induced anemia. However, the short duration of the present study is regarded as a limitation, and therefore a longer duration is required for obtaining better responses.

Key words: *Tamarindus indica*, haematinic activity, phenylhydrazine

ÖZ

Amaç: *Tamarindus indica* L. Hindistan'da çok amaçlı kullanılan geleneksel bir bitki olarak bilinmektedir. Bazı bakteriyel ve parazit enfeksiyonlarının tedavisinde, kabızlık ve inflamasyonun tedavisinde kullanılmaktadır. Kan toniği ve yara iyileştirici amaçla da kullanımı kayıtlıdır. Bu çalışma, *T. indica*'nın geleneksel kullanımının doğruluğunun araştırılması amacıyla yapılmıştır.

Gereç ve Yöntemler: *T. indica* yaprağından hazırlanan ekstre oral dağılmayan karışım (TIM) halinde formüle edilmiş ve fenilhidrazin-nedenli (8 gün boyunca 10 mg/kg *tek doz, oral*) anemi modeli üzerindeki hematinik etkisi değerlendirilmiştir. Wistar sıçanları altı gruba ayrılmıştır (n=6). Grup I ve II sırasıyla normal kontrol ve hastalık kontrol grupları olarak ayrılmıştır. Grup III'e standart ilaç (hematinik süspansiyon 2 mL/kg) verilmiştir. Grup IV, V ve VI'ya, sırasıyla 100, 200 ve 400 mg/kg'lık dozlarda oral dağılmayan karışım şeklinde formüle edilmiş olan *T. indica* ekstresi uygulanmıştır.

Bulgular: TIM formüle edilmiş ve farmasötik olarak optimize edilmiştir. Bu karışımın kırmızı kan hücreleri, hemoglobin ve paketlenmiş hücre hacminde önemli artış ve ortalama kan hacminde azalmaya neden olduğu bulunmuştur.

Sonuç: Bu sonuçlar, *T. indica* yaprak ekstresinden hazırlanan TIM'nin, fenilhidrazin-nedenli aneminin etkilerini tersine çevirdiğini göstermiştir. Bununla birlikte, bu çalışmanın kısa süreli olması bir sınırlama olarak kabul edilmiştir, bu nedenle daha iyi yanıtlar elde edebilmek için daha uzun bir süreye ihtiyaç duyulmaktadır.

Anahtar kelimeler: *Tamarindus indica*, hematinik etki, fenilhidrazin

*Correspondence: E-mail: sathya.pharma@gmail.com, Phone: 9035919823 ORCID-ID: orcid.org/0000-0003-3474-7033

Received: 13.09.2017, Accepted: 07.12.2017

©Turk J Pharm Sci, Published by Galenos Publishing House.

INTRODUCTION

All through history, irrespective of culture, plants have been a dependable source of medicine.^{1,2} Plants and their derived products are considered to be the main source for food and medicines. Plant derived medicines, popularly known as “herbal drugs” or “phytomedicines”, are well known and accepted as the most common form of alternative medicine. Almost 70-90% of the world’s rural population still depends on herbal remedies for health care.³ Plants produce a good deal of secondary metabolites that have benefited mankind in various ways, including treatment of diseases.⁴ They are mostly used in Ayurveda, Unani, Siddha, homeopathy, allopathy, and other alternative medicinal practices.⁵

Anaemia is defined as a reduction in haemoglobin level and oxygen carrying capacity below the normal range and is the most common disorder of the blood. It is characterised by a decrease in haemoglobin level to less than 13 g/dL in males or 12 g/dL in females.⁶ In anaemia the rate of production of mature red blood cells entering the blood from the red bone marrow does not keep pace with the rate of haemolysis.⁷ Iron is the main constituent of haemoglobin, which is accountable for transporting oxygen, and of myoglobin in muscles and is part of many enzymes concerned with cellular processes, respiration, and cell division.⁸ Low haemoglobin (Hb) levels result in a corresponding decrease in the oxygen carrying capacity of blood⁷ and other parameters such as total red blood cell (RBC) count, packed cell volume (PCV), mean corpuscular volume (MCV), mean corpuscular haemoglobin (MCH), and MCH concentration (MCHC).^{7,9}

Tamarindus indica is the third largest family of flowering plants, with a total of 727 genera and 19,327 species.¹⁰ *T. indica* is known to have mild laxative, preservative, and anti-measles effects due to the presence of tartaric acid and malic acid.¹¹ Polysaccharide obtained from *T. indica* pulp showed significant antipyretic activity against bacterial pyrogen.¹² Aqueous fruit extract of *T. indica* was shown to possess both central and peripherally acting analgesic activity.¹³ Traditionally, *T. indica* leaves are used as a blood tonic¹⁴ and for their wound healing, antimalarial, aphrodisiac, antihistaminic, antitussive, anti-inflammatory, antidiabetic, hepatoprotective, and antimeasles properties.¹¹ The bark and stem possess anti-asthmatic, antitussive, anti-inflammatory, astringent, hepato-protective, anthelmintic, and abdominal pain relieving effects.¹¹ The antioxidant property (flavonoids) of leaves of *T. indica* and also the existence of iron content in the leaves of *T. indica* have been previously reported.¹⁵⁻¹⁷ Taking this into consideration, the present study was undertaken to substantiate the traditional claim of haematinic activity for leaves of *T. indica* in phenylhydrazine (PHZ) induced anaemia in Wistar rats.

MATERIALS AND METHODS

Plant material and preparation of T. indica leaf extract

Fresh leaves of *T. indica* were collected in the field of the KMF Society Hostel farm, Bangalore, Karnataka. The plant material was identified and authenticated by Dr. S. N. Yoganarasimhan,

plant taxonomist. The taxonomic identification was carried out following Flora of the Presidency of Madras (2005), Flora of Hassan District (1976), and Flora of Bombay (1967). The voucher specimen was deposited at the herbarium of the Faculty of Pharmacy, M. S. Ramaiah University of Applied Sciences, Bangalore. The plant material was shade dried, coarsely powdered, and stored in an airtight container. These shade dried leaves were extracted with 95% v/v ethanol in a Soxhlet apparatus. The alcohol extract was filtered, the solvent was evaporated, and accurate weight of the extract was recorded. The colour and consistency of the extract were noted.

Phytochemical screening

Preliminary phytochemical screening of *T. indica* extract involved qualitative determination of the following substances: alkaloids, carbohydrates, glycosides, phytosterols, phenolic compounds, tannins, saponins, terpenes, and flavonoids. It was carried out in accordance with procedures described by Kokate.¹⁸

Formulation of oral indiffusible mixture

The ethanolic extract of *T. indica* leaf was formulated into an oral indiffusible mixture by hydrating overnight an accurately weighed quantity of ethanolic extract of *T. indica* and cross povidone (1%) solution. Sodium CMC (2%) was taken in separate beaker and kept for overnight hydration. These mucilages were put into a mortar along with glycerine (10%) and triturated to obtain a uniform mixture. Calcium chloride (0.8%) was added dropwise to the above mixture and it was triturated continuously until a uniform dispersion of extract was obtained. The prepared formulation was transferred to a measuring cylinder and the volume was adjusted. Three formulations were prepared as per the dose required for the pharmacological studies^{19,20} (Table 1). Formulation codes are given as follows: TIM1 - 100 mg/kg (15.8 mg/mL), TIM2 - 200 mg/kg (31.6 mg/mL), TIM3 - 400 mg/kg (54 mg/mL).

The oral indiffusible mixture of *T. indica* leaf ethanolic extract was evaluated for pH using a digital pH meter, viscosity using a Brookfield viscometer,²¹ redispersibility,¹⁹ flow rate (F) using

Table 1. Formulation of TIM

Sl. no.	Ingredients	TIM1	TIM2	TIM3
1	Ethanolic extract (g)	8	18	27
2	Sodium CMC (2%) (g)	10	10	10
3	Cross povidone (1%) (g)	5	5	5
4	Glycerine (10%) (mL)	50	50	50
5	Calcium chloride (0.8%) (g)	4	4	4
6	Methyl paraben (g)	0.5	0.5	0.5
7	Propyl paraben (g)	0.5	0.5	0.5
8	Raspberry flavour (mL)	5	5	5
9	Amaranth solution (g)	0.02	0.02	0.02
10	Purified water (q.s.)	Make up to 500 mL		

TIM: *T. indica* mixture, CMC: Carboxymethyl cellulose

a 10 mL pipette, particle size measurement using an Olympus microscope,²² and sedimentation volume using a 100 mL measuring cylinder.^{23,24}

Experimental animals

Wistar rats of 8-12 weeks old, weighing between 140 and 230 g of either sex were used for the study. The animals were bred, reared, and housed in the animal house of the Department of Pharmacology, Faculty of Pharmacy, M. S. Ramaiah University of Applied Sciences. The animal house was well maintained under standard hygienic conditions, at a temperature of 22±2°C and room humidity of 60±10%, with 12-h day and night cycle, and with food and water *ad libitum*. Paddy husk was provided as bedding material and cleaning was done on alternate days. The animals were housed in groups of 3 per cage. The pharmacological study was approved by the Institutional Animal Ethics Committee of the Faculty of Pharmacy (IAEC certificate no. Ref. No. MSRCP/SP-51/2014).

Acute toxicity study

The oral indiffusible mixture of ethanolic extract of *T. indica* leaf was screened for its toxicity following the OECD guidelines 423. A limit test was carried out with a dose of 2000 mg/kg in 3 female Wistar rats.²⁵

Experimental design

Anaemia was induced by oral administration of PHZ at a dose of 10 mg/kg per day for 8 days. The animals were divided into six groups. Each group consisted of six animals of either sex.

Groups I and II served as normal control and disease control groups, respectively. Group III received the standard drug (haematinic suspension 2 mL/kg). Groups IV, V, and VI received formulated oral indiffusible mixture of *T. indica* at a dose of 100, 200, and 400 mg/kg, respectively.

The animals were treated once daily for 14 days with different doses of the oral indiffusible mixture. After day 14 of treatment, blood was collected from the retro-orbital plexus under light ether anaesthesia from overnight fasted experimental animals. Physical parameters (body weight and food and water intake) were evaluated during treatment of the animals. Haematological parameters including RBC and Hb were estimated using automatic analysers. PCV was evaluated by centrifugation. MCV, MCH, and MCHC were calculated using the standard formulae according to Ghai.²⁶

Statistical analysis

The results of haematinic activity of the oral indiffusible mixture of *T. indica* leaf extract were subjected to statistical analysis. The data were expressed as mean ± standard error mean. Significant differences between groups were determined using one-way ANOVA followed by Tukey's multiple comparison; p<0.05 was considered significant.

RESULTS AND DISCUSSION

Preliminary phytochemical analysis

The phytochemical screening of *T. indica* revealed the presence of alkaloids, flavonoids, saponins, phenols, oils and fatty acids, carbohydrates, and tannins.

Evaluation of the oral indiffusible mixtures

The oral indiffusible mixtures were evaluated for pH, redispersibility, flow rate, particle size, viscosity, and sedimentation volume. The results of these parameters are reported in Tables 2 and 3. The pH of these formulations was in the range of 4.5-4.8, which is slightly acidic. In sedimentation TIM3 showed greater sedimentation volume when compared to the other two formulations. Slightly higher viscosity was observed in the higher dose formulation. The flow rate of the mixtures was in the range of 0.10-0.14. Particle size was determined using a microscope and was between 215 and 230 µm (Table 2). After the complete sedimentation of the suspension, formulations were redispersed. In that, the TIM1 formulation took fewer cycles to redisperse (Table 3).

Acute toxicity

A limit test was carried out following OECD guidelines 423. The results are reported in Table 4. All the animals were free of intoxication signs and there were no signs of mortality in the acute toxicity study (Table 4).

Table 2. Evaluation parameters of TIM1, TIM2, and TIM3 formulations

Sl. no.	Parameters	TIM1	TIM2	TIM3
1	pH	4.5±0.2	4.8±0.1	4.5±0.2
2	Redispersibility	3 times	4 times	6 times
3	Flow rate (mL/s)	0.1388±0.002	0.1250±0.005	0.1041±0.003
4	Particle size (µm)	220±25	230±29	215±35
5	Viscosity (cp)	9.0±0.23	12.6±0.43	13.5±0.31

TIM: *T. indica* mixture

Table 3. Sedimentation volume of different formulations

Formulation	$F = V_u/V_o$							
	1 h	2 h	6 h	12 h	1 st day	2 nd day	3 rd day	4 th day
TIM1	1	0.96	0.91	0.88	0.85	0.81	0.78	0.74
TIM2	1	0.96	0.90	0.87	0.83	0.78	0.75	0.70
TIM3	1	0.95	0.90	0.85	0.81	0.77	0.75	0.70

TIM: *T. indica* mixture

Haematinic activity

The haematological parameters of the experimental animals after treatment with oral indiffusible mixtures of *T. indica* leaf extract are presented in Table 5. PHZ treated animals showed reductions in the levels of RBC and Hb, while MCV and MCHC increased significantly, resulting in macrocytic anaemia. There was also a slight increase in MCH, which supports the induction of macrocytic anaemia by PHZ. Fourteen day treatment of anaemic rats (groups IV, V, and VI) with oral indiffusible mixture

Table 4. Acute toxicity results

Dose	1	2	3	4	5	6	7	8	9	10	11	12	13	14	15	16	17	18	19	20
2000 mg/kg	+	-	-	-	-	+	-	-	-	-	-	-	-	-	-	-	-	-	+	-

1. Alertness, 2. Aggressiveness, 3. Pile erection, 4. Grooming, 5. Gripping, 6. Touch response, 7. Decreased motor activity, 8. Tremors, 9. Convulsions, 10. Muscle spasm, 11. Catatonia, 12. Muscle relaxant, 13. Hypnosis, 14. Analgesia, 15. Lacrimation, 16. Exophthalmos, 17. Diarrhoea, 18. Writhing, 19. Respiration, 20. Mortality

Table 5. Haematinic activity of oral indiffusible mixture of *T. indica* leaf extract

Parameters	Normal control	Disease control	Standard	TIM1	TIM2	TIM3
RBC (millioncells/mm ³)	5.68±0.07	5.06±0.17 ^a	5.75±0.12 [*]	5.46±0.14	5.68±0.19 [*]	5.48±0.11
Hb (g/dL)	17.32±0.23	15.31±0.5 ^a	17.33±0.33 [*]	16.50±0.42	17.15±0.57 [*]	16.58±0.33
PCV	58.68±1.72	51.69±1.70	58.85±2.78	52.40±3.02	52.96±3.51	57.90±1.30
MCV	96.30±1.99	102.1±0.78 ^a	102.1±2.08	95.49±3.57	92.67±3.24 [*]	105.6±0.41
MCH	30.19±0.04	30.20±0.09	30.15±0.07	30.18±0.06	30.18±0.07	30.24±0.06
MCHC	35.08±0.85	29.61±0.17 ^a	29.66±0.87	32.72±1.24	32.72±1.24	28.64±0.12

RBC: Red blood cell, Hb: Hemoglobin, PCV: Packed cell volume, MCV: Mean corpuscular volume, MCH: Mean corpuscular haemoglobin, MCHC: Mean corpuscular haemoglobin concentration, Values are expressed as mean ± standard error mean; n=6; ^ap<0.001 in comparison with normal control; ^{*}p<0.05 in comparison with disease control

of *T. indica* leaf extract reversed the effect of PHZ induced anaemia. The treatment resulted in a significant increase in the level of RBC and Hb (p<0.05) and a significant decrease in MCV (p<0.05).

Table 5 represent the changes in RBC, Hb, PCV, MCV, MCH, and MCHC in each group after 14 days of treatment. Administration of PHZ resulted in megaloblastic anaemia characterised by decreases in RBC, Hb, and PCV. Treatment for 14 days with the oral indiffusible mixture of *T. indica* leaf extract reversed the effects of PHZ induced anaemia. There were also increases in MCV and MCH due to PHZ, which indicated macrocytic anaemia. The recovery time for the haematological parameters was low for the lowest dose but there was progressive recovery in RBC, HB, and PCV after 14 days.

All three formulations showed increases in RBC, Hb, and PCV and a decrease in MCV. There was a statistically significant improvement in the level of RBC and Hb (p<0.05) after treatment with TIM2 (200 mg/kg). The improvement seen after treatment with TIM2 was comparable with that of the standard drug. There was no further increase in the levels of RBC or Hb with TIM3 (400 mg/kg). This shows that the response to treatment with the oral indiffusible mixture of *T. indica* leaf extract was dose related. TIM1 caused increases in RBC, Hb, and PCV to submaximal levels when compared to TIM2. There were no large changes in MCH in the groups including the standard, whereas MCV significantly decreased (p<0.05) after treatment with TIM2. However, the short duration of the present study can be considered a limitation; therefore, a longer duration is required for obtaining better responses.

CONCLUSIONS

It is postulated that the presence of flavonoids, phenols, and iron in herbal extracts is responsible for haematinic activity. The oral indiffusible mixture of *T. indica* leaf extract significantly increased the haemoglobin and RBC count in anaemic rats, indicating haematinic activity at a dose of 200 mg/kg. Thus, the oral indiffusible mixture of *T. indica* L. leaf extract was proven

to possess haematinic activity. Further studies are needed to elucidate the mechanism (s) involved in the haematinic activity.

ACKNOWLEDGEMENTS

The authors are grateful to the Faculty of Pharmacy, M. S. Ramaiah University of Applied Sciences, for providing the required facilities and support.

Conflict of Interest: No conflict of interest was declared by the authors.

REFERENCES

1. Stockwell S. Nature's Pharmacy. London: Century Hutchinson Ltd; 1988.
2. Thomson. Medicines from the Earth. Maidenhead, UK: McGraw-Hill Book Co; 1978.
3. Lai PK, Roy J. Antimicrobial and chemopreventive properties of herbs and spices. *Curr Med Chem.* 2004;11:1451-1460.
4. Souza-Fagundes EM, Queiroz AB, Martins Filho OA, Gazzinelli G, Corrêa-Oliveira R, Alves TM, Zani CL. Screening and fractionation of plant extracts with antiproliferative activity on human peripheral blood mononuclear Cells. *Mem Inst Oswaldo Cruz.* 2002;97:1207-1212.
5. Chaudhuri AB. Endangered Medicinal plants, New Delhi: Daya Publishing House; 2001.
6. Ogbe RJ, Aduga GI, Abu AH. Antianemic potentials of some plants extracts on phenyl hydrazine induced anemia in rabbits. *J Medicinal Plants Res.* 2010;4:680-684.
7. Waugh A, Grant A. Ross and Wilson Anatomy and Physiology in health and illness, UK: Elsevier Churchill Livingstone; 2006.
8. Benoist B, McLean E, Cogswell M, Egli I, Wojdyla D, Worldwide prevalence of anaemia, WHO Global Database on Anaemia World Health Organization, Geneva; 2008
9. Tortora GJ, Derrickson BH. Principles of Anatomy and Physiology, NJ: John Wiley and Sons; 2009.
10. Samina KK, Shaikh W, Sofia S, Kazi TK, Amina KK, Usmanhani K, Sheerazi TH, Chemical constituents of *T. indica* L in Sindh. *Pak J Bot.* 2008;40:2553.

11. Havinga RM, Hartl A, Putscher J, Prehler S, Buchmann C, Vogl CR. *Tamarindus indica* L. (Fabaceae): patterns of use in traditional African medicine. *J Ethnopharmacol.* 2010;127:573-588.
12. Izquierdo T, Gracia - Tamayo F, Soto C, Castrillon LE. A *Tamarindus indica* Linn pulp polysaccharide inhibits fever *in-vivo* and IL-1 β release by murine peritoneal exudates cell. *Pharmaceu Bio.* 2007;45:22-30.
13. Khalid S, Shaik Mossadeq WM, Israf DA, Hashim P, Rejab S, Shaberi AM, Mohamad AS, Zakaria ZA, Sulaiman MR. *In Vivo* Analgesic effect of aqueous extract of *Tamarindus indica* L. *Fruits. Med Princ Pract.* 2010;19:255-259.
14. Doughari JH. Antimicrobial activity of *Tarindus indica* Linn. *Trop J Pharmaceu Res.* 2006;5:597-603.
15. Bhadoriya SS, Ganeshpurkar A, Narwaria J, Rai G, Jain AP. *Tamarindus indica*: extent of explored potential. *Pharmacog Rev.* 2011;5:73-81.
16. De Caluwé E, Halamova K, Van Damme P. *Tamarindus indica* L a review of traditional uses, Phytochemistry and Pharmacology. *Afrika Focus.* 2010;23:53-83.
17. Khairunnuur FA Jr, Zulkhairi A, Azrina A, Moklas MM, Khairullizam S, Zamree MS, Shahidan MA. Nutritional composition, *in vitro* antioxidant activity and *Artemia salina* L. lethality of pulp and seed of *Tamarindus indica* L. extracts. *Malays J Nutr.* 2009;15:65-75.
18. Kokate CK. *Practical Pharmacognosy* (4th ed). New Delhi; Vallabh prakashan; 1999.
19. Chukka S, Puligilla S, Yamsani MR. New formulation and evaluation of domperidone suspension. *World J Pharmacy and Pharma Sci.* 2014;3:1867-1884.
20. Dhanapal CK, Manavalan R, Chandar N, Chenthilnathan F. Formulation development of pediatric rifampicin oral suspension. *Der Pharmacia Lettre.* 2012;4:845-853.
21. Weiland RH, Dingman JC, Cronin DB, Browning GJ. Density and Viscosity of Some Partially Carbonated Aqueous Alkanolamine Solutions and Their Blends. *J Chem Eng Data.* 1998;43:378-382.
22. Gaikar NV, Sandhya P, Chaudhari CA. Evaluation of *Curculigo orchoides* Mucilage as Suspending Agent. *Int J Pharm Tech Res.* 2011;3:831-835.
23. Banker SG, Rhodes CT. *Modern Pharmaceutics.* New York, Marcel Dekker; 1998.
24. Patel NK, Kenon L, Levinson RS. *The Theory and Practice of Industrial Pharmacy.* (3rd Indian Edn. Mumbai; Vargheese Publishing House;1986.
25. Ramachander T, Rajkumar D, Sravanprasad M, Goli V, Dhanalakshmi CH, Arjun. Antidiabetic activity of aqueous methanolic extracts of leaf of *Tamarindus indica*. *Int J Pharm Phy Res.* 2012;4:5-7.
26. Ghai CL. *A Text book of Practical Physiology* (6th ed). New Delhi; Jaypee Brothers; 2005.



Quantification of Galantamine in *Sternbergia* Species by High Performance Liquid Chromatography

Sternbergia Türlerinde Yüksek Performanslı Sıvı Kromatografisi ile Galantamin Miktar Tayini

Özlem Bahadır ACIKARA, Betül Sever YILMAZ*, Dilhun YAZGAN, Gülçin Saltan İŞCAN

Ankara University, Faculty of Pharmacy, Department of Pharmacognosy, Ankara, Turkey

ABSTRACT

Objectives: This study describes the qualitative and quantitative analysis of galantamine in *Sternbergia* species growing in Turkey.

Materials and Methods: Galantamine was isolated from *Sternbergia fischeriana* bulbs and the structure of the compound elucidated by spectroscopic methods. The qualitative and quantitative analysis of galantamine was investigated in *Sternbergia lutea* subsp. *lutea*, *S. lutea* subsp. *sicula*, *Sternbergia candida*, *S. fischeriana*, and *Sternbergia clusiana* using a specially developed and validated high performance liquid chromatography (HPLC) method.

Results: *S. lutea* subsp. *sicula* had the highest content of galantamine, i.e., 0.0165 ± 0.0002 g/100 g. The limits of detection and quantification were 7.5 µg and 25 µg, respectively.

Conclusion: Isolation of galantamine from *S. fischeriana* growing in Turkey is reported for the first time. An HPLC method was developed for identification and quantification of galantamine in *Sternbergia* species.

Key words: Galantamine, HPLC, *Sternbergia* spp.

ÖZ

Amaç: Bu çalışmada Türkiye’de yetişen *Sternbergia* türlerinin galantamin içeriklerinin kalitatif ve kantitatif analizi amaçlanmıştır.

Gereç ve Yöntemler: Galantamin *Sternbergia fischeriana* yumrularından izole edilmiş ve yapısı spektroskopik yöntemler kullanılarak aydınlatılmıştır. *Sternbergia lutea* subsp. *lutea*, *S. lutea* subsp. *sicula*, *Sternbergia candida*, *S. fischeriana* ve *Sternbergia clusiana* türlerinin galantamin içeriği kalitatif ve kantitatif olarak yeni geliştirilen ve valide edilmiş bir yüksek performanslı sıvı kromatografisi (HPLC) yöntemi kullanılarak yapılmıştır.

Bulgular: *S. lutea* subsp. *sicula* türünün 0.0165 ± 0.0002 g/100 g olarak en yüksek galantamin içeriğine sahip olduğu belirlenmiştir. Galantamin için saptama ve kantifikasyon sınırı değerleri sırasıyla 7.5 µg ve 25 µg olarak belirlenmiştir.

Sonuç: Türkiye’de yetişen *S. fischeriana* türünden galantamin izolasyonu ilk kez bu çalışma ile rapor edilmiştir. Ayrıca bu çalışma ile *Sternbergia* türlerinin galantamin içeriğinin tespit edilmesi ve miktar tayini için yeni bir HPLC metodu geliştirilmiştir.

Anahtar kelimeler: Galantamin, HPLC, *Sternbergia* spp.

*Correspondence: E-mail: sever@pharmacy.ankara.edu.tr, Phone: +90 532 300 69 94 ORCID-ID: orcid.org/0000-0003-2084-9514

Received: 22.09.2017, Accepted: 28.12.2017

©Turk J Pharm Sci, Published by Galenos Publishing House.

INTRODUCTION

Galantamine is approved by the Food and Drug Administration for the treatment of mild to moderate Alzheimer's disease.¹ Razadyne® (formerly Reminyl®) and Nivalin® are licensed drugs of galantamine, currently available on the market.² This drug inhibits acetylcholinesterase enzyme reversibly and acts as an allosteric modulator of the nicotinic cholinergic receptor. Interaction potentiates cholinergic nicotinic neurotransmission by modulating ion channel activity in the presence of acetylcholine.¹⁻⁴ This drug provides the requisite cholinergic stimulation without producing desensitization. Furthermore, galantamine appears to be a more powerful elevator of frontal cortical dopamine levels compared to other cholinesterase inhibitors such as donepezil.¹ Galantamine exerts neuroprotection on neuronal cell cultures subjected to oxidative stress or amyloid beta stress. Neuroprotection in rat hippocampal slices subjected to oxygen and glucose deprivation followed by a reoxygenation period was also demonstrated by galantamine. Galantamine also acts as a neuroprotective agent in an *in vivo* model of global cerebral ischemia, even when given after the ischemic insult.^{5,6}

Galantamine was firstly isolated from the snowdrop, *Galanthus woronowii*. Generally Amaryllidaceae plants including *Narcissus*, *Galanthus*, *Lycoris*, and *Leucojum* species are used for extraction of galantamine. *Leucojum aestivum* is known as the main source of this compound. *Narcissus* species also contain galantamine in varying amounts from trace amounts to as much as 2.5% of dry weight. Synthetic methods for production of galantamine have been developed; however due to their high cost, plants are still the main sources for galantamine production.⁷

The galantamine content of Amaryllidaceae plants was investigated using different high performance liquid chromatography (HPLC) methods.⁷ An isocratic solvent system consisting of an acetonitrile:methanol:water (containing 7.5 mM triethanolamine, pH 6.9) mixture as mobile phase was used for detecting galantamine on an RP-C8 column in *L. aestivum*.⁸ In another study conducted on *L. aestivum*, an acetonitrile:methanol:buffer pH 4.5 (10:10:80) mixture was used for elution on an RP-C18 column to determine galantamine amount.⁹ Lubbe et al.¹⁰ also reported HPLC analysis of galantamine in *Narcissus pseudonarcissus* on a C18 column using 10% (v/v) acetonitrile in water containing 0.1% trifluoroacetic acid (TFA) as mobile phase. *Galanthus elwesii* was also analyzed for its galantamine content by using a mobile phase comprising a TFA:water:ACN (0.01:90:10) mixture on an RP-

C18 column.¹¹ Petruczynik et al.¹² analyzed galantamine on an RP-C18 column with a mobile phase containing 5% MeCN, 20% acetate buffer at pH 3.5, and 0.025 mL⁻¹ diethylamine as well as on an SCX column using an 8% MeCN and phosphate buffer at pH 2.5 mixture as mobile phase in *L. aestivum*, *Leucojum vernum* var. *carpathicum*, *Galanthus nivalis*, *Zephyranthes rosea*, and *Clivia minata*. The genus *Sternbergia* Waldst. and Kit. (Amaryllidaceae) is represented by eight species and they are widely distributed from the East Mediterranean to Caucasia. In Turkey six taxa of this genus grow naturally.¹³ *Sternbergia* species are well known due to their alkaloid contents, i.e., lycorine and galantamine, with interesting pharmacological properties.^{14,15} Alkaloids including lycorine, homolycorine, haemanthidine, haemanthamine, 6 α - and 6 β -hydroxy-haemanthamine, and tazettine have been isolated from *Sternbergia* species.¹⁴⁻¹⁸ It has been reported that *Sternbergia* species contain especially crinine-type and lycorine-type Amaryllidaceae alkaloids.¹³

In order to investigate new sources for galantamine, *Sternbergia* species were investigated using HPLC in the current study. *Sternbergia lutea*, *Sternbergia sicula*, *Sternbergia fischeriana*, *Sternbergia clusiana*, and *Sternbergia colchiciflora*, which were collected from different locations of Anatolia, were analyzed using HPLC. An isocratic system was developed and used for HPLC analysis. Galantamine, which was isolated from *S. fischeriana* bulbs previously, was used for quantification of the galantamine contents of *S. lutea*, *S. sicula*, *S. fischeriana*, *S. clusiana*, and *S. colchiciflora*.

EXPERIMENTAL

Plant materials

Sternbergia species were collected from different parts of Anatolia as shown in Table 1. Voucher specimens are kept at the Herbarium of Ankara University, Faculty of Pharmacy with their herbarium numbers (Table 1).

Isolation of galantamine

Galantamine was isolated from *S. fischeriana* bulbs. The dried bulbs (500 g) were extracted with ethanol (5 L) by percolation. Ethanolic extract was filtered and concentrated under vacuum at 50°C by evaporation. The pH of the extract was adjusted to 3 by addition of 5% HCl. After filtration CHCl₃ was used for liquid-liquid extraction. The chloroform part was concentrated under vacuum by evaporation to obtain extract A (13.7538 g), which contained lycorine and tazettine. The remaining acidic-water part was extracted with CHCl₃ after addition of alkali solution

Table 1. Plant materials, collected places, and herbarium numbers

Species	Herbarium numbers	Collection sites
<i>Sternbergia candida</i> Mathew & T.Baytop	AEF 23794	Muğla-Fethiye
<i>Sternbergia clusiana</i> (Ker Gawl.) Ker Gawl. ex Sprengel	AEF 23697	Kahramanmaraş-Göksun
<i>Sternbergia fischeriana</i> (Herbert) Rupr.	AEF 23793	Antakya-Yayladağ
<i>Sternbergia lutea</i> subsp. <i>lutea</i> Waldst. & Kit.	AEF 23694	İzmir-Torbalı
<i>Sternbergia lutea</i> subsp. <i>sicula</i> Tineo ex Guss.	AEF 23695	Muğla-Marmaris

(NH₄OH 25% to obtain pH 8). The concentrated chloroform part gave extract B (1.9712 g). Extract B was separated by Chromatotron on aluminum oxide GF Gypsum (Merck 1092) plates. Elution was performed with a CHCl₃:MeOH (9:1) mixture. Fractions 1-4 were subjected to further separation by preparative TLC on precoated TLC sheets (Merck 5744) eluting with CHCl₃:MeOH (85:15) to obtain galantamine (5.04 mg).¹⁹ The structure of the isolated compound was elucidated by ¹H-NMR and comparison of these data with the literature.¹⁹⁻²³

Galantamine: ¹H-NMR (CDCl₃, 400 MHz, δ, ppm, J/Hz): 6.63 (1H, d, J=8 Hz, H-12); 6.53 (1H, d, J=8 Hz, H-11); 6.02 (1H, d, J=10.3 Hz, H-4); 6.00 (1H, d, J=10.3 Hz, H-3); 4.47 (1H, brs, H-16); 4.10 (1H, m, H-2α); 4.06 (1H, d, J=15.2 Hz, H-9β); 3.98 (1H, d, J=15.2 Hz, H-9α); 3.05 (1H, m, H-7α); 2.95 (1H, m, H-7β); 2.56 (1H, m, H-1α), 2.45 (1H, m, H-1β); 1.50 (1H, m, H-6α); 1.47 (1H, m, H-β), 3.72 (s, O-CH₃), 2.51 (s, N-CH₃).

HPLC analysis

HPLC analyses were carried out using an Agilent LC 1100 model chromatograph (Agilent Technologies, Inc., Santa Clara, CA, USA). The diode-array detector was set at wavelength 292 nm and peak areas were integrated automatically by computer using Agilent software. The chromatograms were plotted and processed using the above-mentioned software. Separation was carried out using a SUPELCOSIL LC-18 column (250×4.6 mm i.d.; 5 μm; Supelco, Bellefonte, PA, USA). The mobile phase was made up of ammonium carbonate (Laboratory BDH Reagent, Poole, UK) water solution (purified water was obtained by using Milli-Q Plus System (Millipore Corp., Molsheim, France) and acetonitrile (HPLC grade 99.93 % purity, Sigma-Aldrich 270717) (85:15 v/v) applied at a flow rate of 1 mL/min, column temperature 24°C, and 20 μL portions were injected into the liquid chromatography system.

Preparation of standard and sample solutions

Standard stock solution was prepared in 1 mg/mL concentration. First 10 mg of galantamine was weighed in a 10 mL volumetric flask and then it was dissolved in 10 mL of 1% H₂SO₄. Different concentration levels (0.025 mg/mL, 0.05 mg/mL, 0.075 mg/mL, 0.1 mg/mL, 0.2 mg/mL, 0.3 mg/mL, and 0.4 mg/mL) were prepared by diluting the stock solution.

Sample solutions were prepared by extraction of dried and powdered bulbs (10 g) of each plant with 1% H₂SO₄ by rinsing at room temperature for 7 days. The extraction procedure was tested with Mayer's reagent to be sure all alkaloids were extracted. Each extract was filtered through a 0.45-mm membrane filter and adjusted to a final volume of 500 mL with acidic solution.

Limits of detection and quantification

The limit of detection (LOD) and limit of quantification (LOQ) were established at a signal to noise ratio (S/N) of 3 and 10, respectively. LOD and LOQ concentrations were experimentally verified by six injections of galantamine. The precision of the method (intra-day variations of replicate determinations) was checked by injecting galantamine nine times at the LOQ level.

RESULTS AND DISCUSSION

To date, any *Sternbergia* species growing in Turkey has been reported that does not contain galantamine. In addition, galantamine has not been determined in any *Sternbergia* species growing in Turkey. However in the present study galantamin was detected and quantified in *Sternbergia* species.^{13,24} This study led to the isolation of this compound from the bulbs of *S. fischeriana* collected from Yayladağ in Antakya Province. Additionally, the current study describes the development of a method for identifying and quantifying galantamine in *Sternbergia* species. Good separation and determination of this compound were achieved using a mobile phase consisting of ammonium carbonate and acetonitrile (85:15 v/v) on a SUPELCOSIL LC-18 column (250×4.6 mm×5 μm) at wavelength 292 nm as shown in Figures 1 and 2.

LOD and LOQ values were 7.5 μg and 25 μg, respectively. Table 2 shows the wavelength measured, the calculated calibration curve, and the LOD and LOQ results for this compound. The precision of the method is expressed as the relative standard

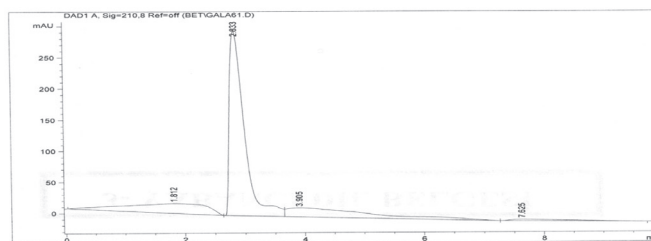


Figure 1. HPLC chromatogram of galantamine

HPLC: High performance liquid chromatography, DAD: Diode-array detector

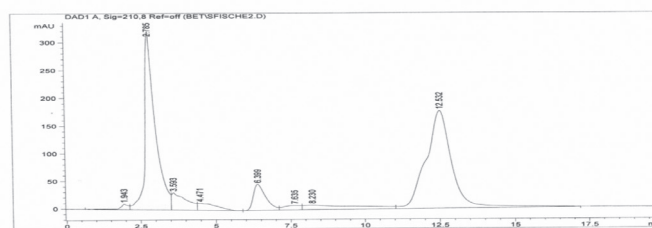


Figure 2. HPLC chromatogram of *Sternbergia fischeriana*

HPLC: High performance liquid chromatography, DAD: Diode-array detector

Table 2. Linearity results, LOQ, and LOD

Compound	λ	Equation	r ²	Slope RSD %	Intercept RSD %	LOQ (μg)	LOD (μg)
Galantamine	292	Y=118484.33X + 448.2	0.995	2.0594	4.4493	25	7.5

LOQ: Limit of quantification, LOD: Limit of detection, RSD: Relative standard deviation

Table 3. Galantamine contents of *Sternbergia* species

Species	Galantamine % (n=3, mean \pm standard deviation)
<i>Sternbergia candida</i>	0.0092 \pm 0.0005
<i>Sternbergia clusiana</i>	0.0077 \pm 0.0001
<i>Sternbergia fischeriana</i>	0.0069 \pm 0.0006
<i>Sternbergia lutea</i> subsp. <i>lutea</i>	0.0100 \pm 0.0005
<i>Sternbergia lutea</i> subsp. <i>sicula</i>	0.0165 \pm 0.0002

deviation at the LOQ level.

The presence of galantamine (Figure 3) in *S. lutea* subsp. *lutea*, *S. lutea* subsp. *sicula*, *S. candida*, *S. fischeriana*, and *S. clusiana* was analyzed quantitatively and qualitatively by HPLC. The current study results, as shown in Table 3, revealed that all plant samples contain galantamine and the highest content was determined in *S. lutea* subsp. *sicula* (0.0165 \pm 0.0002% dw) followed by *S. lutea* subsp. *lutea* (0.0100 \pm 0.0005% dw). According to previous studies, *G. woronowii* and *L. aestivum* contain 0.003–0.506% and 0.0028–0.2104% galantamine, respectively.^{25,26} The galantamine content ranged from 0.05 to 0.36 mg/g dw in the bulbs of *G. nivalis* and from 0.3 to 0.033 mg/g dw in the bulbs of *Narcissus tazetta* samples collected from different locations in Iran. According to the results, geographical regions and cultural practices affected the chemical composition of the plants. The chemical variations can be attributed to environmental factors.⁷ *L. aestivum* plants collected during different periods of vegetation were analyzed for their galantamine contents and the amounts were determined as 0.13% and 0.14%, respectively, for the plant in bloom and fructification, respectively.⁹ According to Petruczynik et al.¹², different extraction procedures such as maceration, extraction in an ultrasonic bath, and extraction in an ultrasonic bath following maceration yielded different amounts of galantamine. Galantamine content in *L. aestivum* was determined as 0.0196 mg/mL, 0.0273 mg/mL, and 0.0949 mg/mL, respectively, by the mentioned extraction procedures. Ultrasonic bath extraction following maceration induced a relatively high amount of galantamine extraction. In the same study the highest amount of galantamine was determined in *L. aestivum* roots with 2.3524 mg/g dw, followed by leaves with

1.6611 mg/g dw. *Z. rosea* bulbs and *C. minata* leaves as well as roots were found to contain 0.8384 mg/g dw and 0.1489 mg/g dw, and 0.0284 mg/g dw galantamine, respectively. In all parts of *G. nivalis* galantamine content varied from 0.0003 mg/g dw to 0.0178 mg/g dw. *G. elwesii* samples collected from two different locations in Turkey, İzmir and Karaburun, contained 0.026% and 0.007% galantamine, respectively.¹¹ The amount of galantamine also varied from 2.36 mg/g dw to 3.32 mg/g dw in *N. pseudonarcissus* bulbs collected from the Netherlands.¹⁰ According to our results, galantamine content of the *Sternbergia* species was lower than that of *L. aestivum* when they were compared. The current study's results revealed that *Sternbergia* species are not valuable sources for galantamine extraction. Differences in galantamine content among all the investigated species could be explained by the existence of chemotype. Furthermore, a number of factors such as temperature, season, stages of maturity, geographical origin, climatic conditions, and soil can affect the phytochemical content of plants.^{27,28} Plants cultivated under different conditions exhibit an alteration in the quantity of phytochemicals and therefore display varied therapeutic effects.^{29,30}

CONCLUSIONS

The present study is the first report of galantamine isolation from *Sternbergia* species growing in Turkey. An HPLC method was developed for identification and quantification of galantamine in the genus *Sternbergia*. The presence of galantamine could be related to growing conditions such as temperature, season, climatic conditions, soil, or stages of maturity as well as geographical origin. Chemotype of the mentioned species could be also the reason for the presence of galantamine in *Sternbergia* species. Therefore, further studies will be planned to investigate *Sternbergia* species collected from different locations in Turkey for their galantamine contents.

Conflict of Interest: No conflict of interest was declared by the authors.

REFERENCES

- Lindenmayer JP, Khan A. Galantamine augmentation of long-acting injectable risperidone for cognitive impairments in chronic schizophrenia. *Schizophr Res.* 2011;125:267-277.
- Berkov S, Codina C, Bastida J. A Global Perspective of Their Role in Nutrition and Health. In *Tech*, Rijeka-Croatia 2012:235-254.
- Heinrich M, Lee Teoh H. Galantamine from snowdrop-The development of a modern drug against Alzheimer's disease from local caucasian knowledge. *J Ethnopharmacol.* 2004;92:147-162.
- Wattmo C, Wallin AK, Minthon L. Progression of mild Alzheimer's disease: knowledge and prediction models required for future treatment strategies. *Alzheimer Res Ther.* 2013;5:44.
- Madrigal JL, Garcia-Bueno B, Caso JR, Perez-Nievas BG, Leza JC. Stress-induced oxidative changes in brain. *CNS Neurol Disord Drug Targets.* 2006;5:561-568.
- Sethi G, Sung B, Aggarwal BB. Nuclear factor-kappaB activation: from bench to bedside. *Exp Biol Med (Maywood).* 2008;233:21-31.

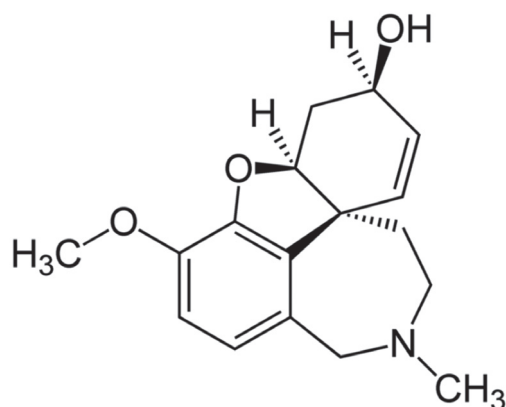


Figure 3. Structure of galantamine

7. Khonakdari MR, Mirjalili MH, Gholipour A, Rezadoost H, Farimani MM. Quantification of galantamine in *Narcissus tazetta* and *Galanthus nivalis* (Amaryllidaceae) populations growing wild in Iran. *Plant Genet Resour.* 2018;16:188-192.
8. Pavlov A, Berkov S, Courot E, Gocheva T, Tuneva D, Pandova B, Georgiev M, Georgiev V, Yanev S, Burrus M, Ilieva M. Galanthamine production by *Leucojum aestivum* *in vitro* systems. *Process Biochem.* 2007;42:734-739.
9. Klosi R, Mersinllari M, Gavani E. Galantamine content in *Leucojum aestivum* populations grown in northwest Albania. *AJPhSci.* 2016;3:1-3.
10. Lubbe A, Pomahacova B, Choi YH, Verpoorte R. Analysis of Metabolic Variation and Galanthamine Content in Narcissus Bulbs by ¹H NMR. *Phytochem Anal.* 2010;21:66-72.
11. Kaya GI, Çiçek Polat D, Emir A, Bozkurt Sarıkaya B, Onur MA, Ünver Somer N. Quantitative Determination of Galantamine and Lycorine in *Galanthus elwesii* by HPLC-DAD. *Turk J Pharm Sci.* 2014;11:107-112.
12. Petruczynik A, Misiurek J, Tuzimski T, Uszynski R, Szymczak G, Chernetsky M, Waksmundzka-Hajnos M. Comparison of different HPLC systems for analysis of galantamine and lycorine in various species of Amaryllidaceae family. *J Liq Chromatogr Relat Technol.* 2016;39:574-579.
13. Saltan Çitoğlu G, Sever Yılmaz B, Bahadır Ö. Quantitative analysis of lycorine in *Sternbergia* species growing in Turkey. *Chem Nat Comp.* 2008;44:826-828.
14. Çitoğlu GS, Acikara OB, Yılmaz BS, Ozbek H. Evaluation of analgesic, anti-inflammatory and hepatoprotective effects of lycorine from *Sternbergia fisheriana* (Herbert) Rupr. *Fitoterapia.* 2012;83:81-87.
15. Tanker M, Çitoğlu GS, Gümüşel B, Şener B. Alkaloids of *Sternbergia clusiana* and their analgesic effects. *Int J Pharmacog.* 1996;34:194-197.
16. Çitoğlu GS. Alkaloids of *Sternbergia candida* Mathew & T. Baytop. *J Fac Phar Gazi.* 1998;15:93.
17. Çitoğlu GS, Tanker M, Gümüşel B. Antiinflammatory effects of lycorine and haemanthidine. *Phytother Res.* 1996;12:205.
18. Yurdaşık D. Pharmacognostical Researches on the Alkaloids of *Sternbergia fisheriana*. Ankara. Master Thesis, Ankara University; 2005.
19. Bastida J, Viladomat F, Llabrés JM, Codina C, Feliz M, Rubiralta M. Alkaloids from *Narcissus confusus*. *Phytochemistry.* 1987;26:1519-1524.
20. Harlem D, Martin MT, Thal C, Guillou C. Synthesis and structure activity relationships of open d-ring galanthamine analogues. *Bioorg Med Chem Lett.* 2003;13:2389-2391.
21. Liang PH, Liu JP, Hsin LW, Cheng CY. Intramolecular Heck Cyclization to the Galanthamine-type Alkaloids: Total Synthesis of (±)-Lycoramine. *Tetrahedron.* 2004;61:11655-11660.
22. Berkov S, Sidjimova B, Eustatieva L, Popov S. Intraspecific variability in the alkaloid metabolism of *Galanthus elwesii*. *Phytochemistry.* 2004;65:579-586.
23. Kaya Gİ. *Sternbergia* Waldst. & Kit. türlerinin kimyasal bileşikleri ve biyolojik aktiviteleri. *Marmara Pharm.* 2001;15:52-57.
24. Çiçek D, Ünver Somer N, Kaya Gİ. Quality control and anticholinesterase activity determinations on *Sternbergia sicula*. *Marmara Pharm.* 2010;14:121-124.
25. Emir A, Çiçek Polat D, Kaya GI, Sarıkaya B, Onur MA, Ünver Somer N. Simultaneous determination of lycorine and galanthamine in *Galanthus woronowii* by HPLC-DAD. *Acta Chromatogr.* 2013;25:755-764.
26. Georgieva L, Berkov S, Kondakova V, Bastida J, Viladomat F, Atanassov A, Codina C. Alkaloid variability in *Leucojum aestivum* from wild populations. *Z Naturforsch C.* 2007;62:627-635.
27. Banerjee SK, Bonde CG. Total phenolic content and antioxidant activity of extracts of *Bridelia retusa* Spreng Bark: Impact of dielectric constant and geographical location. *J Med Plants Res.* 2011;5:817-822.
28. Gull J, Sultana B, Anwar F, Naseer F, Ashraf M, Ashrafuzzaman M. Variation in Antioxidant Attributes at Three Ripening Stages of Guava (*Psidium guajava* L.) Fruit from Different Geographical Regions of Pakistan. *Molecules.* 2012;17:3165-3180.
29. Sun YF, Liang ZS, Shan CJ, Viernstein H, Unger F. Comprehensive evaluation of natural antioxidants and antioxidant potentials in *Ziziphus jujuba* Mill. var. *spinosa* (Bunge) Hu ex H. F. Chou fruits based on geographical origin by TOPSIS method. *Food Chem.* 2011;124:1612-1619.
30. Kolawole OT, Ayankunle AA. Seasonal Variation in the Anti-Diabetic and Hypolipidemic Effects of *Momordica charantia* Fruit Extract in Rats. *Eur J Med Plant.* 2012;2:177-185.



Antiplasmodial Activity of the *n*-Hexane Extract from *Pleurotus ostreatus* (Jacq. ex. Fr) P. Kumm.

Pleurotus ostreatus (Jacq. ex. Fr) P. Kumm. *n*-Hekzan Ekstresinin Antiplazmodiyal Etkisi

© Ozadheoghene Eriarie AFIEROHO^{1*}, © Xavier Siwe NOUNDOU², © Chiazor P. ONYIA¹, © Osamuyi H. FESTUS¹, © Elizabeth C. CHUKWU¹, © Olutayo M. ADEDOKUN³, © Michelle ISAACS⁴, © Heinrich C. HOPPE⁴, © Rui WM. KRAUSE², © Kio A. ABO¹

¹University of Port Harcourt, Faculty of Pharmaceutical Sciences, Department of Pharmacognosy and Phytotherapy, Port Harcourt, Nigeria

²Rhodes University, Faculty of Science, Department of Chemistry, Grahamstown, South Africa

³University of Port Harcourt, Faculty of Agriculture, Department of Crop and Soil Sciences, Port Harcourt, Nigeria

⁴Rhodes University, Faculty of Science, Department of Biochemistry and Microbiology, Grahamstown, South Africa

ABSTRACT

Objectives: Several mushrooms species have been reported to be nematophagous and antiprotozoan. This study reported the antiplasmodial and cytotoxic properties of the *n*-hexane extract from the edible mushroom *Pleurotus ostreatus* and the isolation of a sterol from the extract.

Materials and Methods: Antiplasmodial and cytotoxicity assays were done *in vitro* using the plasmodium lactate dehydrogenase assay and human HeLa cervical cell lines, respectively. The structure of the isolated compound from the *n*-hexane extract was elucidated using spectroscopic techniques.

Results: The *n*-hexane extract (yield: 0.93% w/w) showed dose dependent antiplasmodial activity with the trend in parasite inhibition of: chloroquine (IC₅₀=0.016 µg/mL) > *n*-hexane extract (IC₅₀=25.18 µg/mL). It also showed mild cytotoxicity (IC₅₀>100 µg/mL; selectivity index >4) compared to the reference drug emetine (IC₅₀=0.013 µg/mL). The known sterol, ergostan-5,7,22-trien-3-ol, was isolated and characterized from the extract.

Conclusion: This study reporting for the first time the antiplasmodial activity of *P. ostreatus* revealed its nutraceutical potential in the management of malaria.

Key words: *Pleurotus ostreatus*, nutraceuticals, malaria, cytotoxicity, ergosterol

ÖZ

Amaç: Bazı mantar türlerinin nematofagöz ve antiprotozoan olduğu bildirilmiştir. Bu çalışmada, yenilebilir mantar *Pleurotus ostreatus* *n*-hekzan ekstresinin antiplazmodiyal ve sitotoksik etkileri araştırılmış ve ekstreten bir sterol izolasyonu yapılmıştır.

Gereç ve Yöntemler: Antiplazmodiyal ve sitotoksikite deneyleri, sırasıyla, plasmodium laktat dehidrojenaz analizi ve insan HeLa servikal hücre hatları kullanılarak *in vitro* gerçekleştirilmiştir. *n*-Hekzan ekstresinden izole edilen bileşiğin yapısı, spektroskopik teknikler kullanılarak aydınlatılmıştır.

Bulgular: *n*-Hekzan ekstresi (verim: %0.93 a/a) parazit inhibisyonunda doza bağlı antiplazmodiyal aktivite gösterdi: klorokin (IC₅₀=0.016 µg/mL) > *n*-hekzan ekstresi (IC₅₀=25.18 µg/mL). Ayrıca referans ilaç emetine kıyasla (IC₅₀=0.013 µg/mL) hafif sitotoksikite (IC₅₀>100 µg/mL; seçicilik indeksi >4) gösterdi. Bilinen sterol bileşiği ergostan-5,7,22-trien-3-ol izole edildi ve yapısı tayin edildi.

Sonuç: *P. ostreatus*'un antiplazmodiyal aktivitesini ilk kez rapor eden bu çalışma, sıtma tedavisindeki nutrasötik potansiyelini ortaya koymuştur.

Anahtar kelimeler: *Pleurotus ostreatus*, nutrasötik, malarya, sitotoksikite, ergosterol

*Correspondence: E-mail: ozadheoghene.afihero@uniport.edu.ng, Phone: +2348063432417 ORCID-ID: orcid.org/0000-0002-5847-161X

Received: 03.12.2017, Accepted: 18.01.2018

©Turk J Pharm Sci, Published by Galenos Publishing House.

INTRODUCTION

The scourge of malaria infections has continued to be a global health burden, with countries in Sub-Saharan Africa contributing about ninety percent.¹ Children and expectant mothers are the worst hit with attendant high mortality if not treated promptly. Malaria remains a threat to the poor people living in endemic regions, where access to quality health facilities is limited and the cost of orthodox drugs is high. More worrisome is the high occurrence of drug resistant *Plasmodium falciparum* strains of the causative parasite. These obstacles to receiving effective treatment for malaria have led to the continued search for new anti-malarial agents that are relatively nontoxic. Bioactive metabolites from nature's flora and fauna are veritable leads in drug development. Mushrooms are basidiomycetous fungi and the edible ones are popular not only for their nutritive value but also as functional foods in the treatment of various diseases. The antiparasitic properties of some mushrooms and closely related fungi species have been reported. Some of these include: the antimalarial properties of *Cordyceps* species² and *Bulgaria inquinans*,³ and the amoebicidal⁴ and anti-trypanosomiasis⁵ properties of *Pleurotus ostreatus*. Other reported biological activities include nematocidal,⁶ anti-inflammatory and immunomodulatory,⁷ and anticancer^{8,9} properties among others. As a follow up to earlier reports on the scientific validation of the health benefits and the characterization of bioactive secondary metabolites from indigenous edible mushrooms in Nigeria,¹⁰⁻¹³ the present study aimed to determine the nutraceutical potentials of the *n*-hexane extract (NHE) of the fruiting bodies of the edible mushroom *P. ostreatus* in the management of malaria infections.

EXPERIMENTAL

Collection of mushroom samples

P. ostreatus (fresh fruiting bodies) was collected from the Dilomat farm, Rivers State University of Science and Technology, Port Harcourt, Rivers State, and identified by a mycologist in the Department of Crop and Soil Sciences, Faculty of Agriculture, University of Port Harcourt, Port Harcourt, Rivers State. After due authentication, a voucher specimen (UPH/C/075) was deposited at the herbarium of the Department of Plant Science and Biotechnology of the same university. The fresh fruiting bodies of *P. ostreatus* were chopped into small pieces, after which they were dried under a current of air in a dehumidified environment. The dried samples were pulverized using an electric blender.

Preparation of extract

The dried pulverized fruiting body (362.1 g) was cold macerated for 72 h with *n*-hexane with fresh replacement of solvent at 24-h intervals to obtain the NHE. The NHE was concentrated using a rotary evaporator (Model RE52A, Labscience made in India for England) and used for this study.

Phytochemical methods

Confirmatory phytochemical tests were carried out on the extract using standard phytochemical screening reagents.^{14,15}

Isolation and purification of compound 1

The bioactive NHE (1g) was dissolved in *n*-hexane and pre-adsorbed on silica gel in the ratio of 1:1 w/w to form a homogeneous paste, which was allowed to air dry in a fume cupboard. The mixture was loaded on a chromatography column (internal diameter 4.1 cm and packed with normal phase silica gel mesh 200-400 to a height of 27 cm). The column was eluted with gradient of increasing order of polarity: *n*-hexane (100%, 500 mL), *n*-hexane:dichloromethane (1:1, 500 mL), and dichloromethane (100%, 500 mL). After thin layer chromatography (TLC) examination of the eluates, they were pooled into 3 subfractions: F1-F3. F2 eluted with *n*-hexane:dichloromethane (1:1) yielded a white solid compound 1 (Figure 1) after re-crystallizing with acetone. Its purity was determined using TLC performed on plates pre-coated with silica gel 60 HF₂₅₄ (Merck, TLC grade, with gypsum binder). The TLC bands were visualized by exposure to iodine and by spraying with concentrated H₂SO₄ using a spray gun. Complementary purity confirmation by melting point determination was recorded on an electrothermal melting point apparatus and the results are uncorrected.

The ¹H and ¹³C-NMR spectra of compound 1 (Figure 1) were recorded at 300 MHz (75 MHz for ¹³C-NMR analysis) on a Bruker Avance spectrometer in deuterated CDCl₃. Chemical shifts are expressed in parts per million (ppm) downfield of trimethylsilane as internal reference for ¹H resonances, and referenced to the central peak of the appropriate deuterated solvent's resonances. Infrared spectra were recorded on a 1600 ATI Matson Genesis series FTIR™ spectrometer. Mass spectra were recorded on a FINNIGAN MAT 12 spectrometer. Unambiguous assignment of the positions was done using two-dimensional nuclear magnetic resonance (2D-NMR) experiments like heteronuclear multiple bond correlation (HMBC), heteronuclear single quantum correlation (HSQC), and proton-proton correlation spectroscopy (H-H-COSY).

Cell viability assay

Briefly mammalian HeLa cells were plated in 96-well plates at 2×10⁴ cell per well in 150 μL the culture medium. The culture medium was prepared from Dulbecco's Modified Eagle's Medium supplemented with 5 mM L-glutamine, 10% (v/v) fetal bovine serum, and antibiotics (penicillin/streptomycin/amphotericin B). After overnight incubation in a 5% CO₂ humidified incubator, various concentrations (0.006104-100 μg/mL) of the test samples prepared following a 10-fold serial dilutions approach in 96-well plates were added to the cultures (duplicate wells; 200 μL of final culture volume) and incubation continued for an additional 48 h. The viability of cells in individual wells was assessed by adding 20 μL of resazurin toxicology reagent (Sigma-Aldrich) per well and measuring fluorescence intensity (exc. 560 nm/em. 590 nm) in a Spectramax M3 plate reader after incubation for 2 h. Fluorescence readings in experimental wells were converted to % cell viability relative to control wells containing untreated cells and used to obtain dose-response plots of mean % cell viability against log (test sample concentration) using the nonlinear regression function

of Microsoft Excel 2007 software with the median inhibition concentration IC_{50} values derived from the plot by extrapolation. Emetine of various concentrations (0.00000325–32.5 $\mu\text{g/mL}$) prepared following a 10-fold serial dilutions approach in 96-well plates was used as standard drug for comparison.

Plasmodium falciparum growth inhibition assay

Briefly, the *P. falciparum* (3D7 strain) parasites were maintained in medium composed of RPMI 1640 supplemented with 2

mM L-glutamine, 25 mM Hepes (buffered between a pH of 7.2 and 7.4), 5% (w/v) Albumax II, 20 mM glucose, 0.65 mM hypoxanthine, 60 $\mu\text{g/mL}$ gentamicin sulfate, and 2–4% (v/v) human red blood cells, in an atmosphere containing a mixture of O_2 , CO_2 , and N_2 (5:5:90 v/v/v). For the growth inhibition assays, parasite cultures were adjusted to 2% parasitaemia and 1% haematocrit (final) and incubated for 48 h, after addition of the test samples (final test concentrations range of 0.006104–100 $\mu\text{g/mL}$ prepared in duplicate following a 4-fold serial dilutions

Table 1. Spectral data of compound 1 isolated from the n-hexane extract of *Pleurotus ostreatus*

S/No.	δ_c ppm	DEPT-135	Published ¹⁷ δ_c ppm	δ_H ppm	H-multiplicity	H-H-COSY	HMBC
1	38.4	CH ₂	38.4	2.08	2 Hm	H ₋₂	C ₋₃
2	32.0	CH ₂	32.0	1.52, 1.91	2 Hm	H _{-3'} , H _{1a}	
3	70.5	CH	70.4	3.65	1 Hm	H _{-2a}	
3-OH	-	-	-				
4	40.8	CH ₂	40.8	2.32	2 Hm	H ₋₃	C ₋₃
5	139.8	C	139.8	-			
6	119.6	CH	119.6	5.60	1 Hd	H ₋₇	C _{-5'} , C ₋₁₀
7	116.3	CH	116.3	5.42	1 Hd	H ₋₆	
8	141.4	C	141.3	-			
9	46.3	CH	46.2	1.99	1 Hm		
10	37.0	C	37.0				
11	21.1	CH ₂	21.1	1.65, 1.70	2 Hm		
12	39.1	CH ₂	39.1	2.05	2 Hm		
13	42.8	C	42.8				
14	54.6	CH	54.6	1.92	1 Hm		
15	23.0	CH ₂	23.0	1.40, 1.70	2 Hm		
16	28.3	CH ₂	28.3	1.38, 1.80	2 Hm		
17	55.8	CH	55.7	1.30	1 Hm		
18	12.0	CH ₃	12.0	0.65	3 Hs		
19	17.6	CH ₃	17.6	0.93	3 Hs		
20	40.4	CH	40.4	2.48	1 Hm		
21	21.1	CH ₃	21.1	1.05	3 Hd (J=6 MHz)		
22	135.6	CH	135.6	5.25	1 Hdd		C _{-20'} , C ₂₃
23	132.0	CH	132.1	5.20	1 Hdd		C ₋₂₀
24	42.8	CH	42.8	1.90	1 Hd		
25	33.1	CH	33.1	1.52	1 Hm	H _{-26'} , H _{-24'} , H ₋₂₇	
26	19.9	CH ₃	19.8	0.86	3 Hd (J=6 MHz)	H ₋₂₅	
27	19.6	CH ₃	19.6	0.84	3 Hd (J=6 MHz)	H ₋₂₅	
28	16.3	CH ₃	17.8	0.97	3 Hd (J=6 MHz)		

s: Singlet, d: Doublet, dd: Doublet of doublet, m: Complex multiplet, HSQC: Heteronuclear single quantum correlation, H-H-COSY: Proton-proton correlation spectroscopy, HMBC: Heteronuclear multiple bond correlation

approach in 96-well plates (200 μL culture/well; two wells per test sample dilution). After the incubation period, the levels of parasite were determined by colorimetric determination of parasite lactate dehydrogenase activity.¹⁶ Chloroquine (eight final test concentrations within the range 0.00000516129–51.6129 $\mu\text{g}/\text{mL}$) prepared following 10-fold serial dilution was used as standard antimalarial drug for comparison. At 620 nm the absorbance values in the wells containing test samples and standard drug (chloroquine) were converted to percentage parasite viability relative to the wells containing untreated parasite cultures. The median pLDH inhibition concentration (IC_{50}) values were derived from graphs of mean % parasite viability against log (test sample concentration) using the nonlinear regression function of Microsoft Excel 2007 software.

RESULTS

Phytochemical analysis of the NHE and structural elucidation of compound 1: The NHE was found to contain isoprenoids (triterpenoid/steroids, cardenolides) and fatty acids as metabolites from phytochemical screening using appropriate standard reagents. Compound 1 (Figure 1) was isolated and characterized from the NHE after chromatography separation and spectroscopic analysis, respectively.

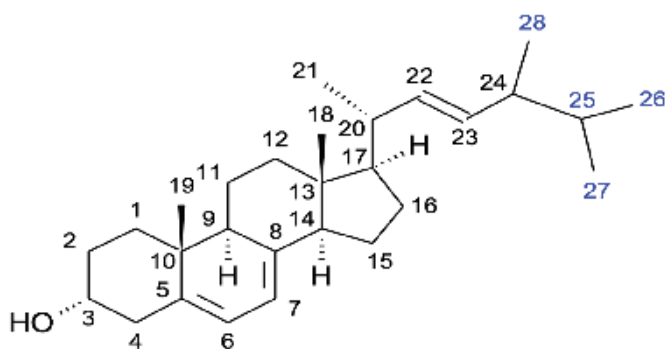


Figure 1. Compound 1: Ergosteran-5,6,22-trien-3-ol (ergosterol)

Structural elucidation/characterization of isolated compound 1:

Appearance: White solid;

Melting point: 155–160°C;

Solubility: Freely soluble in chloroform, dichloromethane;

Molecular Mass: 396.7 (calculated for $\text{C}_{28}\text{H}_{44}\text{O}$).

IR spectrum: [frequency, V, cm^{-1}]: 3412; 3404 [OH str], 3060 [=CH str], 2951; 2868 [CH_2/CH_3 str], 1655; 1600 [C=C str], 1053/1030 [C-O str], 727 [CH_2 rocking].

EI-Mass spectrum: [m/z (rel. int)]: 396 (62.66) [M^+], 378 [$\text{M}^+ - \text{H}_2\text{O}$], 363 (42.96) [$\text{M}^+ - (18+15)$], 271 (20.45) [$\text{M}^+ - \text{aliphatic chain}$], 253 (30.95) [$\text{M}^+ - \text{H}_2\text{O} - \text{aliphatic chain}$], 285 [$\text{M}^+ - \text{H}_2\text{O} - 15\text{-ring A}$], 69 (100), 55 (80.83), 57 (43.95), 43 (74.37).

$^1\text{H-NMR}$ (300 MHz, CDCl_3 , δppm): Details of the spectra data are presented in Table 1.

$^{13}\text{C-NMR}$ (75 MHz, CDCl_3 , δppm): Details of the spectra data are presented in Table 1.

Cytotoxicity activity: A marked onset of cytotoxicity for the NHE (Figure 2, Table 2) was observed at the highest screened concentration of 100 $\mu\text{g}/\text{mL}$ ($\approx 75\%$ cell viability translating to $\approx 25\%$ cell death and a selectivity index >4). This is indicative of low cytotoxicity ($\text{IC}_{50} > 100 \mu\text{g}/\text{mL}$) compared to the reference drug emetine with $\text{IC}_{50} = 0.013 \mu\text{g}/\text{mL}$.

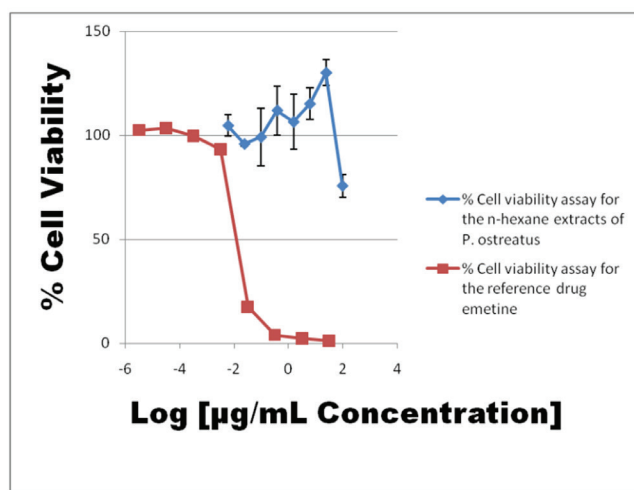


Figure 2. Dose dependent mammalian HeLa cell viability profile of the n-hexane extracts of *Pleurotus ostreatus*

Antiplasmodial activity

The NHE inhibited *Plasmodium* parasite lactate dehydrogenase activity in a dose dependent manner *in vitro* (Figure 3, Table 2) with a median inhibition concentration (IC_{50}) of 25.18 $\mu\text{g}/\text{mL}$.

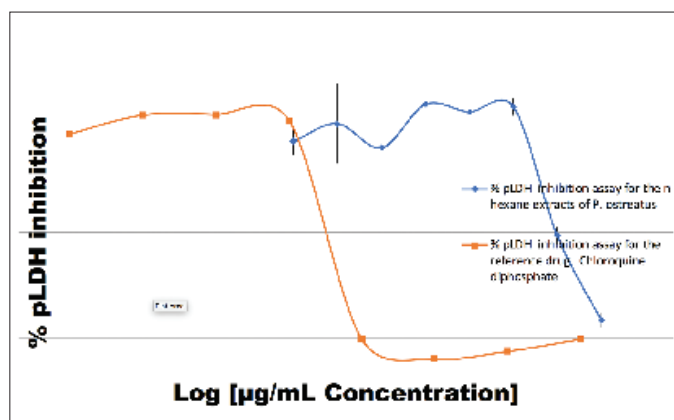


Figure 3. Dose dependent plasmodium parasite growth inhibition profile of the n-hexane extracts of *Pleurotus ostreatus*

mL . It was, however, significantly ($p=0.02$, <0.05) less active compared to the standard drug chloroquine diphosphate ($\text{IC}_{50} = 0.016 \mu\text{g}/\text{mL}$); see Figure 3 and Table 2.

DISCUSSION

The *Plasmodium* pLDH is an essential energy-producing enzyme. It is the last enzyme in the parasite glycolytic pathway. It is produced by both the sexual and asexual stages

Table 2. pLDH inhibition and mammalian cell (HeLa) viability assay results for the n-hexane extract from *Pleurotus ostreatus* fruiting bodies

n-hexane extracts			Reference drug Emetine		Reference drug	Chloroquine diphosphate
Concentration $\mu\text{g/mL}$	pLDH inhibition %	Cell viability %	Concentration $\mu\text{g/mL}$	Cell viability %	Concentration $\mu\text{g/mL}$	pLDH inhibition %
0.006	93.160 \pm 6.067	104.670 \pm 5.054	0.00000325	102.571	0.00000516129	9.677.495
0.024	101.742 \pm 19.000	95.809 \pm 1.053	0.0000325	103.607	0.0000516129	1.056.567
0.098	90.250 \pm 2.164	99.096 \pm 13.659	0.000325	99.648	0.000516129	1.059.009
0.391	110.896 \pm 0.239	111.970 \pm 11.730	0.00325	93.383	0.00516129	1.033.283
1.563	107.290 \pm 4.063	106.438 \pm 13.305	0.0325	17.465	0.0516129	0.032861
6.250	109.731 \pm 4.222	115.149 \pm 7.605	0.325	3.878	0.5161289	-946.859
25.000	48.751 \pm 3.997	130.106 \pm 6.337	3.250	2.282	5.161.289	-591.963
100.000	8.830 \pm 3.466	75.664 \pm 5.530	32.50	1.032	516.129	-0.2488
IC ₅₀ ($\mu\text{g/mL}$)	25.179 \pm 2.456	>100	0.013		0.016	
Selectivity index	>4	NA		NA		NA

pLDH: Plasmodium lactate dehydrogenase

of parasites, as well as the mature gametocytes of all human *Plasmodium* species.¹⁸⁻²⁰ The parasite and erythrocytic cells (human host) lack a complete citric acid cycle for mitochondrial ATP production, making dependence on anaerobic glucose metabolism an imperative. Thus, the pLDH plays an important role in catalyzing energy production in the parasite.^{18,21} The activity of the enzyme pLDH is reported to disappear within 24 h of effective malaria treatment.²¹ The pLDH antigen is considered a specific marker for the presence of viable plasmodium in blood. A report by the United States National Cancer Institute regards plant extract with cytotoxic IC₅₀ 20 $\mu\text{g/mL}$ or lower as being highly cytotoxic.²²⁻²⁴ Those with IC₅₀ greater than 100 $\mu\text{g/mL}$ are regarded to be of low to zero toxicity.²² The observed low cytotoxicity of the NHE is suggestive that the observed antiplasmodium activity may not necessarily be due to general cytotoxicity of the extract thus is a clue to its potential as a source of nontoxic agents for drug development.

The presence of isoprenoids (triterpenoid/steroids, cardenolides) and fatty acids as metabolites in the NHE from phytochemical screening using appropriate standard reagents corroborated our earlier report about the presence of these metabolites in a closely related species *Pleurotus tuber regium*.¹¹ The observed dose-dependent *plasmodium* pLDH inhibition by the NHE from the fruiting bodies of *P. ostreatus* could be due to the presence of these observed metabolites. Similar reports on the antimalarial activities of edible mushroom and related fungi have been documented.^{2,3,25} After chromatography separation of the NHE, compound **1** was isolated and its structure elucidated using mass spectrometry, nuclear magnetic resonance (1D and 2D), and fourier transform infrared spectroscopic techniques to be the known compound, ergostan-5,7,22-trien-3-ol. Compound **1** gave positive Liebermann and Salkowski phytochemical test reagents confirming it to have a steroidal nucleus. The NMR spectra data (Table 2) are evident with the ¹H and ¹³C chemical shift signals for a conjugated di-substituted olefinic bond in ring B and the isolated olefinic bond in the aliphatic side chain,

and six methyl (two angular and four at the aliphatic side chain) and one secondary carbinol (CHOH) at position 3 of ring A, which were unambiguously assigned as stated in Table 2 using 2D-NMR (HMBC, H-H-COSY, and HSQC) experiments. In all, a total of 28 carbon signals, i.e., four quaternary (4 \times C), eleven methine (11 \times CH) of which one is the CHOH at position 3 of ring A, seven methylene (7 \times CH₂), and six upfield methyl (6 \times CH₃), were observed, which corresponded to the molecular formula C₂₈H₄₄O, corroborating the observed molecular ion peak at m/z 396 from the EI-mass spectrum analysis. These trends in the spectra data are characteristic of an unsaturated steroidal alcohol and when compared to literature reports for ergosterol¹⁷ were similar. Owing to solubility limitations, compound **1** was, however, not evaluated for the reported biological activities. Ergosterol derivatives like ergosterol endoperoxide isolated from *P. ostreatus* have been reported to exhibit antiparasitic properties like trypanocidal⁵ and amoebicidal⁴ activities.

CONCLUSIONS

This study showed the first time the nutraceutical potential in the management of malaria infection of the edible mushroom *P. ostreatus* cultivated in Nigeria. The isolation and characterization of the known steroid ergostan-5,6,22-trien-3-ol (commonly called ergosterol) from the bioactive extracts from spectroscopic analysis was also reported. After further investigation, this edible mushroom species may be recommended in the diet as a prophylaxis against malaria infection.

ACKNOWLEDGEMENTS

AOE gratefully acknowledges financial support from the Royal Society of Chemistry JWT Jones travelling Fellowship award of 28th August 2015 to visit Rhodes University, Grahamstown, South Africa, where the spectroscopy and bioassay components of this project was done. The bioassay component of the project was funded by the South African Medical Research Council

with funds from the National Treasury under its Economic Competitiveness and Support Package. XSN is grateful for a Rhodes University Postdoctoral Fellowship.

Conflict of Interest: No conflict of interest was declared by the authors.

REFERENCES

- Malaria fact sheet N° 94. In: www.who.int/mediacentre/factsheets/fs094/en/ Accessed December 2015
- Isaka M, Tantichareon M, Kongsaree P, Thebtaranonth Y. Structures of Cordopyridones A-D, Antimalarial N-Hydroxy- and N-Methoxy-2-pyridones from the Insect Pathogenic Fungus *Cordyceps nipponica*. *J Org Chem*. 2001;66:4803-4808.
- Bi H, Han H, Li Z, Ni W, Chen Y, Zhu J, Gao T, Hao M, Zhou Y. A Water-Soluble Polysaccharide from the Fruit Bodies of *Bulgaria inquinans* (Fries) and Its Anti-Malarial Activity. *Evid Based Complement Alternat Med*. 2011;2011:973460.
- Meza-Menchaca T, Suarez-Medellin J, Del Angel-Pina C, Trigos A. The Amoebicidal Effect of Ergosterol Peroxide Isolated From *Pleurotus Ostreatus* *Phytother Res*. 2015;29:1982-1986.
- Ramos-Ligonio A, Lopez-Monteon A, Trigos A. Trypanocidal Activity of Ergosterol Peroxide From *Pleurotus Ostreatus*. *Phytother Res*. 2011;26:938-943.
- Degenkolb T, Vilcinskis A. Metabolites from nematophagous fungi and nematocidal natural products from fungi as alternatives for biological control part II: Metabolites from nematophagous basidiomycetes and non-nematophagous fungi. *Appl Microbiol Biotechnol*. 2016;100:3813-3824.
- Lull C, Wichers HJ, Savelkoul HF. Antiinflammatory and Immunomodulating Properties of Fungal Metabolites. *Mediators Inflamm*. 2005;2005:63-80.
- Wu JY, Chen CH, Chang WH, Chung KT, Liu YW, Lu FJ, Chen CH. Anti-cancer effects of protein extracts from *Calvatia lilacina*, *Pleurotus ostreatus* and *Volvariella volvacea*. *Evid Based Complement Alternat Med*. 2011;2011:982368.
- Elsayed AE, El Enshasy H, Wadaan MAM, Aziz R. Mushrooms: A Potential Natural Source of Anti-Inflammatory Compounds for Medical Applications. *Mediators Inflamm*. 2014;2014:805841.
- Afiero OE, Chukwu EC, Festus OH, Onyia CP, Suleiman M, Adedokun OM. Evaluation of the anti-mitotic and bacteriostatic activities of the fruiting bodies of *Pleurotus ostreatus* (Jacq. Ex. Fr) P. Kumm. (Pleurotaceae). *Malaysian Journal of Medical and Biological Sciences*. 2017;4:15-20.
- Afiero OE, Lawson L, Adedokun OM, Emenyonu N. Antituberculosis and phytochemical investigation of the dichloromethane extract of *Pleurotus tuber-regium* (Fries) Singer sclerotium. *IRJP*. 2013;4:255-257.
- Afiero OE, Ollornwi KV, Elechi N, Okwubie L, Okoroafor D, Abo KA. Free radical scavenging potentials and level of some heavy metals in *Pleurotus flabellatus* Berk and Broome (Pleurotaceae). *The Global Journal of Pharmaceutical Research*. 2013;2:1807-1812.
- Afiero OE, Ugoeze KC. Gas Chromatography-Mass Spectroscopic (GC-MS) Analysis of n-Hexane Extract of *Lentinus tuber-regium* (Fr) Fr (Polyporaceae) Syn *Pleurotus tuber regium* Fr sclerotia. *Trop J Pharm Res*. 2014;13:1911-1915
- Harborne JB. *Phytochemical Methods- a Guide to Modern Techniques of Plant Analysis* 3rd ed. Chapman and Hall; London; 1998.
- Houghton PJ, Raman A. *Laboratory Handbook for the Fractionation of Natural Extracts*. Chapman and Hall; London; 1998.
- Makler MT, Ries JM, Williams JA, Bancroft JE, Piper RC, Gibbins BL, Hinrichs DJ. Parasite lactate dehydrogenase as an assay for *Plasmodium falciparum* drug sensitivity. *Am J Trop Med Hyg*. 1993;48:739-741.
- Martinez M, Alvarez ST, Campi MG, Bravo JA, Vila JL. Ergosterol from the mushroom *Laetiporus* sp.; Isolation and structural characterization. *Bolivian Journal of Chemistry*. 2015;32:90-94.
- Brown WM, Yowell CA, Hoard A, Vander Jagt TA, Hunsaker LA, Deck LM, Royer RE, Piper RC, Dame JB, Makler MT, Vander Jagt DL. Comparative structural analysis and kinetic properties of lactate dehydrogenases from the four species of human malarial parasites. *Biochemistry*. 2004;43:6219-6229.
- Piper R, Lebras J, Wentworth L, Hunt-Cooke A, Houze S, Chiodini P, Makler M. Immunocapture diagnostic assays for malaria using *Plasmodium lactate dehydrogenase* (pLDH). *Am J Trop Med Hyg*. 1999;60:109-118.
- Makler MT, Hinrichs DJ. Measurement of the lactate dehydrogenase activity of *Plasmodium falciparum* as an assessment of parasitemia. *Am J Trop Med Hyg*. 1993;48:205-210.
- Oduola AM, Omitowoju GO, Sowunmi A, Makler MT, Falade CO, Kyle DE, Fehintola FA, Ogundahunsi OA, Piper RC, Schuster BG, Milhous WK. *Plasmodium falciparum*: evaluation of lactate dehydrogenase in monitoring therapeutic responses to standard antimalarial drugs in Nigeria. *Exp Parasitol*. 1997;87:283-289.
- Malek SN, Phang CW, Ibrahim H, Norhanom AW, Sim KS. Phytochemical and Cytotoxic Investigations of *Alpinia mutica* Rhizomes. *Molecules*. 2011;16:583-589.
- Lee CC, Houghton P. Cytotoxicity of plants from Malaysia and Thailand used traditionally to treat cancer. *J Ethnopharmacol*. 2005;100:237-243.
- Geran RI, Greenberg NH, McDonald MM, Schumacher A, Abbott BJ. Protocols for screening chemical agents and natural products against animal tumour and other biological systems. *Cancer Chemotherapy Reports*. 1972;3:17-19.
- Lovy A, Knowles B, Labbe R, Nolan L. Activity of edible mushrooms against the growth of human T4 leukemia cancer cells, and *Plasmodium falciparum*. *Journal of Herbs, Spices and Medicinal Plants*. 2000;6:49-57.



Characterization of Gamma-Irradiated *Rosmarinus officinalis* L. (Rosemary)

Gama Işınlanmış *Rosmarinus officinalis* L. (Biberiye)

Reza REZANEJAD^{1,2}, Seyed Mahdi OJAGH^{1*}, Marzieh HEIDARIEH^{2*}, Mojtaba RAEISI³, Gholamreza RAFIEE⁴, Alireza ALISHAH²

¹Gorgan University of Agriculture Sciences and Natural Resources, Faculty of Fisheries and Environmental Science, Department of Seafood Science and Technology, Gorgan, Iran

²Nuclear Agriculture Research School, Nuclear Science and Technology Research Institute, Karaj, Iran

³Golestan University of Medical Sciences, Cereal Health Research Center, Gorgan, Iran

⁴University of Tehran, Faculty of Natural Resources, Department of Fisheries, Karaj, Iran

ABSTRACT

Objectives: *Rosmarinus officinalis* L., a member of the family Lamiaceae, is regarded as the spice with the highest antioxidant activity.

Materials and Methods: In this study, the transmission electron microscopy, X-ray diffraction, and fourier transform infrared spectroscopy (FTIR) physicochemical characteristics of the nanostructure of gamma-irradiated rosemary were investigated.

Results: The particle size distribution of the gamma-irradiated rosemary prepared under irradiation at 30 kGy in a Cobalt-60 irradiator exhibited a very narrow size distribution with average size of 70 nm. The results showed that irradiated (30 kGy) and crude rosemary had similar patterns of FTIR spectra, typical of phenol compound, without any notable changes in the key bands and functional groups status. Rosemary irradiated with 50 kGy and 10 kGy showed the highest and lowest crystallinity, respectively. Rosemary crystallinity of irradiated samples was lower compared with the nonirradiated sample.

Conclusion: Therefore, 30 kGy can be optimum for the synthesis of nanoparticles, average size of 70 nm, with low crystallinity and without any notable change in key bands compared to nonirradiated samples.

Key words: Rosemary, gamma irradiation, FTIR, transmission electron microscopy, nanoparticles, X-ray diffraction

ÖZ

Amaç: Lamiaceae familyası bitkisi olan *Rosmarinus officinalis* L., en yüksek antioksidan aktiviteye sahip baharat olarak kabul edilmektedir.

Gereç ve Yöntemler: Bu çalışmada, gama ışınlarıyla ışınlanmış biberiyenin nanoyapılarının fizikokimyasal özellikleri transmisyon elektron mikroskobu, X-ışını difraksiyonu ve fourier dönüşümü kızılötesi spektroskopisi (FTIR) kullanılarak incelenmiştir.

Bulgular: Bir kobalt-60 ışınlayıcıda 30 kGy'de ışınlama altında hazırlanan gama ışınlanmış biberiyenin partikül büyüklüğü dağılımı, ortalama büyüklüğü 70 nm olan çok dar bir boyut dağılımı sergilemiştir. Sonuçlar, ışınlanmış (30 kGy) ve ham biberiyenin, tipik fenol bileşiğinin, fonksiyonel gruplara ilişkin bantlarda kayda değer bir değişiklik göstermeden benzer FTIR spektrum paternine sahip olduğunu göstermiştir. 50 kGy ve 10 kGy ile ışınlanmış biberiye sırasıyla en yüksek ve en düşük kristallenme özelliği gösterdi. Işınlanmış örneklerin kristallenme özelliğinin, ışınlanmamış numuneye kıyasla daha düşük olduğu belirlendi.

Sonuç: Bu nedenle, 30 kGy'nin ortalama boyutu 70 nm olan nanopartiküllerin sentezi için ideal olduğu, ışınlanmamış örnekler ile karşılaştırıldığında düşük kristallenme ve bantlardaki kayda değer olmayan değişikliklere neden olduğu belirlenmiştir.

Anahtar kelimeler: Biberiye, gama radyasyon, FTIR, transmisyon elektron mikroskobu, nanopartikül, X-ışını difraksiyonu

*Correspondence: E-mail: haidariehm81@gmail.com-mahdi_ojagh@yahoo.com, Phone: +0982634411102 ORCID-ID: orcid.org/0000-0003-2097-960X

Received: 24.06.2017, Accepted: 07.12.2017

©Turk J Pharm Sci, Published by Galenos Publishing House.

INTRODUCTION

Synthetic antioxidants are widely used to retard undesirable changes as a result of oxidation in many foods. Many synthetic substances such as butylated hydroxyanisol (BHA), propyl gallate, and citric acid are commonly used in lipids to prevent oxidation. Recently, these synthetic substances have been shown to cause effects such as enlarged liver size and increased microsomal enzyme activity. Therefore, there is a need for other compounds to use as antioxidants and to render safer food products for mankind.¹⁻³ Plant originated antioxidants are more suitable as food additives, not only for their free radical scavenging properties, but also because of the belief that natural products are safer than synthetic antioxidants.^{4,5} Chang et al.⁶ reported the results of investigations of the antioxidative effect of rosemary and sage due to the peroxide value. Naturally occurring compounds in rosemary extracts have been reported to exhibit antioxidant properties greater than BHA and equal to BHT.^{7,8} *Rosmarinus officinalis* L. (rosemary), a member of the family Lamiaceae, is an attractive evergreen shrub with pine needle-like leaves that grows wild in most Mediterranean countries. Rosemary has been accepted as the spice with the highest antioxidant activity. Many compounds have been isolated from rosemary such as flavones, diterpenes, steroids, and triterpenes.⁹

On the other hand, nanoparticles produced by plant extracts are more stable and the rate of synthesis is faster than that in the case of other organisms.¹⁰ Various methods of synthesizing nanoparticles are namely chemical reduction, interfacial polymerization, solvent evaporation, solvent deposition, nanoprecipitation, emulsification-diffusion, controlled jellification, microwave processing, and irradiation.¹¹⁻¹³ Irradiation induced reduction synthesis, which offers some advantages over the conventional methods; it provides metal nanoparticles in fully reduced, highly pure, and highly stable state due to its simplicity.^{11,14} Moreover, gamma irradiation of natural polysaccharides, such as chitosan, carrageenan, and sodium alginate, offers a clean method for the formation of low molecular weight oligomers. These oligomers have valid applications as antibiotic, antioxidant, and plant-growth promoting substances.^{11,15}

Therefore, this study aimed to investigate the transmission electron microscopy (TEM), X-ray diffraction (XRD), and fourier transform infrared spectroscopy (FTIR) physicochemical properties of the nanostructure of gamma-irradiated *R. officinalis* L. (rosemary).

MATERIALS AND METHODS

Plant material

Rosemary leaves were obtained from the Institute of Medicinal Plants herbarium (1394/O/037 for *R. officinalis* L.), Karaj, Iran. The leaves were washed first under running tap water, followed by sterilized distilled water, and dried at room temperature in the dark without applying any heat treatment to minimize the loss of active components; then they were ground into powder using an electrical blender (SME GmbH).

Preparation of gamma-irradiated R. officinalis L. (Rosemary)

Ground rosemary powder was suspended in sterile 0.15 M phosphate buffered saline (pH 7.2). A sample was sonicated for 30 min in a water bath sonicator (Jencons, Leighton Buzzard, UK) and centrifuged at 5000 rpm for 15 min.¹⁶ After precipitation in 2.5 volumes of 96% ethanol, the ground rosemary powder sample was dried at 40°C and then milled to the mesh size of 53-125 µm. The remaining powder was packed in a plastic cover and weighed. Irradiation was carried out at a dose rate 10, 20, 30, 40, and 50 kGy with a Cobalt-60 gamma irradiator (PX-30 Issledovapel, Russia) at a dose rate of 0.22 Gy s⁻¹. Furthermore, dosimetry was performed with a Fricke reference standard dosimetry system and after the irradiation process the gamma-irradiated rosemary was stored at 4°C for further experiments.

Characterization of gamma-irradiated R. officinalis L. (Rosemary)

Fourier transform infrared spectroscopy

An amount of irradiated rosemary powder was mixed with KBr powder and, after drying, was compressed to form a disc. The discs were later subjected to FTIR spectroscopy measurement. These measurements were recorded on a Bruker spectrophotometer (EQUINOX 55, Germany) in transmittance mode with a resolution of 4 cm⁻¹ in the wavenumber region of 400 to 4000 cm⁻¹. FTIR measurements were carried out in order to obtain information about the chemical groups present around gamma-irradiated rosemary for their stabilization and to understand the transformation of functional groups due to the reduction process.

X-ray diffraction

XRD was carried out using a Philips PW-1710 diffractometer (with sample holder PW 1729 X-ray generator, target copper) fixed at 20 mA and 40 kV. It employed Cu-Kα X-radiation of wavelength λ=1.54060 Å, between a 2θ angle. XRD was used to determine whether a material was amorphous or crystalline.

Transmission electron microscopy

The nanoparticles were immobilized on a coated copper grid and were allowed to dry at room temperature. The particle size and shape were observed using an FEI/Philips EM 208S TEM.

RESULTS AND DISCUSSION

Gamma irradiation has been extensively used to generate nanoscale metals and nanocomposites at room temperature and normal pressure.¹⁷ Recently, polymeric nanoparticles have been focused on for their use as clinical diagnostics, therapeutics, and carriers for delivery systems.¹⁷ In the present study, the particle size of gamma-irradiated rosemary prepared under irradiation of 30 kGy exhibited a very narrow size distribution. This means that the size of the prepared gamma-irradiated rosemary gets smaller and the particle size is 70 nm. TEM micrographs were taken into account. Figure 1 represents TEM images of the gamma-irradiated rosemary at different doses ranging from 10 to 50 kGy.

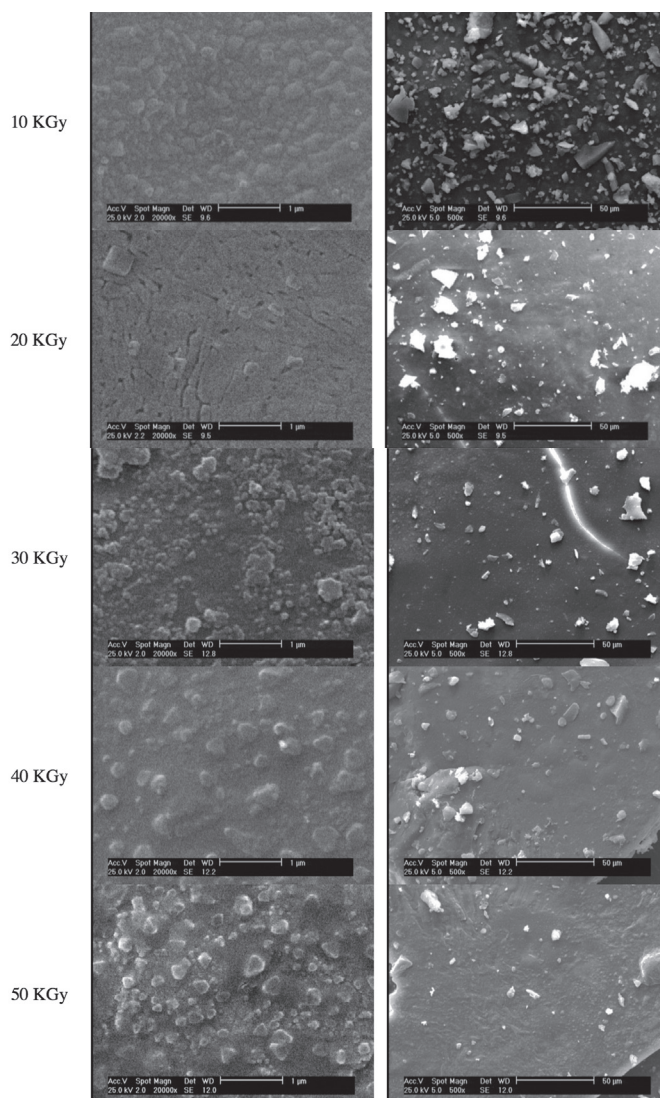


Figure 1. TEM images of gamma-irradiated rosemary at different doses ranging from 10 to 50 KGy

TEM: Transmission electron microscopy

To investigate whether any structural changes occurred during gamma irradiation, FTIR spectra were recorded. FTIR is one of the most widely used tools for the detection of functional groups in pure compounds and mixtures and for compound comparison.¹⁸ The FTIR spectra are shown in Figure 2, and the wavenumbers of characteristic bands and corresponding assignments for the gamma-irradiated rosemary with different doses are listed in Table 1.

The key bands of rosemary are at 1735.62, 1672.95, 1454.06, 1366.32, 1242.9, 1078.01, 987.37, 886.13, 839.84, and 787.79 cm^{-1} .¹⁹

The FTIR spectra of rosemary exhibited the following absorption bands: broad absorption, band peaking at 3414.50 cm^{-1} , corresponding to OH stretching bands of alcohols and/or carboxylic acids vibrations, followed by peaks at 2929.63 cm^{-1} and 2854.70 cm^{-1} , assigned to vibration of the $-\text{CH}_3$ asymmetric stretching and symmetric stretching absorption band of the methylene group vibration, respectively. Other bands in this

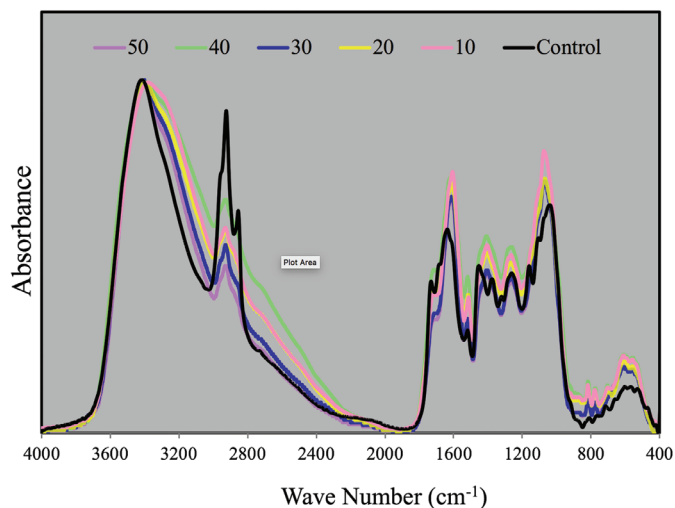


Figure 2. FTIR spectra of rosemary gamma irradiated with different doses
FTIR: Fourier transform infrared spectroscopy

spectrum are observed at 1636.57 cm^{-1} , 1453.40 cm^{-1} , 1375.98 cm^{-1} , 1262.36 cm^{-1} , 1039.65 cm^{-1} , and 603.35 cm^{-1} due to the bond vibrations of the asymmetrical carboxylic acid and C=O stretching vibration, C-N stretching, symmetrical carboxylic acid group, C-O stretching vibrations (amide) and phenyl groups and of the C-O stretching, and at last attributed to C-O stretching vibrations of mono-, oligo-, and carbohydrates, respectively (Table 1).

According to Hollenstein et al.²⁰, FTIR spectroscopy can be used to determine particle configuration. As particle size increases, the width of the peak decreases and intensity increases. Furthermore, the intensity of an absorption peak depends on the path length, concentration, and strength of the absorption band.^{20,21}

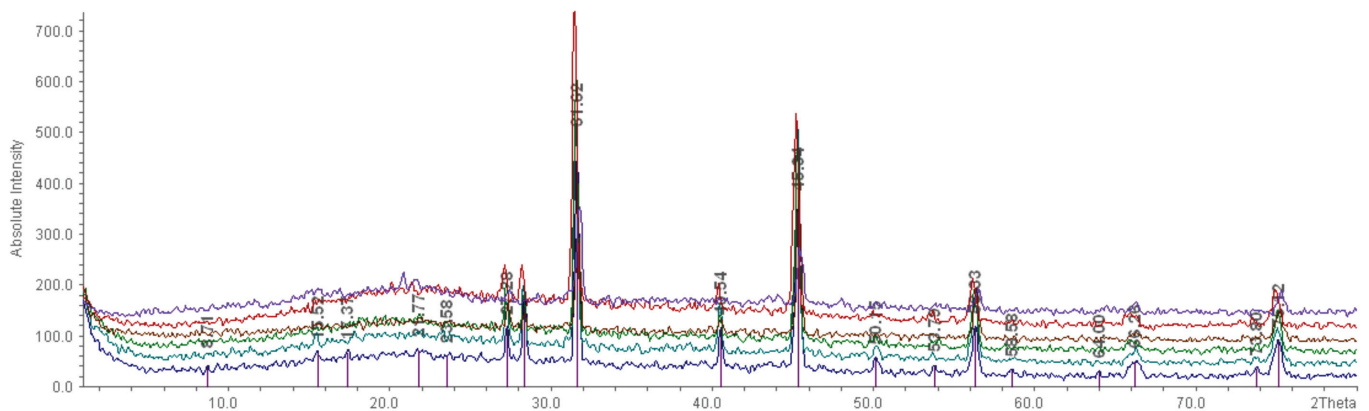
In this research, after radiation, two C-H stretching vibrations became merged and appeared as a single vibration in all groups; this was due to the increased peak width. The shift of this band could be attributed to the weakening of hydrogen bonds.²² As mentioned above, the width and intensity of the peak can reveal the particle size.^{20,21} Therefore, increased peak width and reduced peak intensity accompany decreased particle size in all treatments.

On the other hand, the results revealed that irradiated (30 kGy) and crude rosemary had similar patterns of FTIR spectra, typical of phenol compound, without any notable changes in the key bands or functional groups status. The results are similar in other herb extracts.

The XRD results of the nonirradiated and irradiated rosemary at 10, 20, 30, 40, and 50 kGy are presented in Figure 3. XRD patterns from materials with different cubic crystal structures provided in textbooks can be used as reference.²³ In the present study, based on XRD pattern, rosemary has a structure that can be described as face centered cubic.²³ Moreover, the nonirradiated rosemary showed diffraction peaks at 20.85°, 31°, 45.47°, 56.51°, 66.28°, 75.29°, and 76.76°. A comparison

Table 1. Wavenumbers of characteristic bands and corresponding assignments for normal and gamma-irradiated rosemary

Wavenumbers (cm ⁻¹) of measured peaks for						Assignment
Irradiated rosemary (kGy)					Normal rosemary	
50	40	30	20	10		
3403.86	3396.13	3400.58	3369.01	3376.18	3414.50	OH stretching bands of alcohols
2927.98	2929	2926.88	2928.49	2929.63	2950.55 2916.81 2870.52 2848.25	C-H stretching vibrations specific to CH ₃ and CH ₂
1710.27 1610.51	1716.76 1608.62	1710.27 1609.04	1716.76 1609.15	1723.24 1607.10	1672.95 1659.45 1641.13 1617.02	C=O stretching vibration, C-N stretching, COO ⁻ antisymmetric stretching
1516.60	1517.95	1516.72	1515.87	1513.52	1572.66	Aromatic domain and N-H bending
1407.30	1408.19	1406.32	1405.73	1406.35	1454.06 1376.93 1366.32	C-O stretching vibration (amide) and C-C stretching from phenyl groups, COO ⁻ symmetric stretching, CH ₂ bending
1262.76	1263.12	1262.61	1264.38	1264.55	1291.11 1242.9 1203.36	C-O stretching
1071.97	1072.16	1072.30	1072.12	1073.83	1190.83 1163.83 1144.85 1116.58 1078.01 1035.59	Stretching vibrations C-O of mono-, oligo-, and carbohydrates
817.19 611.99	817.25 776.65 609.22	817.07 609.93	817.56 776.84 608.13	818.39 778.50 611.77	987.35 960.37 917.95 886.13 787.77	C-H out-of-plane bending vibrations from isoprenoids

**Figure 3.** X-ray diffraction of Irradiated and non-irradiated Rosemary

among diffraction patterns of the rosemary, before and after irradiation, showed that the intensity of the reflection markedly declined with gamma irradiation compared to the control. The order of irradiated rosemary reflection intensity was 50, 40, 30, 20, and 10 kGy. The rosemary irradiated with 50 kGy and 10 kGy had the highest and lowest crystallinity, respectively.

Therefore, the rosemary crystallinity of irradiated samples was lower as compared with the nonirradiated sample.

CONCLUSIONS

This work presents a simple, available, and effective method for preparation of rosemary nanoparticles. The purpose of

the research was to synthesize new rosemary nanoparticles using gamma irradiation. The developed nanoparticles were characterized for particle size and structural and optical properties of the irradiated rosemary via TEM, XRD, and FTIR. The particle size distribution of the gamma-irradiated rosemary prepared under irradiation at 30 kGy in a Cobalt-60 irradiator exhibited a distribution with average size 70 nm. In addition, the results showed that irradiated (30 kGy) and crude rosemary had similar patterns of FTIR spectra, typical of phenol compound, without any notable changes in the key bands or functional groups status. The rosemary crystallinity of irradiated samples was lower than that of the nonirradiated sample. The rosemary irradiated with 50 kGy and 10 kGy had the highest and lowest crystallinity, respectively. Therefore, 30 kGy can be optimum for synthesis nanoparticles, average size of 70 nm, with low crystallinity and without any notable change in key bands compared to nonirradiated samples.

ACKNOWLEDGEMENTS

The authors would like to thank the Research Council of Nuclear Science and Technology Research Institute, Karaj, Iran, and Gorgan University of Agricultural Sciences and Natural Resources for their financial and technical support of this study.

Conflict of Interest: No conflict of interest was declared by the authors.

REFERENCES

- Farag RS, Badei AZMA, El-Baroty GSA. Influence of thyme and clove essential oils on cotton seed oil oxidation. *J Am Oil Chem Soc.* 1989;66:800-804.
- Farag RS, Ali MN, Taha SH. Use of some essential oils as natural preservatives for butter. *Am Oil Chem Soc.* 1990;68:188-191.
- Brookman P. Antioxidants and consumer acceptance. *Food Pharm Ind.* 1991.
- Almey A, Khan AJ, Zahir S, Suleiman M, Aisyah MR, Rahim K. Total phenolic content and primary antioxidants activity of methanolic and ethanolic extracts of aromatic plant's leaves. *Int Food Res J.* 2010;17:1077-1084.
- Gür E, Gulden O. Oregana (*Oreganum onites* L.) ekstraktlayný rafine zeytinyaoyndaki antioksidatif etkilerinin incelenmesi. (Antioxidative activity of oregano (*Oreganum onites* L.) extracts in refined olive oil. *Gida Teknolojisi.* 1997;7:56-64.
- Chang SS, Ostric-Matijasevic BO, Hsieh OAL, Huang CL. Natural antioxidant from Rosemary and Sage. *J Food Sci.* 1977;42:1102-1106.
- Wu JW, Lee MH, Ho CT, Chang SS. Elucidation of the chemical structures of natural antioxidants isolated from rosemary. *J Am Oil Chem Soc.* 1982;59:339-345.
- Ho CT, Houlihan CM, Chang SS. Structural determination of two antioxidants isolated from Rosemary. Abstract of papers presented at the (186th) Amer Chem Soc Meeting Washington DC; 1983.
- Pintore G, Usai M, Bradesi P, Juliano C, Boatto G, Tomi F, Chessa M, Cerri R, Casanova J. Chemical composition and antimicrobial activity of *Rosmarinus officinalis*. *Flavour Fragr J.* 2002;17:15-19.
- Mason C, Vivekanandhan S, Misra M, Mohanty AK. Switchgrass (*Panicum virgatum*) Extract Medicated green Synthesis of Silver Nanoparticles. *World Journal of Nano Science and Engineering.* 2012;2:47-52.
- Press CMcL, Evensen Ø, Reitan LJ, Landsverk T. Retention of furunculosis vaccine components in Atlantic salmon Salmon solar L., following different routes of dministration. *J Fish Dis.* 1996;19:215-224.
- Joosten PHM, Kruijjer WJ, Rombout JHWM. Anal immunisation of carp and rainbow trout with different fractions of a *Vibrio anguillarum* bacterin. *Fish Shellfish Immunol.* 1996;6:541-551.
- Chen VJ, Ma PX. Nano-fibrous poly (L-lactic acid) scaffolds with interconnected spherical macropores. *Biomaterials.* 2004;25:2065-2073.
- Heidarieh M, Daryalal F, Mirvaghefi A, Rajabifar S, Diallo A, Sadeghi M, Zeiai F, Moodi S, Maadi E, Sheikhzadeh N, Heidarieh H, Hedyati M. Preparation and anatomical distribution study of 67 Ga-alginate acid nanoparticles for SPECT purposes in rainbow trout (*Oncorhynchus mykiss*). *Nukleonika.* 2014;59:153-159.
- Christopher Marlowe AC, Carlo CL, Ingvild B, Monica FB, Viswanath K. Influence of alginate acid and fucoidan on the immune responses of head kidney leukocytes in cod. *Fish Physiol Biochem.* 2012;37:603-612.
- Toma M, Vinatoru M, Mason TJ. Ultrasonically assisted extraction of bioactive principles from plants and their constituents. *Advances in Sonochemistry.* 1999;5:209-248.
- Karim MR, Lim KT, Lee CJ, Bhuiyan MI, Kim HJ, Park LS, Lee MS. Synthesis of core-shell silver-polyaniline nanocomposites by gamma radiolysis method. *J Polym Sci.* 2007;45:5741-5747.
- Bhattacharya S, Srivastava A. Synthesis of gold nanoparticles stabilised by metal-chelator and the controlled formation of close-packed aggregates by them. *Chem Sci.* 2003;115:613-619.
- Schulz H, Quilitzsch R, Krüger H. Rapid evaluation and quantitative analysis of thyme, origano and chamomile essential oils by ATR-IR and NIR spectroscopy. *J Mol Struct.* 2003;661:299-306.
- Hollenstein Ch, Howling AA, Courteille C, Magni D, Scholz SM, Kroesen GMW, Simons N, de Zeeuw W, Schwarzenbach W. Silicon oxide particle formation in RF plasmas investigated by infrared absorption spectroscopy and mass spectrometry. *J Phys D Appl Phys.* 1998;31:74-84.
- Tourinho FA, Depeyrot J, da Silva GJ, Lara MCL. Electric double layered magnetic fluids (EDL-MF) based of spinel ferrite nanostructures [(M1-x+2Fex+3)+2 1-x Fe+3]A[(Fe2-x+3Mx+2)]BO4-2. *Braz J Phys.* 1998;28:413.
- Nasab MM, Taherian A, Bakhtiyari M, Farahnaky A, Askari H. Structural and rheological properties of succinoglycan biogums made from low-quality date syrup or sucrose using agro-bacterium radiobacter inoculation. *Food Bioprocess Technol.* 2012;5:638-647.
- Suryanarayana C, Norton MG. "X-Ray Diffraction a Practical Approach. Plenum Press, New York; 1998:3-19.



Enhancement of Dissolution of Fenofibrate Using Complexation with Hydroxy Propyl β -Cyclodextrin

Hidroksi Propil β -Siklodekstrin ile Kompleksasyon Kullanılarak Fenofibratın Çözünmesinin Arttırılması

✉ Sachin K. JAGDALE^{1*}, ✉ Mohammad H. DEGHAN², ✉ Nilesh S. PAUL³

¹Marathwada Mitra Mandal's College of Pharmacy, Pune, India

²Y. B. Chavan College of Pharmacy, Aurangabad, India

³MGM Institute of Bioscience and Technology, Aurangabad, India

ABSTRACT

Objectives: The aim of the present study was to enhance the dissolution rate of fenofibrate using complexation with hydroxy propyl β -cyclodextrin (HP β CD).

Materials and Methods: The phase solubility behavior of fenofibrate was studied in various concentrations of (HP β CD) aq. solution at 37°C. The solubility of fenofibrate increased with an increase in the amount of HP β CD aq. solution. Gibbs free energy (ΔG°)_r values were all negative. Complexes of fenofibrate with HP β CD were prepared in 1:1 ratio by kneading and coprecipitation. These complexes were evaluated by dissolution studies, fourier transform infrared (FTIR) spectroscopy, and differential scanning calorimetry (DSC) studies.

Results: The complexation of fenofibrate with HP β CD exhibited an enhanced dissolution rate. The mean dissolution time of fenofibrate decreased significantly upon complexation. FTIR studies showed the formation of intermolecular hydrogen bonding between fenofibrate and HP β CD. DSC studies indicated a loss in crystalline state of fenofibrate in complexes.

Conclusion: Complexation with HP β CD can be used as a useful tool for the enhancement of dissolution of fenofibrate.

Key words: Fenofibrate, hydroxy propyl β -cyclodextrin, solubility, Gibbs free energy, dissolution rate

ÖZ

Amaç: Bu çalışmanın amacı, hidroksi propil β -siklodekstrin (HP β CD) ile kompleksasyon kullanarak fenofibratın çözünme hızını arttırmaktır.

Gereç ve Yöntemler: Fenofibratın faz çözünürlük davranışları (HP β CD) çeşitli konsantrasyonlardaki sulu çözeltisinde, 37°C'de çalışıldı. Fenofibratın çözünürlüğü, artan miktarda HP β CD'nin sulu çözeltisi ile arttı. Gibbs serbest enerji (ΔG°)_r değerlerinin hepsi negatifti. HP β CD ile fenofibrat kompleksleri, 1:1 oranında yoğurma ve kopresipitasyon ile hazırlandı. Bu kompleksler, çözünme çalışmaları, fourier dönüşümü kızılötesi spektroskopisi (FTIR) ve diferansiyel tarama kalorimetrisi (DSC) çalışmaları ile değerlendirildi.

Bulgular: Fenofibratın HP β CD ile kompleksasyonu, gelişmiş bir çözünme hızı sergiledi. Fenofibratın ortalama çözünme süresi, kompleksasyon üzerine önemli ölçüde azaldı. FTIR çalışmaları fenofibrat ve HP β CD arasında moleküller arası hidrojen bağlanmasının oluşumunu göstermiştir. DSC çalışmaları komplekslerde kristalin fenofibrat durumunda bir kayıp olduğunu gösterdi.

Sonuç: HP β CD ile kompleksasyon, fenofibratın çözünmesinin arttırılması için yararlı bir araç olarak kullanılabilir.

Anahtar kelimeler: Fenofibrat, hidroksi propil β -siklodekstrin, çözünürlük, Gibbs serbest enerjisi, çözünme hızı

*Correspondence: E-mail: sachin10pharmacy@gmail.com, Phone: +91-7588938173 ORCID-ID: orcid.org/0000-0001-5714-5508

Received: 09.11.2017, Accepted: 14.12.2017

©Turk J Pharm Sci, Published by Galenos Publishing House.

INTRODUCTION

Fenofibrate, propan-2-yl 2-[4-(4-chlorobenzoyl) phenoxy]-2-methylpropanoate, is a fibric acid derivative useful as an antilipidemic agent. Fenofibrate is a hypolipidemic drug that reduces the levels of lipids (fats) in the blood. It is a white crystalline powder, practically insoluble in water (log p=5.24).¹ Its low water solubility and poor dissolution rate cause problems in formulation development and restrict its therapeutic application by influencing the rate of absorption and the onset of action.

Consequently, its bioavailability is incomplete, irregular, and often varies from one person to another. As a result, commercially available doses are of higher strength and require repeated dosing. From an economic point of view, this low bioavailability of drug leads to wastage of more amounts of drug after oral administration, increasing the cost of medication. Therefore, it is very important to find appropriate formulation approaches to enhance the aqueous solubility, dissolution rate, and thus the bioavailability of poorly soluble drugs. Nowadays, many approaches are used to enhance the solubility and dissolution rate of poorly soluble drugs by the use of pharmaceutical technology.² Physical modification often aims to increase the surface area, solubility, and/or wettability of the powder. Other approaches include cosolvency using various solvent blends, cyclodextrin complexation,³ use of surfactants,⁴ salt forms,⁵ prodrugs,⁶ and alteration of crystal properties.^{7,8}

A number of different microorganisms and plants produce certain enzymes called cyclodextrin glucosyltransferases, which degrade starch to cyclic products called cyclodextrins. These cyclodextrins are cyclic oligosaccharides involving (α-1,4)-associated α-D-glucopyranose units and contain a genuinely lipophilic cavity and a hydrophilic external surface. They are shaped like truncated cones rather than perfect cylinders. In light of such qualities, cyclodextrins are able to form inclusion complexes both in solid state and in solution state, in which every guest entity is surrounded by the hydrophobic environment of the cyclodextrin cavity. Upon inclusion, the water solubility of the guest can increase as well as its bioavailability.^{9,10} This inclusion complex formation leads to alteration of the physicochemical and biological properties of the guest molecules and may eventually have considerable pharmaceutical potential.^{11,12}

The naturally occurring α-, β-, and γ-cyclodextrin consist of six, seven, and eight glucopyranose units, respectively. Natural cyclodextrins like β-cyclodextrin have limited aqueous solubility and the complexes formed from the interaction of lipophilic/hydrophobic drugs with these cyclodextrins may be of limited solubility. This may result in precipitation of solid cyclodextrin complexes from water and other aqueous systems. Cyclodextrin derivatives of pharmaceutical interest include the derivatives of these naturally occurring β- and γ-cyclodextrins. Out of these cyclodextrin derivatives, hydroxy propyl β-cyclodextrin (HPβCD) appears the most useful as a pharmaceutical complexing agent because of its complexing ability, low cost, and other properties. The approach of

cyclodextrin complexation can be used to increase the water solubility and dissolution rate of poorly soluble drugs and to solve bioavailability problems.

As fenofibrate dissolves very slightly in water, the present study was undertaken to overcome the limitations existing in available fenofibrate products so as to improve the dissolution profile, absorption characteristics, and bioavailability and to reduce the dose required for administration to attain a desired effect.

The study also aimed to develop a method for preparation of an inclusion complex of fenofibrate with HPβCD that is efficient and economical, simple, and less time consuming than other methods.

Thus, the present study was performed to enhance the solubility and dissolution rate of fenofibrate using complexation with HPβCD in order to attain a therapeutic effect. The possible interactions between fenofibrate and HPβCD in both solid state and liquid states were investigated. The solid state interaction was investigated by fourier transform infrared (FTIR) spectroscopy and differential scanning calorimetry (DSC) studies. The interaction in solution was studied by phase solubility analysis and dissolution experiments.

MATERIALS AND METHODS

Materials

A gift sample of fenofibrate was received from Shreya Life Sciences, (Aurangabad, India). HPβCD was obtained from Wockhardt Pharmaceuticals (Aurangabad, India). All other solvents and ingredients used were of analytical grade.^{13,14}

Methods

Phase solubility studies

Phase solubility studies were performed in triplicate according to the method reported by Higuchi and Connors.¹⁵ An excess of drug was added to 5-mL portions of distilled water in vials each containing a variable amount of HPβCD (2 mM to 10 mM). All the above solutions were subjected to sonication for 30 min and then allowed to stand at room temperature (~25°C) for 48 h without disturbance to attain saturation equilibrium. These saturated systems were carefully filtered through Whatman filter paper (no. 41) and were analyzed spectrophotometrically at 287 nm after appropriate dilutions on a ultraviolet (UV)-visible spectrophotometer.

The solubility of fenofibrate in every HPβCD solution was calculated and a phase solubility diagram was drawn between solubility of fenofibrate and different concentrations of HPβCD. The apparent stability constant (Kc) was calculated by using the formula¹⁵;

$$\text{Stability constant (Kc)} = \frac{\text{Slope}}{\text{So (1-slope)}} \dots\dots\dots 1$$

where So=aqueous solubility of fenofibrate.

The Gibbs free energy of transfer (ΔG°_{tr}) of fenofibrate from pure water to the aqueous solution of carrier was calculated as¹⁴;

$$\Delta G_{tr} = 2.303 RT \log \text{So} / \text{Ss}, \dots\dots\dots 2$$

where S_o/S_s is the ratio of molar solubility of fenofibrate in aqueous solution of HP β CD to that of the same medium without HP β CD.

Preparation of solid binary systems

Preparation of physical mixture of fenofibrate with HP β CD

The physical mixture of fenofibrate with HP β CD containing molar weight ratio 1:1 (fenofibrate:HP β CD) was prepared, followed by passing through a sieve (no. 72) with minimum abrasion.

Preparation of inclusion complex by kneading method¹⁵

Stoichiometric quantities (1:1) of fenofibrate:HP β CD were accurately weighed. HP β CD was added to the mortar, and a small amount of ethanol:water (1:1 v/v) was added while triturating to get a slurry-like consistency. Then slowly the drug was incorporated into the slurry, and trituration was continued for a further 45 min. The slurry was then dried at 50°C for 24 h, pulverized, passed through a no. 72 sieve, and stored in desiccators until further use.

Preparation of inclusion complex by coprecipitation

Fenofibrate and HP β CD in 1:1 molar ratio were accurately weighed. Saturated cyclodextrin solution was prepared with HP β CD and water. Then fenofibrate solution in methanol was added slowly and a suspension was formed. The suspension was stirred at 40°C for 30 min and the stirring was continued at room temperature (25°C) for 30 min. The obtained masses were filtered through Whatman filter paper no. 41 and dried at 50°C in an oven for 24 h. The dried complexes were pulverized and passed through a no. 72 sieve and stored in desiccators until further use.¹⁶

The yield for HP β CD complex was not significant. Therefore, we used the following method for coprecipitation.

Fenofibrate and HP β CD in 1:1 molar ratio were accurately weighed. Cyclodextrin solution was prepared with HP β CD and water. Then fenofibrate solution in methanol was added slowly to the above solution and a suspension was formed. The suspension was stirred at 40°C for 30 min and kept stirring at room temperature for 12 h. The obtained masses were refrigerated for 24 h. Then these masses were filtered through Whatman filter paper no. 41 and dried at 50°C in an oven for 24 h. The dried complexes were pulverized and passed through a no. 72 sieve and stored in desiccators until further use.¹⁷

Dissolution studies

As fenofibrate is a lipophilic compound and practically insoluble in water, dissolution study of fenofibrate dosage forms necessitates modifications in the dissolution medium. Sodium lauryl sulfate (SLS) of concentration 20 mM and above provides sink conditions.^{18,19}

Dissolution studies of fenofibrate, physical mixture, kneaded product, and coprecipitated product were performed using the U.S. Pharmacopeia (USP) model digital tablet dissolution test apparatus II (Electrolab, Mumbai) at paddle rotation speed of 75 rpm in 900 mL of 20 mM SLS at 37.0 \pm 0.5°C.

The physical mixture equivalent to 145 mg of fenofibrate was weighed using a digital balance (Make Eagle, India) and added to dissolution medium. Then 5-mL samples were withdrawn at predetermined intervals and replaced with fresh dissolution medium and suitably diluted. Diluted samples were then assayed for fenofibrate content by measuring the absorbance at 287 nm using a UV-visible spectrophotometer (Jasco model V630, Japan). The dissolution studies were either performed until all the solids were completely dissolved or stopped at 2 h if the duration of dissolution was longer. Studies were performed in triplicate (n=3). Mean values of cumulative drug release were calculated for plotting the release curve.

Fourier transform infrared spectroscopy

FTIR spectra were obtained using an FT/IR-4100 spectrophotometer (Jasco, Japan). The samples (fenofibrate, physical mixture, and drug:cyclodextrin complexes) were previously ground and mixed thoroughly with potassium bromide, an infrared transparent matrix, at 1:5 (sample: KBr) ratio, respectively. Forty scans were obtained from 4000 to 400 cm⁻¹.

Differential scanning calorimetry studies

The DSC thermograms were obtained on a DSC (Shimadzu DSC-60 thermal analyzer, Japan). The instrument was calibrated using indium as standard. Samples (5 mg) were heated in sealed aluminum pans under nitrogen using the following program: hold for 10 min at 40°C and heat from 40.0 to 250.0°C at a scanning rate of 10°C/min. Then the samples were subjected to DSC studies. Samples were sealed in 40- μ L aluminum pans. An identical empty pan was used as a reference. The samples were scanned at 10°C/min with a 50 mL/min nitrogen purge.

RESULTS AND DISCUSSION

Phase solubility studies

The phase solubility profiles of fenofibrate-HP β CD are presented in Figure 1. This plot showed that aqueous solubility of the drug increases linearly as a function of HP β CD. The phase solubility profile of fenofibrate with HP β CD can be classified as A_L-type. The linear host-guest correlation coefficient $r=0.9969$ ($r^2=0.994$) with a slope (m) of 0.004 suggested the formation

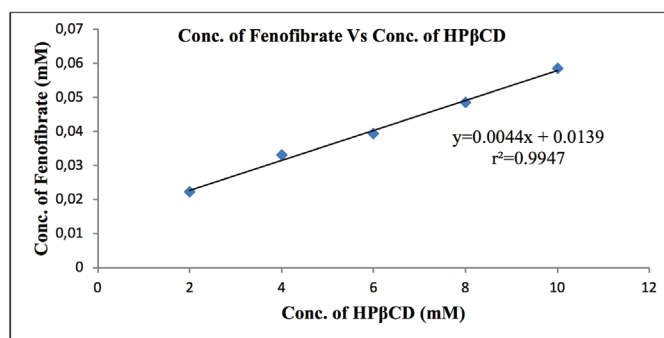


Figure 1. Phase solubility diagram of the fenofibrate-HP β CD system in water

HP β CD: Hydroxy propyl β -cyclodextrin

of a 1:1 complex with respect to HPβCD concentrations. The apparent stability constants, $K_{1:1}$, obtained from the slope of the linear phase solubility diagram was 630.0006 M^{-1} for HPβCD [Eq. (1)]. The $K_{1:1}$ value suggested that fenofibrate formed more stable complex with HPβCD.

An indication of the process of transfer of fenofibrate from pure water to the aqueous solution of HPβCD may be obtained from the values of the Gibbs free energy change (Table 1). The values of Gibbs free energy associated with the aqueous solubility of fenofibrate in the presence of HPβCD (were all negative for HPβCD at various concentrations, indicating the spontaneous nature of the drug solubilization. The values decreased with increasing HPβCD concentration, demonstrating that solubilization was more favorable as concentration of HPβCD increased.

Table 1. Effect of HPβCD concentration and Gibbs free energy on solubility of fenofibrate

Sr. no.	Concentration of HPβCD (mM)	Concentration of fenofibrate (mM)	(ΔGtr) (J/Mol)
1	0	0.007012	0
2	2	0.022256	-684.006
3	4	0.033079	-918.699
4	6	0.039483	-1023.508
5	8	0.048561	-1146.070
6	10	0.058632	-1257.683

HPβCD: Hydroxy propyl β-cyclodextrin

Dissolution studies

The results of the dissolution studies for individual samples (fenofibrate alone, PMs, and complexes) over 2 h are shown in Figure 2. Onset of dissolution of pure fenofibrate is very slow, with about 13.29% of drug being dissolved in 120 min. Complexes of fenofibrate with HPβCD had considerably enhanced dissolution rates as compared to pure drug fenofibrate and PMs.

Percentage dissolution efficiencies (%DE) values were computed for comparative analysis of all the formulations. The %DE values in the initial time period of the dissolution study, i.e.,

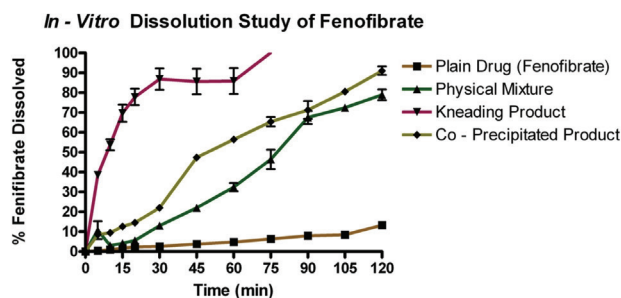


Figure 2. *In vitro* dissolution study of fenofibrate-HPβCD complexes

HPβCD: Hydroxy propyl β-cyclodextrin

%DE_{10min}, provide comparative information for very fast releasing formulations, whereas those for %DE_{60min} provide relative information about both fast and slow releasing formulations. The values of %DE_{60min} for the pure drug increased to 32.45% in PMs and up to 87.39% in kneaded product and 56.46% in coprecipitated products. The change in DE_{60min} of the drug in its PMs and complexes is statistically significant ($p < 0.05$).

The results of % dissolution and dissolution efficiency study indicate an improvement in the dissolution rate of fenofibrate in cyclodextrin complexes by both techniques. The improvement in dissolution rate is possibly caused by several factors:

- the strong hydrophilic character of HPβCD, which improves the water penetration and wettability of the hydrophobic fenofibrate,
- the optimal dispersion of fenofibrate to HPβCD,
- the absence of crystals corresponds to lower energy required for dissolution, and
- the intermolecular hydrogen bonds and the molecular dispersion of fenofibrate on HPβCD lead to partial miscibility, improving the hydrophilic characteristics of the drug substance via interactions with βCD the improvement of dissolution rate of fenofibrate in the physical mixture is due to increased wettability of the drug powder.²⁰

Kneading showed better dissolution than coprecipitation. This could be attributed to the improved wetting provided by cyclodextrins in kneading than in coprecipitation, as earlier reported by Mukne for triamterene²¹ and Deshmukh for ziprasidone.²² Thus it can be concluded that kneading is better for complexation than coprecipitation.

FTIR spectroscopy

The FTIR spectra of the systems of fenofibrate-HPβCD and those of pure components are shown in Figure 3. When the systems are compared, it can be observed that the ester group stretching band at 1727.91 cm^{-1} broadens and shifts towards higher wavenumbers, indicating change in the intermolecular H-bonds of the drug upon complexation. Similar modifications

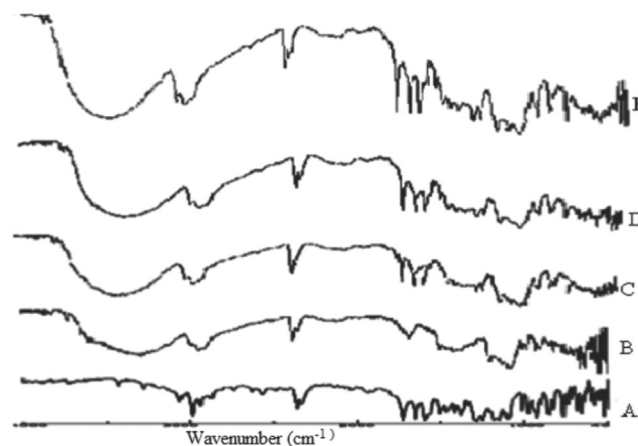


Figure 3. FTIR spectrograms of a) pure drug fenofibrate, b) HPβCD, c) physical mixture, d) kneading product, e) coprecipitated product

FTIR: Fourier transform infrared, HPβCD: Hydroxy propyl β-cyclodextrin

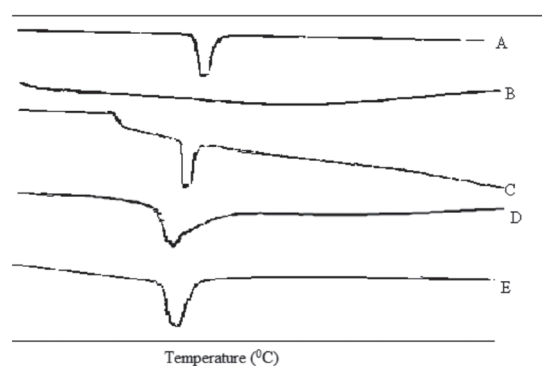


Figure 4. DSC curves of a) fenofibrate, b) HPβCD, c) physical mixture, d) kneading product, e) coprecipitation product

DSC: Differential scanning calorimetry, HPβCD: Hydroxy propyl β-cyclodextrin

were seen in the combination signal of the ester group, which indicates change in the interaction of this group when the complex is formed. In addition, the bands at 1050–1340 cm^{-1} corresponding to antisymmetric vibrations of the aryl ether group and C–O stretching of esters broaden in some cases and in others peaks vanish upon complexation. The decreased intensity and vanishing of the band are associated with the out-of-plane bending of the aromatic C–H bonds at 824–844 cm^{-1} , evidence of the inclusion of the benzene ring.²³

Finally, the C–H stretching seen at 3032–3052 cm^{-1} vanishes in the complexes, indicating that complexation has occurred.

DSC studies

The DSC thermogram of HPβCD showed a straight line. The DSC curve of fenofibrate showed a broad endothermic peak in the range of 80–90°C owing to the melting point of the drug. The peak of fenofibrate showed changes in terms of peak area and ΔH (heat of fusion) value (Table 2) in the case of the complexes as compared to the physical mixture comprising drug:HPβCD in the same ratio. This suggested that the presence of HPβCD resulted in complexation of fenofibrate. The change in peak height and broadening of peaks may be attributed to loss of crystallinity.²⁴

Table 2. Peak area and heat of fusion (ΔH) values obtained from DSC curves

Sample	Height mW	ΔH (J/gm)
Fenofibrate	-8.82	93.83
Physical mixture (P1)	-5.35	20.21
Kneading product (B1)	-2.44	12.03
Coprecipitation product (C1)	-3.41	12.7

DSC: Differential scanning calorimetry

CONCLUSIONS

The solubility and dissolution rate of fenofibrate can be enhanced by the use of complexes of fenofibrate with HPβCD. The solubilization effects of HPβCD, reduction of particle

aggregation of the drug, loss in crystallinity, increased wettability and dispersibility, and alteration in the surface properties of the drug particles might be responsible for the enhanced solubility and dissolution rate of fenofibrate from its complexes and physical mixtures.

Kneading showed better dissolution than coprecipitation. This could be attributed to the improved wetting provided by cyclodextrins in kneading than in coprecipitation.

It is concluded that fenofibrate–HPβCD complexation results in an increase in the solubility and dissolution rate of the drug, suggesting a possible enhancement of its oral bioavailability.

ACKNOWLEDGEMENTS

The authors are grateful to Shreya Life Sciences Ltd and Wockhardt for providing gift samples of fenofibrate and cyclodextrin, respectively. The authors are thankful to Y B Chavan College of Pharmacy, Aurangabad, and Marathwada Mitra Mandal's College of Pharmacy, Kalewadi, Pune.

Conflict of Interest: No conflict of interest was declared by the authors.

REFERENCES

- Gidwani SK, Singurkar PS. Fenofibrate- Cyclodextrin Inclusion Complexes and Other Pharmaceutical Composition. US patent US 2003/0220293A1. 2003 Nov 27.
- Yalkowsky SH. Solubility and Solubilization in Aqueous Media. Oxford University Press; Cambridge; 1999.
- Loftsson T, Brewster ME. Pharmaceutical application of cyclodextrins. 1. Drug solubilization and stabilization. *J Pharm Sci.* 1996;85:1017-1025.
- Rangel-Yagui CO, Pessoa A Jr, Tavares LC. Micellar Solubilization of drugs. *J Pharm Pharm Sci.* 2005;8:147-163.
- Serajuddin ATM, Pudipeddi M. Salt selection strategies. In: Stahl PH, Wermuth CG. eds. Handbook of Pharmaceutical Salts Properties Selection and Use. Verlag Helvetica Chimica Acta/Wiley-VCH, Switzerland; Federal Republic of Germany; 2002:158-159.
- Stella VJ, Nti-Addae KW. Prodrug strategies to overcome poor water solubility. *Adv Drug Deliv Rev.* 2007;59:677-694.
- Blagden N, de Matas M, Gavan PT, York P. Crystal engineering of active pharmaceutical ingredients to improve solubility and dissolution rates. *Adv Drug Deliv Rev.* 2007;59:617-630.
- Shefter E, Higuchi T. Dissolution behavior of crystalline solvated and nonsolvated forms of some pharmaceuticals. *J Pharm Sci.* 1963;52:781-791.
- Hickey MB, Peterson ML, Scoppettuolo LA, Morrisette SL, Vetter A, Guzmán H, Remenar JF, Zhang Z, Tawa MD, Haley S, Zaworotko MJ, Almarsson O. Performance comparison of a co-crystal of carbamazepine with marketed product. *Eur J Pharm Biopharm.* 2007;67:112-119.
- Szejtli, J. Cyclodextrins in drug formulations: Part I. *Pharmaceutical Technology.* 1991;3:15-22.
- Uekama K, Hirayama F, Irie T. Cyclodextrin drug carrier systems. *Chem Rev.* 1998;98:2045-2076.
- Loftsson T, Masson M. Cyclodextrin in topical drug formulations: theory and practice. *Int J Pharm.* 2001;225:15-30.

13. Rawat S, Jain SK. Solubility enhancement of celecoxib using beta-Cyclodextrin inclusion complexes. *Eur J Pharm Biopharm.* 2004;57:263-267.
14. Hamada H, Ishihara K, Masuoka N, Mikuni K, Nakajima N. Enhancement of Water-Solubility and Bioactivity Paclitaxel Using Modified Cyclodextrins. *J Biosci Bioeng.* 2006;102:369-371.
15. Higuchi T, Connors K. Phase solubility techniques. *Advances in Analytical Chemistry and Instrumentation.* 1965;7:117-212.
16. Asker AF, Whitworth CW. Dissolution of acetylsalicylic acid from acetylsalicylic acid-polyethylene glycol 6000 coprecipitates. *Pharmazie* 1975;30:530-531.
17. Veiga F, Dias T, Kedzierewicz F, Sousa A, Maincent P. Inclusion complexation of tolbutamide with β -cyclodextrin and hydroxypropyl- β -cyclodextrin. *Int J Pharm.* 1996;129:63-71.
18. Liu L, Zhu S. Preparation and characterization of inclusion complexes of prazosin hydrochloride with β -cyclodextrin and hydroxypropyl-beta-cyclodextrin. *J Pharm and Biomed Anal.* 2006;40:122-127.
19. Stancanelli R, Crupi V, De Luca L, Ficarra P, Ficarra R, Gitto R, Guardo M, Iraci N, Majolino D, Tommasini S, Venuti V. Improvement of water solubility of non- competitive AMPA receptor antagonist by complexation with beta-cyclodextrin. *Bioorg Med Chem.* 2008;16:8706-8712.
20. Crison JR, Shah VP, Skelly JP, Amidon GL. Drug dissolution into micellar solutions: development of a convective diffusion model and comparison to the film equilibrium model with application to surfactant-facilitated dissolution of carbamazepine. *J Pharm Sci.* 1996;85:1005-1011.
21. Jamzad S, Fassihi R. Role of Surfactant and pH on Dissolution Properties of Fenofibrate and Glipizide A Technical Note. *AAPS PharmSciTech.* 2006;7:33.
22. Van den MG, Augustijns P, Bleton N, Kinget R. Physico chemical characterization of solid dispersions of temazepam with polyethylene glycol 6000 and PVP K30. *Int J Pharm.* 1998;164:67-80.
23. Mukne AP, Nagarsenkar MS. Triamterene-beta- cyclodextrin systems: Preparation, Characterization and *in vivo* evaluation. *AAPS Pharmasci Tech.* 2004;5:19.
24. Deshmukh SS, Potnis VV, Shelar DB, Mahaparale PR. Studies on inclusion complexes of ziprasidone hydrochloride with β cyclodextrin and hydroxyl propyl β cyclodextrin. *Indian Drugs,* 2007;44:677-682.



Effect of the Lipid Peroxidation Product 4-Hydroxynonenal on Neuroinflammation in Microglial Cells: Protective Role of Quercetin and Monochloropivaloylquercetin

Mikroglial Hücrelerde Lipid Peroksidasyon Ürünü 4-Hidroksinonenalin Nöroinflamasyon Üzerine Etkisi: Kersetin ve Monokloropivaloilkersetinin Koruyucu Rolü

Ahmet CUMAĞLU*, Aslı Özge AĞKAYA, Zehra ÖZKUL

Erciyes University, Faculty of Pharmacy, Department of Biochemistry, Kayseri, Turkey

ABSTRACT

Objectives: The lipid peroxidation-derived aldehyde 4-hydroxynonenal (HNE) has been implicated in a number of oxidative stress-induced inflammatory pathologies such as neurodegenerative diseases and aging. In this regard, we investigated the effects of HNE on neuroinflammatory responses by measuring cyclooxygenase-2 (COX-2) and inducible nitric oxide synthase (iNOS) induction with cytokine production. In addition, we measured nuclear factor erythroid 2-related factor 2 (Nrf-2)/Kelch-like ECH-associated protein 1 (Keap1) signaling proteins, and antioxidant enzymes heme oxygenase-1 (HO-1) and nicotinamide adenine dinucleotide phosphate dehydrogenase, quinone 1 (NQO1), and compared the results with quercetin and monochloropivaloylquercetin (MPQ) pretreated microglial cells.

Materials and Methods: Cytotoxicity was determined by MTT (3-(4,5-dimethylthiazol-2-yl)-2,5-diphenyltetrazolium bromide) assay and production of cytokines was determined by cytokine array. Furthermore, intracellular Nrf2/Keap1 signaling proteins, HO-1, NQO1, and COX-2 expression were analyzed by western blot in 2.5 µM HNE treated BV-2 cells.

Results: Inducible nitric oxide synthase (iNOS) and COX-2 mRNA levels were measured with reverse transcription-quantitative polymerase chain reaction. HNE induced both COX-2 mRNA and protein levels, iNOS mRNA expression, and cytokine production. In addition, HNE markedly increased Keap1 levels and decreased cytoplasmic Nrf-2 expression with antioxidant enzyme HO-1 levels. Quercetin and monochloropivaloylquercetin treatment alleviated neuroinflammatory responses in microglial cells, by decreasing COX-2 mRNA expression. Monochloropivaloylquercetin decreased cytoplasmic Keap1 levels and increased nuclear translocation of Nrf-2 resulted in induction of HO-1 and NQO1 expression.

Conclusion: These results suggest that HNE could be a link between oxidative stress and inflammation in BV-2 microglia cells. In particular, monochloropivaloylquercetin alleviated inflammation, probably by decreasing the expression of proinflammatory genes and strengthening the antioxidant defense system.

Key words: 4-Hydroxynonenal, microglia, quercetin, inflammation, cyclooxygenase-2, hemeoxygenase-1

ÖZ

Amaç: Lipit peroksidasyonu ürünü aldehit, 4-hidroksinonenal (HNE), nörodejeneratif hastalıklar ve yaşlanma gibi oksidatif strese bağlı inflamatuvar patolojilerle ilişkilendirilmiştir. Bu bağlamda, HNE'nin nöroinflamatuvar cevap üzerine etkisini siklooksijenaz-2 (COX-2), indüklenebilir nitrik oksit sentaz (iNOS) ifadenmeleri ve sitokin üretimi üzerinden incelenmiştir. Bunlara ek olarak, nükleer faktör eritroid 2-ilişkili faktör 2 (Nrf2)/Kelch-benzeri ECH-ilişkili protein 1 (Keap1) sinyal proteinleri, antioksidan enzimler hemoksijenaz-1 (HO-1) ve nikotinamid adenin dinükleotit fosfat dehidrojenaz, kinon 1 (NQO1) ifadenme düzeyleri ölçüldü ve sonuçlar kersetin ve monokloropivaloilkersetin uygulanan hücrelerle karşılaştırılmıştır.

Gereç ve Yöntemler: Sitotoksikite MTT (3-(4,5-dimetiltiyazol-2-yl)-2,5-difeniltetrazolyum bromit) indirgenme yöntemi ile ölçüldü ve sitokin üretimi ise sitokin array ile belirlendi. Bununla birlikte, 2,5 µM HNE uygulanmış BV-2 hücrelerinde hücre içi Nrf2/Keap1 sinyal proteinleri, HO-1, NQO1

*Correspondence: E-mail: ahmetcumaoglu@yahoo.com, Phone: +90 533 340 51 04 ORCID-ID: orcid.org/0000-0002-3997-7746

Received: 26.09.2017, Accepted: 14.12.2017

©Turk J Pharm Sci, Published by Galenos Publishing House.

ve COX-2 ifadeleri Western blot ile analiz edildi. iNOS ve COX-2 mRNA düzeyleri ters transkripsiyon-kantitatif polimeraz zincir reaksiyonu ile ölçülmüştür.

Bulgular: HNE mikroglial hücrelerde COX-2 mRNA ve protein düzeylerini, iNOS mRNA düzeylerini ve bunlarla birlikte sitokin üretimini artırdı. Buna ek olarak, HNE uygulaması Keap1 düzeyinde belirgin bir artışla birlikte, sitoplazmik Nrf2 ifadeleri ve antioksidan enzim HO-1 düzeylerini azaltmıştır. Kersetin ve monokloropivaloilkersetin ile tedavi COX-2 mRNA ifadenme düzeylerini azaltarak nöroinflamasyonu hafifletmiştir. Monokloropivaloilkersetin sitoplazmik Keap1 seviyelerini azaltırken Nrf2'nin nükleer translokasyonunu artırmıştır, bu durum HO-1 ve NQO1 ifadenmelerini uyarımı ile sonuçlanmıştır.

Sonuç: Bu sonuçlar BV-2 mikroglial hücrelerde HNE'nin oksitativ stres ve inflamasyon arasında bağlayıcı olabileceğini göstermektedir. Özellikle monokloropivaloilkersetin, proinflamatuvar genlerin ifadenme düzeylerini azaltıp, antioksidan savunma sistemini güçlendirerek inflamasyonu hafifletmiştir.

Anahtar kelimeler: 4-Hidroksinonenal, mikroglia, kersetin, inflamasyon, siklooksijenaz-2, hemoksijenaz-1

INTRODUCTION

Lipid peroxidation causes generation of highly reactive aldehydes such as acrolein, malondialdehyde, and hydroxynonenal (HNE). This lipid by-product is capable of modifying nucleophilic side chains on amino acid residues (Cys, His, Arg, Lys) primarily through 1,4-Michael-type conjugate reactions.¹ The formation of these adducts (mostly irreversible) can lead to multiple deleterious events such as inhibition of DNA, RNA, and protein synthesis; and disruption of protein and cell membrane functions.² Oxidative stress and associated membrane lipid peroxidation are involved in the pathogenesis of ageing³ and neurodegenerative diseases,⁴ which include Alzheimer disease (AD) and others.⁵ Previous studies reported an important role of HNE in the development of AD.^{6,7} Thus, significant increases in free HNE in the cerebrospinal fluid,⁸ amygdala, hippocampus, and parahippocampal gyrus⁹ were detected in the brains of AD patients compared to control subjects. The central nervous system (CNS) is sensitive to oxidative stress because of the high levels of polyunsaturated lipids in neuronal cell membranes and poor antioxidant defense.¹⁰ HNE-mediated oxidative stress may indirectly contribute to brain damage by activating a number of cellular pathways, resulting in the expression of stress-sensitive genes and proteins to cause oxidative damage. Moreover, oxidative stress also may activate glia cell-mediated inflammation, which also causes secondary neuronal damage. Microglia are unique resident immune cells of the CNS acting as primary mediators of inflammation.¹¹ Under physiological conditions, microglia have small cell bodies (surveillance mode) and have low levels of reactive free radicals. When hazardous signals excite microglial cells, cells pass to the pro-inflammatory phase. The characteristics of the inflammatory phase (M1 stage) are induction of stress-sensitive genes in NFκB signaling and proinflammatory cytokines (IL-6, TNF-α, and IF-γ). The pro-inflammatory polarization of microglia is often followed by a long-lasting repair stage (M2 stage) The M2 program is activated by anti-inflammatory cytokines such as IL-4, IL-13, and IL-10.¹² Finally, activated glial cells are thus histopathological hallmarks of neurodegenerative diseases. When activated by proinflammatory stimuli, microglia release substantial levels of cytokines, chemokines, and other neurotoxins and mounting evidence suggests this contributes to neuronal damage during neuroinflammation.¹³

Nuclear factor erythroid 2-related factor 2 Nrf-2 (NF-E2-related factor-2) transcription factor regulates oxidative

stress response and represses inflammation. Nrf-2 deficiency causes an exacerbation of inflammation and an inducer of Nrf-2 such as dimethyl fumarate has been approved for the treatment of multiple sclerosis¹⁴ in part based on its anti-inflammatory function. In physiological condition, Nrf-2 is sequestered by Keap1 (kelch-like ECH-associated protein 1). Keap1 is a key regulator of the Nrf-2 signaling pathway and serves as a molecular switch to turn on and off the Nrf-2/Keap1-ARE pathway. When oxidative modification of one of the Keap1 occurs, Nrf-2 escapes from this proteolytic pathway, then translocates to the nucleus, and binds to the antioxidant response element (ARE). Nrf-2-mediated ARE activation leads to the expression of cytoprotective enzymes, such as NAD(P)H: quinone oxidoreductase 1 (NQO1) and heme oxygenase 1 (HO-1).^{15,16} Cyclooxygenase-2 (COX-2) is mainly expressed in activated macrophages and other inflammatory cells and is upregulated after exposure to inflammatory stimuli, but the use of COX-2 inhibitors is a successful approach to counter the damaging effects of inflammation.¹⁷

Flavonoids comprise a large group of compounds occurring widely throughout the plant kingdom and exert several biological activities, which are mainly related to their antioxidant properties,¹⁸ and they are able to regulate immune responses.¹⁹ Quercetin is the most common flavonoid in nature and fruits and vegetables, especially berries and onions, are the primary sources of naturally occurring dietary quercetin derivatives. Quercetin bioavailability is generally poor and characterized by high intersubject variability.²⁰ To find new analogues with increased bioavailability and enhanced pharmacological activity, researchers have attempted the chemical modification of quercetin.

Monochloropivaloylquercetin was prepared by Bel/Novamann International s.r.o. according to Veverka et al.²¹ Its antioxidant potential and enzyme inhibitory activity (aldose reductase, glycosidase, and sarcoplasmic/endoplasmic reticulum calcium ATPases 1) were shown by Žižková et al.²² In addition, chloropivaloylquercetin has an anti-inflammatory effect on lipopolysaccharide induced neuroinflammation by downregulating NFκB activity.²³

In the present study, we aimed to investigate the influence of HNE-mediated oxidative stress on the induction of inflammatory response in BV-2 (mouse microglia cells) and present some emerging therapeutic options for antioxidant/anti-inflammatory therapy, together with the therapeutic potential of quercetin and monochloropivaloylquercetin.

MATERIALS AND METHODS

Cell culture

BV-2 mouse microglial cells were kindly donated by Lucia Rackova PhD (Slovak Academy of Sciences, Slovakia). The cells were cultured in either 75 cm² flasks or 6-well dishes containing Dulbecco's Modified Eagle Medium (DMEM) supplemented with 10% fetal bovine serum (FBS), 2 mM glutamine, 100 U/mL penicillin, and 10 µg/mL streptomycin and grown in a 5% CO₂ atmosphere at 37°C.

Determination of cytotoxicity (MTT assay)

The cytotoxic effect of HNE was evaluated by MTT (3-[4,5-dimethylthiazol-2-yl]-2,5 diphenyl tetrazolium bromide) reduction assay. BV-2 cells were treated with 0-50 µM of HNE without phenol red 1% FBS supplemented DMEM for 6 h and then rinsed three times with ice-cold phosphate-buffered saline (PBS). MTT was added to the final concentration of 0.5 mg/mL. After 4 h of MTT incubation, solubilization buffer (10% sodium dodecyl sulfate in 0.01 mol/L HCl) was added and the colored formazan crystals were gently resuspended. The absorbance at 570 nm was recorded with a microplate reader (Bio-Tek ELX800, BioTek Instruments Inc., Winooski, VT, USA).

Western blot analysis of antioxidant proteins (Nrf-2/Keap-1, HO-1, and NQO1)

Cells were pretreated with N-acetyl-L-cysteine (Sigma-Aldrich, St. Louis, MO, USA), quercetin (Sigma-Aldrich), and monochloropivaloylquercetin (indicated concentrations for 3 h) and treated with HNE (2.5 µmol/L, 6 h). After the treatment procedure the cells were washed in ice cold PBS three times and lysed in radio immunoprecipitation assay buffer supplemented with 2 mM Na₃VO₄ and protease inhibitor cocktail (Complete Mini™, Roche, Mannheim, Germany) at 4°C. The lysate was clarified by centrifugation at 10,000 rpm for 10 min at 4°C to remove insoluble components. We used Ne-PER (Pierce, Rockford, IL, USA) nuclear and cytoplasmic extraction reagents to prepare fractions according to the manufacturer's instructions. Cell lysates were normalized for protein content using bicinchoninic acid assay reagent (Pierce). Equal amounts (30 µg) of protein were loaded onto 10% PAGE gels and separated by standard SDS-PAGE procedure. Proteins were transferred to a polyvinylidene difluoride membrane (Bio-Rad, Hercules, CA, USA) and blocked with 5% nonfat dry milk in TBST. To detect protein expression, the blots were probed with the specific antibodies against HO-1, Keap1, Nrf-2 (Bioss, Woburn, MA, USA), COX-2 (Santa Cruz Biotechnology, Santa Cruz, CA, USA), and NQO1 (Abcam, Cambridge, MA, USA) followed by the secondary antibodies coupled to horseradish peroxidase. The detection of GAPDH (Cell Signaling Technology Inc., Beverly, MA, USA) with a specific antibody was used as an internal control. The immunoreactive proteins on the membrane were detected by chemiluminescence using the SuperSignal® West Pico (Pierce) on X-ray film.

Determination of COX-2 and inducible nitric oxide synthase mRNA levels with quantitative real-time polymerase chain reaction

Total RNA isolation from cells was performed via phenol-guanidine thiocyanate extraction using RNAzol isolation

reagent (Sigma-Aldrich), according to the manufacturer's instructions. Total RNA (1 µg) was reverse-transcribed to cDNA using a Transcriptor High Fidelity cDNA Synthesis Kit (Roche) in a 20 µL reaction mixture. Real-time polymerase chain reaction (PCR) was carried out using a LightCycler Nano System (Roche). To quantify cDNA, qPCR was performed using FastStart Essential DNA probe master mix (Roche). The reaction mixture (15 µL) was prepared in LightCycler 8-tube strips (Roche) and included 10 µL of 2' Master Reaction Mix (Roche), 4 µL of PCR grade water, 1 µL of catalogue assay kit (kits consist mix of primers and probes for determination of iNOS, COX-2, β-actin), and 5 µL of cDNA. Real-time PCR was performed according to the following conditions: activation of Taq DNA polymerase and DNA denaturation at 95°C for 10 min, followed by 45 amplification cycles for 10 s at 95°C and for 30 s at 60°C. For each sample the level of target gene transcripts was normalized to β-actin.

Cytokine profiling of BV-2 cells by cytokine array

BV-2 cells (1×10⁶) were treated with HNE (2.5 µmol/L, 6 h) and the released cytokines were determined semiquantitatively by mouse cytokine antibody array (Abcam) according to the manufacturer's protocol. The density of the cytokine spots was analyzed by using the ImageJ densitometric analysis program. We used the intensity of positive control spots for normalization of array results.

Statistical analysis

Possible associations between groups were analyzed with SigmaPlot 12 statistical software using the t test. P values <0.05 were considered statistically significant. Fold increases or decreases in mRNA levels were also calculated by relative expression software tool developed for group-wise comparison and statistical analysis of relative expression results.

RESULTS

HNE induces microglial cell death

Firstly, we investigated the cytotoxic activity of HNE in BV-2 cells. As shown in Figure 1, HNE dose-dependently triggered cell death. After 6 h of incubation, HNE significantly reduced

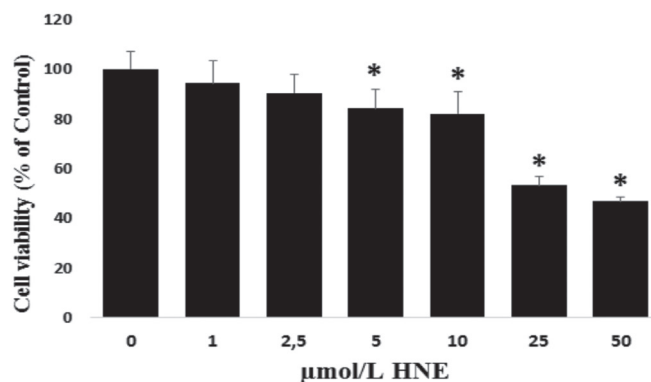


Figure 1. Effect of HNE on cell viability assessed by MTT reduction assay in BV-2 cell line

n=4, *p<0.05 vs. control (0)

HNE: 4-hydroxynonenal

the viability of cultured microglial cells at the conc. >2.5 μmol/L, whereas 2.5 μmol/L or lower concentrations of HNE decreased cultured cell viability, but the differences were not statistically significant. The nontoxic highest concentration of HNE was used for induction of neuroinflammation. Quercetin and monochloropivaloylquercetin were toxic over 10 μM (data not shown). Thus, for all the further studies these nontoxic doses of quercetin and monochloropivaloylquercetin were used, ranging from 2.5 to 5.0 μM.

Modulation of the cytokine secretion in BV-2 cells in response to HNE

We then examined the inflammatory effect of HNE on cytokine production in BV-2 cells. A mouse cytokine antibody array was applied to broadly observe the effects of HNE on cytokine secretion. After the cells were incubated with HNE for 6 h, the cytokine expression pattern in the treated cells was differentially compared to that in the control cells (Figure 2). According to the array results, under basal conditions (in control cells), IL-5, IL-17, SCF, and VEGF protein expressions were at undetectable levels. After HNE treatment, cytokine protein expressions of granulocyte colony stimulating factor, granulocyte/macrophage colony stimulating factor, IL-2, IL-3, IL-4, IL-5, IL-9, IL-10, IL-13, IL-17, IF-γ, SCF, p60/p70, VEGF, and TNF-α all were increased. Expressions of IL-6, RANTES, MCP-1, and sTNHR1 were slightly increased in HNE-treated cells, compared to those

of the untreated group. IL-12p70, MCP-5, and thrombopoietin expression patterns did not change in HNE-treated cells, when compared with those of the untreated group.

Changes in proinflammatory gene expression in response to oxidative stress: effects of quercetin and monochloropivaloylquercetin pretreatment

After BV-2 cells were exposed to HNE for 0, 1, 3, 6, and 12 h, we performed mRNA and protein expression analysis of the COX-2 and mRNA expression of iNOS. Real-time PCR analysis confirmed that there was a time-dependent increase in the expressions of COX-2 and inducible nitric oxide synthase (iNOS) in the HNE-treated BV-2 cells compared with the control (Figure 3). In parallel to these results, HNE exposure increased COX-2 protein expression. Although pretreatment with quercetin and monochloropivaloylquercetin did not affect iNOS mRNA expression in HNE-treated BV-2 cells, monochloropivaloylquercetin pretreatment significantly decreased COX-2 mRNA expression (Figure 4).

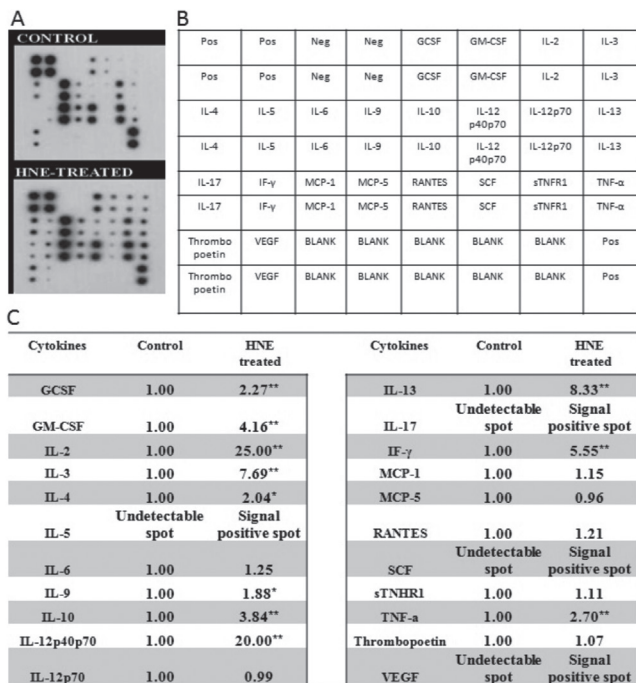


Figure 2. Effect of HNE treatment on cytokine production in BV-2 cells. (A) Image of cytokine array. (B) Gene map of cytokine array. All spots are in duplicate. (C) the quantification by image of cytokine secretion in nontreated control cells and HNE-treated BV-2 cells. Fold changes were given in the table after average spot signals of control cells were assumed as 1.00 *p<0.05, **p<0.01

Pos: Positive controls, Neg: Negative controls, HNE: 4-hydroxynonenal, GCSF: Granulocyte colony stimulating factor, GM-CSF: Granulocyte/macrophage colony stimulating factor

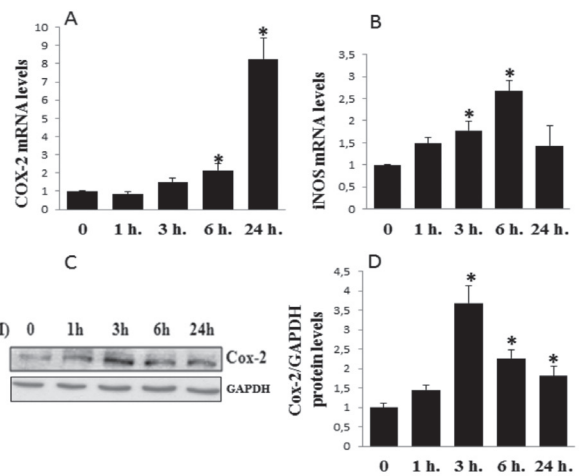


Figure 3. Time-dependent changes in COX-2 mRNA expression (A), iNOS mRNA expression (B), and COX-2 protein expression (C, D) in HNE-treated BV-2 cells

n=3, *p<0.05 vs. control (0)

COX-2: Cyclooxygenase-2, HNE: 4-hydroxynonenal, iNOS: Inducible nitric oxide synthase, GAPDH: Glyceraldehyde-3-phosphate dehydrogenase

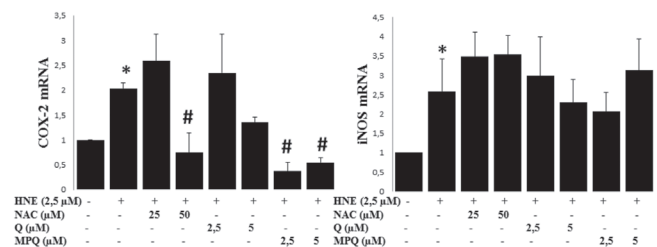


Figure 4. Effects of quercetin and monochloropivaloylquercetin on COX-2 mRNA expression and iNOS expression in HNE-treated BV-2 cells

n=3, *p<0.05 vs. control (0), #p<0.05 vs. HNE

COX-2: Cyclooxygenase-2, HNE: 4-hydroxynonenal, NAC: N-acetyl-L-cysteine, Q: Quercetin, MPQ: Monochloropivaloylquercetin, iNOS: Inducible nitric oxide synthase

Quercetin and monochloropivaloylquercetin induce HO-1 and NQO1 expression by inducing nuclear translocation of Nrf-2 in HNE-treated BV-2 cells

It is known that the redox-sensitive transcription factor Nrf-2 plays an important role in cellular defense against oxidative stress by inducing the expression of phase II genes (Figure 5). Western blot analysis was performed to determine the cytoplasmic expression and nuclear translocation of Nrf-2 in response to 2.5 $\mu\text{mol/L}$ HNE, quercetin, and monochloropivaloylquercetin. Although HNE did not cause any nuclear translocation of Nrf-2 at 6 h, it increased the cytoplasmic expression of Keap1 and decreased the cytoplasmic expression of Nrf-2. In addition, HNE treatment caused a slight alteration in HO-1 and NQO1 expression but the difference was not statistically significant (Figure 6). Pretreatment with quercetin and

monochloropivaloylquercetin markedly decreased cytoplasmic Keap1 levels with increased cytoplasmic Nrf-2 levels. At the same time, monochloropivaloylquercetin pretreatment induced expression of the antioxidant proteins HO-1 and NQO1, while quercetin pretreatment induced NQO1 expression with both molecules increased nuclear translocation of Nrf-2.

DISCUSSION

The aim of this study was firstly to test the effect of mild-type oxidative/electrophilic stress on neuro-inflammatory response in microglial cells induced by HNE, and secondly to investigate the protective ability of quercetin and monochloropivaloylquercetin. We found that HNE induced inflammatory response by increasing both COX-2 mRNA and protein expression as well as iNOS mRNA levels in a time-dependent manner and augmenting cytokine production. Quercetin and monochloropivaloylquercetin exerted a significant antioxidant effect by strengthening the antioxidant defense system via induced nuclear translocation of Nrf-2 and decreased Keap1 expression in addition to increased NQO1. Additionally, monochloropivaloylquercetin induced HO-1 expression and behaved as an anti-neuroinflammatory agent by decreasing COX-2 expression against HNE-induced inflammatory in BV-2 cells.

HNE is thought to contribute to the dysfunction and death of neurons in the pathogenesis of neurodegenerative diseases. Oxidative stress also activates mechanisms that result in glia cell-mediated inflammation, also causing secondary neuronal damage. Several studies have shown that when the oxidative stress is induced by several agents, brain cells like microglia and astrocytes release diverse inflammatory mediators.^{24,25} Moreover, oxidative stress indicators [reactive oxygen species (ROS), reactive lipid peroxidation products] act as critical signaling molecules to trigger inflammatory responses in the CNS through activation of redox sensitive transcription factors.^{26,27} The ability of HNE to exert a number of toxicological effects has been attributed to its electrophilic α , β -unsaturated carbonyl moiety that can react through 1, 2 and 1, 4 additions with nucleophiles such as cysteine, lysine, and histidine residues.^{28,29} The normal, physiological level of HNE in human tissues and plasma range from 0.07 to 2.8 μM , while in diseased states and near the core of lipid peroxidation sites, its concentration can be greatly increased (even above 100 μM).³⁰ Treatment with low (1 and 10 μM) concentrations of HNE caused significant induction of cell death.^{31,32} As expected, in our study, starting with the concentration of 5 $\mu\text{mol/L}$ HNE, a significant drop in BV-2 cell viability was assessed by MTT ($84.19 \pm 7.61\%$ of control) after 6 h of treatment. Previous studies reported that HNE showed toxic effects in neuron cultures and therefore our data are in agreement with those studies.³³⁻³⁵

The goal of the present study was to identify whether HNE is a possible intracellular mediator between oxidative stress and inflammation in microglia cells. Our results reveal that oxidative stress is an iNOS and COX-2 activator in BV-2 microglia cells. Indeed, COX-2 expression was significantly increased and similarly release of proinflammatory cytokines

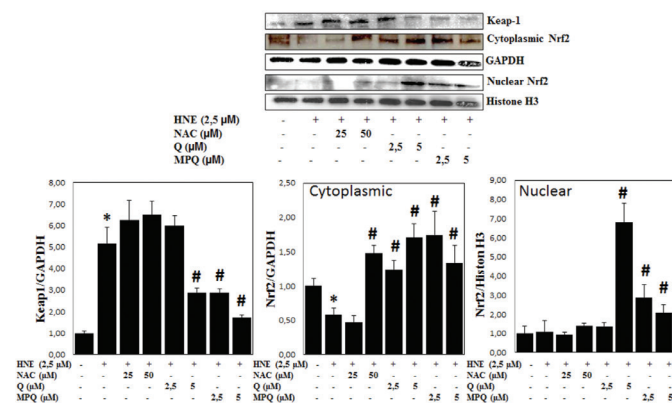


Figure 5. Effects of quercetin and monochloropivaloylquercetin on cytoplasmic Nrf-2/Keap1 protein expression and nuclear Nrf-2 translocation in HNE-treated BV-2 cells

n=3, *p<0.05 vs. control (0), #p<0.05 vs. HNE

HNE: 4-hydroxynonenal, NAC: N-acetyl-L-cysteine, Q: Quercetin, MPQ: Monochloropivaloylquercetin, GAPDH: Glyceraldehyde-3-phosphate dehydrogenase

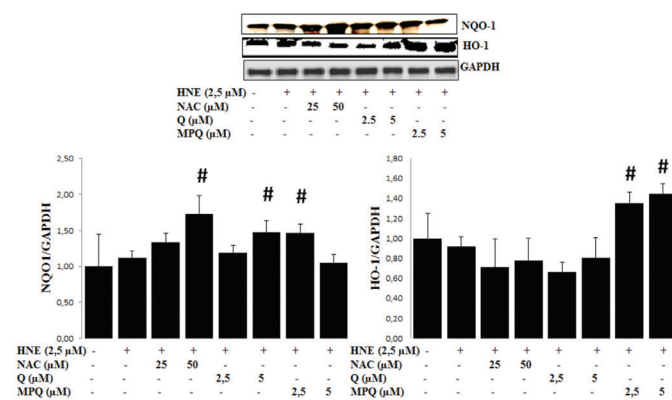


Figure 6. Effects of quercetin and monochloropivaloylquercetin on phase II protein NQO1 expression and antioxidant HO-1 protein expression in HNE-treated BV-2 cells

n=3, *p<0.05 vs. Control (0), #p<0.05 vs. HNE

COX-2: Cyclooxygenase-2, HNE: 4-hydroxynonenal, NAC: N-acetyl-L-cysteine, Q: Quercetin, MPQ: Monochloropivaloylquercetin, GAPDH: Glyceraldehyde-3-Phosphate Dehydrogenase

was significantly raised in response to HNE-mediated oxidative stress. Previous studies have reported that 4-HNE is an inducer of COX-2 expression in several types of cells including 3T3-L1 adipocytes,³⁶ epithelial RL34 cells,³⁷ and macrophages.³⁸ Our data extend these results to BV-2 microglia cells. Given that lipid peroxidation reactions are an important source of advanced glycation end products (AGEs),³⁹ the production of lipid peroxidation-derived aldehyde fragments such as HNE may indicate a mechanism by which AGE epitopes are generated. Other than HNE, advanced lipid peroxidation end products induced proinflammatory response by activating proinflammatory gene expression in monocytes.⁴⁰ In addition, activation of the receptor for advanced glycation end product mediated pathway on mononuclear phagocytes has been reported to give rise to this phenotype of activated macrophages that is manifested by the induction of some proinflammatory cytokines (IL-1 β and TNF- α), platelet-derived growth factor, and insulin-like growth factor-1. Moreover, it was emphasized in these studies that HNE is a possible link between oxidative stress and inflammation. Our results are also in agreement with those published by Kauppinen et al.⁴¹ who reported that 24-h HNE treatment induced inflammasome signaling by increased inflammasome component NRLP3 (NLR family, pyrin domain containing 3) mRNA levels in retinal pigment epithelial cells (ARPE-19), raising the IL-1 β and IL-18 release. Additionally, the inflammatory role of HNE was reported by Chen et al.⁴², who stated that single treatment with 10 μ M HNE induced proinflammatory prostaglandin E₂ (PGE₂) release as well as COX-2 and microsomal PGE₂ synthase-1 (mPGES-1) expression in osteoarthritic chondrocytes. Another key piece of evidence for the inflammatory effect of HNE was that HNE may contribute to osteoarthritis development via its ability to alter cellular phenotype and metabolic activity of osteoblasts by modulating inflammatory processes. HNE induced PGE₂ release and COX-2 expression and COX-2 promoter activity with activated MAPK signaling pathway in osteoblasts.⁴³ Although quercetin and its derivatives have been shown to have anti-inflammatory and antioxidant effects in several *in vivo* and *in vitro* studies, the effect of a new quercetin derivative monochloropivaloylquercetin on the HNE-stimulated activation of inflammatory COX-2 expression and Nrf-2/HO-1 and NQO1 antioxidant signaling pathway, which may be involved in the neuroinflammation and immune response, has not been studied before. Nrf-2 is sequestered in the cytoplasm with its cytosolic repressor Keap1. The dissociation of Nrf-2 from Keap1 is crucial for its nuclear translocation, followed by binding to the ARE.⁴⁴ The innate immune response involves generation of ROS, which can act as second messengers activating proinflammatory signaling pathways such as NF κ B.⁴⁵ Accordingly, inhibition of NF κ B and herewith activation of the Nrf-2 signaling pathway may be a beneficial strategy for reduction of the deleterious effects of inflammation and it is well known that anti-inflammatory agents suppress NF κ B signaling while activating the Nrf-2/ARE pathway.⁴⁶⁻⁴⁸ Activation of the Nrf-2 mediated signaling pathway results in upregulation of HO-1 expression. HO-1 is known to play an anti-inflammatory role due to carbon monoxide

production and NF κ B inhibition.⁴⁹ In our study, pretreatment with quercetin and monochloropivaloylquercetin activated Nrf-2/Keap1 signaling by decreasing cytoplasmic expression and inducing nuclear translocation of Nrf-2, resulting in upregulation of downstream genes HO-1 and NQO1 in HNE-treated BV-2 cells. Additionally, COX-2 mRNA stimulation by 4-HNE was inhibited when BV-2 cells were preincubated with quercetin and monochloropivaloylquercetin. In this regard, there remains the possibility that induction of Nrf-2 target genes contributes to both quercetin and monochloropivaloylquercetin's efficacy to inhibit COX-2 expression. Ramyaa et al.⁵⁰ have already reported the modulatory effect of quercetin on oxidative stress by upregulating Nrf-2 expression and downregulating NF κ B and COX-2 expression. The anti-inflammatory properties of quercetin accompanied by an increase in HO-1 protein levels associated with elevated nuclear translocation of Nrf-2 were previously exhibited by Boesch-Saadatmandi et al.⁵¹ in murine RAW 264.7 macrophages. On the other hand, quercetin acts as an anti-inflammatory agent in lipopolysaccharide-induced acute lung injury by significantly reducing COX-2 and iNOS expression, and NF κ B p65 phosphorylation.⁵² In another study, intratracheal administration of quercetin affected the protective agent by modulating HO-1 activity against lipopolysaccharide-induced acute lung injury.⁵³ Quercetin was previously shown to downregulate proinflammatory responses, involving iNOS expression and NO generation in BV-2 cells through inducing Nrf-2 mediated HO-1 expression.⁵⁴ In contrast, quercetin pretreatment did not affect iNOS mRNA expression in our study; this may be associated with the dose of quercetin or incubation time.

CONCLUSIONS

Our data provide new evidence for the inflammatory role of HNE, an oxidative stress-related product, in the physiopathology of neuro-inflammation and we propose that the activation of the Nrf-2/HO-1 pathway by quercetin and monochloropivaloylquercetin may mediate its anti-inflammatory properties.

ACKNOWLEDGEMENTS

This article was part of the master's thesis by Zehra Özkul.

Conflict of Interest: No conflict of interest was declared by the authors.

REFERENCES

1. Esterbauer H, Schaur RJ, Zollner H. Chemistry and biochemistry of 4-hydroxynonenal, malonaldehyde and related aldehydes. *Free Radic Biol Med.* 1991;11:81-128.
2. Schaur, RJ. Basic aspects of the biochemical reactivity of 4-hydroxynonenal. *Mol Aspects Med.* 2003;24:149-159.
3. Yan LJ. Positive oxidative stress in aging and aging-related disease tolerance. *Redox Biol.* 2014;2:165-169.
4. Zarkovic K. 4-hydroxynonenal and neurodegenerative diseases. *Mol Aspects Med.* 2003;24:293-303.

5. Csala M, Kardon T, Legeza B, Lizák B, Mandl J, Margittai É, Puskás F, Száraz P, Szelényi P, Bánhegyi G. On the role of 4-hydroxynonenal in health and disease. *Biochim Biophys Acta*. 2015;1852:826-838.
6. Sayre LM, Zelasko DA, Harris PL, Perry G, Salomon RG, Smith MA. 4-Hydroxynonenal-derived advanced lipid peroxidation end products are increased in Alzheimer's disease. *J Neurochem*. 1997;68:2092-2097.
7. Drake J, Petroze R, Castegna A, Ding Q, Keller JN, Markesbery WR, Lovell MA, Butterfield DA. 4-Hydroxynonenal oxidatively modifies histones: implications for Alzheimer's disease. *Neurosci Lett*. 2004;356:155-158.
8. Lovell MA, Ehmann WD, Mattson MP, Markesbery WR. Elevated 4-hydroxynonenal in ventricular fluid in Alzheimer's disease. *Neurobiol Aging*. 1997;18:457-461.
9. Markesbery WR, Lovell MA. Four-hydroxynonenal, a product of lipid peroxidation, is increased in the brain in Alzheimer's disease. *Neurobiol Aging*. 1998;19:33-36.
10. Halliwell B. Oxidative stress and neurodegeneration: where are we now? *J Neurochem*. 2006;97:1634-1658.
11. Liu B, Hong JS. Role of microglia in inflammation-mediated neurodegenerative diseases: mechanisms and strategies for therapeutic intervention. *J Pharmacol Exp Ther*. 2003;304:1-7.
12. Rojo AI, McBean G, Cindric M, Egea J, López MG, Rada P, Zarkovic N, Cuadrado A. Redox control of microglial function: molecular mechanisms and functional significance. *Antioxid Redox Signal*. 2014;21:1766-1801.
13. Suzumura A. Neuron-microglia interaction in neuroinflammation. *Curr Protein Pept Sci*. 2013;14:16-20.
14. Gopal S, Mikulskis A, Gold R, Fox RJ, Dawson KT, Amaravadi L. Evidence of activation of the Nrf2 pathway in multiple sclerosis patients treated with delayed-release dimethyl fumarate in the Phase 3 DEFINE and CONFIRM studies. *Mult Scler*. 2017;23:1875-1883.
15. Venugopal R, Jaiswal AK. Nrf1 and Nrf2 positively and c-Fos and Fra1 negatively regulate the human antioxidant response element-mediated expression of NAD(P)H:quinone oxidoreductase1 gene. *Proc Natl Acad Sci USA*. 1996;93:14960-14965.
16. Itoh K, Wakabayashi N, Katoh Y, Ishii T, Igarashi K, Engel JD, Yamamoto M. Keap1 represses nuclear activation of antioxidant responsive elements by Nrf2 through binding to the amino-terminal Neh2 domain. *Genes Dev*. 1999;13:76-86.
17. O'Banion MK. Cyclooxygenase-2: molecular biology, pharmacology, and neurobiology. *Crit Rev Neurobiol*. 1999;13:45-82.
18. Kozłowska A, Szostak-Wegierek D. Flavonoids food sources and health benefits. *Rocz Państw Zakł Hig*. 2014;65:79-85.
19. Middleton E Jr, Kandaswami C. Effects of flavonoids on immune and inflammatory cell functions. *Biochem Pharmacol*. 1992;43:1167-1179.
20. Guo Y, Bruno RS. Endogenous and exogenous mediators of quercetin bioavailability. *J Nutr Biochem*. 2015;26:201-210.
21. Veverka M, Gallovic J, Svaidlenka E, Veverkova E, Pronavova N, Milackova I, Stefek M. Novel quercetin derivatives: synthesis and screening for anti-oxidant activity and aldose reductase inhibition. *Chemical Papers*. 2013;67:76-83.
22. Žižková P, Blaškovič D, Májeková M, Švorc L, Račková L, Ratkovská L, Veverka M, Horáková L. Novel quercetin derivatives in treatment of peroxynitrite-oxidized SERCA1. *Mol Cell Biochem*. 2014;386:1-14.
23. Mrvová N, Škandlík M, Kuniaková M, Račková L. Modulation of BV-2 microglia functions by novel quercetin pivaloyl ester. *Neurochem Int*. 2015;90:246-254.
24. Bradley MA, Xiong-Fister S, Markesbery WR, Lovell MA. Elevated 4-hydroxyhexenal in Alzheimer's disease (AD) progression. *Neurobiol Aging*. 2012;33:1034-1044.
25. Williams TI, Lynn BC, Markesbery WR, Lovell MA. Increased levels of 4-hydroxynonenal and acrolein, neurotoxic markers of lipid peroxidation, in the brain in Mild Cognitive Impairment and early Alzheimer's disease. *Neurobiol Aging*. 2006;27:1094-1099.
26. Yoritaka A, Hattori N, Uchida K, Tanaka M, Stadtman E, Mizuno Y. Immunohistochemical detection of 4-hydroxynonenal protein adducts in Parkinson disease. *Proc Natl Acad Sci USA*. 1996;93:2696-2701.
27. Hsieh HL, Yang CM. Role of redox signaling in neuroinflammation and neurodegenerative diseases. *Biomed Res Int*. 2013;2013:484613.
28. Min KJ, Yang MS, Kim SU, Jou I, Joe EH. Astrocytes induce hemeoxygenase-1 expression in microglia: a feasible mechanism for preventing excessive brain inflammation. *J Neurosci*. 2006;26:1880-1887.
29. Melo A, Monteiro L, Lima RM, Oliveira DM, Cerqueira MD, El-Bachá RS. Oxidative stress in neurodegenerative diseases: mechanisms and therapeutic perspectives. *Oxid Med Cell Longev*. 2011;2011:467180.
30. Adibhatla RM, Hatcher JF. Lipid oxidation and peroxidation in CNS health and disease: from molecular mechanisms to therapeutic opportunities. *Antioxid Redox Signal*. 2010;12:125-169.
31. Siems W, Grune T. Intracellular metabolism of 4-hydroxynonenal. *Mol Aspects Med* 2003;24:167-175.
32. Wildburger R, Mrakovcic L, Stroser M, Andricic L, Borovic Sunjic S, Zarkovic K, Zarkovic N. Lipid peroxidation and age-associated diseases cause or consequence? *Türkiye Klinikleri J Med Sci*. 2009;29:189-193.
33. Milkovic L, Cipak Gasparovic A, Zarkovic N. Overview on major lipid peroxidation bioactive factor 4-hydroxynonenal as pluripotent growth-regulating factor. *Free Radic Res*. 2015;49:850-860.
34. Cumaoglu A, Aricioglu A, Karasu C. Redox status related activation of endoplasmic reticulum stress and apoptosis caused by 4-hydroxynonenal exposure in INS-1 cells. *Toxicol Mech Methods*. 2014;24:362-367.
35. Bali EB, Ergin V, Rackova L, Bayraktar O, Küçükboyacı N, Karasu C. Olive leaf extracts protect cardiomyocytes against 4-hydroxynonenal-induced toxicity in vitro: comparison with oleuropein, hydroxytyrosol, and quercetin. *Planta Med*. 2014;80:984-992.
36. Zarrouki B, Soares AF, Guichardant M, Lagarde M, Géloën A. The lipid peroxidation end-product 4-HNE induces COX-2 expression through p38MAPK activation in 3T3-L1 adipose cell. *FEBS Lett*. 2007;581:2394-2400.
37. Uchida K, Kumagai T. 4-hydroxy-2-nonenal as a COX-2 inducer. *Mol Aspects Med*. 2003;24:213-218.
38. Kumagai T, Matsukawa N, Kaneko Y, Kusumi Y, Mitsumata M, Uchida K. A lipid peroxidation-derived inflammatory mediator: identification of 4-hydroxy-2-nonenal as a potential inducer of cyclooxygenase-2 in macrophages. *J Biol Chem*. 2004;279:48389-48396.
39. Fu MX, Requena JR, Jenkins AJ, Lyons TJ, Baynes JW, Thorpe SR. The advanced glycation end product, Ne-(carboxymethyl)lysine, is a product of both lipid peroxidation and glycoxidation reactions. *J Biol Chem*. 1996;271:9982-9986.
40. Shanmugam N, Figarola JL, Li Y, Swiderski PM, Rahbar S, Natarajan R. Proinflammatory effects of advanced lipoxidation end products in monocytes. *Diabetes*. 2008;57:879-888.

41. Kauppinen A, Niskanen H, Suuronen T, Kinnunen K, Salminen A, Kaarniranta K. Oxidative stress activates NLRP3 inflammasomes in ARPE-19 cells implications for age-related macular degeneration (AMD). *Immunol Lett.* 2012;147:29-33.
42. Chen SH, Fahmi H, Shi Q, Benderdour M. Regulation of microsomal prostaglandin E2 synthase-1 and 5-lipoxygenase-activating protein/5-lipoxygenase by 4-hydroxynonenal in human osteoarthritic chondrocytes. *Arthritis Res Ther.* 2010;12:21.
43. Shi Q, Vaillancourt F, Côté V, Fehmi H, Lavigne P, Afif H, Di Battista JA, Fernandes JC, Benderdour M. Alterations of metabolic activity in human osteoarthritic osteoblasts by lipid peroxidation end product 4-hydroxynonenal. *Arthritis Res Ther.* 2006;8:159.
44. Zenkov NK, Menshchikova EB, Tkachev VO. Keap1/Nrf2/ARE redox-sensitive signaling system as a pharmacological target. *Biochemistry (Mosc).* 2013;78:19-36.
45. Morgan MJ, Liu ZG. Crosstalk of reactive oxygen species and NF- κ B signaling. *Cell Res.* 2011;21:103-115.
46. Wagner AE, Boesch-Saadatmandi C, Dose J, Schultheiss G, Rimbach G. Anti-inflammatory potential of allyl-isothiocyanate role of Nrf2, NF-(κ) B and microRNA-155. *J Cell Mol Med.* 2012;16:836-843.
47. Manandhar S, You A, Lee ES, Kim JA, Kwak MK. Activation of the Nrf2-antioxidant system by a novel cyclooxygenase-2 inhibitor furan-2-yl-3-pyridin-2-yl-propenone: implication in anti-inflammatory function by Nrf2 activator. *J Pharm Pharmacol.* 2008;60:879-887.
48. Yao J, Zhao L, Zhao Q, Zhao Y, Sun Y, Zhang Y, Miao H, You QD, Hu R, Guo QL. NF- κ B and Nrf2 signaling pathways contribute to wogonin-mediated inhibition of inflammation-associated colorectal carcinogenesis. *Cell Death Dis.* 2014;5:1283.
49. Bellezza I, Tucci A, Galli F, Grottelli S, Mierla AL, Pilolli F, Minelli A. Inhibition of NF- κ B nuclear translocation via HO-1 activation underlies α -tocopheryl succinate toxicity. *J Nutr Biochem.* 2012;23:1583-1591.
50. Ramyaa P, Krishnaswamy R, Padma VV. Quercetin modulates OTA-induced oxidative stress and redox signalling in HepG2 cells - up regulation of Nrf2 expression and down regulation of NF- κ B and COX-2. *Biochim Biophys Acta.* 2014;1840:681-692.
51. Boesch-Saadatmandi C, Loboda A, Wagner AE, Stachurska A, Jozkowicz A, Dulak J, Döring F, Wolfram S, Rimbach G. Effect of quercetin and its metabolites isorhamnetin and quercetin-3-glucuronide on inflammatory gene expression: role of miR-155. *J Nutr Biochem.* 2011;22:293-299.
52. Wang L, Chen J, Wang B, Wu D, Li H, Lu H, Wu H, Chai Y. Protective effect of quercetin on lipopolysaccharide-induced acute lung injury in mice by inhibiting inflammatory cell influx. *Exp Biol Med (Maywood).* 2014;239:1653-1662.
53. Takashima K, Matsushima M, Hashimoto K, Nose H, Sato M, Hashimoto N, Hasegawa Y, Kawabe T. Protective effects of intratracheally administered quercetin on lipopolysaccharide-induced acute lung injury. *Respir Res.* 2014;15:150.
54. Kang CH, Choi YH, Moon SK, Kim WJ, Kim GY. Quercetin inhibits lipopolysaccharide-induced nitric oxide production in BV2 microglial cells by suppressing the NF- κ B pathway and activating the Nrf2-dependent HO-1 pathway. *Int Immunopharmacol.* 2013;17:808-813.



Development of a Discriminative and Biorelevant Dissolution Test Method for Atorvastatin/Fenofibrate Combination with Appliance of Derivative Spectrophotometry

Türev Spektrofotometrik Yöntem ile Atorvastatin/Fenofibrat Kombinasyonunda Ayırıcı ve Biyoyumlu Çözünme Testi Metodunun Geliştirilmesi

© Panukumar Durga ANUMOLU*, © Sunitha GURRALA, © Subrahmanyam Chavali VENKATA SATYA, © Santoshi Vani POLISETTY, © Anjana RAVINDRAN, © Radhagayathri ACHANTA

Osmania University, Gokaraju Rangaraju College of Pharmacy, Department of Pharmaceutical Analysis, Hyderabad, India

ABSTRACT

Objectives: Nowadays, the market is flooded with combinations of drugs in various dosage forms, but there is a lack of official methods to quantify them. A single dissolution test method for the analysis of combined dosage form is preferred for simplification of quality control testing.

Materials and Methods: If the developed dissolution medium mimics the biorelevant and discriminating dissolution procedure for drug products with limited drug aqueous solubility it is a useful tool for qualitative forecasting of the *in vivo* behavior of formulations.

Results: Dissolution profiles were evaluated for atorvastatin and fenofibrate in capsules, using a paddle-type United States Pharmacopeia dissolution apparatus in 900 mL of medium at 50 rpm and 37±0.5°C. The best medium was 900 mL of 0.5% w/v sodium lauryl sulfate. The cumulative % dissolution was more than 85% within 45 min for marketed tablets. The proposed dissolution test conditions have discriminative power, dissimilarity factor (f_1) values are low (12-16%), and similarity (f_2) factor values are also low (45-48%). Hence the use of 0.5% w/v sodium lauryl sulfate solution is justified.

Conclusion: The dissolution method was validated (% relative standard deviation <2). To quantify both drugs simultaneously, a second derivative spectrophotometric method was established (λ_{max} 281 nm and 296 nm, respectively, for atorvastatin and fenofibrate) in acetate buffer, pH 2.8 solution.

Key words: Derivative spectrophotometry/quantification simultaneously, atorvastatin/fenofibrate combined dosage form, biorelevant/discriminative dissolution method

ÖZ

Amaç: Günümüzde, çeşitli dozaj formlarında etkin madde kombinasyonlarına rağbet edilmektedir, ancak bunlardaki etkin maddeleri tayin etmek için farmakope yöntemleri bulunmamaktadır. Bu çalışmada, kombine dozaj formunun analizi için kalite kontrol testini sadeleştirmek amacıyla tek bir çözünme testi yöntemi tercih edilmiştir.

Gereç ve Yöntemler: Suda çözünürlüğü sınırlı olan ilacın çözünme yöntemi için geliştirilen çözünme ortamı *in vivo* davranışlarının kalitatif tahmininde biyoyumlu bir yöntem olarak kullanışlı bulunmuştur.

Bulgular: Atorvastatin ve fenofibrat içeren kapsüllerde çözünme profilleri, 37±0.5°C'de, 50 rpm ve 900 mL ortam içinde bir palet tipi Amerikan Farmakopesi çözünme cihazı ile değerlendirildi. En iyi ortam, 900 mL %0.5 a/h sodyum lauril sülfattır. Piyasadaki tabletler için kümülatif % çözünme, 45 dakika içinde %85'ten fazla olmuştur. Önerilen çözünme testi koşulları ayırt edici bir güce sahiptir, farklılık faktörü (f_1) değerleri düşüktür (%12-16) ve benzerlik (f_2) faktör değerleri de düşüktür (%45-48). Bu nedenle, %0.5 w/v sodyum lauril sülfat çözeltisinin kullanımı uygundur.

*Correspondence: E-mail: panindrapharma@yahoo.co.in, Phone: +09010014734 ORCID-ID: orcid.org/0000-0001-5010-7488

Received: 14.11.2017, Accepted: 20.12.2017

©Turk J Pharm Sci, Published by Galenos Publishing House.

Sonuç: Çözünme yöntemi valide edilmiştir (% relatif standart sapma <2). Her iki etkin maddeyi pH 2.8 asetat tamponu çözeltisi içinde aynı anda tayin etmek için, ikinci türev spektrofotometrik yöntemde atorvastatin ve fenofibrat için sırasıyla λ_{\max} 281 nm ve 296 nm kullanılmıştır.

Anahtar kelimeler: Atorvastatin/fenofibrat kombine dozaj formu, biyoyoumlu/ayırıcı çözünme yöntemi

INTRODUCTION

Dissolution is considered one of the most routinely performed quality control tests on dosage forms to ensure uniformity and reproducibility of production batches. Process parameters and ingredients are optimized during product development,¹⁻³ and whether changes made to the formulations or their manufacturing processes are likely to affect the performance in the clinic or not are decided on using dissolution methods.⁴ An immediate release dosage form is designed to deliver the drug rapidly into systemic circulation. Hence, dissolution may become the rate limiting step for its absorption. The absorption of a drug substance may vary with diverse parameters like its solubility and permeability in the conditions associated with the gastro-intestinal (GI) tract after oral administration.⁵⁻⁷ Taking all these points into consideration, there is a need to put more research efforts into developing *in vitro* GI fluids that mimic *in vivo* conditions. Discriminative dissolution has the ability to differentiate the dissolution profiles between manufacturing process variations and product composition variations.⁸⁻¹⁰

Fenofibrate, chemically known as isopropyl 2-[4-(4-chlorobenzoyl)2-phenoxy] methyl propanoate, is a fibric acid derivative with lipid regulating properties exerting its therapeutic effects through activation of peroxisome proliferator activated receptor α (Figure 1A). Atorvastatin calcium, chemically [R-(R',R'')]-2-(4-Fluorophenyl)- β,δ -dihydroxy-5-(1-methylethyl)-3-phenyl [(phenylamino)carbonyl]-1H-pyrrole-1-heptanoic acid, is an HMG-Co A reductase inhibitor with hypolipidemic properties (Figure 1B).^{11,12} The combined dosage form of fenofibrate and atorvastatin is therapeutically used for hyperlipidemic patients. Fixed dose combination of drugs has been a challenge; if possible a single dissolution method is preferred to simplify quality control testing procedures.¹³⁻¹⁵ Few analytical methods were reported for simultaneous quantification of atorvastatin calcium and fenofibrate by high-performance liquid chromatographic and spectrophotometric methods.¹⁶⁻¹⁹ Derivative spectroscopy may be used with minimum error for the quantification of one analyte.^{20,21} Overlaid zero-order spectra exhibit a similar nature and overlapping for atorvastatin calcium with fenofibrate denotes development of the derivative graphical method. To the best of our knowledge, only one first and second derivative spectrophotometric method have been reported for simultaneous quantification of atorvastatin (ATV)

and fenofibrate (FEN) in methanol as solvent, but methanol is environmentally toxic and more expensive than aqueous buffers and one wavelength is 245 nm, which is normally originated from the benzenoid ring system. Since several compounds may contain benzene rings, it is always better to avoid 245 nm and select a wavelength away from it. Literature data signify the need for a simple, economical, ecofriendly, and specific analytical method for simultaneous quantification of ATV and FEN combination in tablets and dissolution samples. The development of a single dissolution method is practically challenging due to their low water solubility for combination of atorvastatin and fenofibrate. Keeping these points in mind, an attempt is made to develop and validate a single dissolution test for simultaneous quantification with application of a simple derivative spectrophotometric technique.

MATERIALS AND METHODS

Materials

Atorvastatin and fenofibrate were obtained as gift samples from Dr. Reddy's Laboratories Limited (Hyderabad, India). Methanol, hydrochloric acid, ortho-phosphoric acid, potassium di hydrogen orthophosphate, sodium hydroxide, sodium chloride, and sodium acetate were purchased from Sd Fine-Chem Limited (Mumbai, India); sodium lauryl sulfate (SLS), tween 80, cetrimide, lecithin, and sodium taurocholate were purchased from Himedia Ltd (Mumbai, India). Double distilled water was used throughout the study. Atorvastatin and fenofibrate combination tablet formulations—Atacor (Dr. Reddy's Laboratories) and Fibator (Sun Pharma, Sikkim, India)—were obtained from the local market.

Instrumentation

A double beam 1800 UV-visible spectrophotometer (Shimadzu, Japan), dissolution apparatus (Electrolab TDT-08L), analytical balance (Shimadzu AUX 220, Japan), tablet compression machine (Lab Press-CIP Machineries, Ahmedabad, India), hardness tester (Secor, Hyderabad, India), pH meter (Elico, Hyderabad, India), and ultrasonic cleaner were used for the study (calibration of instruments were done according to standard procedures).

Analytical method

The first-order derivative overlaid spectra of atorvastatin calcium and fenofibrate denoted that there was no zero crossing point for atorvastatin calcium for quantification of fenofibrate (Figure 2). Hence, the first-order derivative spectrum was not suitable for simultaneous estimation and this problem was minimized by the second-order derivative method, which permitted selection of the suitable wavelengths to make the quantification possible with zero crossing, where fenofibrate had zero absorbance at 281 nm, while atorvastatin calcium gave a significant derivative response; likewise atorvastatin gave zero absorbance at 296

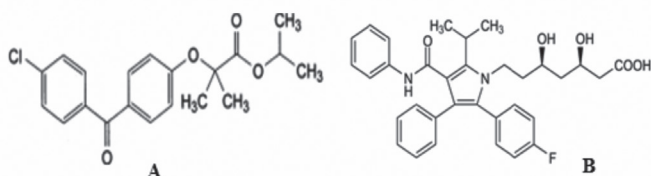


Figure 1. Chemical structure of fenofibrate (A) and atorvastatin (B)

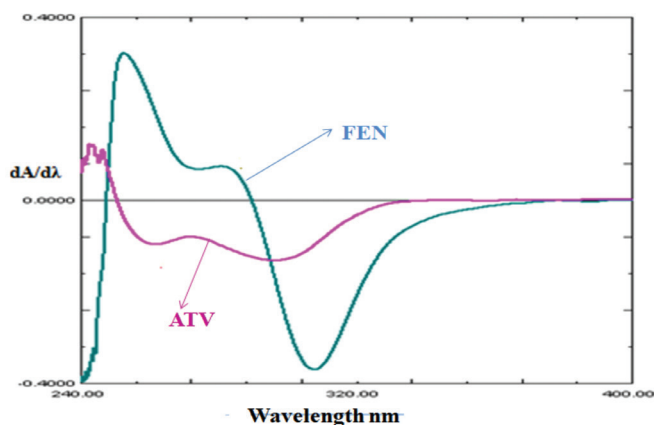


Figure 2. First-order UV overlay spectra of atorvastatin (10 µg/mL) and fenofibrate (10 µg/mL) in acetate buffer, pH 2.8

UV: Ultraviolet, ATV: Atorvastatin, FEN: Fenofibrate

nm, while fenofibrate gave a significant derivative response. Therefore, 281 nm and 296 nm were selected for estimation of atorvastatin calcium and fenofibrate, respectively.

Dissolution test conditions

The log *p* values of atorvastatin calcium and fenofibrate were 6.36 and 5.28, respectively, indicating low water solubility and so the development of a single dissolution method for this combination is a challenge and single *in vitro* dissolution studies were not reported for this combination along these lines. An attempt was made to develop and validate a single dissolution test for atorvastatin calcium and fenofibrate in combined tablets.

Atorvastatin (10 mg) and fenofibrate (145 mg) bulk drug filled capsules were evaluated for dissolution profile in 900 mL of seven buffers of distinct pH (1.2/2.8/3.6/4.7/5.6/6.8 and 7.4), biorelevant media such as SGF (pH 1.2), SIF (pH 7.5), FaSSIF (pH 6.5), FeSSIF (pH 5.0), modified fasted state (pH 6.5) and fed state (pH 5.0) simulated intestinal fluids) and three different surfactants and at 2 different concentrations at 50 rpm using type 2 - United States Pharmacopeia dissolution apparatus and samples were withdrawn for 60 min, being replaced with the same volume of fresh medium. Samples withdrawn were evaluated with the regression equation of the proposed analytical technique for quantification of dissolved drug, followed by a plot against time. A combination of these media was utilized for identifying the optimized dissolution medium, in which the highest drug release, stability, and sink conditions were obtained, and it was chosen as the *in vitro* dissolution medium.

Discriminatory power of the dissolution method

The dissolution method's ability to discriminate was ascertained using tablets punched under distinct conditions, such as a discrete manufacturing process (hardness of 5.0 kg/cm² and 8.0 kg/cm²) and discrete product composition (with/without disintegrant). The dissolution-profiles in test conditions were examined and their data were estimated with factors of comparison (f_1 and f_2).

Stability determination

Sample solutions withdrawn for the optimized dissolution medium were analyzed at time 0; consequently samples were kept for 24 h and 48 h and analyzed by the proposed method.

Validation of the dissolution method

Validation of the dissolution method is required to ensure that a proposed dissolution method is scientifically and experimentally sound, obtaining results for specificity, linearity, accuracy, and precision as per standard guidelines.

The method's specificity was assessed by comparing the spectra obtained from the commercial formulations and the synthetic mixture from standard solutions by preparing similar dose ratios of synthetic and tablet dosage forms. Then the analytical method was applied in order to check if any component of the formulation could generate a response or an absorption wavelength similar to that of the drugs.

Linearity was determined with standard concentrations of atorvastatin (2-12 µg/mL) and fenofibrate (1-35 µg/mL) quantified with the second derivative spectrophotometric technique. Then absorbance was recorded and a calibration curve was constructed by plotting the analyte response versus the drug concentrations.

Intra-day and inter-day precision studies were evaluated as per International Conference on Harmonization guidelines, in which six tablets were subjected to the dissolution test conditions, on the same day (intra-day precision) and for three consecutive days (inter-day precision); then % RSD was calculated.

Accuracy studies were conducted using standard addition method where known amounts of drugs at 80%, 100% and 120% of the formal assay of atorvastatin and fenofibrate were added to the placebo sample in the dissolution medium, which was further subjected to the proposed method; then percentage recovery and relative standard deviation (% RSD) were computed for each concentration.

RESULTS AND DISCUSSION

Development of the dissolution method

The selection of the dissolution test method was based on the dissolution profiles of atorvastatin (10 mg) and fenofibrate (145 mg) bulk drug filled capsules using a USP type 2 apparatus at a paddle speed of 50 rpm and selection of a dissolution medium for adequate solubility and stability of both atorvastatin calcium and fenofibrate was necessary for this dissolution method. The log *p* values of atorvastatin calcium and fenofibrate respectively were 6.36 and 5.28, denoting low water solubility. Several compendia dissolution media were screened; these include various buffer media (pH 1.2 to 7.4), surfactant media, and several biorelevant media. However, the results showed that the dissolution rate of atorvastatin was maximum in weak acidic buffers because of the specific interaction but the dissolution rate of fenofibrate was less than 2% in all buffers, indicating that fenofibrate dissolution was independent of pH due to the absence of ionizable groups (Table 1). Both drugs showed higher dissolution in 0.5% w/v SLS medium than in other dissolution media. Dissolution medium with low concentration

of SLS may resemble the gastric environment of our body, and hence this medium is useful for correlating *in vitro* dissolution behavior of atorvastatin and fenofibrate in combined dosage form with their *in vivo* performance. This medium can also be a useful quality control tool and the selected dissolution test conditions are USP apparatus 2 at paddle speed 50 rpm in a medium of 0.5% w/v SLS. Therefore, dissolution studies were performed for commercial tablets (Atocor and Fibator) in optimized dissolution test conditions.

In vitro dissolution profiles of commercial tablets

Dissolution studies on Atocor and Fibator tablets were performed with the optimized dissolution test medium of 0.5% w/v SLS, using a USP type 2 apparatus at paddle speed of 50 rpm at temperature $37\pm 0.5^\circ\text{C}$ and these results are shown in Figure 3 and 4. They indicated that about 85% of both atorvastatin and fenofibrate was released in 45 min from the two brands. In fact, fenofibrate exhibited only 50% dissolution in 60 min (Table 1). On the other hand, tablets exhibited 85%

Table 1. Screening study results for ATV (10 mg) and FEN (145 mg) bulk drug using a USP type II apparatus at 50 rpm, temperature $37\pm 0.5^\circ\text{C}$ for 60 min

Dissolution media	% Drug release mean \pm standard deviation (n=12)	
	ATV	FEN
0.1 N hydrochloric acid	18.40 \pm 0.09	1.16 \pm 0.07
Acetate buffer, pH 2.8	29.56 \pm 0.04	1.47 \pm 0.07
Acetate buffer, pH 3.6	41.40 \pm 1.66	1.14 \pm 0.08
Acetate buffer pH 4.7	48.43 \pm 2.16	1.12 \pm 0.10
Phosphate buffer, pH 5.6	92.45 \pm 2.96	0.93 \pm 0.04
Phosphate buffer, pH 6.8	95.45 \pm 4.18	1.02 \pm 0.02
Phosphate buffer, pH 7.4	86.59 \pm 1.40	1.04 \pm 0.05
SGF (simulated gastric fluid without enzyme)	50.28 \pm 3.71	1.04 \pm 0.06
SIF (simulated intestinal fluid)	87.59 \pm 2.40	1.94 \pm 0.05
BFaSSIF (blank fasted state simulated intestinal fluid)	95.88 \pm 1.76	1.20 \pm 0.06
BFeSSIF (blank fed state simulated intestinal fluid)	92.46 \pm 2.45	1.33 \pm 0.08
MFaSSIF (modified fasted state simulated intestinal fluid)	98.00 \pm 1.19	5.33 \pm 0.75
MFeSSIF (modified fed state simulated intestinal fluid)	92.45 \pm 0.60	4.15 \pm 0.21
Cetrimide, 0.25% w/v	98.33 \pm 5.41	7.08 \pm 0.07
SLS 0.25% w/v	94.00 \pm 5.27	30.54 \pm 0.54
Tween 80 0.25% v/v	40.87 \pm 0.02	2.36 \pm 0.17
SLS 0.5% w/v	95.42 \pm 2.56	50.54 \pm 0.53

ATV: Atorvastatin, FEN: Fenofibrate, USP: United States Pharmacopeia, SLS: Sodium lauryl sulfate

dissolution in 45 min; this means that the inactive ingredients in the tablets also supported the dissolution. Such a factor should also be kept in mind while optimizing the dissolution conditions. Atorvastatin components of the tablet formulation exhibited 88% dissolution in 45 min, whereas the pure drug exhibited 92% dissolution in 45 min in the same medium. Thus the proposed dissolution medium satisfactorily reproduced the dissolution characteristics of atorvastatin and fenofibrate with initial lag time of 5 min for drug dissolution but lag time was more pronounced in the case of fenofibrate. This trend was familiar from the chemical structure of fenofibrate (no functional groups responsible for ionization). Furthermore, both drugs are hydrophobic as indicated by the log *p* values, 6.36 and 5.28, respectively, for atorvastatin and fenofibrate. From 5 min to 60 min, the dissolution behavior was gradual and linear, which again reflected the hydrophobic nature of the drugs.

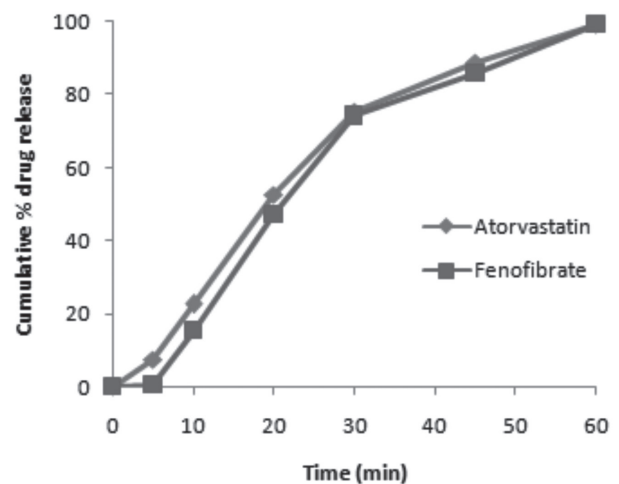


Figure 3. *In vitro* dissolution profiles of Atocor tablets in 0.5% W/V SLS medium

SLS: Sodium lauryl sulfate

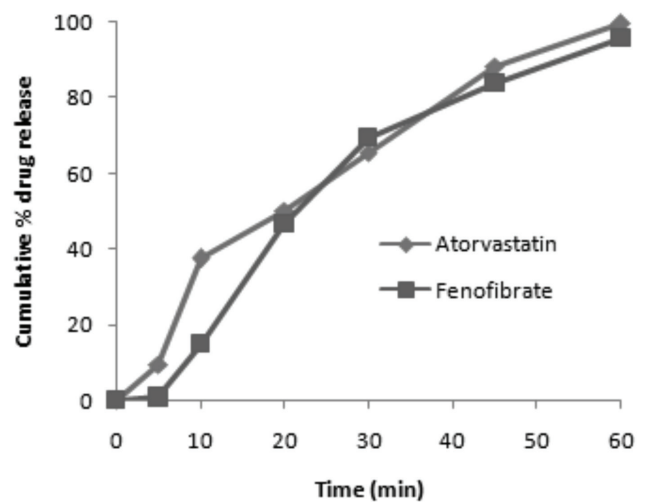


Figure 4. *In vitro* dissolution profiles of Fibator tablets in 0.5% W/V SLS medium

SLS: Sodium lauryl sulfate

Discriminatory power of the dissolution method

The discriminatory power of the dissolution method was determined by manufacturing tablets under different conditions and studying the behavior of those products in the proposed dissolution method. The effects of tablet hardness (5 kg/cm² vs. 8 kg/cm²) and disintegrant (with vs. without) are shown in Figure 5. The dissolution data were calculated with the help of factors of comparison using 6 points; among these, one point was found to specify the drug release more than 85% (Table 2). These results confirmed that the dissolution test procedure has the ability to discriminate for distinct composition and process, and, based on these results, 0.5% w/v SLS medium has discriminating power.

Stability determination of atorvastatin and fenofibrate in dissolution medium

The stability of drugs in dissolution medium at different time periods was calculated in order to demonstrate the integrity

Table 2. Dissimilarity factor (f_1) and similarity factor (f_2) for dissolution profiles of tablets

Name of the drug	Tablets with hardness of 5 kg/cm ² vs. 8 kg/cm ²		Tablets with disintegrant vs. no disintegrant	
	f_1 value	f_2 value	f_1 value	f_2 value
Atorvastatin	16	45.44	12	46.70
Fenofibrate	17	48.30	16	47.81

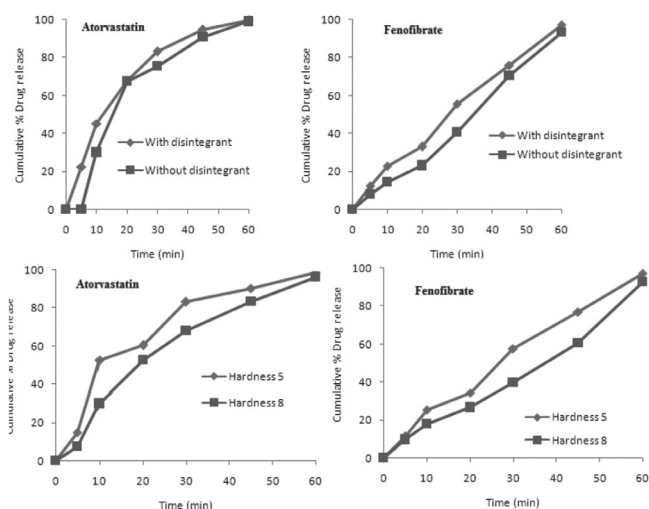


Figure 5. Dissolution profiles of atorvastatin/fenofibrate self-punched tablets in 0.5% w/v SLS medium

SLS: Sodium lauryl sulfate

Table 4. Precision data of atorvastatin and fenofibrate for the proposed dissolution method

Product	Percent amount of atorvastatin				Percent amount of fenofibrate			
	Intra-day		Inter-day		Intra-day		Inter-day	
	Mean ± SD	% RSD	Mean ± SD	% RSD	Mean ± SD	% RSD	Mean ± SD	% RSD
Atocor	98.86±1.751	1.77	99.45±1.82	1.83	99.17±2.203	0.22	98.24±2.02	1.05
Fibator	98.49±1.604	1.62	98.49±1.54	1.56	95.89±0.479	0.49	96.84±0.54	0.55

SD: Standard deviation, RSD: Relative standard deviation

of the drugs and is given in Table 3, showing that both drugs were stable under dissolution test conditions. The change in drug content was not assessed and likewise no evidence of degradation denotes that the solutions were stable for more than 48 h.

Table 3. Data for stability of atorvastatin and fenofibrate dissolution samples

Analyte	% Amount of drug found (AM ± SD) (n=3)		
	Initial time	After 24 h	After 48 h
Atorvastatin	98.24±0.45	99.47±1.24	99.05±0.58
Fenofibrate	99.54±0.34	100±0.32	98.54±0.98

SD: Standard deviation

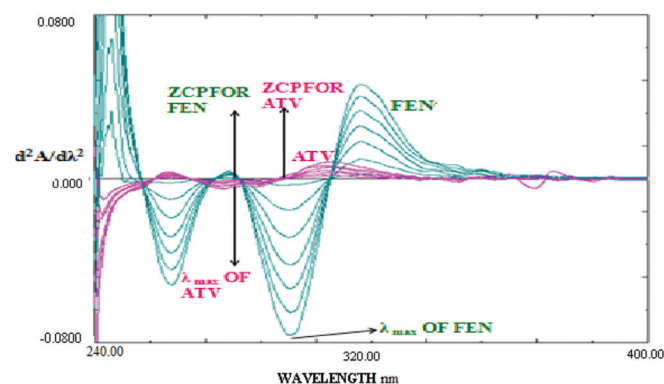


Figure 6. Second-order derivative linearity spectra of ATV and FEN

ATV: Atorvastatin, FEN: Fenofibrate

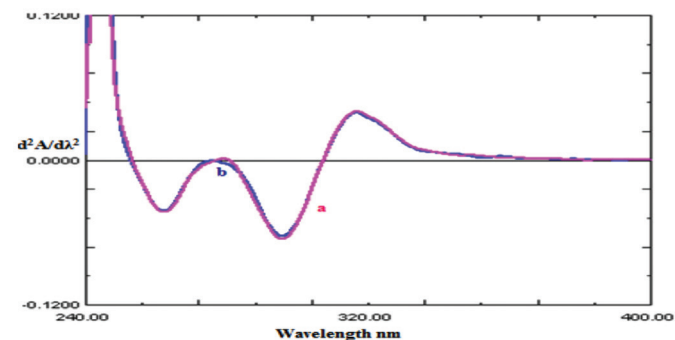


Figure 7. Second-order derivative overlay spectra of commercial formulation (a), standard mixture (b)

Dissolution method validation

Linearity

Linearity was assessed by the regression equation of calibration curve method. The responses for atorvastatin at 281 nm were linear in the concentration range of 2-12 µg/mL, with a correlation coefficient (R^2) of 0.9971; likewise the responses for fenofibrate at 296 nm were linear in the concentration range of 1-35 µg/mL, with a R^2 of 0.998. The results indicate a good linear relationship between derivative response and concentrations at 281 nm and 296 nm (Figure 6).

Specificity

The derivative spectrum attained from the commercial formulation solution was correlated with the spectrum of the synthetic mixture of standard solutions (atorvastatin and fenofibrate). The spectra of the commercial formulation and synthetic mixture were superimposed. No interference was seen from excipients with derivative response of either of the drugs (atorvastatin and fenofibrate) at their respective analytical wavelengths of 281 nm and 296 nm (Figure 7); hence the method was found to be specific.

Precision

The precision evaluation data for the dissolution studies are given in Table 4, and they show that percent relative standard deviation values for intra-day and inter-day precision studies were less than 2 and there were no significant differences, indicating that the proposed method was reproducible and precise.

Accuracy

The accuracy assessment data for the dissolution studies are given in Table 5. They show that percent recovery was from 96% to 106% and percent relative standard values were less than 2, indicating that an agreement between the standard values and ascertained values signifies that the dissolution method was accurate.

CONCLUSIONS

The present investigation was undertaken with the objective to develop and validate a single test method for the dissolution evaluation of atorvastatin calcium and fenofibrate simultaneously. The optimal conditions for dissolution testing of atorvastatin and fenofibrate are as follows: 900 mL of 0.5% w/v SLS, using a paddle-type USP dissolution apparatus, stirring speed of 50 rpm, a temperature of $37 \pm 0.5^\circ\text{C}$, and collection time of 60 min. The proposed dissolution test conditions have discriminative power, substantiated the usefulness of this biorelevant medium for the two drugs, and the dissolution method was validated (% RSD < 2). The developed dissolution method can be fruitfully employed as a quality control tool as well as a research tool.

ACKNOWLEDGEMENTS

The authors are grateful to the management of Gokaraju Rangaraju College of Pharmacy for providing the necessary facilities and infrastructure to carry out this research work.

Conflict of Interest: No conflict of interest was declared by the authors.

REFERENCES

- Dressman J, Kramer J. Pharmaceutical dissolution testing (1st ed). London; Taylor and Francis; 2007:92-98.
- Subrahmanyam CVS. Physical pharmaceutics (2nd ed). Delhi, India; Vallabh Prakashan; 2005:85-96. p.
- Wang J, Flanagan DR. Fundamentals of dissolution (1st ed). New York; Academic Press; 2009:309-318.
- Anumolu PD, Sunitha G, Bindu SH, Satheshbabu PR, Subrahmanyam CV. Development and validation of discriminating and biorelevant dissolution test for lornoxicam tablets. Indian J Pharm Sci. 2015;77:312-320.
- Soni T, Nagda E, Tejal G, Chotai N. Development of discriminating method for dissolution of aceclofenac marketed formulations. Dissolution Technologies. 2008;15:31-34.
- Dressman JB, Amidon GL, Reppas C, Shah VP. Dissolution testing as prognostic tool for oral drug absorption: immediate release dosage forms. Pharm Res. 1998;15:11-22.
- Oliveira EFS, Aievedo RCP, Bonfilio R, Oliveira DB, Rebeiro GP, Araujo MB. Dissolution test optimization for meloxicam in the tablet pharmaceutical form. Braz J Pharm Sci. 2009;45:67-73.
- He Z, Zhong D, Chen X, Liu X, Tang X, Zhao L. Development of a dissolution medium for nimodipine tablets based on bioavailability evaluation. Eur J Pharm Sci. 2004;21:487-491.
- Anumolu PD, Venkataraju Y, Gurralla S, Puvvadi S, Subrahmanyam CVS. Development of biorelevant and discriminating method for dissolution of efavirenz and its formulations. Asian J Pharm Clin Res. 2012;5:220-223.
- Menegola J, Steppe M, Schapoval EE. Dissolution test for citalopram in tablets and comparison of *in vitro* dissolution profiles. Eur J Pharm Biopharm. 2007;67:524-530.
- Anthony CM, David MO, Brian W. Clarke's analysis of drugs and poisons (3rd ed). London; Pharmaceutical Press, 2004:654.
- Indian pharmacopoeia (7th ed). Ghaziabad; The Indian Pharmacopoeia Commission; 2014:1099-1744.
- Vignaduzzo SE, Castellano PM, Kaufman TS. Development and validation of a dissolution test for meloxicam and pridinol mesylate from combined tablet formulation. India J Pharm Sci. 2010;72:197-203.
- Anumolu PD, Neeli S, Anuganti H, Ranganatham SBP, Satya SCV. Development of dissolution test method for a telmisartan/amlodipine besylate combination using synchronous derivative spectrofluorimetry. Braz J Pharm Sci. 2014;50:330-336.
- Huang Z, Lozano R, Francis R, Aubry AF, Stebeck A, Sociascia DO. Development of a single *in vitro* dissolution method for a combination trilayer tablet formulation of clopidogrel and pravastatin. Dissolution Technologies. 2011;18:12-19.
- Bhokare PS, Kane RN, Desai DS. Simultaneous spectrophotometric estimation of atorvastatin and fenofibrate in bulk drug and dosage form by using dual wavelength method. IJRPBS. 2012;3:1448-1453.
- Deepan T, Paul Ambethkar K, Vijaya Laksjmi G, Dhanaraju MD. Analytical method development and validation of RP-HPLC for estimation of atorvastatin calcium and fenofibrate in bulk drug and tablet dosage forms. Eur J App Sci. 2011;3:35-39.

18. Dhabale PN, Gharge DS. Simultaneous spectrophotometric estimation of atorvastatin and fenofibrate in bulk drug and dosage form by using simultaneous equation method. *International Journal of Chem Tech Research*. 2010;2:325-328.
19. Hirave R, Bendagude R, Kondawar M. RP-HPLC method for simultaneous estimation of atorvastatin calcium and fenofibrate in tablet dosage forms. *J Pharm Res*. 2010;3:2400-2402.
20. Anumolu PD, Gurralla S, Yeradesi VR, Puvvadi SBR, Chavall SVS. Development of dissolution test method for drotaverine hydrochloride/mefenamic acid combination using derivative spectrophotometry. *Trop J Pharm Res*. 2013;12:227-232.
21. Mark H, Workman J. Derivatives in spectroscopy Part II- The true derivative. *Spectroscopy* 2003;18:32-33.
22. Raymond CR, Paul JS, Sian CO. *Hand book of pharmaceutical excipients* (2nd ed). Chicago; London; Pharmaceutical Press: American Pharmacists Association; 2007;132:385-725.



Comparison of the Essential Oils of *Ferula orientalis* L., *Ferulago sandrasica* Peşmen and Quézel, and *Hippomarathrum microcarpum* Petrov and Their Antimicrobial Activity

Ferula orientalis L., *Ferulago sandrasica* Peşmen ve Quézel ve *Hippomarathrum microcarpum* Petrov'un Uçucu Yağ ve Antimikrobiyal Etkilerinin Karşılaştırılması

© Songül KARAKAYA^{1*}, © Gamze GÖGER², © Fatmagül D. BOSTANLIK³, © Betül DEMİRCİ⁴, © Hayri DUMAN⁵, © Ceyda Sibel KILIÇ³

¹Atatürk University, Faculty of Pharmacy, Department of Pharmacognosy, Erzurum, Turkey

²Trakya University, Faculty of Pharmacy, Department of Pharmacognosy, Edirne, Turkey

³Atatürk University, Faculty of Pharmacy, Department of Pharmaceutical Botany, Ankara, Turkey

⁴Anadolu University, Faculty of Pharmacy, Department of Pharmacognosy, Eskişehir, Turkey

⁵Gazi University, Faculty of Art and Sciences, Department of Biological Sciences, Ankara, Turkey

ABSTRACT

Objectives: To determine the chemical composition and antimicrobial activity of the essential oils of the aerial parts of *Ferula orientalis* L., roots of *Ferulago sandrasica* Peşmen and Quézel, and aerial parts of *Hippomarathrum microcarpum* Petrov.

Materials and Methods: Essential oils were analyzed by gas chromatography and gas chromatography/mass spectrometry. The antimicrobial activity of the essential oils was determined by bioautography assay.

Results: α -Pinene (75.9%) and β -pinene (3.4%) were the major components of the aerial parts of *F. orientalis*; with limonene (28.9%), α -pinene (15.6%), and terpinolene (13.9%) for *F. sandrasica*; and β -caryophyllene (31.4%) and caryophyllene oxide (23.1%) for the aerial parts of *H. microcarpum*. Essential oils from the aerial parts of *F. orientalis*, the roots of *F. sandrasica*, and the aerial parts of *H. microcarpum* were active against *Staphylococcus aureus* and *Candida albicans* strains. However, essential oils were not active against *Pseudomonas aeruginosa* or *Escherichia coli*.

Conclusion: The antimicrobial activities against *S. aureus* and *C. albicans* of these species may be attributed to the presence of the main components in the essential oils.

Key words: Antimicrobial, bioautography, *Ferula*, *Ferulago*, *Hippomarathrum*

ÖZ

Amaç: *Ferula orientalis* L.'nin toprak üstü kısımlarından, *Ferulago sandrasica* Peşmen ve Quézel'in köklerinden ve *Hippomarathrum microcarpum* Petrov'un toprak üstü kısımlarından elde edilen uçucu yağların içeriğini ve antimikrobiyal aktivitelerini belirlemektir.

Gereç ve Yöntemler: Bu çalışmada türlerden elde edilen uçucu yağların içerikleri gaz kromatografisi ve gaz kromatografisi/kütle spektrometresi ile analiz edilmiştir. Antimikrobiyal aktivite biyootografi yöntemiyle incelenmiştir.

Bulgular: Sırasıyla; α -pinen (%75.9) ve β -pinen (%3.4) *F. orientalis*'in toprak üstü kısımlarının; limonen (%28.9), α -pinen (%15.6) ve terpinolen (%13.9) *F. sandrasica*'nın köklerinin; β -karyofillen (%31.4) ve karyofillen oksit (%23.1) *H. microcarpum*'un toprak üstü kısımlarının ana bileşenleri olarak bulunmuştur. *F. orientalis*'in toprak üstü kısımlarından ve *F. sandrasica*'nın köklerinden elde edilen uçucu yağlar *Staphylococcus aureus* ve *Candida albicans* türlerine karşı etkili olduğu görülürken, *Pseudomonas aeruginosa* ve *Escherichia coli*'ye karşı etkisiz olduğu görülmüştür. *H. microcarpum*'un toprak üstü kısımlarının *P. aeruginosa*, *S. aureus*, *C. albicans* ve *E. coli*'ye karşı etkisiz olduğu tespit edilmiştir.

Sonuç: Bu türlerin *S. aureus* ve *C. albicans*'a karşı antimikrobiyal aktiviteleri uçucu yağlarında bulunan ana bileşenlerin varlığından kaynaklanabilir.

Anahtar kelimeler: Antimikrobiyal, biyootografi, *Ferula*, *Ferulago*, *Hippomarathrum*

*Correspondence: E-mail: ecz-songul@hotmail.com, Phone: +90 553 461 66 41 ORCID-ID: orcid.org/0000-0002-3268-721X

Received: 04.10.2017, Accepted: 28.12.2017

©Turk J Pharm Sci, Published by Galenos Publishing House.

INTRODUCTION

The genus *Ferula* L. is a member of the family Apiaceae and has been found to be a rich source of gum resin.¹ *Ferula* species are known in Turkey as “çakşır”, “asaotu”, “kingor”, “heliz” etc.,² and *Ferula orientalis* is known as “heliz”,³ and they have been used as a carminative, sedative, laxative, antispasmodic, digestive, expectorant, diuretic, aphrodisiac, antiseptic, anthelmintic, analgesic,⁴ and stimulant.⁵ *Ferula* species have been found to contain sesquiterpenes and sesquiterpene coumarins.⁶ Fresh peeling stems of *F. orientalis* L., known as “at kasnisi” are used by local people to give flavor to pickles.⁵ It is 100-150 cm high, grows on rocky slopes at 1600-2900 m, and has distinguished yellow flowers, with a flowering time in late May and June.⁷ *Ferulago* W. Koch. is represented by approximately 83 taxa throughout the world and is a perennial genus of Apiaceae.⁸ *Ferulago* species are known as “çakşır”, “şeytanteresi”, and “kişniş” in Turkey and *Ferulago sandrasica* is known as “kuzu kişnişi”.² Since ancient times *Ferulago* species have been used for the treatment of intestinal worms and hemorrhoids; as a tonic, aphrodisiac, digestive, and sedative; and against ulcers, snake bites, spleen diseases, and headache. These species have been found to contain coumarins, quinones, flavonoids, and sesquiterpenes.⁹ *F. sandrasica* Peşmen and Quézel is an endemic glabrous species, 30-35 cm high; it grows on rocky serpentine slopes at 2000 m and its flowering time is in June and July.⁷

The genus *Hippomarathrum* link is a member of the family Apiaceae and it has five species. *Hippomarathrum* is an erect, much-branched perennial genus, 50-100 cm high, and distributed on rocky slopes and in fields. *Hippomarathrum microcarpum* is also used as food and is known as “çakşır” or “çaşır” by local people in Eastern Anatolia in Turkey.¹⁰ The species of this genus have long been used as spices in ethnobotany.¹¹ *H. microcarpum* Petrov is a gray shrub with yellowish flowers⁷ and it is reported that coumarins and furanocoumarins are found in the roots and fruits of the genus *Hippomarathrum*.¹² Essential oils or their components have been shown to exhibit antimicrobial, antiviral, antimycotic, antitoxigenic, antiparasitic, and insecticidal properties. It is considered that these characteristics are related to the function of these compounds in plants.¹³

The aim of the present study was to present and compare the chemical compositions of the essential oils of the aerial parts of *F. orientalis*, roots of *F. sandrasica*, and aerial parts of *H. microcarpum* growing wild in Turkey. We determined the chemical composition of the essential oils by gas chromatography (GC) and GC/mass spectrometry (MS) analysis and examined the antimicrobial activities of the essential oils by thin-layer chromatography (TLC)-bioautography assay. To the best of our knowledge, this is the first report on the chemical composition and antimicrobial activity of the essential oils in *F. orientalis*, *F. sandrasica*, and *H. microcarpum*.

MATERIALS AND METHODS

Plant material

The plant materials were collected from different parts of Turkey and were identified by Prof. Dr. Hayri Duman (Gazi University,

Faculty of Science, Department of Biology) and the voucher specimens are kept in AEF (Herbarium of Ankara University Faculty of Pharmacy). The localities where these species were found are given in Table 1.

Table 1. Localities of the species

Species	Locality	Herbarium number
<i>Ferula orientalis</i>	B9: Between Ağrı and Erzurum, Mount Tahir, 2475 m, 13.07.2014	AEF 10966
<i>Ferulago sandrasica</i>	C2: Mount Sandras 3 km to Lake Kartal, Under <i>Pinus nigra</i> trees, in Muğla, 1675 m, 10.6.2013	AEF 26274
<i>Hippomarathrum microcarpum</i>	C5: Adana, south of Tufanbeyli, 13.07.2014	AEF 26699

Isolation of the essential oil

The roots and aerial parts were subjected to hydrodistillation for 3 h using a Clevenger-type apparatus in accordance with the method recommended in the European Pharmacopoeia. The oils obtained were dried in anhydrous sodium sulfate and stored in sealed vials at +4°C in the dark until analyzed and tested. All oils were pleasant smelling and transparent with a faint yellow and greenish color. The essential oil % yields of the aerial parts of *F. orientalis*, roots of *F. sandrasica*, and aerial parts of *H. microcarpum* were 0.022%, 0.019%, and 0.048%, respectively.

GC/MS analysis

GC/MS analysis was performed with an Agilent 5975 GC-MSD system. An Innovax FSC column (60 m×0.25 mm, 0.25 mm film thickness) was used with helium as carrier gas (0.8 mL/min). GC oven temperature was kept at 60°C for 10 min and programmed to 220°C at a rate of 4°C/min, and kept constant at 220°C for 10 min and then programmed to 240°C at a rate of 1°C/min. Split ratio was adjusted to 40:1 and injector temperature was set to 250°C. Mass spectra were recorded at 70 eV and mass range was from m/z 35 to 450.

GC analysis

GC analysis was performed with an Agilent 6890N GC system. The temperature of the flame ionization detector (FID) detector was 300°C. In order to obtain the same elution order as GC/MS, simultaneous auto-injection was done on a duplicate of the same column conforming with the same operational conditions. Relative percentage quantities of the separated compounds were calculated from FID chromatograms. The results of the analysis are given in Table 2. Identification of the essential oil components was performed by comparison of their relative retention times with those of authentic samples or by comparison of their relative retention index to series of *n*-alkanes. Computer matching against commercial sources^{14,15} and the in-house “Başer Library of Essential Oil Constituents” established with genuine compounds and components of

known oils, alongside MS literature data,^{16,17} was used for the identification.

Determination of antimicrobial compounds of the essential oils by TLC-bioautography assay

Chromatography was carried out on 0.2 mm silica gel 60 F₂₅₄ aluminum sheet TLC plates. To the plates was applied 10 μ L of essential oils with a minicaps capillary pipette. The plates were then developed with toluene:ethyl acetate, 93:7, as a mobile phase and another TLC plate for bioautography was prepared in parallel. After the development, the TLC plates were evaluated at UV 254 nm and 366 nm for determination of fluorescent compounds. Alcoholic vanillin-sulfuric acid reagent was used to visualize the separated compounds and they were heated for 3 min at 110°C.

Preparation of microorganisms and the TLC-bioautography assay

After TLC separation, the antimicrobial activity of the essential oils was determined by direct bioautography.^{18,19} *Pseudomonas aeruginosa* ATCC 13388, *Staphylococcus aureus* ATCC BAA 1026, *Candida albicans* ATCC 24433, and *Escherichia coli* NRRL B-3008 strains were used for bioautography. Microbial suspensions were grown overnight in double strength Mueller-Hinton broth standardized to 10⁸ CFU mL⁻¹ (corresponding to McFarland no. 0.5). TLC plates were placed on nutrient agar plates and molten agar culture medium containing inocula was overlaid on the TLC plates and they were incubated at 37°C for 24 h. Then, by incubation, 2,3,5-triphenyl-2H-tetrazolium chloride solution was sprayed on the TLC plates. The treated plates were incubated at 37°C for 2 h and after incubation the inhibition zones were visible as pale spots against a red background.

RESULTS

Thirteen compounds were identified in the essential oil of the aerial parts of *F. orientalis*, representing 96.6% of the oil. α -Pinene (75.9%), β -pinene (3.4%), trans-verbenol (3.0%), and β -caryophyllene (2.5%) were the major components. The analysis on the roots of *F. sandrasica* resulted in the identification of 69 essential compounds representing 96.0% of the oil. Limonene (28.9%) was the most abundant compound in the essential oil, followed by α -pinene (15.6%), terpinolene (13.9%), camphene (2.6%), myrcene (2.8%), p-cymene (2.8%), and 2,3,6-trimethylbenzaldehyde (3.2%).

Twenty-one compounds were characterized in the oil of the roots of *H. microcarpum*, representing 98.7% of the oil. The major constituents were β -caryophyllene (31.4%), caryophyllene oxide (23.1%), bornyl acetate (9.1%), α -humulene (4.9%), germacrene D (4.2%), β -phellandrene (4.6%), α -pinene (3.0%), and caryophylla-2(12),6-dien-5 β -ol (=caryophyllenol II) (3.0%). The essential oils obtained from these species did not show much qualitative and quantitative similarity. α -Pinene, camphene, β -pinene, limonene, β -phellandrene, p-cymene, and β -caryophyllene were the main compounds in the three species. Trans-verbenol was the main compound in the essential oils of *F. orientalis* and *F. sandrasica*. Thuja-2,4(10)-diene, pinocarvone,

trans-pinocarveol, myrtenol, and cuparene were only found in the essential oils of the aerial parts of *F. orientalis*.

Sabinene, α -phellandrene, (Z)- β -ocimene, γ -terpinene, (E)- β -ocimene, terpinolene, α -copaene, bornyl acetate, α -humulene, germacrene D, δ -cadinene, caryophyllene oxide, and humulene epoxide-II were the main compounds in the essential oils of *F. sandrasica* and *H. microcarpum*. Caryophylla-2(12),6-dien-5 β -ol (=Caryophyllenol II) was only found in the essential oils of the aerial parts of *H. microcarpum*. The composition of the essential oils obtained from these species and their relative percentages are given in Table 2.

The results for antimicrobial activity by bioautography showed that essential oils from the aerial parts of *F. orientalis* and roots of *F. sandrasica* were active against *S. aureus* and *C. albicans* strains. However, they were not active against the *E. coli* strain. Similarly, essential oil from the aerial parts of *H. microcarpum* was found to contain compounds active against *S. aureus* and *C. albicans*. The essential oil was more effective against *C. albicans* than against *S. aureus*. However, it did not have good activity against *E. coli*. The essential oils did not give any inhibition zone against *P. aeruginosa*. The TLC evaluation of the essential oils is shown in Figure 1.

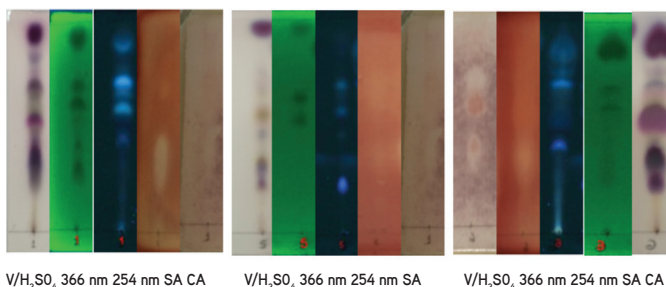


Figure 1. TLC separation of the essential oil from the *Ferula orientalis*, *Ferulago sandrasica*, and *Hippomarathrum microcarpum* on silica gel 60 F₂₅₄

V/H₂SO₄: Vanillin/H₂SO₄ reagent, SA: *Staphylococcus aureus* ATCC 6538, CA: *Candida albicans* ATCC 90028, TLC: Thin-layer chromatography

DISCUSSION

Monoterpene hydrocarbons (P-cymene, myrcene, γ -terpinene, limonene, terpinolene, and (Z)- β -ocimene), oxygenated monoterpenes (carvacrol methyl ether, 2,5-dimethoxy-p-cymene, trans-chrysanthenyl acetate, cis-chrysanthenyl acetate, and ferulagone), aldehydes (like 2,3,6-trimethylbenzaldehyde, (E)-2-decenal, and octanal), alkane derivatives (hexadecanoic acid), sesquiterpene hydrocarbons (α -humulene, 4,6-guaiadiene, and 7-epi-1,2-dehydrosesquicineole), and oxygenated sesquiterpenes (like cubenol, humuleneepoxide II, and spathulenol) were the major components of some *Ferulago* species.

Some *Ferula* species contain monoterpene hydrocarbons [β -pinene, sabinene, camphene, β -phellandrene, and (E)- β -ocimene], alkane derivatives (nonane), sesquiterpene hydrocarbons (germacrene D, germacrene B, δ -cadinene, (Z)-

Table 2. Chemical composition of the essential oil of *Ferula orientalis*, *Ferulago sandrasica*, and *Hippomarathrum microcarpum*

RRI	Compound	<i>Ferula orientalis</i> %	<i>Ferulago sandrasica</i> %	<i>Hippomarathrum microcarpum</i> %
1032	α -Pinene	75.9	15.6	3.0
1072	α -Fenchene	0.6	0.3	-
1076	Camphene	3.4	2.6	1.5
1093	Hexanal	-	0.1	-
1118	β -Pinene	-	0.3	tr
1132	Sabinene	-	0.1	1.1
1135	Thuja-2,4(10)-diene	2.0	-	-
1151	δ -4-Carene	-	tr	-
1159	δ -3-Carene	-	0.1	-
1174	Myrcene	-	2.8	-
1176	α -Phellandrene	-	-	2.0
1188	α -Terpinene	-	0.2	-
1203	Limonene	1.4	28.9	1.9
1218	β -Phellandrene	1.3	0.6	4.6
1244	2-Pentyl furan	-	0.1	-
1246	(Z)- β -Ocimene	-	0.8	tr
1255	γ -Terpinene	-	1.9	tr
1266	(E)- β -Ocimene	-	tr	2.0
1280	<i>p</i> -Cymene	2.2	2.8	1.9
1290	Terpinolene	-	13.9	1.4
1294	1,2,4-Trimethyl benzene	-	0.1	-
1452	α , <i>p</i> -Dimethylstyrene	-	0.8	-
1468	<i>trans</i> -1,2-Limonene epoxide	-	0.3	-
1479	δ -Elemene	-	0.3	-
1497	α -Copaene	-	0.2	0.6
1532	Camphor	-	0.3	-
1538	<i>trans</i> -Chrysanthenyl acetate	-	0.2	-
1586	Pinocarvone	tr	-	-
1591	Fenchyl alcohol	-	1.3	9.1
1598	Camphene hydrate	-	0.1	-
1600	β -Elemene	-	0.6	-
1612	β -Caryophyllene	2.5	0.8	31.4
1614	Carvacrol methyl ether	-	1.3	-
1670	<i>trans</i> -Pinocarveol	2.0	-	-
1683	<i>trans</i> -Verbenol	3.0	-	-
1684	Isoborneol	-	1.3	-
1683	<i>trans</i> -Verbenol	-	0.2	-
1687	α -Humulene	-	0.3	4.9

Table 2. Continued

1704	γ -Muurolene	-	0.2	-
1706	α -Terpineol	-	1.8	-
1707	δ -Selinene	-	0.3	-
1719	Borneol	-	0.8	-
1726	Germacrene D	-	1.4	4.2
1742	β -Selinene	-	0.3	-
1744	α -Selinene	-	0.3	-
1751	Carvone	-	0.1	-
1773	δ -Cadinene	-	1.6	0.6
1776	γ -Cadinene	-	0.9	-
1779	(<i>E,Z</i>)-2,4-Decadienal	-	0.1	-
1786	<i>ar</i> -Curcumene	-	0.3	-
1796	Selina-3,7(11)-diene	-	0.4	-
1804	Myrtenol	1.6	-	-
1807	α -Cadinene	-	0.4	-
1827	(<i>E,E</i>)-2,4-Decadienal	-	0.4	-
1849	Cuparene	0.7	-	-
1864	<i>p</i> -Cymen-8-ol	-	0.2	-
1878	2,5-Dimethoxy- <i>p</i> -cymene	-	0.3	-
1918	β -Calacorene	-	tr	-
1941	α -Calacorene	-	0.1	-
1945	1,5-Epoxy-salvia(4)14-ene	-	0.2	-
2008	Caryophyllene oxide	-	0.3	23.1
2019	2,3,6-Trimethylbenzaldehyde	-	3.2	-
2037	Salvia-4(14)-en-1-one	-	0.1	-
2071	Humulene epoxide-II	-	0.1	2.4
2073	β -Caryophyllene alcohol	-	0.1	-
2080	Cubenol	-	0.6	-
2080	Junenol (=Eudesm-4(15)-en-6-ol)	-	0.2	-
2096	Elemol	-	0.1	-
2130	Salviadienol	-	0.2	-
2144	Spathulenol	-	0.1	-
2209	T-Muurolol	-	0.1	-
2255	α -Cadinol	-	0.5	-
2256	Cadalene	-	0.2	-
2269	Guaia-6,10(14)-dien-4 β -ol	-	0.2	-
2369	Eudesma-4(15),7-dien-4 β -ol	-	0.2	-
2392	Caryophylla-2(12),6-dien-5 β -ol (=Caryophyllenol II)	-	-	3.0
Total		96.6	96.0	98.7

RRI: Relative retention indices, calculated against *n*-alkanes, % calculated from flame ionization detector data, tr: trace (<0.1%)

β -farnesene, dehydrosesquicineole, and eremophilene), and oxygenated sesquiterpenes (germacrene D-4-ol, α -cadinol, shyobunone, epi-shyobunone, 6-epi-shyobunone, β -eudesmol, and α -eudesmol) were the major components of some *Ferula* species.

In addition, esters like bornyl acetate were major components of some *Ferula* and *Ferulago* species.²⁰

Previous studies demonstrated that the major components of the essential oil of leaves from *F. sandrasica* were ocimene (30.5%), carene- δ -3 (27.4%), and α -pinene (17.8%).¹⁹ Baser and Kırimer²⁰ studied 12 *Ferulago* species (*F. asparagifolia* Boiss., *F. aucheri* Boiss., *F. confusa* Velen, *F. galbanifera* (Mill.) W. D. J. Koch, *F. humilis* Boiss., *F. idaea* Özhatay and Akalın, *F. macrosciadia* Boiss. and Balansa, *F. mughlae* Peşmen, *F. sandrasica* Peşmen and Quézel, *F. silaifolia* (Boiss.) Boiss., *F. sylvatica* (Besser) Rchb., and *F. trachycarpa* Boiss.) growing in Turkey and that study showed that the major components of essential oils were 2,3,6-trimethylbenzaldehyde (38.9%) and myrcene (18.2%), α -pinene (35.9%), 2,5-dimethoxy-p-cymene (63.4%), α -pinene (31.8%) and sabinene (15.8%), (Z)- β -ocimene (32.4%), p-cymene (18.4%), carvacrol methyl ether (78.1%), α -pinene (25.4%), α -pinene (40.8%), trans-chrysanthenyl acetate (83.5%), p-cymene (45.8%), and (Z)- β -ocimene (30.7%).²¹

The major components of essential oils of some *Ferula* species were reported as phenol, 2-methyl-5-(1-methylethyl) (18.2%), cyclopropa [α] naphthalene-octahydro-tetramethyl (6.6%), and α -bisabolol (10.4%) (3); α -pinene (18.3%), β -pinene (50.1%), and Δ -3-carene (6.7%).²² Comparing these results with previous studies of *F. orientalis* showed that the major components were nonane (45.6%) and 2-methyloctane (19.4%).²³ Furthermore, essential oils from the aerial parts of *F. orientalis* were obtained: β -phellandrene (24%), (E)- β -ocimene (14%), α -pinene (13%), α -phellandrene (12%), and dehydrosesquicineole (10%),²⁴ but α -pinene (75.9%) was a major component in our study.

Comparison of these results with previous studies of *Hippomarathrum boissieri* from Turkey¹⁸ showed that the major component of the essential oils from both species was β -caryophyllene (31.4% for aerial parts oil of *H. microcarpum*, 25.6% for aerial parts oil of *H. boissieri*). Another study showed that the major components of essential oils of the leaf and flower of *H. microcarpum* were α -caryophyllene (26.4%), γ -muurolene (19.0%), and linalool (6.1%); and β -caryophyllene (18.5%), γ -muurolene (19.2%), thymol (6.9%), and linalool (5.9%), respectively.¹⁰ The results gained in this investigation suggest that this chemical diversity may be useful in taxonomic classification.

There are not enough data on antimicrobial activity for these species. In a previous survey, the essential oil of *F. sandrasica* was tested against *E. coli* MC 400, *E. coli* ATCC 25922, *E. coli* 0157 H7, *Enterobacter colaecea* ATCC 23355, *Enterococcus faecalis* ATCC 19433, *P. aeruginosa* NRRL B-2679, *S. aureus* ATCC 25923, *S. aureus* ATCC 33862, *Bacillus cereus* NRRL B-3711, *Bacillus subtilis* ATCC 6633, *B. subtilis* NRRL B-209, *Bacillus licheniformis* NRRL B-1001, *Micrococcus luteus* NRRL B-1013, and *Listeria monocytogenes* ATCC 7644 by disk diffusion method.

The results showed that the essential oil was active against all tested microorganisms.¹⁸ It was previously reported that the essential oil of *H. microcarpum* was studied for antimicrobial and antifungal activity. The results showed that the essential oil of *H. microcarpum* had antimicrobial activity against *C. albicans* A117 and *S. aureus* ATCC-29213 but had no activity against *E. coli* A1 or *Pseudomonas* sp.¹⁰ Our finding concur with this study.

Bioautography is a suitable method for evaluating essential oils because they contain mixtures of compounds. Therefore, there is a need for the detection of common antimicrobial compounds in essential oils. Additionally, this method is rapid, easy, economical, and inexpensive.²⁵ In the present study, our aim was the chemical characterization of the essential oils of *F. orientalis*, *F. sandrasica*, and *H. microcarpum* and the detection of antimicrobial activity of essential oils and their main components against some pathogenic bacteria and yeast by TLC-bioautography. The antimicrobial activity test performed against four different microorganisms showed that the essential oils were active against *S. aureus* and *C. albicans* strains; however, they were not active against *P. aeruginosa* or *E. coli* strains.

CONCLUSIONS

These data provide an abundance of information on the essential oil compositions of *F. orientalis*, *F. sandrasica*, and *H. microcarpum* and their antimicrobial activities against some pathogenic microorganisms. As far as we know, this is the first report on the antimicrobial activity of essential oils by TLC-bioautography. The antimicrobial activities against *S. aureus* and *C. albicans* of these species may be attributed to the presence of the main components in the essential oils. A comprehensive study should be conducted including the main compounds isolated from the essential oils or their combinations against different pathogenic microorganisms.

Conflict of Interest: No conflict of interest was declared by the authors.

REFERENCES

1. French D. Ethnobotany of the Umbelliferae. In: Heywood VH, ed. The Chemistry and Biology of the Umbellifera. London; Academic Press; 1971:285-412.
2. Güner A. Türkiye Bitkileri Listesi (Damarlı Bitkiler), Flora Dizisi 1 (1st ed). İstanbul Nezahat Gökyiğit Botanik Bahçesi Yayınevi; 2012:62-64.
3. Behçet L, Arik M. An Ethnobotanical Investigation in East Anatolia (Turkey). Tr J Nature Sci. 2013;2:86-110.
4. Dehpour AA, Ebrahimzadeh MA, Fazel NS, Mohammad NS. Antioxidant activity of the methanol extract of *Ferula assafoetida* and its essential oil composition. Grasas Y Aceites. 2009;60:405-412.
5. Duke JA. Dr. Dukes phytochemical and ethnobotanical databases, Agricultural Research Service Publication; 2002.
6. Kojima K, Isaka K, Ondognii P, Zevgeegiino O, Gombosurengyin P, Davgiin K. Sesquiterpenoid derivatives from *Ferula feruloides*. Chem Pharm Bull. 2000;48:353-356.

7. Davis PH. Flora of Turkey and the East Aegean Islands (4th ed). Edinburgh; University Press; 1972; 4:462-464.
8. http://www.ipni.org/ipni/advPlantNameSearch.do?find_family=&find_genus=ferulago&find_species=&find_infrafamily=&find_infragenus=&find_infraspecies=&find_authorAbbrev=&find_includePublicationAuthors=on&find_includePublicationAuthors=off&find_includeBasionymAuthors=on&find_includeBasionymAuthors=off&find_publicationTitle=&find_isAPNIREcord=on&find_isAPNIREcord=false&find_isGCIREcord=on&find_isGCIREcord=false&find_isIKRecord=on&find_isIKRecord=false&find_rankToReturn=all&output_format=normal&find_sortByFamily=on&find_sortByFamily=off&query_type=by_query&back_page=plantsearch
9. Kılıç CS, Coskun M, Demirci B, Baser KHC. Composition of the essential oil of fruits and roots of *Ferulago isaurica* Pesmen and *F. syriaca* Boiss. (Umbelliferae) from Turkey. *Flavour Fragr J.* 2006;21:118-121.
10. Ozer H, Sökmen M, Güllüce M, Adigüzel A, Sahin F, Sökmen A, Kiliç H, Baris O. Chemical composition and antimicrobial and antioxidant activities of the essential oil and methanol extract of *Hippomarathrum microcarpum* (Bieb.) from Turkey. *J Agric Food Chem.* 2007;55:937-942.
11. Baytop T. Türkçe Bitki Adları Sözlüğü (A Dictionary of Vernacular Names of Wild Plants of Turkey) (1st ed). Ankara; Turkish Language Society; 1997:294.
12. Sefidkon F, Shaabani A. Analysis of the oil of *Hippomarathrum micocarpum* (M. B) B. Fedtsch. from Iran. *J Essent Oil Res.* 2003;15:261-262.
13. Burt S. Essential oils: their antibacterial properties and potential applications in foods a review. *Int J Food Microbiol.* 2004;94:223-253.
14. Mc Lafferty FW, Stauffer DB. The Wiley/NBS Registry of Mass Spectral Data. J Wiley and Sons; New York; 1989.
15. Koenig WA, Joulain D, Hochmuth DH. Terpenoids and related constituents of essential oils. MassFinder 3, Hamburg, Germany; 2004.
16. Joulain D, Koenig WA. The Atlas of spectra data of sesquiterpene hydrocarbons. EB Verlag, Hamburg; 1998.
17. ESO 2000. The Complete database of essential oils, boelens aroma chemical information service, The Netherlands; 1999.
18. Baser KHC, Ozek T, Aytac Z. Essential oil of *Hippomarathrum boissieri* Reuteret Hausskn. *J Essent Oil Res.* 2000;12:231-232.
19. Celik A, Arslan I, Herken EN, Ermis A. Constituents, oxidant-antioxidant profile, and antimicrobial capacity of the essential oil obtained from *Ferulago sandrasica* Peşmen and Quézel. *International Journal of Food Properties.* 2013;16:1655-1662.
20. Baser KHC, Kırımer N. Essential Oils of Anatolian Apiaceae a Profile. *Nat Vol Essent Oils.* 2014;1:1-50.
21. Başer KHC, Demirci B, Özek T, Akalin E, Özhatay N. Micro-distilled volatile compounds from *Ferulago* species growing in western Turkey. *Pharm Biol* 2002;40:466-471.
22. Sayyah M, Kamalinejad M, Hidage RB, Rustaiyan A. Iranian antiepileptic potential and composition of the fruit essential oil of *Ferula gummosa* Boiss. *Biomed J.* 2001;5:69-72.
23. Kanani MR, Rahiminejad MR, Sonboli A, Mozaffarian V, Kazempour Osalo S, Nejad Ebrahimi S. Chemotaxonomic significance of the essential oils of 18 *Ferula* Species (Apiaceae) from Iran. *Chem Biodivers.* 2011;8:503-517.
24. Kartal N, Sokmen M, Tepe B, Daferera D, Polissiou M, Sokmen A. Investigation of the antioxidant properties of *Ferula orientalis* L. using a suitable extraction procedure. *Food Chemistry.* 2007;100:584-589.
25. Horváth G, Jámbor N, Végh A, Böszörményi A, Lemberkovics É, Héthelyi É, Kovács K, Kocsis B. Antimicrobial activity of essential oils: the possibilities of TLC-bioautography. *Flavour Fragr J.* 2010;25:178-182.



Microanatomical and Physicochemical Characterization and Antioxidative Activity of Methanolic Extract of *Oudemansiella canarii* (Jungh.) Höhn

Oudemansiella canarii (Jungh.) Höhn Metanollü Ekstresinin Mikroanatomik ve Fizikokimyasal Karakterizasyonu ve Antioksidan Aktivitesi

© Krishnendu ACHARYA*, © Sudeshna NANDI, © Arun Kumar DUTTA

University of Calcutta, Department of Botany, Kolkata, India

ABSTRACT

Objectives: *Oudemansiella canarii* is an edible mushroom highly appreciated throughout the world due to its being a gastronomic delicacy. To date, no extensive work has been reported on the pharmacological or antioxidative aspects of this macrofungus. The present study focuses on the micromorphological features, confirmation of its identity based on molecular sequence (nrITS rDNA) data, and determination of its physicochemical parameters such as organoleptic features and fluorescent behavior.

Materials and Methods: Collected basidiocarps were powdered and used for microscopic and organoleptic evaluation. 2,2-Diphenyl-1-picrylhydrazyl (DPPH) radical scavenging method, total antioxidant activity methods, and 2,2-azinobis (3-ethylbenzothiazoline-6-sulfonic acid) (ABTS) assay were used for evaluating the antioxidant capacities of the methanolic extract. High-performance liquid chromatography (HPLC) analysis profile was also recorded to analyze the phenolic fingerprint.

Results: The DPPH radical scavenging activity was determined with an EC_{50} value of 0.912 μ g, total antioxidant activity was found to be 15.33 μ g ascorbic acid equivalent/mg of extract, and the ABTS assay revealed 12.91 μ m TE/mg of extract antioxidant activity. The HPLC chromatogram revealed the presence of 12 peaks. Several parameters were tested for the determination of chemical composition, revealing the existence of major bioactive components in the extract in the following order: phenol>flavonoid>ascorbic acid> β -carotene-lycopene.

Conclusion: The present work suggests that *O. canarii* may be considered a novel prospect as a functional food and antioxidant supplement.

Key words: Chromatographic fingerprinting, edible mushroom, fluorescence analysis, internal transcribed spacer, phytochemicals, West Bengal

ÖZ

Amaç: *Oudemansiella canarii*, gastronomik lezzeti nedeniyle dünya çapında değerli, yenilebilir bir mantardır. Bugüne kadar, bu makrofungusun farmakolojik veya antioksidan özellikleri hakkında kapsamlı bir çalışma bildirilmemiştir. Bu çalışmada, mikro-morfolojik özellikler, moleküler dizi (nrITS rDNA) verisine dayanarak kimliğinin doğrulanması, organoleptik özellikler ve floresan davranışı gibi fizikokimyasal parametrelerinin belirlenmesi amaçlanmıştır.

Gereç ve Yöntemler: Toplanan basidiokarplar toz haline getirilmiş ve mikroskopik ve organoleptik değerlendirme için kullanılmıştır. Metanollü ekstrenin antioksidan kapasitelerini değerlendirmek için 2,2-difenil-1-picrylhydrazyl (DPPH) radikal süpürme yöntemi, toplam antioksidan aktivite yöntemleri ve 2,2-azinobis (3-etilbenzotiyazolin-6-sülfonik asit) (ABTS) analizi kullanılmıştır. Fenolik parmakizi analizi için yüksek performanslı sıvı kromatografisi (HPLC) profili alınmıştır.

Bulgular: DPPH radikal süpürücü etki tayininde EC_{50} değeri 0.912 μ g olarak belirlenmiş, toplam antioksidan aktivitenin 15.33 μ g askorbik asit eşdeğeri/mg ekstre olduğu bulunmuş ve ABTS analizinde 12.91 μ m TE/mg ekstre ile antioksidan aktivite gösterdiği belirlenmiştir. HPLC kromatogramı 12 pikin

*Correspondence: E-mail: krish_paper@yahoo.com, Phone: +91 8013167310 ORCID-ID: orcid.org/0000-0003-1193-1823

Received: 06.09.2017, Accepted: 28.12.2017

©Turk J Pharm Sci, Published by Galenos Publishing House.

varlığını ortaya çıkarmıştır. Ekstrenin kimyasal bileşiminin belirlenmesi ve majör biyoaktif bileşenlerin (sırasıyla; fenol>flavonoit>askorbik asit> β -karoten-likopen) varlığının ortaya konulması için çeşitli parametreler incelenmiştir.

Sonuç: Bu çalışma, *O. canarii*'nin fonksiyonel bir gıda ve antioksidan takviyesi olarak yeni bir olasılık olarak kabul edilebileceğini göstermektedir.

Anahtar kelimeler: Kromatografik parmakizi, yenilebilen mantar, floresans analizi, dahili kopyalanan aralayıcı, fitokimyasal, West Bengal

INTRODUCTION

For millennia mushrooms have had a prolonged connection with humankind and have had profound biological and economic impact. A recent assessment implied the existence of around 140,000 species, of which only 10% have been identified. Recently, scientists have reported that there are at least 7000 unrevealed macrofungi in the world that may have beneficial effects for mankind.¹ Thus, there is a recent trend among mycologists to document edible mushrooms all around the globe.

West Bengal (21°38'-27°10'N latitude and 85°50'-89°50'E longitude) possesses unique phytogeographical features with variable altitudinal, climatic, and edaphic amalgamations. It is the only state in India that topographically extends from the Himalayas in the north to the Bay of Bengal in the south, with regions such as a plateau and the Ganges delta prevailing in between. These outspread ranges of topographical features and classes of soils and substrata make the state an ideal place for hosting a rich diversity of mushrooms.² In previous years, our research team conducted extensive field works and recorded an immense number of wild edible mushrooms from different corners of the state with the help of tribal and ethnic forest dwellers of the regions who consume them as part of their daily diet.³ Taxonomic and molecular exploration revealed that many of them are new to science,^{4,5} new records for India,^{6,7} and additions to the macrofungal flora of West Bengal.^{8,9}

Throughout the globe, mushrooms are well known to human civilizations because of having nutritional and culinary value and medicinal potential. In contemporary terms, they can be regarded as functional foods that can furnish health benefits beyond the traditional nutrients.¹⁰ Mushrooms are known to be rich sources of various bioactive substances like antioxidant,¹¹⁻¹³ antimicrobial,^{14,15} immunomodulatory,^{16,17} and anticancer¹⁸ substances. Despite all the mentioned health promoting effects, this diverse group is still largely unknown as more than half of the species remain undescribed.

Most of the species belonging to the genus *Oudemansiella* (Basidiomycota, Agaricales, Physalacriaceae) are consumed worldwide.¹⁹ Many *Oudemansiella* species are known to contain bioactive compounds, such as oudenone and lectin (obtained from *Oudemansiella radicata*),^{20,21} and mucidin and oudemansin (from *Oudemansiella mucida*).^{22,23} The edible mushroom *Oudemansiella canarii* (Jungh.) Höhn was found to be present in various biomasses, where it colonizes with several plant species. Morphologically, the taxon is characterized by the presence of a medium to considerably larger pileus with glutinous to viscid surface colored gray-orange to orange white or with paler to white margin; adnate to shallowly adnexed, white, distant lamellae with 2-3 series of lamellulae; globose to subglobose basidiospores measuring 19-25×18-23 μ m in

diameter; an ixotrichoderm type of pileipellis; well-developed, stalked, pleuro- and cheilocystidia; presence of one- to few-celled caulocystidia with heterogeneous contents; and lignicolous habit.²⁴ As it is considered an edible mushroom with good potential as a food source, it is highly cultivated artificially on various lignocellulosic substrates.²⁵ Very few literature reports were found related to their physicochemical, nutritional, and medicinal value. Only one report has been published regarding the antifungal and biological activities of *O. canarii*.²⁶ Therefore, in the present study we documented molecular parameters with the phylogeny, physicochemical profile, and antioxidant potentiality of *O. canarii*.

MATERIALS AND METHODS

Sample collection and microscopic and organoleptic characterization of powdered basidiocarps

Living basidiocarps of *O. canarii* were collected from the Gangetic plains of West Bengal, India. The basidiocarps were found to grow on dead and decayed woods of dicotyledonous plants. Identification of the specimen was done based on the standard literature.^{24,27} Collected basidiocarps were then dried overnight at 40°C using a field drier. A sample of the voucher specimen was deposited in Calcutta University Herbarium (CUH) following the protocol described by Pradhan et al.²⁸ with the accession number CUH AM26. The remaining basidiocarps were used to make powder and then the powdered sample was hydrated and macerated with 10% potassium hydroxide (KOH) and mounted on a glass slide for microscopic observations. For effective results, various stains (lactophenol and cotton blue, Melzer's reagent, congo red, etc.) were used to visualize different cellular structures such as hyphae, basidia, and spores. The slides were then viewed under a Leica DMLS microscope and images were captured at the desired magnification. Different organoleptic characters (i.e., color, odor, taste, and nature) of the powdered sample were evaluated.

DNA extraction and polymerase chain reaction and cycle sequencing

Genomic DNA was extracted and the desired region (nrDNA ITS) was amplified using the method described by Dutta et al.²⁹ with the help of the primer pair ITS1 (forward) and ITS4 (reverse).³⁰

Fluorescence analysis

Fluorescence analysis was performed as per the standard protocol.³¹ A small amount of sieved powder was kept on a clean grease-free microscopic slide and treated with prepared chemical agents including Hager's, Mayer's, Dragendroff's, phloroglucinol, and Barfoed's reagent and were mixed by gently tilting the slide. Then the slide was placed within a ultraviolet (UV) viewer chamber and viewed against visible, long (365 nm), and short

(254 nm) UV radiations. Then the changes in color on application of these reagents in different radiations were recorded.

Preparation of methanol extract

Initial extraction was done using 100 mL of methanol overnight from the dried powdered fruit bodies (5 g) and then the solution was filtered using Whatman no. 1 filter paper. The residue was then re-extracted using 30 mL of methanol. Volume reduction of the combined methanolic extracts was done by evaporating at 40°C using a Buchi Rotavapor R3 (Switzerland). The methanolic fraction was then kept at -20°C in a dark bottle until analysis, for not more than 1 month. Percentage yield and organoleptic features of the extract were recorded.

Quantitative estimation of some important bioactive compounds

Freshly prepared methanolic extract was subjected to several quantitative biochemical assays to investigate the presence and amounts of different phytochemicals. Folin-Ciocalteu reagent was used to estimate the content of total phenolic compounds in the extract³² with gallic acid as a standard. The results were expressed comparing with µg of gallic acid equivalents/mg of dry extract. Potassium acetate and aluminum nitrate were used to detect the presence of total flavonoid content.³³ A standard curve was prepared with the help of quercetin (5-20 µg/mL). The results were expressed as µg of quercetin equivalents per mg of dry extract. β-Carotene and lycopene contents were estimated by measuring absorbance at 453, 505, and 663 nm wavelengths following the standard protocol.³⁴ Ascorbic acid was determined by titration against 2,6-dichlorophenol indophenol dye.³⁵

High performance liquid chromatographic profile of methanol soluble extract

High performance liquid chromatographic (HPLC) analysis was performed to produce a fingerprinting profile of the extract. A 0.2 µm filter was used to filter the methanolic extract and then 20 µL of the filtrate was loaded in the HPLC system (Agilent, USA). Separation was performed on an Agilent Eclipse Plus C18 column (100 mm×4.6 mm, 3.5 µm) with a flow rate of 0.8 mL/min at 25°C. The mobile phase comprised eluent A (acetonitrile) and eluent B (aqueous phosphoric acid solution, 0.1% v/v). Further a gradient program was utilized for elution: 0-2 min, 5% A; 2-5 min, 15% A; 5-10 min, 40% A; 10-15 min, 60% A; 15-18 min, 90% A. Finally, at 280 nm, absorbance of the sample solution was measured.³⁶

Antioxidant activity

For evaluation of the antioxidant potential of *O. canarii*, the methanolic extract was tested for several *in vitro* antioxidant activities by 2,2-diphenyl-1-picrylhydrazyl (DPPH) radical scavenging assay, 2,2'-azinobis-(3-ethyl-benzothiazoline-6 sulfonic acid (ABTS) assay, and total antioxidant assay.

DPPH radical scavenging activity

The radical scavenging activity of the extract was tested using DPPH radicals following Mitra et al.³⁷ Two milliliters of the reaction mixture contained several concentrations of the extract along with 0.1 mM methanolic solution of DPPH. After 30 min

of incubation at room temperature in the dark, the absorbance was measured against a methanol blank at 517 nm. The EC₅₀ value denotes an effective concentration at which 50% of the DPPH radicals are scavenged. Ascorbic acid was used for comparison. The scavenging ability was calculated using the following equation:

$$\text{Scavenging effect (\%)} = \left\{ \frac{A_0 - A_1}{A_0} \right\} \times 100$$

A₀ was absorbance of the control and A₁ was absorbance in the presence of sample. The percentage of inhibition was plotted against respective concentrations used.

Total antioxidant activity

Measurement of total antioxidant activity was solely based on the reduction of molybdenum (from VI to V) by the sample analyte and thereby formation of phosphate/molybdenum (V) complex at acidic pH.³⁸ The sample was mixed with reagent solution, prepared with 28 mM sodium phosphate, 0.6 M sulfuric acid, and 4 mM ammonium molybdate, and incubated at 95°C for 90 min. The mixture was then cooled to room temperature. Absorbance was spectrophotometrically recorded for each solution at 695 nm using a blank sample as control. For reference antioxidant, various concentrations (1-30 µg/mL) of ascorbic acid were used and the total antioxidant capacity was expressed equivalent to ascorbic acid.

ABTS radical scavenging activity

ABTS is well regarded as a peroxidase substrate that generates a metastable radical cation when oxidized.³⁹ The ability to inhibit the accumulation of ABTS radical cation by methanol extract and antioxidant standard, Trolox, was measured spectrophotometrically. ABTS dissolved in methanol to yield 7.4 mM concentration. ABTS radical solution was prepared by reacting ABTS (7.4 mM) with 2.6 mM potassium persulfate solution and permitting the mixture to stand in the dark for 12-16 h at room temperature before use. The mother stock was diluted to achieve an absorbance of 0.7±0.02 at 734 nm. Methanol extract at 1 mg/mL concentration was allowed to react with the ABTS working solution for 5 min and the absorbance was measured.

Statistical analysis

All the assays were performed in triplicate and the results are expressed by the mean values and standard deviation. For determining the significant difference among samples, the results were compared by means of Student's t-test. The analysis was carried out using Microsoft® Office Excel (Microsoft®, USA), where values of p≤0.05 were considered statistically significant.

RESULTS AND DISCUSSION

Microscopic and organoleptic characterization of the powdered basidiocarps

Dried powder of the fresh basidiocarps that was passed through sieve and further macerated with KOH showed basidiospores and fragmented hyphae (Figure 1). The hyphal system was

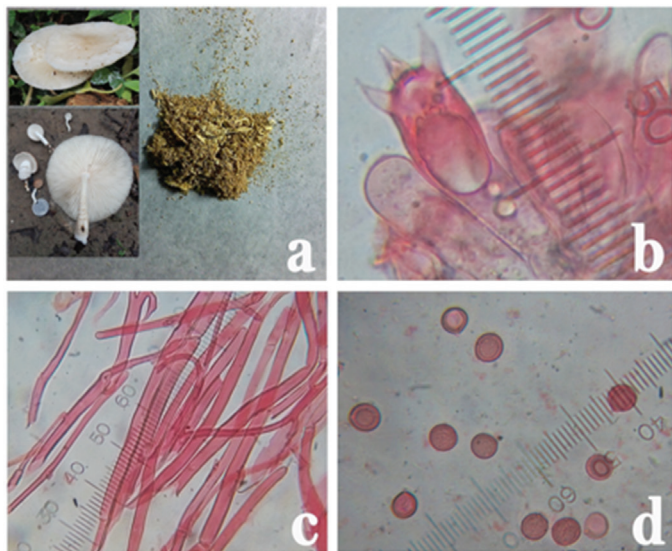


Figure 1. Macroscopic and microscopic characters of *Oudemansiella canarii*. a) sieved powder (fresh basidiocarps in insets), b) basidium, c) hyphae, d) basidiospores

monomitic in nature with generative hyphae that were 4–6 μm broad, septate, branched, hyaline, thin-walled, clamped. The basidia were 64–83 \times 11–22 μm in diam., shaped clavate to broadly clavate and 4-spored at the apex. Basidiospores were 14–21 \times 10.5–18 μm in diam., hyaline, globose to sub-globose with hilar appendage, and thick-walled. Melzer's reaction showed a negative result, which signifies the non-amyloid nature of the basidiospores.

Sieved powder was used for the organoleptic study. The powder was yellowish, with no odor, tasteless, and fibrous in texture.

Molecular analysis

The newly generated sequence of *O. canarii* was manually edited using the BioEdit sequence alignment editor v.7.0.9.0 (Ibis Biosciences, Carlsbad, CA, USA). The edited DNA sequence of the collected specimen produced 747-bp-long stretches that include the ITS1, 5.8S, ITS2, and 28S ribosomal RNA genes. The edited sequence was then used for the Basic Local Alignment Search Tool (BLAST) searches in the NCBI GenBank database (www.ncbi.nlm.nih.gov).

BLAST analyses with our newly generated sequence showed similarity with the genus *Oudemansiella*, with the highest similarity shown by *O. canarii* [AF321476, Identities= 681/698 (98%), Gaps= 7/698 (1%); KR265132, Identities= 690/690 (100%), Gaps= 0/690 (0%)]. Hence, the result of the BLAST search easily helps to identify our collected specimen as *O. canarii* (family Physalacriaceae). The newly generated sequence of *O. canarii* was then deposited in the GenBank database with accession number KU647631.

Fluorescence analysis

The fluorescence test of the powdered sample was carried out for qualitative assessment of crude drug to give an idea of its chemical nature. The colors developed by these reagents represent the presence of active constituents. Analysis of

powdered drug through fluorescence is a vital and very useful pharmacognostic technique for identification of authentic samples and recognizing adulterates and substituents to help in maintaining the quality, reproducibility, and efficacy of natural drugs.^{40,41} Here, powdered sample was treated with seven different chemical reagents and the characteristic fluorescence properties or colors were recorded (Table 1).

Table 1. Fluorescence analysis of dry powder of *Oudemansiella canarii*

Sl. no.	Reagent	Visible	UV	
			Long (365 nm)	Short (254 nm)
1	Blank	Straw yellow	Brown	Straw yellow
2	Water	Cinnamon brown	Cinnamon brown	Light brown
3	Mayer's	Grayish orange	Dark brown	Pastel yellow
4	Hager's	Cream	Grayish brown	Grayish orange
5	Phloroglucinol	Brownish yellow	Violet brown	Dark brown
6	Barfoed's reagent	Dark brown	Grayish brown	Violet brown
7	Dragendorff's reagent	Brownish orange	Brown	Light brown

UV: Ultraviolet

Quantitative estimation of bioactive compounds

The quantitative estimation of several marked phytochemicals of the methanolic extract was carried out based on the standard protocols as described above. Phenolic compounds are well regarded as a powerful chain-breaking antioxidant because of the presence of hydroxyl groups with scavenging ability. It was found that the extract contained phenol as high as 5.38 \pm 0.55 μg gallic acid equivalent/mg of extract. Total flavonoid content was estimated using quercetin as the standard. The flavonoid content was 1.875 \pm 0.78 μg quercetin equivalent/mg of the extract while the ascorbic acid content was 1.10 \pm 0.42 $\mu\text{g}/\text{mg}$. β -Carotene and lycopene were present in negligible amounts: 0.0342 \pm 0.004 $\mu\text{g}/\text{mg}$ and 0.0238 \pm 0.004 $\mu\text{g}/\text{mg}$ of the extract, respectively.

Chromatographic fingerprinting by HPLC

For preliminary determination of the presence of chemical constituents in any sample, one of the popular and efficient chromatographic methods is HPLC. Thus, HPLC analysis was carried out using the methanolic extract of *O. canarii*. The UV spectrum analysis of the chromatogram (278 nm) depicts the presence of 12 peaks excluding the mobile phase peak. The represented chromatogram may serve as a phenolic fingerprint for this mushroom. The HPLC chromatogram of methanolic extract of the sample identifies the presence of cinnamic acid (retention time 15.358 min) and pyrogallol (retention time 15.966

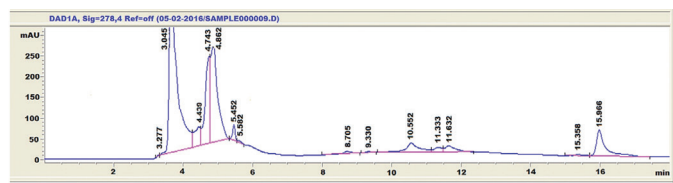


Figure 2. Enlarged HPLC chromatogram of methanol extract from *Oudemansiella canarii*

HPLC: High-performance liquid chromatography

Table 2. HPLC profile at 278 nm of methanol extract from *Oudemansiella canarii*

Peak no.	Retention time (min)	Area (AU)	Maximum height (AU)
1	4.439	593.86871	46.60723
2	4.743	2061.23242	211.45323
3	4.862	3274.20972	239.57074
4	5.452	198.42529	38.72375
5	5.582	36.55459	4.50278
6	8.705	85.07185	5.29850
7	9.330	26.53930	2.48095
8	10.552	623.75525	22.86010
9	11.333	187.39143	11.74532
10	11.632	341.26938	15.61782
11	15.358	67.66934	4.10833
12	15.966	1172.96606	63.93803

min) based on the standard as provided in our previous study.¹⁵ The chromatographic profile along with the retention time of each peak is presented in Figure 2 and respective areas of each peak are documented in Table 2.

Antioxidant activity

DPPH radical scavenging activity

The DPPH assay has been popularly used for testing the free radical scavenging ability of various natural samples. DPPH receives electrons or hydrogen to gain stability. Antioxidants, on the other hand could donate electrons or hydrogen atoms. In methanol solution, DPPH produces a violet color. However, when electrons are donated to DPPH, the solution starts losing color from purple to yellow and the reduction capacity of DPPH is determined by the decrease in its absorbance at 517 nm.⁴² The extract showed high effective free radical scavenging activity in the DPPH assay at the rate of 6.53%, 55.85%, and 78.74% at 0.5, 1, and 1.5 mg/mL concentrations (Figure 3). The EC_{50} value was 0.912 ± 0.38 mg/mL.

Total antioxidant activity

One of the simplest methods for evaluating total antioxidant capacity is the phosphomolybdenum method. The total antioxidant capacity of the methanol fraction was investigated and compared against ascorbic acid. The extract revealed antioxidant capacity of 15.33 ± 0.67 μ g/mg ascorbic acid equivalent.

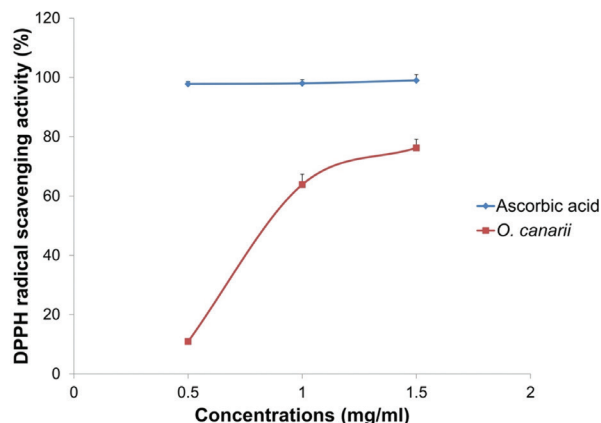


Figure 3. DPPH assay of methanol extract from dried basidiocarp of *Oudemansiella canarii*

DPPH: 2,2-Diphenyl-1-picrylhydrazyl

ABTS radical scavenging activity

The ABTS assay is based on the inhibition of the formation of ABTS⁺, a stable radical cation by one electron oxidants. The methanolic extract of the sample showed 12.91 ± 0.26 μ M Trolox equivalents/mg of extract antioxidant activity.

CONCLUSIONS

The present work allocates standards of the macrofungus *O. canarii* with the help of pharmacognostic, molecular, and chemical characteristics. Various standardization parameters such as microscopy, molecular characteristics, physicochemical constants, preliminary mycochemical quantification, HPLC analysis, and antioxidant activity were studied, and were reported for the first time for this mushroom. All these combined data indicate this edible mushroom is a valuable source of bioactive molecules like phenolic compounds and has enormous antioxidant potential.

Conflict of Interest: No conflict of interest was declared by the authors.

REFERENCES

1. Thatoi H, Singdevsachan SK. Diversity, nutritional composition and medicinal potential of Indian mushrooms: a review. *Afr J Biotechnol.* 2014;13:523-545.
2. Dutta AK, Acharya K. Traditional and ethno-medicinal knowledge of mushrooms in West Bengal, India. *Asian J Pharm Clin Res.* 2014;7:36-41.
3. Dutta AK, Pradhan P, Basu SK, Acharya K. Macrofungus diversity and ecology of the mangrove ecosystem in the Indian part of Sundarbans. *Biodiversity.* 2013;14:196-206.
4. Acharya K, Dutta AK, Pradhan P. A new variety of *Volvariella pusilla* from West Bengal, India. *Mycosphere.* 2012;3:13-17.
5. Dutta AK, Chandra S, Pradhan P, Acharya K. A new species of *Marasmius* sect. *Sicci* from India *Mycotaxon.* 2014;128:117-125.
6. Dutta AK, Pradhan P, Roy A, Acharya K. A subtropical agaric new to India. *Kavaka.* 2011;39:37-39.

7. Dutta AK, Pradhan P, Roy A, Acharya K. Agaricales of West Bengal, India. I. Clavariaceae: Clavaria and Scytinopogon. Ind J Appl Pure Biol. 2012;27:53-58.
8. Dutta AK, Chakraborty N, Pradhan P, Acharya K. Phallales of West Bengal, India. II. Phallaceae: Phallus and Mutinus. Researcher. 2012;4:21-25.
9. Acharya K, Pradhan P, Sherpa NL, Dutta AK. Favolaschia a new fungal genus record for Eastern India. Ind For. 2014;140:639-640.
10. Rathee S, Rathee D, Rathee D, Kumar V, Rathee P. Mushrooms as therapeutic agents. Rev Bras Farmacogn. 2012;22:459-474.
11. Khatua S, Mitra P, Chandra S, Acharya K. *In vitro* protective ability of *Ramaria aurea* against free radical AND identification of main phenolic acids by HPLC. J Herbs Spices Med Plants. 2015;21:380-391.
12. Pattanayak M, Samanta S, Maity P, Sen IK, Nandi AK, Manna DK, Mitra P, Acharya K, Islam SS. Heteroglycan of an edible mushroom *Termitomyces clypeatus*: structure elucidation and antioxidant properties. Carbohydr Res. 2015;413:30-36.
13. Dasgupta A, Paloi S, Acharya K. Mycochemical analysis and antioxidant efficacy of a wild edible mushroom from the Eastern Himalayas. Res J Pharm Biol Chem Sci. 2015;6:943-948.
14. Mallick S, Dey S, Mandal S, Dutta A, Mukherjee D, Biswas G, Chatterjee S, Mallick S, Lai TK, Acharya K, Pal C. A novel triterpene from *Astraeus hygrometricus* induces reactive oxygen species leading to death in *Leishmania donovani*. Future Microbiol. 2015;10:763-789.
15. Khatua S, Dutta AK, Acharya K. Prospecting *Russula senecis*: a delicacy among the tribes of West Bengal. Peer J. 2015;3:810.
16. Maity P, IK S, Majia PK, Paloi S, Devi KS, Acharya K, Maiti TK, Islam SS. Structural, immunological, and antioxidant studies of β -glucan from edible mushroom *Entoloma lividoalbum*. Carbohydr Polym. 2015;123:350-358.
17. Samanta S, Nandi AK, Sen IK, Maity P, Pattanayak M, Devi KS, Khatua S, Maiti TK, Acharya K, Islam SS. Studies on antioxidative and immunostimulating fucogalactan of the edible mushroom *Macrolepiota dolichaula*. Carbohydr Res. 2015;413:22-29.
18. Chatterjee S, Biswas G, Chandra S, Saha GK, Acharya K. Chemopreventive effect of *Tricholoma giganteum* against benzo[a]pyrene-induced forestomach cancer in Swiss albino mice. Int J Pharm Sci Rev Res. 2014;26:189-196.
19. Xu F, Li Z, Liu Y, Rong C, Wang S. Evaluation of edible mushroom *Oudemansiella canarii* cultivation on different lignocellulosic substrates. Saudi J Biol Sci. 2016;23:607-613.
20. Tsantrizos YS, Yang X, McClory A. Studies on the Biosynthesis of the Fungal Metabolite Oudenone. 2. Synthesis and Enzymatic Cyclization of an alpha-Diketone, Open-Chain Precursor into Oudenone in Cultures of *Oudemansiella radicata*. J Org Chem. 1999;64:6609-6614.
21. Liu Q, Ng T, Wang H. Isolation and characterization of a novel lectin from the wild mushroom *Oudemansiella radicata* (Relhan.: Fr.) Sing. Biotechnol Bioprocess Eng. 2013;18:465-471.
22. Subik J, Behun M, Smigan P, Musilek V. Mode of action of mucidin, a new antifungal antibiotic produced by the basidiomycete *Oudemansiella mucida*. Biochim Biophys Acta. 1974;343:363-370.
23. Anke T, Hechi HJ, Schramm G, Steglich W. Antibiotics from Basidiomycetes. IX. Oudemansin, an antifungal antibiotic from *Oudemansiella mucida* (Schrader ex Fr.) Hochnel (Agaricales). J Antibiot (Tokyo) 1979;32:1112-1117.
24. Petersen RH, Desjardin DE, Krüger D. Three type specimens designated in *Oudemansiella*. Fungal Divers. 2008;32:81-96.
25. Silveira RMJ, Tauk TSM, Bonomi VLR, Capelari M. Cultivation of the edible mushroom *Oudemansiella canarii* (Jungh.) Höhn. In Lignocellulosic substrates. Braz J Microbiol. 2001;32:211-214.
26. Rosa LH, Cota BB, Machado KMG, Rosa CA, Zani CL. Antifungal and other biological activities from *Oudemansiella canarii* (Basidiomycota). World J Microbiol Biotechnol. 2005;21:983-987.
27. Corner EJH. On the Agaric genera Hohenbuehelia and Oudemansiella. Part II: Oudemansiella, Gard Bull Singapore, 1994:49-75.
28. Pradhan P, Dutta AK, Acharya K. A low cost long term preservation of macromycetes for fungarium. Protocol Exchange; 2015.
29. Dutta AK, Wilson AW, Antonin V, Acharya K. Taxonomic and phylogenetic study on gymnopoid fungi from Eastern India. I. Mycol Progress. 2015;14:79.
30. White TJ, Bruns T, Lee S, Taylor J. PCR Protocols: a Guide to Methods and Applications. In: Innis MA, Gelfand DH, Sninsky DH, White TJ, eds. Amplification and direct sequencing of fungal ribosomal RNA genes for phylogenetics. Orlando; Florida; 1990:315-322.
31. Kokashi CJ, Kokashi RJ, Sharma M. Fluorescence was powdered vegetable drugs under ultraviolet radiation. J Am Pharm Assoc Am Pharm Assoc. 1958;47:715-717.
32. Singleton VL, Rossi JA. Colorimetry of total phenolics with phosphomolybdic- phosphotungstic acid reagents. Am J Enol Viticult. 1965;16:44-158.
33. Adebayo EA, Oloke JK, Ayandele AA, Adegunlola CO. Phytochemical, antioxidant and antimicrobial assay of mushroom metabolite from *Pleurotus pulmonarius* -LAU 09 (JF736658). J Microbiol Biotech Res. 2012;2:366-374.
34. Nagata M, Yamashita I. Simple method for simultaneous determination of chlorophyll and carotenoids in tomatoes fruit. J Jpn Soc Food Sci. 1992;39:925-928.
35. Rekha C, Poornima G, Manasa AV, Pavithra DJ, Vijay KHT, Prashith KTR. Ascorbic acid, total phenol content and antioxidant activity of fresh juices of four ripe and unripe citrus fruits. Chem Sci Trans. 2012;1:303-310.
36. Mitra P, Mandal N, Acharya K. Biocomponents and bioprospects of ethanolic extract of *Termitomyces heimii*. Asian J Pharm Clin Res. 2015;8:331-334.
37. Mitra P, Mandal NC, Acharya K. Phytochemical characteristics and free radical scavenging activity of ethanolic extract of *Termitomyces microcarpus* R. Heim. Der Pharmacia Lettre. 2014;6:92-98.
38. Prieto P, Pineda M, Aguilar M. Spectrophotometric quantitation of antioxidant capacity through the formation of phosphomolybdenum complex: specific application to the determination of vitamin E. Anal Biochem. 1999;269:334-337.
39. Arnao MB, Cano A, Hernandez-Ruiz J, Garcia-Canovas F, Acosta M. Inhibition by L-ascorbic acid and other antioxidants of the 2,2'-azino-bis (3-ethylbenzthiazoline-6-sulfonic acid) oxidation catalyzed by peroxidase: a new approach for determining total antioxidant status of foods. Anal Biochem. 1996;236:255-261.
40. Bhattacharya S, Zaman MK. Pharmacognostical evaluation of *Zanthoxylum nitidum* bark. Int J Pharm Tech Res. 2009;1:292-298.
41. Sonibare MA, Olatubosun OV. Pharmacognostic and free radical scavenging evaluation of *Cyathula prostata* (Blume) L. Phcog J. 2015;7:107-116.
42. Shimada K, Fujikawa K, Yahara K, Nakamura T. Antioxidative properties of Xanthan on the autoxidation of soybean oil in cyclodextrin emulsion. J Agric Food Chem. 1992;40:945-948.



Degradation Kinetics, *In Vitro* Dissolution Studies, and Quantification of Praziquantel, Anchored in Emission Intensity by Spectrofluorimetry

Degradasyon Kinetiği, *In Vitro* Çözünme Çalışmaları ve Bağlanmış Prazikuantelin Emisyon Yoğunluklu Spektrofluorimetri ile Miktar Tayini

© Panikumar D. ANUMOLU, © Sunitha GURRALA*, © Ceema MATHEW, © Vasavi PANCHAKATLA, © Veda MADDALA

Osmania University, Gokaraju Rangaraju College of Pharmacy, Department of Pharmaceutical Analysis, Hyderabad, India

ABSTRACT

Objectives: A simple, rapid, specific, and highly sensitive ecofriendly spectrofluorimetric method has been developed for the quantification of praziquantel.

Materials and Methods: A linear relationship was found between fluorescence intensity and praziquantel concentration in the range of 1-20 µg/mL in water at emission wavelength of 286 nm after excitation wavelength at 263 nm with a good correlation coefficient (0.999).

Results: The proposed method was validated according to International Conference on Harmonization guidelines and statistical analysis of the results revealed high accuracy and good precision with the percentage relative standard deviation values less than 2. The detection and quantification limits were 0.27 and 0.81 µg/mL, respectively. The proposed method was extended to investigate the stability of the drug and its degradation kinetics in the presence of acidic, alkaline, and oxidative conditions.

Conclusion: The method was utilized for *in vitro* dissolution studies of praziquantel tablet formulation. The suggested procedures could be used for the assessment of praziquantel in drug substance and drug products as well as in the presence of its degradation products.

Key words: Praziquantel, excitation wavelength-263 nm, emission wavelength-286 nm, dissolution, forced degradation

ÖZ

Amaç: Prazikuantel miktar tayini için basit, hızlı, spesifik ve yüksek duyarlılığa sahip, çevre dostu spektrofluorimetrik bir yöntem geliştirilmiştir.

Gereç ve Yöntemler: Prazikuantel konsantrasyonu ile floresan yoğunluğu arasında, 1-20 µg/mL aralığında su içinde, 286 nm emisyon ve 263 nm eksitasyon dalga boyunda, iyi bir korelasyon katsayısı (0.999) olan doğrusal bir ilişki bulundu.

Bulgular: Önerilen yöntem Uluslararası Uyumlaştırma Konferansı yönergelerine göre doğrulanmıştır ve sonuçların istatistiksel analizi, 2'den düşük bağıl standart sapma değerleri ile yüksek doğruluk ve hassasiyet göstermiştir. Saptama ve miktar limitleri sırasıyla 0.27 ve 0.81 µg/mL'dir. Önerilen yöntem, ilacın stabilitesini ve asidik, alkali ve oksidatif koşullar varlığında bozunma kinetiklerini araştırmak için genişletilmiştir.

Sonuç: Yöntem, prazikuantel tablet formülasyonunun *in vitro* çözünme çalışmaları için kullanılmıştır. Önerilen prosedürler, prazikuantelin ilaç maddesi ve ilaç ürünlerinde ve degradasyon ürünlerinin varlığının değerlendirilmesi için kullanılabilir.

Anahtar kelimeler: Prazikuantel, eksitasyon dalga boyu-263 nm, emisyon dalga boyu-286 nm, çözünme, zorla bozunma

*Correspondence: E-mail: g.sunitha88@gmail.com, Phone: 09966556830 - 919966556830 ORCID-ID: orcid.org/0000-0001-6251-2763

Received: 17.11.2017, Accepted: 18.01.2018

©Turk J Pharm Sci, Published by Galenos Publishing House.

INTRODUCTION

Chemically, praziquantel is 2-cyclohexanecarbonyl-1H,2H,3H,4H,6H,7H,11bH-piperazino [2,1-a] isoquinolin-4-one (Figure 1). It is within the category of anthelmintics, used for the treatment of schistosome and many cestode infestations. Schistosomiasis is a parasitic disease caused by worms that penetrate the skin of people through water. Praziquantel is the only drug for treatment of schistosomiasis and it is effective and safe. Work is ongoing to expand the treatment with praziquantel to young children as well.^{1,2}

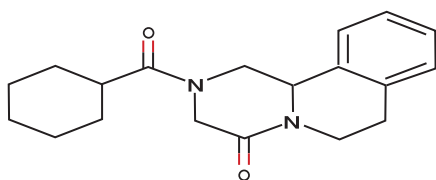


Figure 1. Chemical structure of praziquantel

An extended literature survey revealed that few analytical methods [using high-performance liquid chromatography (HPLC) and HPLC-mass spectrometry] have been reported for estimation of praziquantel.³⁻⁷ To date, one spectrofluorimetric method has been reported for praziquantel quantification in blood plasma and urine. However, the method was complicated because of drug chemical derivatization with dansyl chloride, which involved various solvents with many extraction procedures. Keeping the above points in mind, our objective in this work was to develop a simple method for praziquantel quantification in pharmaceutical dosage forms in the presence of degradation products and *in vitro* dissolution samples. Spectrofluorimetry has implicit a foremost role in drug analysis because of its greater sensitivity and specificity than absorption spectrophotometry. Fluorimetry involves the estimation of drug solution at two wavelengths, excitation and emission in fluorescence; an emission spectrum is acquired by scanning the emission monochromator at determined emission wavelengths (λ_{em}), at a particular excitation wavelength (λ_{ex}).⁸⁻¹³

Nowadays, dissolution tests are routinely used in the pharmaceutical industry in a wide variety of applications, to identify which sort of formulation will produce the best results in the clinic, to release products into the market, and to verify batch-to-batch reproducibility.^{14,15} International Conference on Harmonization (ICH) Q1A guidelines suggested procedures to carry out stress degradation studies to ensure the high quality, safety, and efficacy of the pharmaceutical product during its storage. Forced degradation (FD) study/stress testing is a process in which the natural degradation rate of a pharmaceutical product is increased by the application of an additional stress. It is an important part of the drug development process as it provides knowledge about the degradation chemistry of drug compounds to develop stability-indicating analytical methods and characterization of degradation products.¹⁶

Taking all these points into consideration, the objective of the present work was to develop and validate a simple spectrofluorimetric method for quantification of praziquantel in pharmaceutical dosage forms. The proposed method was applied to study the *in vitro* dissolution profiles of praziquantel and further extended to stress degradation studies of praziquantel and degradation kinetics were also calculated.

MATERIALS AND METHODS

Chemicals and reagents

All chemicals and reagents were of analytical grade. Pure praziquantel (99.50%) was obtained as gift samples from Taj Pharmaceutical Ltd. (Mumbai, India). Tablets (Zenticide) were obtained from local pharmacies. Glacial acetic acid (99.8-100.5%), ethanol, methanol, hydrochloric acid (36.46%), ortho-phosphoric acid, sodium hydroxide, hydrogen peroxide, dimethyl sulphoxide (DMSO), dimethyl formamide (DMF), acetonitrile, and potassium di-hydrogen phosphate were purchased from SD Fine Chemicals Ltd. (Mumbai, India). Series of buffer solutions of acetate buffers (pH 3.7-4.7) and phosphate buffers (pH 5.8-7.8) were prepared as per the Indian Pharmacopoeia.¹⁷

Instrumentation

A Shimadzu (Japan) RF-5301 PC spectrofluorophotometer was used for measurement of the fluorescence intensity of the selected drug. It was equipped with a 150-W Xenon arc lamp, a 1-cm non-fluorescent quartz cell was used, and it was connected to RFPC software. The instrument was operated at both low and high sensitivity with excitation and emission slit width set at 5 nm. An analytical balance (Shimadzu AUX 220, Japan), dissolution apparatus (Electro Lab, TDT-08L, India), pH meter (Elico), hot air oven, and ultraviolet (UV)-cabinet (Bio-Technics, India) were also used.

Preparation of standard stock solutions

Pure praziquantel drug of 10.0 mg was weighed and placed into a 10.0-mL volumetric flask and dissolved in methanol. The flask was shaken and volume was made up to the mark with distilled water. Then 0.1 mL of prepared solution was diluted to 10.0 mL with distilled water to attain praziquantel end concentration of 10.0 $\mu\text{g/mL}$.

Construction of the calibration graph

The standard stock solution of praziquantel (100 $\mu\text{g/mL}$) was used to prepare a set of diluted standard solutions of various concentrations (1-20 $\mu\text{g/mL}$) prepared by pipetting appropriate volumes (0.1, 0.5, 1, 1.5, 2 mL) of stock solution into 10.0-mL volumetric flasks and adjusting the volume to the mark with distilled water. These solutions were scanned in a spectrofluorimeter at λ_{ex} of 263 nm.

Determination of praziquantel in tablet dosage form (assay)

Twenty tablets of marketed formulation (Zenticide®), each containing 600 mg of praziquantel, were taken and accurately weighed. Average weight was determined and they were crushed into fine powder. An accurately weighed profusion of powder equivalent to 10.0 mg of praziquantel was transferred

to a 10.0 mL volumetric flask. Methanol was added to this volumetric flask and it was sonicated for 15 min. The flask was shaken and volume was made up to the mark with water. The above solution was filtered through Whatman filter paper (no. 41). From the filtrate, a final concentration of solution was prepared for the estimation of drug content by the proposed method.

Dissolution studies

Dissolution testing of the praziquantel tablet formulation (Zenticide®) was carried out in 0.1 M HCl (900 mL) containing 2 mg of sodium lauryl sulfate according to the Food and Drug Administration (FDA) dissolution database, using a paddle apparatus (type 2) at 50 rpm and $37 \pm 0.5^\circ\text{C}$ for 60 min. Sampling aliquots of 5.0 mL were withdrawn at 10, 20, 30, 40, 50, and 60 min and reconstituted with an equal volume of the fresh medium to maintain the sink conditions. At the end of each test time, sample aliquots were filtered, diluted with water, and quantified. Samples withdrawn were evaluated with the regression equation of the proposed analytical technique for quantification of the dissolved drug followed by a plot against time.

Forced degradation studies

FD studies were carried out by exposing the sample solution to stress conditions like acidic, alkaline, thermal, oxidative, and UV effects.

Sample solution (10 $\mu\text{g}/\text{mL}$) was prepared by adding 1.0 mL of stock solution and 2.0 mL of 5 M HCl to a 10.0 mL volumetric flask. Then the volumetric flask was kept under 60°C reflux conditions for 5 h and neutralized with 5 M NaOH; then the volume was made up to the mark with distilled water. Similarly, alkaline degradation (5 M NaOH), oxidative degradation (1% H_2O_2), and thermal degradation (heated at 105°C) were performed. UV degradation was performed with 10 mg of praziquantel placed in a UV cabinet at short wavelength (254 nm), then subjected to the proposed sample procedure, and fluorescence intensity was measured every 1 h up to 24 h.

RESULTS AND DISCUSSION

Selection of wavelength

To attain a sensitive and specific spectrofluorimetric method for the quantification of praziquantel, several solvent systems were investigated such as methanol, DMSO, ethanol, DMF, and glacial acetic acid. Fluorescence intensity was higher in methanol:water (1:9) than in the other solvent systems (Figure 2) and exhibited native fluorescence at emission wavelength 286 nm after excitation at 263 nm in the presence of a polycyclic aromatic system like pyrazino and isoquinolin rings with more π electrons (Figure 3). Hence methanol:water (1:9) was selected as the solvent for quantification, FD studies, and *in vitro* dissolution studies of praziquantel.

Analytical method validation

Linearity and range

Linearity was verified qualitatively by running the plot; at several concentrations, the plot showed that amplitudes

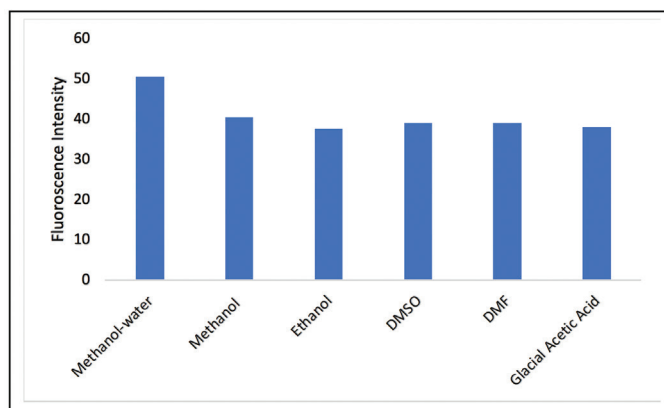


Figure 2. Effect of various solvents on fluorescence intensity of praziquantel

DMSO: Dimethyl sulphoxide, DMF: Dimethyl formamide

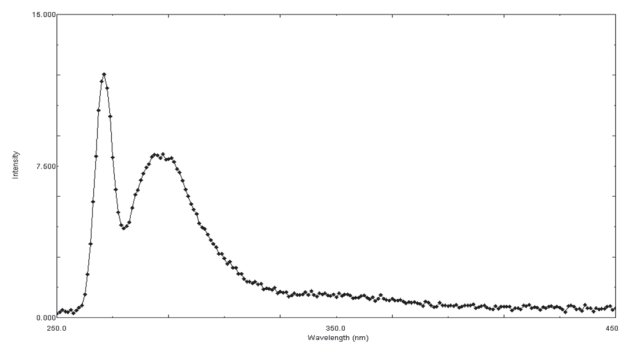


Figure 3. Emission spectrum (286 nm) of praziquantel in methanol water as solvent

gradually changed (increased) at 286 nm (Figure 4). This was clear evidence of the suitability of the method for analysis. The linearity was assessed by the regression equation of the calibration curve; furthermore, the data and regression equation of calibration curves shown in Table 1 and Figure 5 denote that responses for praziquantel at 286 nm were linear in the concentration range of 1-20 $\mu\text{g}/\text{mL}$, with a correlation coefficient (R^2) value of 0.996.

Selectivity

The fluorescence spectrum attained from the commercial formulation solution was compared with the spectrum

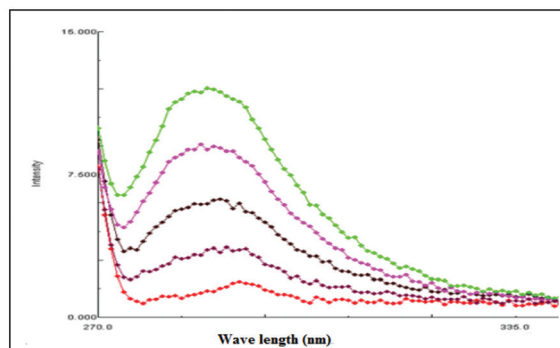


Figure 4. Linearity spectra of praziquantel at 286 nm (1-20 $\mu\text{g}/\text{mL}$)

Table 1. Optimized parameters for the proposed method

Parameter	Value
Excitation wavelength (nm)	263
Emission wavelength (nm)	286
Linearity range ($\mu\text{g/mL}$)	1-20
Limit of detection ($\mu\text{g/mL}$)	0.27
Limit of quantification ($\mu\text{g/mL}$)	0.81
Correlation coefficient (r^2)	0.996
Slope (m)	0.574
Intercept (c)	0.409
Regression equation	$Y=0.574x+0.409$

of standard solution (praziquantel). Both the commercial formulation spectrum and the standard solutions spectrum were superimposed; they denoted no interference from excipients with response of praziquantel at analytical wavelength 286 nm. Hence the method was found to be specific and selective.

Accuracy (recovery studies)

Accuracy was assessed by standard addition method at three distinct levels (80%, 100%, and 120%) of standards coalesced to commercial tablets in triplicate and the mean of percentage recoveries and % relative standard deviation (RSD) values were computed and are given in Table 2. The % RSD values at relevant concentration level was 2 and % recoveries of praziquantel were assessed to be in the range of 99-101, thus suggesting the accuracy of the method.¹⁸

Table 2. Accuracy (% recovery) of the proposed method

Formulation	Recovery level (%)	Theoretical content ($\mu\text{g/mL}$)	Concentration found ($\mu\text{g/mL}$) (mean \pm SD)	% Amount recovered (mean \pm SD)	% RSD
Zenticide [®]	80	18	17.93 \pm 0.072	99.6 \pm 0.677	0.679
	100	20	20.12 \pm 0.164	100.6 \pm 1.361	1.352
	120	22	22.45 \pm 0.390	102.0 \pm 0.264	0.258

SD: Standard deviation, RSD: Relative standard deviation

Precision

Intra-day and inter-day precision harmony was appraised as per ICH guidelines, in which samples containing praziquantel (5/10 and 15 $\mu\text{g/mL}$) were analyzed six times on the same day (intra-day precision) and for three consecutive days (inter-day precision); then % RSD was calculated. Results of intra-day and inter-day precision data are given in Table 3, which revealed that there was no significant distinction between the % RSD values of intra-day and inter-day analysis, which indicates that the proposed method is highly precise.

Limit of detection and limit of quantitation

The limit of detection and limit of quantitation were discretely appraised based on the standard calibration curve, and the results are presented in Table 1.

Table 3. Precision data of the proposed analytical method

Theoretical concentration ($\mu\text{g/mL}$)	Intra-day		Inter-day	
	Concentration (mean ^a \pm SD)	% RSD	Concentration (mean ^b \pm SD)	% RSD
5	4.9 \pm 0.018	0.36	5.0 \pm 0.016	0.32
10	9.8 \pm 0.0169	0.17	9.9 \pm 0.024	0.24
15	15.1 \pm 0.023	0.15	14.9 \pm 0.035	0.23

^a: Mean values of six different standards for each concentration, ^b: Inter-day reproducibility was quantified from six different standards of each concentration for three consecutive days, SD: Standard deviation, RSD: Relative standard deviation

Applications

Assay

The proposed method was employed for the assay of commercial tablets (Zenticide[®]) containing praziquantel (600 mg). The results were correlated with consequent labeled amounts and are shown in Table 4. The best peaks of the assay in tablets were found to be 100.1 (% RSD<2), which indicates the accuracy of the proposed method.

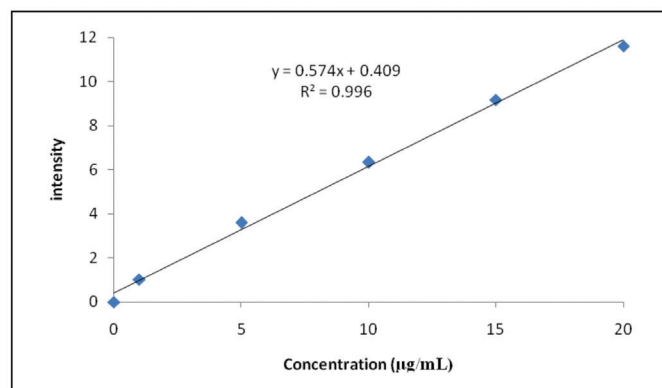
Table 4. Assay results of marketed tablets of praziquantel

Formulation	Praziquantel			
	Label claim (mg)	Amount found (mg) (mean \pm SD) (n=3)	% Assay	% RSD
Zenticide	600	600.8 \pm 0.08	100.1%	0.013

SD: Standard deviation, RSD: Relative standard deviation

In vitro dissolution testing

Dissolution studies on praziquantel tablets were performed with the FDA dissolution test medium as United States Pharmacopeia dissolution apparatus type 2 containing 900 mL of 0.1 M HCl with 2.0 mg of sodium lauryl sulfate as dissolution medium at a paddle speed of 50 rpm at temperature 37 \pm 0.5 $^{\circ}\text{C}$. These results and profiles are given in Figure 6, which revealed that 95% of praziquantel was dissolved from the tablet dosage form.

**Figure 5. Linearity plot of praziquantel**

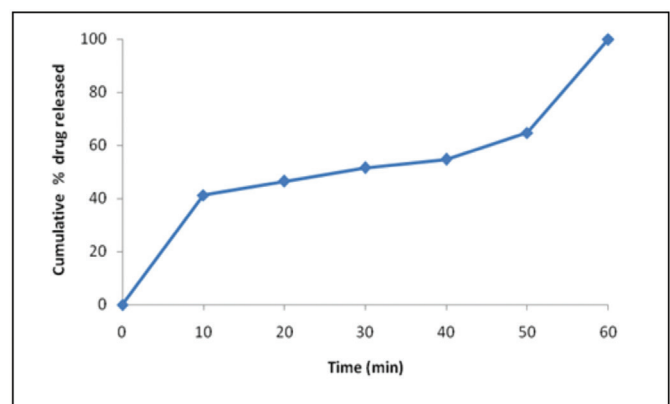


Figure 6. Cumulative % drug release of praziquantel from Zenticide tablets

Forced degradation studies

The stability of praziquantel was studied to elucidate its inherent stability characteristics in terms of fluorescence intensity in acid/alkali hydrolysis, oxidative, thermal, and UV light conditions. Anon constructed the plot between % drug degraded vs time interval. Degradation was observed in 5 M HCl (81% up to 60 min) and 5 M NaOH (1.0% up to 60 min) and 1% H_2O_2 (84% up to 60 min) but there was no evidence of degradation under UV light or thermal conditions (data not shown). For acidic and oxidative degradation it was observed that relative fluorescence intensity decreased gradually with increased heating time (Figure 7). Constructed the plot between logarithmic concentration against time shown in Figures 8, 9, calculated the half-life and first order rate constants for acid and oxidative degradation.

CONCLUSIONS

The proposed spectrofluorimetric method has the advantages of being economical, simple, sensitive, specific, and extraction free for quantification of praziquantel in tablets and *in vitro* dissolution samples. Furthermore, the present work examined the degradation kinetics of praziquantel under stress conditions as per ICH guidelines. Fortunately, considerable degradation

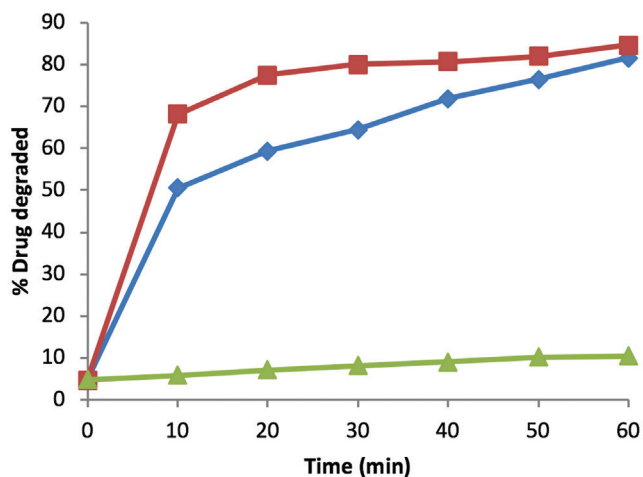


Figure 7. Stability profile of praziquantel in the presence of peroxide (◆) basic (▲) and acidic (■) degradation conditions

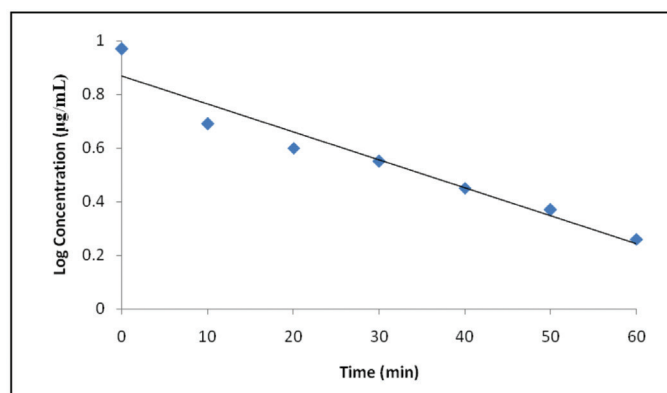


Figure 8. Plot of praziquantel degradation in the presence of 5 N HCl solution

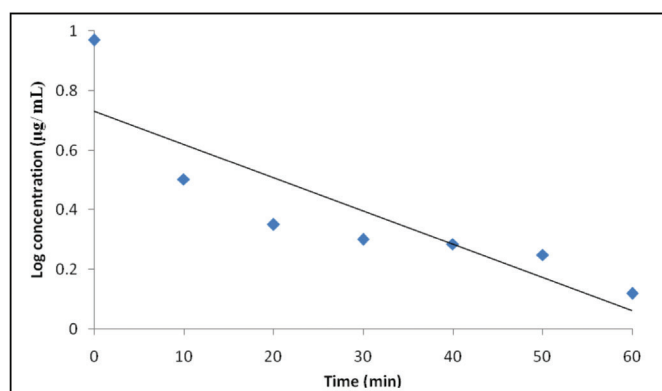


Figure 9. Plot of praziquantel degradation in the presence of 1% H_2O_2 solution

Table 5. Results of the degradation study of praziquantel under acidic and oxidative conditions on the kinetic parameters of praziquantel

Degradation condition	Reaction rate constant (K min ⁻¹)	Half-life time ($t_{1/2}$, min)
Acidic degradation (5 N HCl, 60°C)	0.027	25.6
Oxidative degradation (1% H_2O_2)	0.030	23

was observed and the rate constant and half-life under acidic and oxidative stress conditions were calculated. The results of the proposed spectrofluorimetric method were clear evidence that it can be employed fruitfully for quantification of praziquantel in tablet dosage form, in *in vitro* dissolution samples without any interference, and in degradation studies.

ACKNOWLEDGEMENT

The authors are thankful to the management and Principal Dr CVS Subrahmanyam, of Gokaraju Rangaraju College of Pharmacy for providing facilities for this research work.

Conflict of Interest: No conflict of interest was declared by the authors.

REFERENCES

1. The United States Pharmacopoeia 26 National formulary 21, Asian edition, Rockville: USP Convention, Inc; 2006.
2. British Pharmacopoeia (6th ed). Volume II. British Pharmacopoeia Commission; London; 2008.
3. Shah SR, Dey S, Pradhana P, Jain HK, Upadhyay M. Method development and validation for simultaneous estimation of albendazole and praziquantel in bulk and in a synthetic mixture. *J Taibah Univ Sci.* 2014;8:54-63.
4. Pontes FLD, Piantavini MS, Uber CP, Gasparetto JC, Campos FR, Pontarolo R, Trindade A. Development and validation of an HPLC-MS/MS method for simultaneous determination of ivermectin, febantel, praziquantel, pyrantel pamoate and related compounds in fixed dose combination for veterinary. *Asian J Pharm Clin Res.* 2013;4:191-200.
5. Hashem H, Ibrahim AE, Elhenawee M. A rapid stability indicating LC-method for determination of praziquantel in presence of its pharmacopoeial impurities. *Arabian J Chem.* 2014;6:194-199.
6. Chaud MV, Lima AC, Vila MMDC, Paganelli MO, Paula FC, Pedreiro LN, Gremiao MPD. Development and evaluation of praziquantel solid dispersions in sodium starch glycolate. *Trop J Pharm Res.* 2013;12:163-168.
7. Vignaduzzo SE, Operto MA, Castellano PM. Development and Validation of a Dissolution Test Method for Albendazole and Praziquantel in Their Combined Dosage Form. *J Brazil Chem Soc* 2015;26:729-735.
8. Gomez-Hens A. Modern aspects of fluorimetry as applied to clinical chemistry. *Pure Appl Chem.* 1991;63:1083-1088.
9. Ibrahim F, El-Din MK, Eid MI, Wahba ME. Validated stability indicating spectrofluorimetric methods for the determination of ebastine in pharmaceutical preparations. *Chem Cent J.* 2011;5:11.
10. Patra D, Mishra AK. Recent developments in multi-component synchronous fluorescence scan analysis. *Trends Anal Chem.* 2002;21:787-797.
11. Andrade-Eiora A, Armas GD, Estela JM, Cerda V. Critical approach to synchronous spectrofluorimetry. *Trends Anal Chem.* 2010;29:885-901.
12. Belal F, El-Brashy A, El-Enany N, Tolba M. Conventional and first derivative synchronous fluorimetric determination of ethamsylate in pharmaceutical preparations and biological fluids- application to stability studies. *J Fluoresc.* 2011;21:1371-1384.
13. Kavitha A, Vijaya D, Bindu H, Kasala ER, Khaleel NP, Anumolu PD. Forced degradation studies, quantification and *in vitro* dissolution studies of tadalafil by spectrofluorimetry. *Asian J Pharm Clin Res.* 2013;6:326-329.
14. Brahmkar DM, Jaiswal SB. *Biopharmaceutics and pharmacokinetics*, first ed. Vallabh Prakashan; New Delhi; 2007.
15. Subrahmanyam CVS. *Physical pharmaceutics (2 nd)*. Vallabh Prakashan; New Delhi; 2005.
16. International Conference on Harmonization, Harmonized Tripartite Guideline, Stability Testing of new Drug Substances and Products, Q1 A (R2); 2003.
17. Indian Pharmacopoeia (7th ed). Ghaziabad. The Indian Pharmacopoeia Commission; 2014:245.
18. International Conference on Harmonization, Harmonized Tripartite Guideline, Validation of Analytical Procedures, Text and Methodology, Q2 (R1); 2005.



Subchronic Toxicity Assessment of Orally Administered Methanol (70%) Seed Extract of *Abrus precatorius* L. in Wistar Albino Rats

Wistar Albino Sıçanlarda Oral Olarak Uygulanmış *Abrus precatorius* L. Tohum Metanol (%70) Ekstraktının Subkronik Toksikite Değerlendirmesi

Shazia TABASUM^{1*}, Swati KHARE², Kirti JAIN¹

¹Government Science and Commerce College, Department of Botany, Bhopal, India

²Government Maharani Laxmi Bai Girls P.G. Autonomous College, Department of Botany, Bhopal, India

ABSTRACT

Objectives: *Abrus precatorius* L. is a famous medicinal plant of the family Fabaceae and is widely used in traditional medicine for the treatment of various ailments. However, there are limited toxicological data available regarding its safety following repeated exposure; therefore, the present study was designed to evaluate the 28-day subchronic toxicity of methanol (70%) crude extract of *A. precatorius* seeds in adult Wistar albino rats.

Materials and Methods: A subchronic toxicity experiment was conducted by oral administration of graded doses (200 mg/kg and 400 mg/kg) of test extract daily for 28 days. Signs of toxicity, food and water consumption, body weight, and gross pathology as well as relative organ weight were evaluated. The toxic effects were also assessed using hematological and biochemical data followed by histopathological examination of various internal organs. All data collected were expressed as mean \pm standard deviation. ANOVA followed by the Bonferroni test was used for data interpretation and $p < 0.05$ was considered significant.

Results: No deaths or evident toxic signs were found during the experimental period. There were no significant differences in body weight, gross pathology, organ weight, or food and water consumption between the control and the treated groups. There were no treatment-related differences in hematological or biochemical indices. Moreover, no gross abnormalities or histological alterations were observed.

Conclusion: The methanol extract of *A. precatorius* seeds was nontoxic in subchronic intake at the dosages tested. Thus, this study is expected to be beneficial for clinical and traditional applications for safe consumption and to utilize *A. precatorius* as a remedy at a recommended dosage.

Key words: *Abrus precatorius*, subchronic toxicity, hematology, histopathology, biochemical indices

ÖZ

Amaç: *Abrus precatorius* L., Fabaceae familyasından ünlü bir şifalı bitkidir ve geleneksel tıpta çeşitli rahatsızlıkların tedavisinde yaygın olarak kullanılır. Bununla birlikte, tekrarlanan maruz kalmanın ardından güvenliği ile ilgili sınırlı toksikolojik veriler mevcuttur; bu nedenle, bu çalışma yetişkin Wistar albino sıçanlarında *A. precatorius* tohumlarının metanol (%70) ham ekstraktının 28 günlük subkronik toksisitesini değerlendirmek üzere tasarlanmıştır.

Gereç ve Yöntemler: Yirmi sekiz gün boyunca, günlük olarak test edilen dozlar (200 mg/kg ve 400 mg/kg) oral yolla uygulanarak bir subkronik toksisite deneyi gerçekleştirildi. Toksikite belirtileri, yiyecek ve su tüketimi, vücut ağırlığı ve makroskopik patolojinin yanı sıra nispi organ ağırlığı değerlendirildi. Toksik etkiler, hematolojik ve biyokimyasal veriler kullanılarak değerlendirildi ve bunu takiben çeşitli iç organların histopatolojik incelemesi yapıldı. Toplanan tüm veriler ortalama \pm standart sapma olarak ifade edildi. Verilerin yorumlanması için ANOVA ve ardından Bonferroni testi kullanıldı ve $p < 0.05$ anlamlı kabul edildi.

Bulgular: Deney süresince hiçbir ölüm ya da belirgin toksik belirti saptanmadı. Kontrol ve tedavi edilen gruplar arasında vücut ağırlığı, makroskopik patoloji, organ ağırlığı veya gıda ve su tüketimi açısından anlamlı fark yoktu. Hematolojik veya biyokimyasal indekslerde tedaviye bağlı fark yoktu. Ayrıca, hiçbir makroskopik anormallik veya histolojik değişiklik gözlenmedi.

Sonuç: *A. precatorius* tohumlarının metanol ekstraktı, test edilen dozajlarda, subkronik alımda toksik değildir. Bu nedenle bu çalışmanın, klinik ve geleneksel uygulamalarda güvenli tüketim için faydalı olması ve *A. precatorius*'un tavsiye edilen bir dozda ilaç olarak kullanılması beklenmektedir.

Anahtar kelimeler: *Abrus precatorius*, subkronik toksisite, hematoloji, histopatoloji, biyokimyasal indeksler

*Correspondence: E-mail: shaziatabasum49@gmail.com, Phone: +91 7006354561 ORCID-ID: orcid.org/0000-0002-6731-1722

Received: 03.11.2017, Accepted: 25.01.2018

©Turk J Pharm Sci, Published by Galenos Publishing House.

INTRODUCTION

Medicinal plants offer numerous opportunities for the development of new drugs, as extract, pure compound, or derivative. The natural origin, however, does not guarantee their safety for medicinal purposes. Most herbal products used in folk medicine have strong scientific evidence regarding their biological activities. However, the main obstruction to the use of herbal preparations is the lack of scientific and clinical data in support of better understanding of the efficacy and safety of drugs. Different toxicological study data like acute and subchronic on medicinal plants or their preparations should be obtained in order to increase the assurance of their safety in humans, particularly for use in the development of pharmaceuticals.^{1,2}

Abrus precatorius L. (family: Fabaceae), locally known as "Gunja" or "Rati", is indigenous to India and is also found in other tropical and subtropical areas of the world. It is a beautiful, perennial, deciduous, twining woody vine with herbaceous branches and pinnate leaves. The flowers are short stalked, white to pink, and are borne in clusters. Fruits are oblong pods that contain characteristic red seeds with a black mark at the hilum/base. After maturation, these open before falling and curl back to reveal seeds. Seeds are of uniform weight (0.1 g) and therefore were used in the past as standard weighing units by jewellers for weighing silver and gold.^{3,4} They are poisonous when taken internally and therefore are used after processing.^{5,6} A number of biochemical constituents have been reported from *A. precatorius* seeds. These are rich in amino acids (like serine, alanine, valine, choline, and methyl ester); proteins (abrin and *A. precatorius* agglutinin), carbohydrates (galactose, arabinose, and xylose), flavonoids (abectorin, dimethoxycentaureidin-7-o-rutinoside, and precatorin I, II, and III), anthocyanins (delphinindin, pelargonindin, and cyaniding), and alkaloids (dimethyl tryptophan, methocation, picatorine, abrine, hypaphorine, choline, and trigonelline). The seed proteins are rich in most of the essential amino acids, and they are deficient only in cystine and threonine. Moreover, various triterpenoids, steroids, and fatty acids have also been isolated from *A. precatorius* seeds.⁷⁻¹¹ The principle poisonous component of the seed is abrin, an albumotoxin.¹² The plant has been used for therapeutic purposes since ancient times. The most widespread use of *A. precatorius* seeds is in the treatment of eye infections and as a potential contraceptive.⁴ Dry seeds are powdered and taken one teaspoonful once a day for two days to cure worm infection. The seeds are considered purgative, emetic, aphrodisiac, diuretic, expectorant, refrigerant, vermifuge, febrifuge, laxative, and abortifacient. They are commonly used to cure leprosy, dysentery, jaundice, fainting, arthritis, paralysis, nervous disorders, ulcer, stiffness of the shoulder joints, tuberculosis, headache, diarrhea, sciatica, tetanus, rabies, convulsions, fever, cold, gastritis, snakebite, conjunctivitis, inflammations, and leucoderma in traditional and folk medicines. Hot water extract of seeds is taken orally to cure malaria. The seeds are nutritious and are eaten boiled in certain parts of India. Various African tribes use powdered seeds as oral contraceptives.^{8,13-18} Seeds of this

plant are also used to lower high blood pressure and relieve painful swellings. In veterinary medicine, seeds are used in the treatment of fractures.^{8,10} *A. precatorius* seeds are also reported to have anticancer,¹⁹ antifertility,⁴ antitumor, antispermatogenic, antibacterial,^{20,21} antidiabetic,²² antioxidant,²³ nephroprotective,²⁴ antiarthritic,²⁵ antimicrobial,¹⁹ and antimalarial activities.²⁶ Despite its popularity in folk medicine, its toxicity profile has not yet been explored. The present study was thus based on the subchronic toxicity of the methanol (70%) extract of *A. precatorius* seeds in Wistar albino rats. Subchronic toxicity tests were designed to examine the effects resulting from repeated exposure over a portion of the average life span of an experimental animal.

MATERIALS AND METHODS

Seed collection and authentication

Seeds of *A. precatorius* were collected from a local market in Bhopal, Madhya Pradesh, India. The seeds were authenticated by Dr. Zia-Ul-Hassan, Head of the Department, Govt. Saifia Science College, Bhopal, and a voucher specimen (reference no. 520/Bot/Saifia/2015) was deposited there for future reference. The seeds were cleaned and washed with distilled water in order to remove the impurities and were shade dried. The seeds were then coarsely powdered in a mixer grinder.

Preparation of methanol (70%) seed extract

Dried coarse powder of *A. precatorius* seeds (250 g) was defatted with petroleum ether and the marc remaining was extracted successively with methanol (70%) using cold maceration. The filtrate obtained was evaporated in a rotary evaporator under reduced pressure and was vacuum dried. The dried extract was packed in an air-tight container, labeled, and stored in a refrigerator (2-4°C) until needed for the experiment.

Ethical approval

The use of animals for the present study was reviewed and approved with approval reference no. PBRI/IAEC/PN-412 by the Institutional Animal Ethical Committee of Pinnacle Biomedical Research Institute (PBRI) Bhopal, Madhya Pradesh (Reg. No. 1283/PO/c/09/CPCSEA) and they were maintained as per the guidelines of the Committee for the Purpose of Control and Supervision of Experiments on Animals (CPCSEA) India.

Selection of animals

For the purpose of subchronic toxicity studies, adult Wistar albino rats weighing about 94-178 g of both sexes were used. The animals were obtained from the animal house of PBRI.

Maintenance of experimental animals

The animals were kept in properly numbered large polypropylene cages with a stainless steel top grill. They were maintained under standard laboratory conditions (24±2°C; 50±5% humidity; 12 hours light/12 hours dark cycle) with standard diet (Hindustan Lever, Mumbai, India) and water *ad libitum* and were acclimatized to the laboratory conditions for a week before starting the experiment. Paddy husk was used as bedding material and it was changed twice a week.

Preparation of test sample

A suspension was made in 0.1% carboxymethyl cellulose solution and administered orally to the animals. The administration was done by straight type oral feeding needle. Individual doses were calculated on the basis of animal weight.

Subchronic toxicity study

Experimental setup

In order to investigate the adverse effects of repeated daily exposure to methanol (70%) crude extract of *A. precatorius* seeds, a subchronic toxicity study was carried out as per Organisation for Economic Co-operation and Development guidelines 407.²⁷ To determine the dose-related toxic effects, doses of 200 mg/kg/day and 400 mg/kg/day body weight of crude seed extract of *A. precatorius* were administered for the experimental period of 28 days. Eighteen rats of each sex were randomized into three groups of six animals each. The animals were marked to permit individual identification. Group 1 was the control group and received orally normal saline. Group 2 and Group 3 were orally administered 200 mg/kg/day and 400 mg/kg/day body weight of crude methanol seed extract of *A. precatorius*, respectively.

Clinical signs and mortality

During the 28 days of the experimental period, all the animals were observed once daily for toxicity signs and mortality immediately after dosing and up to 4 h after dosing.

Weekly body weight

Individual body weights of rats were recorded initially and every week and the individual doses were adjusted according to body weight to maintain the target dose level for all experimental animals.

Weekly food and water consumption

Food and water consumption parameters were also taken into consideration during the study. Consumption of food and water was measured initially and weekly for each rat.

Blood sample collection

At the end of the experimental period, blood samples were collected under diethyl ether anesthesia from all animals through a retro-orbital plexus puncture using capillary tubes on day 29. The blood from each animal was collected in ethylenediaminetetraacetic acid (EDTA) and non-EDTA tubes to determine hematological and biochemical parameters, respectively. For biochemical analysis, the blood samples were allowed to coagulate for 30 min and the clear serum was separated by centrifuging at 3000-4000 rpm using a cooling microcentrifuge for 15 min. The serum was introduced into new tubes and stored at -20°C until analyzed.

Hematological investigations

The blood collected in EDTA-containing tubes was taken immediately for hematological investigation. The blood or hematological parameters were analyzed using an automated hematology analyzer (Procan Electronics, Model PE6800). The parameters included hemoglobin (HGB), red blood cell (RBC)

count, hematocrit (HCT), RBC distribution width, mean cell volume, mean cell HGB concentration (MCHC), white blood cell count, lymphocytes, granulocytes, platelet (PLT), PLT distribution width, mean PLT volume, and PLT large cell ratio.

Biochemical estimations

The effect of seed extract of *A. precatorius* on the activity of the serum biochemical enzymes was estimated calorimetrically. All the biochemical investigations were performed on an automated biochemical analyzer (Rapid, Model Star 21). The biochemical estimations evaluated were as follows:

- Kidney function tests: blood urea nitrogen, creatinine, uric acid,
- Liver function tests: total bilirubin, aspartate aminotransferase, alanine aminotransferase, alkaline phosphatase, total proteins,
- Lipid profile: total cholesterol, triglycerides (TG), high density lipoproteins, low density lipoproteins.

Gross pathology and relative organ weight

Following blood collection, the animals were anesthetized and dissected out. Immediately the liver, kidneys, heart, spleen, stomach, adrenal glands, duodenum, brain, colon, and lungs were excised, freed of fat, washed in cold saline, blotted with clean tissue paper, and observed for gross pathological changes. Then the organs were weighed in grams using a calibrated balance. The relative organ weight of each animal was then calculated as follows:

$$\text{Relative organ weight} = \frac{\text{Absolute organ weight}}{\text{Body weight of rat on sacrifice day}} \times 100$$

Histopathological examination

Defined samples of the liver, heart, kidneys, spleen, lungs, brain, stomach, and duodenum were collected for histological studies. The tissues were fixed immediately in 10% formalin for at least 24 h, dehydrated through a series of ethanol solutions, and embedded in paraffin. Then 4-5- μ m-thick sections were cut in a rotary microtome and were stained with hematoxylin and eosin for photomicroscopic observation. All histopathological changes were examined by a pathologist. The microscopic features of the organs of both treated groups were then compared with those of the control group.

Statistical analysis

All the experimental data collected from various subchronic parameters were statistically analyzed using SIGMA STAT-3.5 software and expressed as mean \pm standard deviation. ANOVA followed by the Bonferroni test was used for interpretation of data. $P < 0.05$ was considered significant.

RESULTS

Clinical changes and mortality

Daily administration of methanol (70%) seed extract of *A. precatorius* at both 200 mg/kg and 400 mg/kg for 28 days did not induce any evident symptom of toxicity in rats of either sex.

No deaths or evident clinical signs were observed in any groups during the study period.

Body weight changes

Oral administration of *A. precatorius* seed extract to experimental animals for 28 successive days caused no statistically significant changes in body weight compared with the control group (Figure 1).

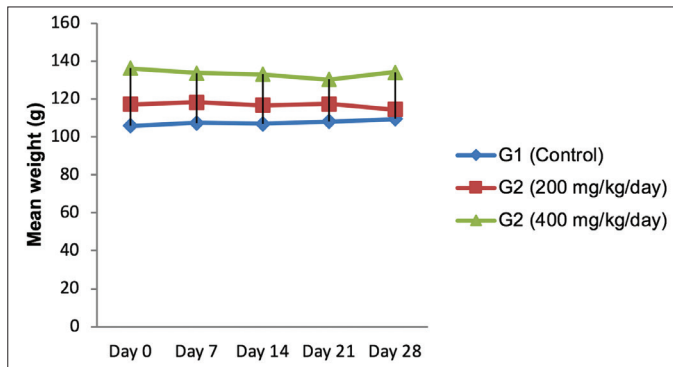


Figure 1. Changes in body weight of rats during the subchronic toxicity study

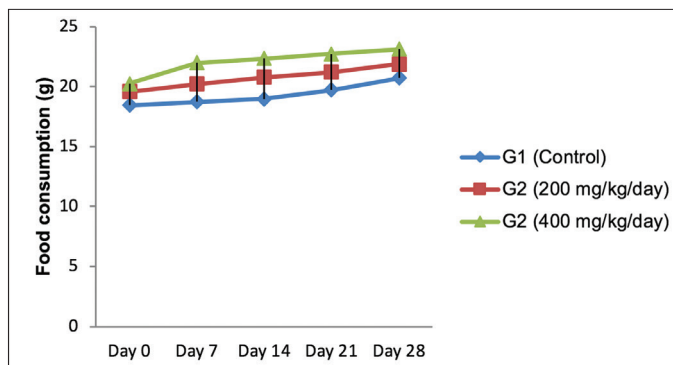


Figure 2. Changes in food consumption of rats during the subchronic toxicity study of methanol (70%) seed extract of *Abrus precatorius*

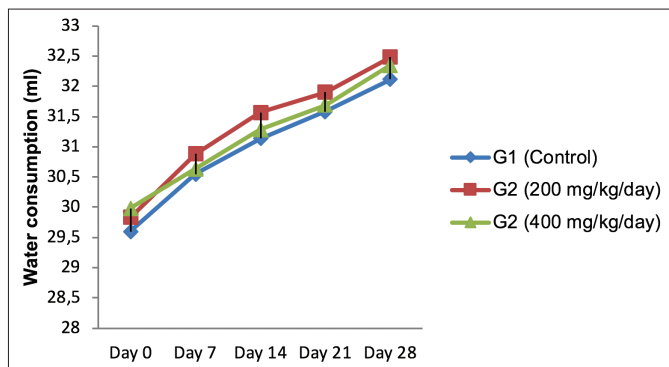


Figure 3. Changes in water consumption of rats during the subchronic toxicity study of methanol (70%) seed extract of *Abrus precatorius*

Food and water consumption changes

Oral administration of extract at 200 and 400 mg/kg body weight for 28 days caused no significant alterations in these indices compared to the control group (Figures 2 and 3).

Hematological effects

The seed extract at both the investigated dose levels had a good hematological tolerance. Hematological parameters of extract-treated rats were not significantly different from those of the control group. Hematological parameters of the test groups and the control group are presented in Table 1.

Biochemical changes

A study of biochemical parameters showed that the seed extract of *A. precatorius* did not induce any harmful biochemical effects in the experimental animals. No significant alterations were observed in the serum concentrations of renal markers, hepatic markers, or lipid profile of extract-treated animals. The results of the biochemical analysis are summarized in Table 2.

Gross pathology and relative organ weight changes

Gross pathology of the liver, kidneys, heart, spleen, stomach, adrenal glands, duodenum, brain, colon, and lungs of treated rats did not show abnormalities in terms of color or texture as compared to the controls. In this study, the relative organ weight of each organ recorded in the treatment groups did not show a significant difference compared to the controls. Relative organ weights of all three groups are shown in Table 3.

Histopathological changes

The light microscopy examinations of the selected organs (heart, liver, lungs, kidneys, spleen, stomach, intestines, and brain) of the extract-treated groups and the control group are shown in Figure 4. The histopathological examination showed normal cytoarchitecture and absence of any gross pathological lesion in the organs of the control as well as the extract-treated rats.

DISCUSSION

Plants provide a wide variety of biochemical components useful to mankind. These substances can be extracted and used in the preparation of drugs or the plant itself can be used directly as a medication.²⁸ However, the main obstacle to the use of traditional herbal plants is the lack of proper clinical and scientific data in support of the safety of drugs. Plants contain some toxic substances and it is better to evaluate them according to standard procedures and their effects on different parameters in order to establish the safety of the plants.²⁹ Toxicity tests are carried out effectively on either rats or mice due to their availability and low cost and the wealth of toxicology data in the literature already available for these species.³⁰ Considering the numerous reported therapeutic potentials of *A. precatorius* seeds as an alternative medicine effective for various diseases, a safety profile was established through a subchronic toxicity study, as a guide for the management of its application and usage in herbal preparations. This study will serve to prevent exposing humans to potential toxicity-related health risks while using *A. precatorius* seeds.

Table 1. Effect on hematological parameters of rats administered with methanol (70%) seed extract of *Abrus precatorius*

Hematological parameters	Group 1 (Control)	Group 2 (200 mg/kg/day)	Group 3 (400 mg/kg/day)
Erythrocyte indices			
HGB (g/dL)	11.6833±0.99401	11.4167±0.78191	10.8067±0.50006
RBC (×10 ⁶ /μL)	6.495±0.34827	6.135±0.59779	5.73833±0.87959
HCT (%)	33.0333±11.56484	24.2667±6.294619	20.63333±7.247912
RDW (fL)	39.16667±2.361967	34.8333±4.399021	35.4±4.642916
MCV (fL)	59.6±2.442676	55.06667±4.454461	55.13333±1.966949
MCHC (g/dL)	30.73333±4.006106	37.23333±2.910708	36.69833±5.43031
Thrombocyte indices			
PLT (×10 ⁶ /μL)	164.666±30.4119	249.666±127.853	279.5±146.459
PDW (%)	9.066667±0.827983	9.23333±0.696818	8.7±1.001665
MPV (fL)	9.716667±1.439232	9.716667±0.982203	8.28333±1.166786
P-LCR (%)	20.03333±5.948856	20.68333±2.319064	18.46667±2.1723
Leucocyte indices			
WBC (×10 ⁶ /μL)	4.71666±3.92785	3.21666±1.66675	5.69833±2.40555
LYM (×10 ⁶ /μL)	3.1±2.20605	1.71666±0.43365	3.05±1.16868
LYM (%)	71.2±13.27717	61.23333±15.20961	55.05±8.147137

HGB: Hemoglobin, RBC: Red blood cell count, HCT: Hematocrit, RDW: Red blood cell distribution width, MCV: Mean cell volume, MCHC: Mean cell hemoglobin concentration, PLT: Platelet, PDW: Platelet distribution width, MPV: mean platelet volume, P-LCR: Platelet large cell ratio, WBC: White blood cell count, LYM: Lymphocytes, values are expressed as mean ± standard deviation of six animals

Table 2. Effect on serum biochemical parameters of rats administered methanol (70%) seed extract of *Abrus precatorius*

Parameter	Group 1 (Control)	Group 2 (200 mg/kg/day)	Group 3 (400 mg/kg/day)
Renal markers			
BUN (mg/dL)	15.07667±2.22464	14.38183±6.688322	15.72833±3.021062
Creatinine (mg/dL)	0.72533±0.15052	0.73833±0.18193	0.7675±0.114176
Uric acid (mg/dL)	2.461833±0.427353	3.426167±1.670978	3.0385±1.280693
Hepatic markers			
Total protein (g/dL)	5.509667±0.500666	7.0215±1.125476	6.672±2.130268
Total bilirubin (mg/dL)	0.23645±0.64627	0.26395±0.17536	0.29115±0.088835
ALP (IU/L)	157.6767±33.2871	168.4167±31.08203	165.5667±20.95387
AST (IU/L)	167.1333±31.34372	172.6322±23.588	164±13.46601
ALT (IU/L)	39.673±9.803	47.595±9.872	51.55333±10.47761
Lipid profile			
Total cholesterol (mg/dL)	44.09667±7.449652	49.15833±12.1925	42.51333±4.353549
Triglycerides (mg/dL)	52.765±54.1075	58.12833±8.903721	50.46±10.90015
HDL (mg/dL)	48.59333±5.753485	49.58±12.66136	43.44±10.9195
LDL (mg/dL)	22.3919±5.490329	21.6345±5.390373	20.42133±6.257871

BUN: Blood urea nitrogen, AST: Aspartate aminotransferase, ALT: Alanine aminotransferase, ALP: Alkaline phosphatase, HDL: High density lipoproteins, LDL: Low density lipoproteins, values are expressed as mean ± standard deviation of six animals

Subchronic toxicity was tested with repeated administration of 200 mg/kg body weight and 400 mg/kg body weight of methanol (70%) seed extract of *A. precatorius*, and its effects in terms of clinical signs, bodyweight, food and water consumption, gross pathology and organ weight, hematological and biochemical parameters, and histopathology were noted.

Mortality, behavioral signs, body weight, and food consumption are very sensitive indicators to assess the toxicity of a substance.³¹ In the present study, all the test animals were physically active during the test period. There were no signs of toxicity or mortality in rats treated with the extract. The lack of significant changes in body weight, food intake, or

Table 3. Effect on relative organ weight of rats administered methanol (70%) seed extract of *Abrus precatorius*

Organ name	Control	200 mg/kg/day	400 mg/kg/day
Liver	3.360333±0.202464	3.342167±0.160833	3.601167±0.22121
R. Kidney	0.5415±0.031154	0.530833±0.042148	0.524167±0.035611
L. Kidney	0.511667±0.018696	0.500333±0.034238	0.524167±0.035611
Heart	0.425333±0.055733	0.473333±0.052908	0.482667±0.074033
Spleen	0.437167±0.054066	0.374333±0.072304	0.497667±0.047971
Stomach	1.135333±0.083194	1.010333±0.136626	0.963833±0.145387
Adrenal glands	0.0375±0.007588	0.033±0.00611	0.0295±0.006922
Duodenum	0.8595±0.211821	0.9065±0.111439	0.754333±0.125298
Brain	1.293±0.192562	1.3015±0.125279	1.127333±0.071818
Colon	0.4825±0.179648	0.635833±0.151786	0.657333±0.082265
Lungs	1.074167±0.070416	1.0225±0.21034	1.040333±0.181494

Values are expressed as mean ± standard deviation of six animals

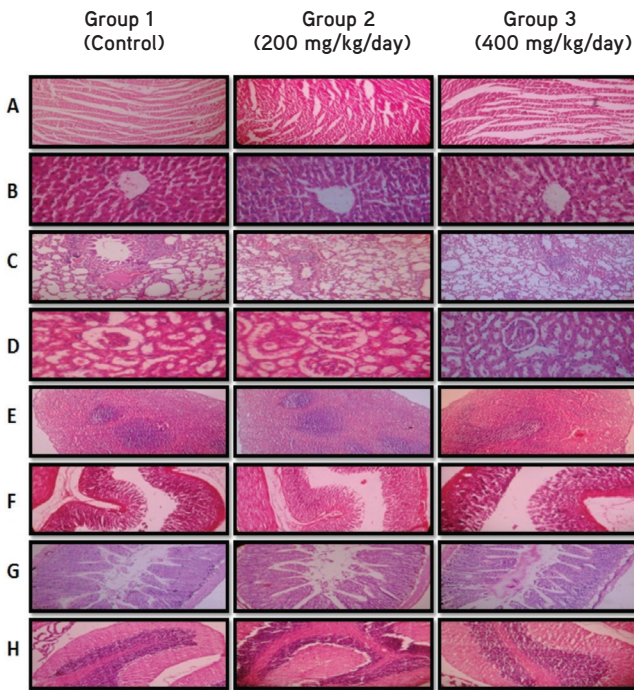


Figure 4. Effect of methanol (70%) seed extract of *A. precatorius* on various rat organ histomorphologies in the subchronic toxicity study (A: Heart, B: Liver, C: Lungs, D: Kidneys, E: Spleen, F: Stomach, G: Intestines, H: Brain)

water consumption of the treated animals also indicates the nontoxicity of the extract.

According to a previous report, the hematopoietic system is one of the most sensitive targets for toxic substances.³² Hematological analysis easily detects the abnormalities in body metabolic processes and reveals very important information about the response of the body to injury, deprivation, and/or stress.³⁰ However, in the present study the mean value of each parameter was within the normal limits and this further supports the nontoxic nature of the extract.

The biochemical investigation showed that no significant modifications of assessed parameters occurred in the rats. The levels of enzymes in the liver and kidneys of all groups of rats stayed within normal ranges, which demonstrated that the test extract had no membrane-labilizing effect on these organs. Enzyme activities in tissues are mostly employed as markers to ascertain early toxic effects of substances administered to experimental animals. Alterations in the lipid profile also show the efficacy and safety of plant extracts. Any deviation in the concentration of lipids can provide information on the status of lipid metabolism as well as the predisposition of animals to atherosclerosis.³³ Cholesterol and TG are the lipid parameters associated with coronary artery diseases and are usually used to ascertain hyperlipidemic conditions.³⁴ In the present study, the normal restoration of lipid parameters in the serum levels of extract-treated rats not only indicates the nontoxic nature of the extract, but also implies that the tested extract may not dispose the animals to cardiovascular risk.

Analysis of organ weight in toxicology studies is an important endpoint for identification of potentially harmful effects of chemicals. A main requirement in toxicological experiments is the ability to assess the effects of xenobiotics on specific organs.³⁵ In the present study, no changes were observed in the gross examination of the organs of treated animals when compared to the control group. The relative organ weight of the liver, kidneys, heart, spleen, stomach, adrenal glands, duodenum, brain, colon, and lungs recorded in the treatment groups did not show a significant difference compared to the control group. This may imply that the extract did not alter the secretory ability of the organs. It is also possible that the extract did not cause any cellular constriction or inflammation of the organs, which would have resulted in a decrease or increase in their weight, respectively.

Histopathological examination of the selected organs provides information to strengthen the findings of hematological and biochemical parameters. Microscopic examinations of sections

of the heart, liver, lungs, kidneys, spleen, stomach, intestines, and brain of all groups revealed no detectable abnormalities.

CONCLUSIONS

Following subchronic treatment, the methanol (70%) seed extract of *A. precatorius* was well tolerated and produced no toxicity signs, lethality, impairments in body and organ weights, or changes in food or water consumption. The extract also produced no signs of hepatotoxicity, nephrotoxicity, or hematotoxicity or detectable abnormalities in the lipid profile or histology of internal organs. Generally, all the values remained within the normal limits and did not suggest toxic effects in subchronic treatment. The present study, therefore, demonstrates the nontoxic nature of the test extract and thus 200 and 400 mg/kg doses may be used in phytomedicine formulations with a low risk of adverse effects. However, further investigations such as to determine its effect in pregnant animals as well as trials in other animals towards the development of drugs from *A. precatorius* should be performed to test its claimed traditional therapeutic value.

Conflict of Interest: No conflict of interest was declared by the authors.

REFERENCES

- Yuet Ping K, Darah I, Chen Y, Sreeramanan S, Sasidharan S. Acute and subchronic toxicity study of *Euphorbia hirta* L. methanolic extract in rats. *Bio Med Res Int*. 2013;2013:182064.
- Sathya M, Kokilavani R, Ananta TKS. Acute and sub-acute toxicity studies of ethanolic extract of *Acalypha indica* Linn. in male Wistar albino rats. *Asian J Pharm Clin Res*. 2012;5(Suppl 1):97-100.
- Shourie A, Kalra K. Analysis of phytochemical constituents and pharmacological properties of *Abrus precatorius* L. *Int J Pharma Bio Sci*. 2013;4:91-101.
- Jahan S, Saeed N, Ijlal F, Khan MA, Ahmad M, Zafar M, Abbasi AM. Histomorphological study to evaluate anti-fertility effect of *Abrus precatorius* L. in adult male mice. *J Med Plants Res*. 2009;3:1021-1028.
- Acharya R, Roy S. A review on therapeutic utilities and purificatory procedure of Gunja (*Abrus precatorius* Linn.) as described in Ayurveda. *J AYUSH*. 2013;2:1-11.
- Chowdhury SR, Sharmin T, Hoque M, Das SM, Das M, Nahar F. Evaluation of Thrombolytic and membrane stabilizing activities of four medicinal plants of Bangladesh. *Int J Pharm Sci Res*. 2013;4:4223-4227.
- Tilwari A, Shukla NP, Pathirissery UD. Immunomodulatory activity of the aqueous extract of seeds of *Abrus precatorius* Linn (Jequirity) in mice. *Iran J Immunol*. 2011;8:96-103.
- Bhatia M, Siddiqui NA, Gupta S. *Abrus precatorius* (L.): An evaluation of traditional herb. *Indo Am J Pharm Res*. 2013;3:3295-3315.
- Garaniya N, Bapodra A. Ethano botanical and phytopharmacological potential of *Abrus precatorius* L.: A review. *Asian Pac J Trop Biomed*. 2014;4:27-34.
- Patil A, Vadera K, Patil D, Phatak A, Chandra N. Phytochemical analysis, in-vitro anticancer activity and HPTLC fingerprint profile of seeds of *Abrus precatorius* L. *Int J Pharm Sci Rev Res*. 2015;33:262-269.
- Tabasum S, Khare S, Jain K. Spectrophotometric quantification of total phenolic, flavonoid and alkaloid contents of *Abrus precatorius* L. seeds. *Asian J Pharm Clin Res*. 2016;9:371-374.
- Arora A. Anti-oogenic evaluation of seed extract of *Abrus precatorius* L. in swiss albino mice. *Int Res J Biol Sci*. 2013;2:27-30.
- Singh RB, Shelly. Polysaccharide structure of degraded glucomannan from *Abrus precatorius* Linn. seeds. *J Environ Biol*. 2007;28(2 Suppl):461-464.
- Upadhyay S, Ghosh AK, Singh V. Anti-lice activity of *Abrus precatorius* Linn (FAM-Fabaceae) seed oil. *Egypt Dermatol Online J*. 2011;7:4.
- Verma D, Tiwari SS, Srivastava S, Rawat AKS. Pharmacognostical evaluation and phytochemical standardization of *Abrus precatorius* L. seeds. *Nat Prod Sci*. 2011;17:51-57.
- Chaudhari KS, Sharma R, Pawar PS, Kashikar VA. Pharmacological activities of *Abrus precatorius* Linn.- A review. *Int J Ayur Herb Med*. 2012;2:336-348.
- Rajani A, Hemamalini K, Begum SKA, Spandana KVLD, Parvathalu, Gowtham B. Antimicrobial activity and phytochemical study of ethanolic seed extract of *Abrus precatorius* Linn. *J Biol Today's world*. 2012;1:23-28.
- Sivakumar R, Ravikumar K. Wound healing activity of two different forms of *Abrus precatorius* L. *Int J Res Eng Biosci*. 2013;1:39-53.
- Anbu J, Ravichandiran V, Sumithra M, Chowdary BS, Kumar KS, Kannadhasan R, Kumar S. Anticancer activity of petroleum ether extract of *Abrus precatorius* on Ehrlich Ascitis carcinoma in mice. *Int J Pharm Bio Sci*. 2011;2:24-31.
- Mistry K, Mehta M, Mendpara N, Gamit S, Shah S. Determination of antibacterial activity and MIC of crude extract of *Abrus precatorius* L. *Adv Biotech*. 2010;10:25-27.
- Bobbarala V, Vadlapudi V. *Abrus precatorius* L. seed extracts antimicrobial properties against clinically important bacteria. *Int J PharmTech Res*. 2009;1:1115-1118.
- Monago CC, Alumanah EO. Antidiabetic effect of chloroform-methanol extract of *Abrus precatorius* Linn seed in Alloxan diabetic rabbit. *J Appl Sci Environ Manage*. 2005;9:85-88.
- Pal RS, Ariharashivakumar G, Girhepunje K, Upadhyay A. *In vitro* antioxidative activity of phenolic and flavonoid compounds extracted from seeds of *Abrus precatorius*. *Int J Pharm Pharm Sci*. 2009;1:136-140.
- Ligha A, Jaja B, Numbere NF. Protective effect of *Abrus precatorius* L. seed extract following alcohol induced renal damage. *Eur J Sci Res*. 2009;25:428-436.
- Sudaroli M, Chatterjee TK. Evaluation of red and white seed extracts of *Abrus precatorius* Linn. against Freund's complete adjuvant induced arthritis in rats. *J Med Plants Res*. 2010;1:86-94.
- Saganuwan SA, Onyeyili PA, Ameh EG, Etuk EU. *In vivo* antiplasmodial activity by aqueous extract of *Abrus precatorius* in mice. *Rev Latinoamer Quim*. 2011;39:32-44.
- OECD. Guidelines for testing of chemicals/No. 407: Repeated dose oral toxicity test method, Organization for Economic Co-operation and Development, Paris; France; 2008.
- Tabasum S, Khare S. Safety of medicinal plants: An important concern. *Int J Pharma Bio Sci*. 2016;7:237-243.
- Shafi S, Tabassum N. Hepatic and hematological activities of hydro-alcoholic extract of *Eriobotrya japonica* fruits in Swiss albino mice. *Int J Pharma Bio Sci*. 2015;6:643-654.

30. Tan PV, Mezui C, Enow-Orock G, Njikam N, Dimo T, Bitolog P. Teratogenic effects, acute and sub-chronic toxicity of the leaf aqueous extract of *Ocimum suave* wild (Lamiaceae) in rats. *J Ethnopharmacol.* 2008;115:232-237.
31. Kebede S, Afework M, Debella A, Ergete W, Makonnen E. Toxicological study of the butanol fractionated root extract of *Asparagus africanus* Lam., on some blood parameter and histopathology of liver and kidney in mice. *BMC Res Notes.* 2016;9:49.
32. Goudah A, Abo-El-Sooud, Yousef MA. Acute and sub-chronic toxicity assessment model of *Ferula assa-foetida* gum in rodents. *Vet World.* 2015;8:584-589.
33. Sairam K, Priyambada S, Aryya NC, Goel RK. Gastroduodenal ulcer protective activity of *Asparagus racemosus*: an experimental, biochemical and histological study. *J Ethnopharmacol.* 2003;86:1-10.
34. Saibu S, Ashafa OT. Toxicological implications and laxative potential of ethanol root extract of *Morella serrata* in loperamide-induced constipated Wistar rats. *Pharm Biol.* 2016;54:2901-2908.
35. Umana UE, Timbuk JA, Musa SA, Asala S, Hambolu J, Anuka JA. Acute and chronic hepatotoxicity and nephrotoxicity study of orally administered chloroform extract of *Carica papaya* seeds in adult Wistar rats. *Int J Sci Res Publ.* 2013;3:1-8.



Is There an Association Between Extreme Levels of Boron Exposure and Decrease in Y:X Sperm Ratio in Men? Results of an Epidemiological Study

Erkeklerde Y:X Sperm Oranındaki Azalma ile Aşırı Düzeyde Bor Maruziyeti Arasında Bir İlişki Var mıdır? Epidemiyolojik Çalışma Sonuçları

© Can Özgür YALÇIN, © Aylın ÜSTÜNDAĞ, © Yalçın DUYDU*

Ankara University, Faculty of Pharmacy, Department of Toxicology, Ankara, Turkey

ABSTRACT

Objectives: A negative association between Y:X sperm ratio and high levels of boron exposure was suggested in an epidemiological study conducted in boron mining areas of China. That study, however, was criticized by many authors due to some weaknesses in the study design. The present epidemiological study was designed to corroborate or refute the above-mentioned negative association between boron exposure and Y:X sperm ratio in men.

Materials and Methods: The study was conducted in a boric acid production zone in Bandırma. One hundred sixty-three male workers voluntarily participated in our study. The workers employed in the boric acid production facilities were assigned as the exposed workers (n=86). The control group was composed of workers employed in the steam power plant, energy supply unit, demineralized water plant, mechanical workshop, etc. (n=77). Blood and semen samples were sampled from the participating workers at the end of the work shift. Y:X sperm ratio in semen samples was determined by fluorescence *in situ* hybridization. Boron concentrations in semen and blood samples were determined using inductively coupled plasma-mass spectrometry.

Results: Boron-mediated adverse effect on the Y:X sperm ratio was not determined in workers in our study even under extreme occupational exposure conditions. The results of our study refute the negative association between Y:X sperm ratio and high levels of boron exposure that was suggested in a previously published epidemiological study conducted in boron mining areas of China.

Conclusion: The results of our study indicate that boron-mediated adverse effects on the Y:X sperm ratio do not seem possible even under occupational boron exposure conditions.

Key words: Boron exposure, blood boron concentration, semen boron concentration, FISH, Y:X sperm ratio

ÖZ

Amaç: Çin'in bor madenciliği yapılan bölgesinde yürütülmüş olan bir epidemiyolojik çalışma sonucunda, erkeklerin Y:X sperm oranı ile yüksek seviyedeki bor maruziyeti arasında negatif bir ilişki olduğu belirtilmiştir. Ancak bu çalışma, çalışmanın tasarımındaki bazı zayıflıklar nedeni ile pek çok bilim insanı tarafından eleştirilmiştir. Bu çalışma, yukarıda söz edilmiş olan erkeklerin Y:X sperm oranı ile yüksek seviyedeki bor maruziyeti arasında negatif bir ilişki olduğu iddiasını doğrulamak ya da çürütmek amacıyla yapılmıştır.

Gereç ve Yöntemler: Bu çalışma Bandırma borik asit üretimi yapılan bölgede gerçekleştirilmiştir. Bu çalışmaya 163 erkek işçi gönüllü olarak katılmıştır. Borik asit üretim tesislerinde istihdam etmekte olan işçiler maruziyet grubu olarak tanımlanmışlardır (n=86). Kontrol grubu ise, buhar santrali, enerji tedarik ünitesi, demineralize su ünitesi, mekanik atölye gibi iş kollarında çalışan işçilerden oluşturulmuştur (n=77). Vardiya sonlarında çalışmaya katılan işçilerden kan ve meni örnekleri alınmıştır. Erkeklerdeki Y:X sperm oranları floresan *in situ* hibridizasyon tekniği ile tespit edilmiştir. Kan ve meni örneklerindeki bor konsantrasyonları indüktif eşleşmiş plazma-kütle spektrometresi ile tayin edilmiştir.

Bulgular: Olağanüstü mesleki maruziyet koşulları altında bile bor maruziyetine bağlı olarak işçilerde Y:X sperm oranlarında olumsuz bir etki gözlenmemiştir. Bizim çalışmamızdan elde etmiş olduğumuz sonuçlar, Y:X sperm oranı ile yüksek seviyedeki bor maruziyeti arasındaki negatif ilişkiyi reddetmektedir.

Sonuç: Bizim çalışmamızdan elde etmiş olduğumuz sonuçlar, ağır mesleki bor maruziyeti koşulları altında bile bor maruziyetinin erkeklerde Y:X sperm oranları üzerinde olumsuz bir etkisinin olmadığını göstermektedir.

Anahtar kelimeler: Bor maruziyeti, kan bor konsantrasyonu, meni bor konsantrasyonu, FISH, Y:X sperm oranı

*Correspondence: E-mail: duydu@pharmacy.ankara.edu.tr, Phone: +90 312 203 31 18 ORCID-ID: orcid.org/0000-0001-7482-086X

Received: 02.06.2018, Accepted: 26.06.2018

©Turk J Pharm Sci, Published by Galenos Publishing House.

INTRODUCTION

Boric acid and borates are classified as toxic to reproduction under "Category 1B" with the hazard statement of "H369 FD" in the European Regulation on Classification, Labelling and Packaging of Substances and Mixtures.¹ The scientific background of this classification is based on the results of animal experiments (hazard assessment). In fact, the boron concentrations tested in animal experiments were too high and from this point of view these dose levels were not relevant to humans. Nevertheless, this classification triggered epidemiological studies in areas of high boron exposure in order to assess the risk of the daily boron exposure levels in those areas. The first study was conducted in mining areas located in Kuandian City, China.² The blood boron concentration reported in that study was 499.2 ± 790.6 (20.4-3568.9) ppb. In spite of this extreme level of boron exposure the reproductive toxicity biomarkers reported in that study did not indicate adverse effects on male reproduction. The second comprehensive epidemiological study was conducted by our study group in workers employed in Bandırma boric acid production plant. The mean blood boron concentration of the high exposure group in our study was 223.89 ± 69.49 (152.82-454.02) ng/g and no boron-mediated unfavorable effects on reproductive toxicity parameters of male workers were observed.^{3,4} The results of our study were in agreement with those of the study conducted in China. Accordingly, both studies clearly indicate that boron-mediated adverse effects on male reproduction do not seem possible even under extreme occupational exposure conditions. However, in 2008 Robbins et al.⁵ reported a boron-mediated decrease in Y:X sperm ratio in workers residing in mining areas of Kuandian City. Essentially, a boron-mediated decrease in Y:X sperm ratio was not observed in earlier epidemiological studies or even in animal experiments. Therefore, the results of the study published by Robbins et al.⁵ had to be verified by an epidemiological study. The major aim of the present epidemiological study was to corroborate or refute the negative association between the high level of boron exposure and the decrease in the Y:X sperm ratio in men suggested by Robbins et al.⁵

MATERIALS AND METHODS

The blood and semen samples were sampled in accordance with the study protocols approved by the Ethics Committee of Hacettepe University School of Medicine (HEK 08/167, date: 22/10/2008). All participants gave their informed consent prior to participation in the project.

Sampling procedure

The present study was performed using the blood and semen samples obtained within the scope of our "Boron Project - I", which was completed in 2010.^{3,4} The "Boron Project - I" was conducted in Bandırma boric acid production zone and 204 workers were enrolled in that study. After the project was completed, the remaining semen samples were stored under appropriate conditions (cryopreserved in liquid nitrogen). The total number of remaining semen samples was 163 and 86 of

them were from workers employed in the boric acid production facilities and were assigned as the samples of the exposed group of workers. The rest of the semen samples, from workers employed in the steam power plant, energy supply unit, demineralized water plant, mechanical workshop etc., were assigned as the control samples (n=77). The demographic information, blood boron concentrations, semen boron concentrations, and sperm concentrations of these 163 workers had been gathered within the scope of the "Boron Project - I". More detailed information about the samples and the sampling area were provided in our previously published studies.^{3,4}

Boron analysis

Blood and semen samples were analyzed by inductively coupled plasma mass spectrometry with a flow injection system. A special sample introduction system that included a perfluoroalkoxy spray chamber and a nebulizer with an alumina injector tube in a quartz torch was used for this study. The details of the above-mentioned analyses were published in our previous study.³

Sperm analysis

The semen samples were sampled and analyzed in accordance with the recommendations of the World Health Organization.⁶ Sperm concentrations were determined in fresh semen samples using an SQA-V Gold Sperm Quality Analyzer. The results were expressed as 10^6 sperm cells/mL.

Determination of Y:X sperm ratios

Y- or X-bearing sperm cells in semen samples were detected using fluorescence *in situ* hybridization (FISH). The Cytocell FAST FISH prenatal X, Y, and 18 Enumeration Probe Kit (LPF 002) was used in the detection and quantification of chromosomes X, Y, and 18 by FISH. The probes are specific for the alpha satellite DNA sequences in the DXZ1, DYZ3, and D18Z1 regions of chromosomes X (green), Y (orange), and 18 (blue), respectively.

The semen samples were removed from the liquid nitrogen, thawed at room temperature in PBS solution, and centrifuged in an appropriate centrifuge tube at $500 \times g$ for 5 min as the initial step of the procedure. The supernatant was gently discarded and the precipitated sperm cells were used in sperm FISH analysis. The cells were resuspended in 10 mL of 0.075 M KCl and left at 37°C for 1 h. After centrifugation for 5 min at 1000 rpm the supernatant was discarded and the precipitated sperm cells were resuspended in 5 mL of (4°C) Carnoy's solution. The cell suspension was centrifuged again for 5 min at 1000 rpm. This process was repeated 3 times. Afterwards, a sufficient amount of these sperm cells was transferred directly onto the slide and allowed to dry at room temperature. The slides then were washed in $2 \times$ saline-sodium citrate (SSC) (3 min), 70% ethanol (3 min), 85% ethanol (3 min), and finally in 100% ethanol (3 min). The slides and the probe were prewarmed on a 37°C hotplate for 10 min. A sufficient amount of probe mixture (10 μ L) was pipetted onto the sperm cells and coverslipped. The slides were placed on a hotplate at 75°C for 5 min for denaturation. Afterwards the slides were transferred into a humid and dark (lightproof)

incubator at 37°C for ~18 h (overnight) for hybridization. After the waiting period, the coverslips were removed and the slides were immersed into 0.4 × SSC at 67°C for 30 s. The washing process continued with 2 × SSC + Tween-20 (room temperature) again for 30 s. The slides were left to drain. Next, 15 µL of DAPI antifade was applied onto each hybridization area, which was then covered with a coverslip. The slides were left in the dark for 15 min to allow color development. Afterwards the slides were viewed under a fluorescence microscope. The sperm cells were analyzed via fluorescence microscopy using a Leica DM1000 microscope with DAPI, AQUA, G/R filters. Leica provided a suitable set-up for simultaneous visualization of DAPI and the triple fluorochromes (spectrum green, orange, and aqua). A total of 5000 morphologically preserved sperm cells were counted per sample by one experienced scorer. The microscopic images of some sperm cells are shown in Figure 1.

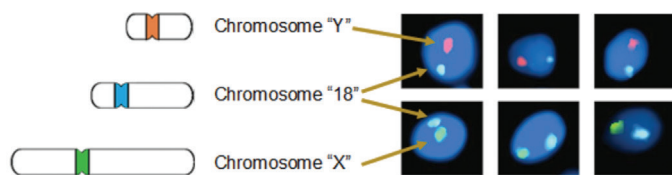


Figure 1. Left illustrations: Probe specifications: “X” centromere, Xp11.1-q11.1 (DXZ1) green; “Y” centromere, Yp11.1-q11.1 (DYZ3) orange; “18” centromere, 18p11.1-q11.1 (D18Z1) blue. Right illustrations: Microscopic sperm images after applying fluorescence *in situ* hybridization. The existence of green and blue dots in sperm cells means that the sperm cell contains chromosomes X and 18 (internal standard). The existence of orange and blue dots in sperm cells means that the sperm cell contains chromosomes Y and 18 (internal standard)

Statistical analysis

The Kruskal-Wallis and Wilcoxon Mann-Whitney U tests were used to analyze some of the variables in Table 1. The statistical significance between the number of girls and boys (at birth) was analyzed using the χ^2 test. Box plots (Figure 2), Pearson’s correlation coefficient, and linear regression (Figure 3) show the empirical distribution and possible linear dependencies.

All statistical tests were performed with IBM SPSS Statistics Version 23. The significance levels of the tests were set at 0.05.

RESULTS

The study population was composed of control (n=77) and exposed (n=86) groups of workers employed in Bandırma boric acid production zone. The “ages” and “years of employment” of the workers did not differ significantly between the control and exposed groups as shown in Table 1. The participating workers were healthy and were not taking any medication during the sampling period.

The mean blood boron concentration of the exposed group (141.55 ng B/g blood) was significantly higher ($p < 0.05$) than that of the control group (63.56 ng B/g blood) (Table 1, Figure 2). This significant difference between the control and exposed groups supports the high level of daily boron exposure for the workers assigned to the exposed group. This finding was also

Table 1. Characteristics of male workers assigned to the control and exposed groups

Parameters	Control group, n=77	Exposed group, n=86	p value
Age	42.86±5.06 (33-48)	42.45±4.61 (33-48)	$p > 0.05$
Years of employment	18.02±6.58 (2-23)	15.76±7.16 (1.62-22)	$p > 0.05$
Sperm concentration ($\times 10^6/\text{mL}$)	68.08±41.37 (9.69-139.21)	64.96±56.09 (11.06-161.98)	$p > 0.05$
Blood boron conc., ng B/g blood	63.56±43.89 (21.45-134.57)	141.55±80.43 (41.28-286.30)	$p < 0.05$
Semen boron conc., ng B/g semen	1127.78±1713.96 (66.4-5115.6)	1703.42±1895.09 (452.60-7067.85)	$p < 0.05$
Y:X sperm ratio	0.99±0.03 (0.94-1.01)	0.99±0.02 (0.96-1.01)	$p > 0.05$
Fathered children	136 (1.77)*	150 (1.74)*	$p > 0.05$
Girls (at birth)	70 (0.91)*	69 (0.80)*	$p > 0.05$
Boys (at birth)	66 (0.86)*	81 (0.94)*	$p > 0.05$
Girls % (at birth)	51.47	46.00	$p > 0.05$

The results are given as mean ± standard deviation (5th-95th), *mean values

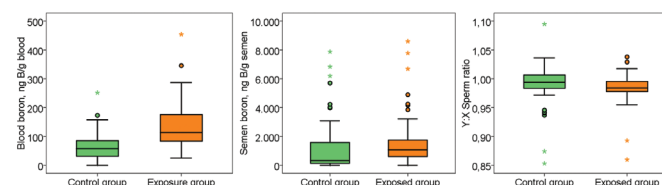


Figure 2. Box-plot graphs of boron concentrations in blood and semen samples of the control and exposed groups are shown in the first two charts. The distribution of Y:X sperm ratio in the control and exposed groups is shown in the rightmost chart

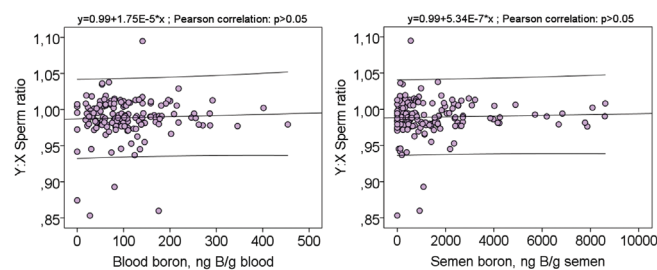


Figure 3. Linear regressions and correlations between blood/semen boron concentrations and Y:X sperm ratios

supported by the semen boron concentrations of workers. The mean semen boron concentrations of the control and exposed groups were significantly different ($p < 0.05$) from each other and thereby provided additional support for the extraordinary daily boron exposure conditions in our study population (Table 1).

The high level of boron exposure in the exposed group of workers did not adversely affect the sperm concentrations

or Y:X sperm ratios of workers as shown in Table 1 and Figure 2. This finding is also supported by the lack of statistically significant correlation (Pearson, $p > 0.05$) between blood/semen boron concentrations and Y:X sperm ratios in workers (Figure 3). Boron-mediated effects on the sex ratio at birth were also investigated within the scope of this study. However, no shift in the sex ratio at birth toward females was observed. As shown in Table 1, the percentage of girls at birth in the exposed group was not significantly higher than that in the control group ($p > 0.05$).

DISCUSSION

Some earlier studies performed on the relation between boron exposure and sex ratio at birth reported an excess of female offspring in highly boron exposed populations. In spite of an increase in female offspring, the increase was not statistically significant in these previously published studies.⁷⁻⁹ In 2008, however, Robbins et al.⁵ reported a statistically significant relation between boron exposure and Y:X sperm ratio in male workers employed in a boron mining company in Kuandian City, China. The authors reported a significant association between a high level of boron exposure and a decrease in Y-bearing versus X-bearing sperm cells. Moreover, the excess of female offspring around the boron mining area in Kuandian City (China) was attributed to the decrease in the Y:X sperm ratios in highly boron exposed men.⁵ Although the results of that study were criticized by some authors due to weaknesses in the study design, a study confirming or rejecting the results of this study has not been performed thus far.¹⁰ Therefore, the major aim of the present study was to corroborate or refute the results reported by Robbins et al.⁵

The Bandırma boric acid production zone is a suitable place for investigating boron-mediated unfavorable effects on the Y:X sperm ratios in men. This study area provided a wide range of daily boron exposure, which made it possible to study dose-dependent responses of the studied parameters.

The high level of daily boron exposure in our study area was supported by using boron exposure biomarkers. Blood boron and to a lesser extent semen boron concentrations were suggested as biomarkers of boron exposure in some earlier studies.^{3,4,11-16} Accordingly, blood boron and semen boron concentrations were used as the biomarkers of boron exposure in order to prove the high level of daily boron exposure of workers classified in the exposed group. The significantly high mean blood boron and semen boron concentrations in the exposed group support the extraordinary daily boron exposure level in our study population as shown in Table 1.

In spite of this high level of daily boron exposure, the mean Y:X sperm ratio of the exposed group was not significantly different from that of the control group ($p > 0.05$) as shown in Table 1. The sex ratio (boys/girls) at birth in the control and exposed groups was 0.94 and 1.17, respectively. In this regard, the numbers of boys and girls in the control and exposed groups were not significantly different ($p > 0.05$) as presented in Table 1.

CONCLUSIONS

Consequently, boron-mediated decrease in Y:X sperm ratios in men or excess of female births were not observed in our highly boron-exposed study population. Under these circumstances, our results refute the association between a high level of boron exposure and decreased Y:X sperm ratios in men that was reported by Robbins et al.⁵

ACKNOWLEDGEMENTS

The study was funded by Eti Mine Works General Management and BOREN (2008-G0207).

Conflicts of Interest: No conflict of interest was declared by the authors.

REFERENCES

1. Regulation (EC) No 1272/2008 on the classification, labelling and packaging of substances and mixtures. 16 December 2008.
2. Xing X, Wu G, Wei F, Liu P, Wei H, Whang C, Xu J, Xun L, Jia J, Kennedy N, Elashoff D, Robbins W. Biomarkers of environmental and workplace boron exposure. *J Occup Environ Hyg.* 2008;5:141-147.
3. Duydu Y, Başaran N, Üstündağ A, Aydın S, Ündeğer Ü, Ataman OY, Aydos K, Düker Y, Ickstadt K, Waltrup BS, Golka K, Bolt HM. Reproductive toxicity parameters and biological monitoring in occupationally and environmentally boron-exposed persons in Bandırma, Turkey. *Arch Toxicol.* 2011;85:589-600.
4. Duydu Y, Başaran N, Üstündağ A, Aydın S, Ündeğer U, Ataman OY, Aydos K, Düker Y, Ickstadt K, Waltrup BS, Golka K, Bolt HM. Assessment of DNA integrity (COMET assay) in sperm cells of boron-exposed workers. *Arch Toxicol.* 2012;86:27-35.
5. Robbins WA, Wei F, Elashoff DA, Wu G, Xun L, Jia J. Y:X sperm ratio in boron exposed men. *J Androl.* 2008;29:115-121.
6. World Health Organization. WHO laboratory manual for the examination and processing of human semen. Fifth Edition; 2010.
7. Whorton D, Haas J, Trent L. Reproductive effects of inorganic borates on male employees: birth rate assessment. *Environ Health Perspect.* 1994;102(Suppl 7):129-132.
8. Chang BL, Robbins WA, Wei F, Xun L, Wu G, Li N, Elashoff DA. Boron workers in China, exploring work and lifestyle factors related to boron exposure. *AAOHN J.* 2006;54:435-443.
9. Sayli BS. An assessment of fertility in boron-exposed Turkish subpopulations, 2. Evidence that boron has no effect on human reproduction. *Biol Trace Elem Res.* 1998;66:409-422.
10. Scialli AR, Bonde JP, Brüske-Hohlfeld I, Culver BD, Li Y, Sullivan FM. An overview of male reproductive studies of boron with an emphasis on studies of highly exposed Chinese workers. *Reprod Toxicol.* 2010;29:10-24.
11. Duydu Y, Başaran N, Bolt HM. Risk Assessment of Borates in Occupational Settings (1st eds.) Elsevier; 2015:65-105.
12. Duydu Y, Başaran N, Bolt HM. Exposure assessment of boron in Bandırma boric acid production plant. *J Trace Elem Med Biol.* 2012;26:161-164.
13. Duydu Y, Başaran N, Üstündağ A, Aydın S, Ündeğer U, Ataman OY, Aydos K, Düker Y, Ickstadt K, Waltrup BS, Golka K, Bolt HM. Is boric acid toxic to

- reproduction in humans? Assessment of the animal reproductive toxicity data and epidemiological study results. *Curr Drug Deliv.* 2016;13:324-329.
14. Basaran N, Duydu Y, Bolt HM. Reproductive toxicity in boron exposed workers in Bandirma, Turkey. *J Trace Elem Med Biol.* 2012;26:165-167.
 15. Bolt HM, Duydu Y, Basaran N, Golka K. Boron and its compounds: current biological research activities. *Arch Toxicol.* 2017;91:2719-2722.
 16. Bolt HM, Basaran N, Duydu Y. Human environmental and occupational exposures to boric acid: reconciliation with experimental reproductive toxicity data. *J Toxicol Environ Health A.* 2012;75:508-514.



Histone Deacetylase Inhibitors: A Prospect in Drug Discovery

Histon Deasetilaz İnhibitörleri: İlaç Keşfinde Bir Aday

© Rakesh YADAV*, © Pooja MISHRA, © Divya YADAV

Banasthali University, Faculty of Pharmacy, Department of Pharmacy, Banasthali, India

ABSTRACT

Cancer is a provocative issue across the globe and treatment of uncontrolled cell growth follows a deep investigation in the field of drug discovery. Therefore, there is a crucial requirement for discovering an ingenious medicinally active agent that can amend idle drug targets. Increasing pragmatic evidence implies that histone deacetylases (HDACs) are trapped during cancer progression, which increases deacetylation and triggers changes in malignancy. They provide a ground-breaking scaffold and an attainable key for investigating chemical entity pertinent to HDAC biology as a therapeutic target in the drug discovery context. Due to gene expression, an impending requirement to prudently transfer cytotoxicity to cancerous cells, HDAC inhibitors may be developed as anticancer agents. The present review focuses on the basics of HDAC enzymes, their inhibitors, and therapeutic outcomes.

Key words: Histone deacetylase inhibitors, apoptosis, multitherapeutic approach, cancer

ÖZ

Kanser tedavisi tüm toplum için büyük bir kıskırtıcıdır ve ilaç keşfi alanında bir araştırma hattını izlemektedir. Bu nedenle, işlemeyen ilaç hedeflerini iyileştirme yeterliliğine sahip, tıbbi aktif bir ajan keşfetmek için hayati bir gereklilik vardır. Artan pragmatik kanıtlar, histon deasetilazların (HDAC) kanserin ilerleme aşamasında deasetilasyonu artırarak ve malignite değişikliklerini tetikleyerek kapana kısıldığını ifade etmektedir. HDAC inhibitörleri, ilaç keşfi bağlamında terapötik bir hedef olarak HDAC biyolojisiyle ilgili kimyasal varlığı araştırmak için, çığır açıcı iskele ve ulaşılabilir bir anahtar sağlarlar. HDAC inhibitörünün gen ekspresyonu yoluyla, kanserli hücrelere sitotoksiteyi ihtiyatlı bir şekilde aktarmak için anti-kanser bir madde olarak geliştirilmesi yaklaşan bir gerekliliktir. Bu derlemede HDAC enziminin temelleri, inhibitörleri ve terapötik sonuçları üzerinde durulmuştur.

Anahtar kelimeler: Histon deasetilaz inhibitörleri, apopitoz, çoklu tedavi yaklaşımı, kanser

INTRODUCTION

In recent years, immense progress has been made in the management of cancer, due to which the life expectancy of cancer patients has been improved remarkably. Cancer is represented by inappropriate cell proliferation or transformation.¹ In cancerous cells, genes undergo various modification processes either by mutation or epigenetics. A number of potential approaches have been proposed for the treatment of cancer, but histone deacetylase inhibitors (HDACIs) are the emerging ones.² Various reports in the literature revealed that certain

histone deacetylase (HDAC) family members are aberrantly expressed in several tumors and have a nonredundant function in controlling the hallmarks of cancerous cells. They are classified into two types, i.e., Zn-dependent (class I and class II) and nicotinamide adenine dinucleotide (NAD)-dependent (class III) enzymes. Currently, researchers around the globe are paying more attention to the modification of the Zn-dependent portion of the histone family. At present, there are a total of 11 HDAC family members identified on the basis of their similarity chain (Figure 1).^{3,4}

*Correspondence: E-mail: rakesh_pu@yahoo.co.in, Phone: 9694891228 ORCID-ID: orcid.org/0000-0002-8932-5076

Received: 24.06.2017, Accepted: 25.01.2018

©Turk J Pharm Sci, Published by Galenos Publishing House.

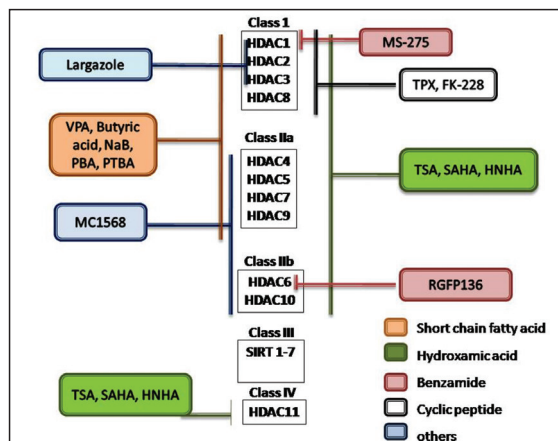


Figure 1. Schematic representation of different histone deacetylase and inhibitors

HDACs are enzymes that catalyze the deacetylation of lysine remnants located at the *N*-terminal of several protein substrates, such as nucleosomal histones. Histone acetylation has an important role in gene expression. Histone acetyl transferases and HDACs are the two types of enzymes that are primarily amenable for the catalysis of particular lysine residues of histones.⁵ Enzymes inhibitors are well known to stimulate cell cycle arrest, p53 sovereign, initiation of cyclin dependent kinase inhibitor, i.e., p21, tumor discriminating apoptosis, and segregation of normal and malignant cells. HDACs have attracted significant interest recently for the treatment of cancer as well as of other human disorders.⁶

A number of HDAC inhibitors have been reported to date that cause tumor cell growth arrest at doses that are apparently nontoxic and appear to be very selective.¹ HDACs consists of three defined structural parts of an ideal pharmacophore, i.e., (a) recognition cap group (b) hydrophobic linker, and (c) the zinc-binding group (Figure 2).^{7,8} Earlier, HDACs highlighted the alteration of the surface recognition site (capping group) and the zinc ion binding group.⁵ Some selective HDACs help in identifying the specific position of the HDAC protein responsible for cancer. This prospective identification by HDACs plays an important role to improve the therapeutic profile of new generation HDACs. In addition to changing the metal binding site, the hydrophobic site is also varied, concentrating on modifying the linker site by varying unsaturation and adding a ring (e.g., aryl, cyclohexyl) inside the series,⁹ but still selective and potent HDACs are yet to be investigated.

On the basis of chemical structures and enzymatic activities, HDACs are (Figure 3)¹⁰ chemically classified as *hydroxamates* (vorinostat, panobinostat, givinostat, quisinostat, abexinostat, belinostat, tefinostat, resminostat, pracinostat), *benzamides* (entinostat, mocetinostat, chidamide), *aliphatic acids* (valproic acid), and *cyclic peptides* (romidepsin).¹¹ These HDACs possess specific structural components that trigger diverse functions like interruption in the cell cycle, angiogenesis, and immunomodulation by acting on histone and non-histone proteins.⁹ A large number of HDACs originate from natural

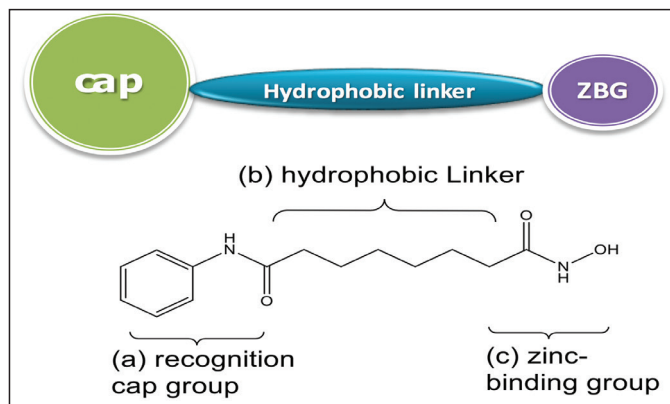


Figure 2. Pharmacophore requirements for histone deacetylase inhibitors sources and show substantial effects against cancer cells. Some examples of natural HDACs are given in Table 1.¹²⁻¹⁴

Food and Drug Administration approved and clinical trial drugs

Vorinostat, romidepsin, belinostat, and romidepsin are HDACs that are approved by the Food and Drug Administration (FDA) for the treatment of cutaneous T-cell lymphoma (CTCL). More than 80 HDACs drugs are under clinical trial at present and 11 of them are particular for solid and hematological tumors. Single and combination drugs for the treatment of other types of cancer are shown in Table 2.³

Hydroxamic acids

A number of HDACs have been identified and some are under clinical trial with a hydroxamic acid scaffold for the treatment of various types of cancer. The hydroxamic acid-based drug molecule consists of three defined structural parts of an ideal pharmacophore, i.e., (a) recognition cap group, (b) hydrophobic linker, and (c) zinc-binding group. HDACs act by binding to the cap bearing amino group, a linker with 4-6 carbon unit and zinc binding group for the inhibition of enzyme.¹⁵

Trichostatin A is the first hydroxamate-based HDACI that was isolated from *Streptomyces hygroscopicus* to inhibit HDACs. Only the R-isomer of Trichostatin A was found to be active against HDACs.¹⁶

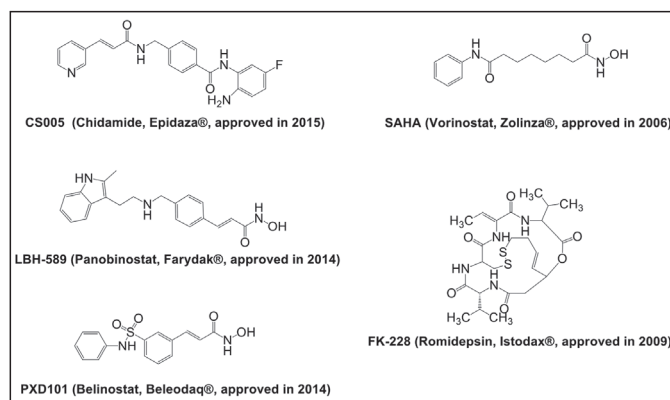


Figure 3. Some of the approved histone deacetylase inhibitors

Table 1. Naturally occurring HDACIs

S. no.	Name	Structure	Natural source	Activity
1	TSA		<i>Streptomyces hygroscopicus</i> (actinomycete)	Anticancer
2	FR235222		<i>Acremonium</i> sp.	Human leukemia cell inhibition (U937) proliferation and arrest cell cycle (G1 phase)
3	Diallyl disulfide		<i>Allium sativum</i>	Antitumor activity
4	Amamistatin (A) R= OMe, (B) R= H		<i>Nocardia asteroides</i>	Anticancer
5	Chlamydocin		<i>Diheterospora chlamydosporia</i>	Antitumor
6	Apicidin		<i>Fusarium</i> sp.	Antitumor
7	Largazole		Cyanobacterium <i>Symploca</i> sp.	Antitumor
8	Spiruchostatin A		<i>Pseudomonas</i>	Anticancer

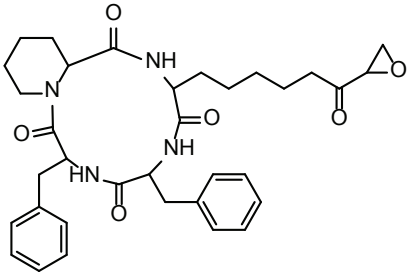
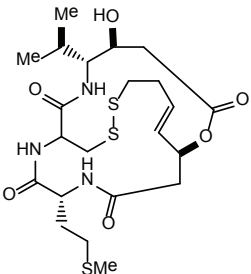
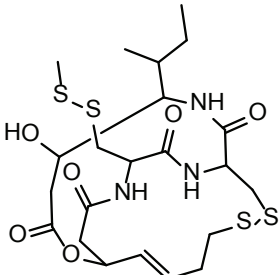
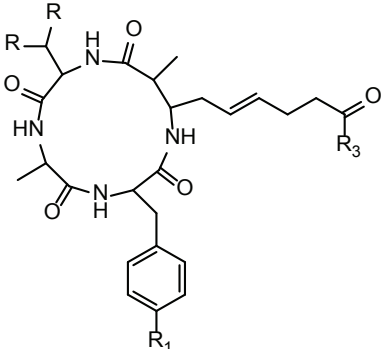
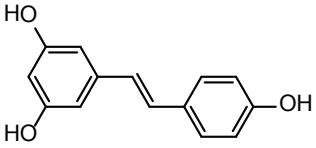
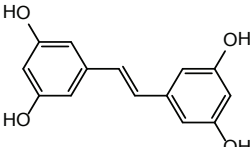
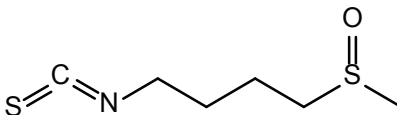
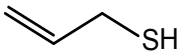
9	Trapoxin A		<i>Corollospora intermedia</i>	Anticancer
10	Burkholdac A		<i>Burkholderia thailandensis</i>	Antiproliferative activity
11	Thailandepsin A		<i>Burkholderia thailandensis</i>	Anticancer and antitumor activity
12	Azumamide (A) R/R1/R2 = CH3/H/ NH2; (B) CH3/OH/ NH2; (C) CH3/OH/OH; (D) H/H/NH2, (E) CH3/H/OH		Marine sponge <i>Mycale izuensis</i>	Anticancer and effective for mammalian solid tumor
13	Resveratrol		<i>Vitisvinifera/ cyanococcus</i>	Anticancer activities
14	Piceatannol		<i>Cyanococcus</i>	Anticancer activities
15	Sulforaphane		<i>Brassica oleracea</i>	Effective against prostate, colon, and breast cancer
16	Allyl mercaptan		<i>Allium sativum</i>	Anticancer

Table 2. Various HDACIs in clinical trials

HDACIs	HDAC specificity (class)	<i>In vitro</i> efficacy	Hydroxamic Acid Based	
			Combination therapy	Types of cancer
Vorinostat (SAHA)	1 and 2	Nanomolar	Temozolomide plus radiation	Glioblastoma multiforme (GBM)
			Cyclophosphamide, Doxorubicin, Vincristine, Prednisone (CHOP)	Peripheral T-cell lymphoma (PTCL)
			X	Gastro-intestinal (GI)
			Whole brain radiation	Brain metastasis
			5-Fluorouracil (5FV)/Leucovorin (LV)	Refractory colorectal and prominent tumors
			Hydroxychloroquine	Modified tumors
			NPI-0052	Pancreatic and lung malignancy
			Velcate®	Multiple myeloma
Beleodaq (Belinostat)	1 and 2	Micromolar	5-fluorouracil (5FV)	Metastatic-colorectal
			X	Malignant pleural mesothelioma
			X	Epithelial and microcapillary ovarian malignancy
			X	Thymus epithelial cancer
			X	Myelodysplastic syndrome (MDS)
			Paraplatin	Platinum resistant ovarian malignancy
			Carboplatin plus Paclitaxel	Ovarian cancer
			X	Acute myeloid leukemia (AML)
PCI-24781 (Abexinostat)	1 and 2	Nanomolar	Cisplatin + doxorubicin + cyclophosphamide	Thymus epithelial tumor
			X	Complex solid cancers
			Pazopanib	Metastatic solid cancer
SB939 (Pracinostat)	1, 2, and 4	Micromolar	Cisplatin + radiation	Naso-pharyngeal carcinoma (NPC)
			X	Myelofibrosis (MF)
			X	Complex solid tumors
Resminostat	1 and 2	Micromolar	X	Intractable solid tumors
			X	Complex solid tumors
			X	Relapsed/refractory Hodgkin's lymphoma (HL)
			Sorafenib	Advanced hepatocellular carcinoma (HCC)
Givinostat (ITF-2357)	1 and 2	Nanomolar	X	Colorectal carcinoma
			X	Myeloproliferative neoplasms (MPN)
Panobinostat	1 and 2	Micromolar	Hydroxycarbamide	Polycythemia vera
			X	Small cell lung malignancy (SCLC)
			X	Myelofibrosis (MF)
			X	Solid tumors
			X	Cutaneous (T-cell) lymphoma
			X	Relapsed or refractory Hodgkin's lymphoma
CUDC-101	1 and 2	Nanomolar	X	Myelodysplastic syndrome (MDS)
			X	Modified solid tumors

Table 2. Continued

Benzamide Based				
HDACIs	HDAC specificity (class)	<i>In vitro</i> potency	Combination	Cancer types
MGCD0103 (Mocetinostat)	1 and 4	Micromolar	X	Leukemia
			X	Myelodysplastic syndrome (MDS)
			X	Chronic lymphocytic leukemia (CLL)
			X	Modified solid malignancy
			X	Relapsed Hodgkin's lymphoma
MS-275 (Entinostat)	1	Micromolar	CRA (13-cis retinoic acid)	Modified solid malignancy
			Erlotinib	Non-small cell lung cancer (NSCLC)
			Exemestane	Breast malignancy
			X	Refractory solid malignancy and lymphoma
CI994 (Tacedinaline)	1	Micromolar	X	Modified solid malignancy
Short Chain Fatty Acid Based				
HDACIs	HDAC specificity (class)	<i>In vitro</i> efficacy	Combination therapy	Cancer types
Valproic acid	1	Micromolar		Refractory/central nervous system (CNS) tumors
				Neuro-endocrine tumors (NET)
			Avastin	Colorectal, prostate, and breast melanoma
			Decitabine	Non-small cell lung cancer (NSCLC)
			(S-1)	Pancreato-biliary
			Apresoline	Solid malignancy
			X	Refractory solid tumor/lymphoma
Phenylbutyrate	1 and 2	Micromolar	X	Persistent brain tumor
			Vidaza®	Acute myeloid leukemia or MDS
			Vidaza®	Prostate malignancy
			Vidaza®	Non-small cell lung cancer (NSCLC)

Vorinostat (*N*-hydroxy-*N'*-phenyl-octanediamide), marketed under the name Zolinza® by Merck, was the one of the first HDACIs permitted for the treatment of CTCL by the FDA, in 2006.¹⁷ *Vorinostat* hinders all classes of HDAC proteins (I, II, and IV), except class III HDAC, which is NAD⁺ dependent.^{18,19}

Panobinostat (LB589) is a new drug developed by Novartis for the treatment of various cancers²⁰ and was approved by the FDA in 2015 for the treatment of multiple myeloma.²¹⁻²³

Givinostat (ITF2357) has been reported as a hydroxamic acid-based HDACI that revealed positive effects in patients with Hodgkin's lymphoma, multiple myeloma, and severe lymphocytic leukemia. The European Union has designated givinostat as an orphan drug for the treatment of systemic juvenile idiopathic arthritis and polycythemia vera.²⁴

Abexinostat (PCI-24781) has been reported as a potent hydroxamate-based HDACI having a wide spectrum of anticancer activity. It is used alone or together with proteasome inhibitors in the treatment of neuroblastoma cell lines.²⁵ *Abexinostat* is used with the usual chemotherapy agents, or is used for different types of carcinomas, e.g., tissue soft-tissue sarcoma (sarcoma models of human).²⁶

Belinostat (*Beleodaq* or *PXD101*) is a novel hydroxamate-type HDAC inhibitor that exhibits *in vitro* cytotoxicity at low micromolar concentrations and it is active for the treatment of ovarian cancer, CTCL, thymoma or thymic carcinoma, and myelodysplastic syndrome. This drug showed remarked effects in single or combined therapy.²⁷

CUDC 101 is multitarget inhibitor of enzymes and receptors like HDAC, tyrosine kinases, epidermal growth factor receptor, and human epidermal growth factor receptor-2 and it possesses potent anti-proliferative and pro-apoptotic activities.²⁸

Pracinostat (SB939) is another clinical trial (phase II) compound with HDAC inhibitory activity. Studies postulated that the activity or acceptability of compound 8 is in transitional/high risk myelofibrosis affected patients.²⁹ The drug has also been tested for modified solid tumors³⁰ but yielded no promising results. The drug also showed greater effectiveness in children with refractory solid tumors.³¹

Resminostat prevents cell growth and robustly induces apoptosis in multiple myeloma cell lines in small μ m concentration.³² This drug shows a significant effect when dispensed in combination with other drugs (melphalan, bortezomib).³³ In phase II clinical

trials, it showed positive effects in Hodgkin's lymphoma and was also evaluated for higher colorectal malignancy.³⁴

Quisinostat (JNJ-26481585) is an experimental drug discovered by Johnson and Johnson through clinical studies. The data suggest that it is a "pan" inhibitor and it was found to be effective for the treatment of CTCL and leukemia myeloid in nanomolar concentration.³⁵

Tefinostat or CHR-2845 (cyclopentyl 2-((4-(N'-hydroxyoctanediamido) cyclohexyl) methylamino)-2-phenylacetate) comes under the hydroxamic acid category used as a particular substrate for hCE-1 (intracellular carboxyl-esterase), whose expression is limited to cells of the family of monocytes/macrophages. It is a monocyte or macrophage focused HDACI that is cleaved to an active acid and has significant effects towards myeloid leukemia. The phase I clinical trial of the drug showed remarkable effects on hematological malignancies and lymphoid tumors.³⁶

CHR-3996 is a next generation HDACI based on hydroxamic acid and showed greater potency towards class I HDAC with latent anti-neoplastic effect and also showed potential effect for modified malignancies in clinical trials.^{37,38}

Benzamide derivatives

This is another class of HDACI having 20 amino anilide moiety which targets specifically class I HDACs. They bind to zinc-chelating moiety for the interaction with the catalytic Zn²⁺ in HDACs' active site.³⁹

Entinostat (MS-275) was found to potentially inhibit various cancer cells like NSCLC, breast malignancy, lympho-blastic cancer, colon and renal cancer, and meta-static tumors and also has a notable effect in different phases of clinical trials and with selectivity towards class I.⁴⁰

Mocetinostat (MGCD0103) is an isotype of HDACI and showed *in vitro* activity against HDAC1 selectively and some activity against the various isoforms of HDAC (2, 3, and 11).⁴¹ The drug showed greater potency in hematological leukemia,⁴² lymphoma cancer,⁴³ and solid malignancy.⁴⁴

Chidamide (Epidaza) is an HDAC inhibitor developed and approved in China (in 2015) that showed potential effects in the treatment of pancreatic cancer.⁴⁵

Short chain fatty acids

The chemical class of short chain fatty acids has been also introduced as HDAC inhibitors. Their mode of action is based on the presence of a COOH group covering the acetate release channel with a Zn binding site and they vie for the acetate group freed from the deacetylation reaction. The best examples of short chain fatty acids are valproic acid and sodium butyrate, which are under clinical trial.⁴⁶

Valproic acid is used as anti-convulsant and mood-stabilizing agent. Recently it was introduced as a pan-HDACI in the third phase of clinical trials for the treatment of cancer, i.e., cervical or ovarian. It shows significant therapeutic effects either alone or in combination therapy.^{47,48}

AN-9 is used for chronic NSCLC and lymphocytic and lymphoma malignancies.⁴⁹

Cyclic peptides

Romidepsin belongs to the class of depsipeptides, and has recently been tested in phase-II clinical trials as well as critical trials in cutaneous and peripheral T-cell lymphomas. An unprejudiced response was seen in 10 of 28 evaluable CTCL affected patients, from an overall response rate of 36%, comprising 3 and 7 complete and partial responses, respectively. Myelotoxicity, nausea, vomiting, and cardiac dysrhythmias are some of the serious side effects. Hematologic and solid malignancies seen in cancer affected patients may be treated with depsipeptides, which are also under clinical trial in single or combination therapy.⁵⁰

Toxicity in clinical trials

Antitumor drugs seem to have more serious toxicity than any other class of drugs. In some cases, thrombocytopenia, neutropenia, anemia, fatigue, and diarrhea are the certain side effects of inhibitors (grades III and IV). By the discontinuation of the (HDAC) drug, some volunteers suffering from thrombocytopenia along with nausea, vomiting, anorexia, constipation, and dehydration were also seen.

Inhibitors of HDAC also have some adverse effects like any class of anticancer agents. The inhibitors (grades III and IV) cause certain side effects like thrombocytopenia, neutropenia, anemia, fatigue, and diarrhea.^{51,52} In some cases, HDAC causes thrombocytopenia but it can be easily resolved by discontinuation of the drug.⁴⁰ Some other side effects were also seen, like nausea, vomiting, anorexia, constipation, and dehydration. Deaths of volunteers in clinical trials involving HDACIs have been reported. For example, during trials of mocetinostat in patients with critical Hodgkin's lymphoma four died, of which two were treatment related deaths.⁵³ Similarly, some other deaths were recorded during clinical trials involving vorinostat and givinostat.^{52,54} Hence, before starting clinical trials some amendments are necessary to reduce the toxicity of HDACIs and curtail the cytotoxicity effects in patients.

Approaches towards the development of HDACIs

Most HDACIs have been recognized but not considered to be competitive inhibitors. The enzymes are inhibited by insertion of the same catalytic site as the usual enzyme substrates called competitive inhibitors. A competitive HDACI normally contributing to the ordinary function of the common model of pharmacophore depends upon the crystal structures of enzyme inhibitor (HDAC-like protein comes from *Aquifex aeolicus*) complex.

Noncompetitive inhibitors selectively disrupting the HDACs' interaction with precise DNA binding proteins and some other regulatory proteins (like 14-3-3 protein) might be potent selective outlines (Figure 4).⁵⁵ Alteration of identified HDACIs is important to recognize the chemical entity that affects the potency of inhibitors and is an important initiative for further investigating a novel chemical molecule.

Some of the new HDACIs with peptoid-based cap groups were synthesized and found to be more selective against HDAC6

isoform than towards other HDAC isoforms (Figure 5).⁵⁶ The compounds obtained from this hypothesis were found to be more active, showing extraordinary chemo-sensitizing effects and remarkable activity against Cal27 and CisR.⁵⁶ Selective inhibition of HDAC6 is a promising target nowadays for a wide range of diseases such as neurodegenerative disorders (Alzheimer's disease, Huntington's disease, and Parkinson's disease), cancers, and hematological malignancies.

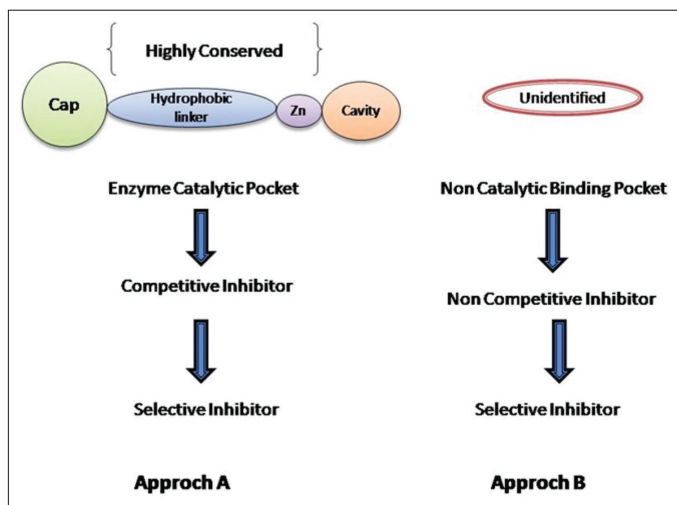


Figure 4. Different approaches for selective histone deacetylase inhibition

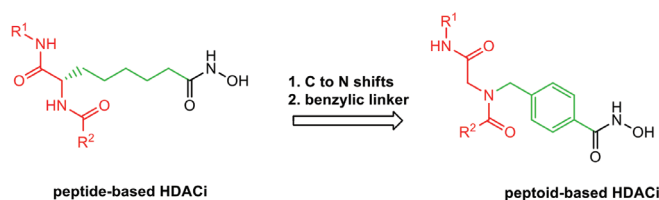
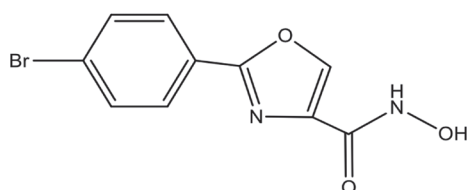


Figure 5. Peptoid-based novel chemical entity effective against HDAC6 isoform

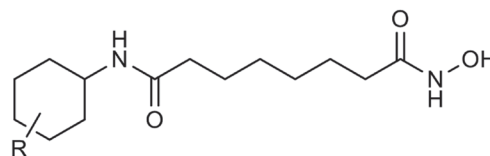
During the identification of some selective HDAC6 inhibitors, a biarylhydroxamate structure was explored without any branching. The heterocycles (thiazole, oxazole, and oxadiazole) attached to the hydroxamate showed a huge impact on HDAC6 potency and selectivity. Compound 1 containing oxazole moiety was identified by Senger et al.⁵⁷ as a potent and selective inhibitor *in vitro* and in cell culture.



(1)

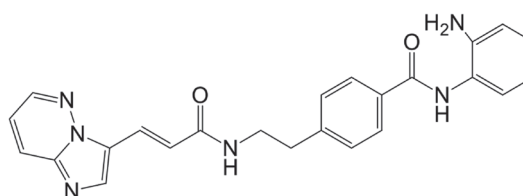
Zhang et al.⁵⁸ outlined the synthesis, characterization, and biological evaluation of suberoylanilide hydroxamic acid (SAHA)-based derivatives with greater binding towards HDAC8 than the SAHA. Compound 2 shows pronounced activity while

inhibiting the cancerous cell lines of human glioma, i.e., MGR2, U251, and U373.



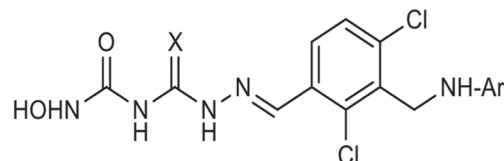
(2)

Bicyclic heterocyclic compounds are well known and widely used in medicinal chemistry, always attracting remarkable attention in the pharmaceutical industry due to their wide therapeutic value. A series of novel acrylamide derivatives based on the lead compound of MS-275 has been synthesized by Li et al.⁵⁹ The synthesized compounds were quantized for antiproliferative activities against cancerous cell lines (HCT-116, MCF-7, and A549). Furthermore, compound 3 manifested an adequate pharmacokinetic profile with 76% bioavailability in rats, and can probably be regarded as a novel compound for drug discovery.



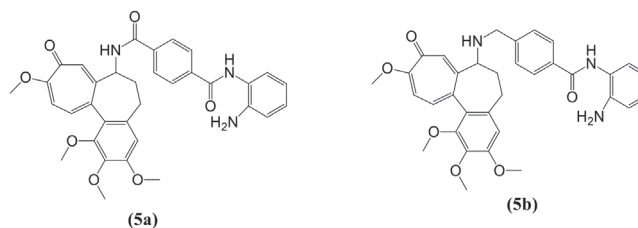
(3)

Chavan and Mahajan⁶⁰ outlined and synthesized a number of derivatives having semi- or thio-carbazone moiety containing hydroxamic acid with average to high G score. Numerous compounds exhibited potent anti-proliferative effects for the MCF7, HCT15, and Jurkat cancer cell lines. Compound 4 showed potential activity against colon cancer.



(4)

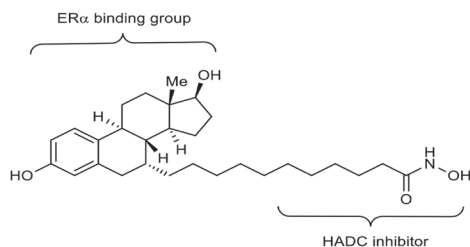
Zhang et al.⁶¹ described colchicine bearing hydroxamate moiety with HDAC inhibitory activity that possesses good effect against HDACs and tubulin. Compounds 5a-b show modest inhibition of HDAC activity and significant action on cytotoxicity.



(5)

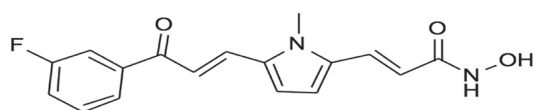
Mendoza-Sanchez et al.⁶² outlined the fusion of antiestrogens with known HDACs to obtain more effective antiproliferative

compounds for the treatment of breast cancer. The fused compound **6** had antiestrogenic and HDACi activity. The benzamide bifunctional molecule was found to be active for class I deacetylases (HDAC3) and class II deacetylases (HDAC6) and was potent in nM concentration in breast cancer models.



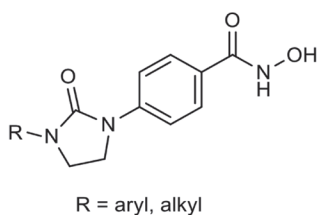
(6)

Fleming et al.⁶³ reported the advanced synthesis and structural modification of MC1568 (**7**), which was found to be selective for class IIa HDACi.



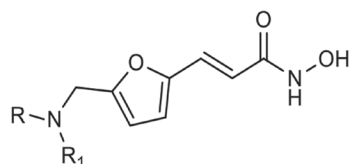
(7)

Cheng et al.⁶⁴ reported the synthesis of phenyl-imidazolidin-2-one derivatives as selective HDACIs. Compound **8** of the series possesses remarkable antitumor activity against cancer cell lines (HCT-116, PC3, and HL-60) in comparison to SAHA. It also showed a major antitumor effect in the xenograft model of HCT 116 mice.



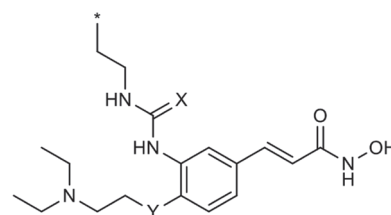
(8)

Feng et al.⁶⁵ described the influence of the insertion of a branched hydrophobic group, e.g., *N*-hydroxyfurylacrylamide, at the cap side of HDACi and was reported to determine the activity in terms of inhibition against tumor cells. All the synthesized compounds were reported to have high selectivity towards HDAC1 and the compound like **9** showed magnificent selectivity next to HDAC6.



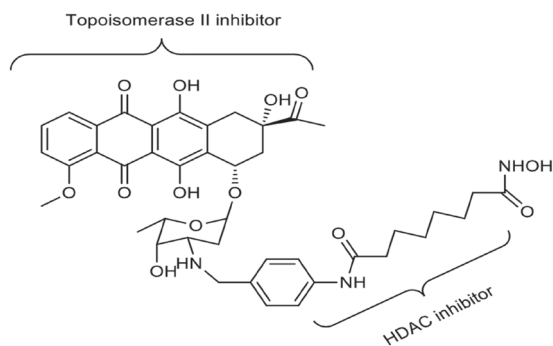
(9)

Ning et al.⁶⁶ stated that the substitution of urea/thiourea on disubstituted cinnamic-based hydroxamates (**10**) has a remarkable HDAC inhibitory effect and antiproliferative activity against tumor cell lines.



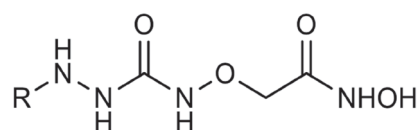
(10)

Guerrant et al.⁶⁷ reported a bifunctional approach to produce chemoactive agents in a single structural design that has 2-fold activity against HDAC and topoisomerase II. Results revealed that compound **11** inhibits both these enzymes with strong inhibitory capacity against different cancerous cell lines.



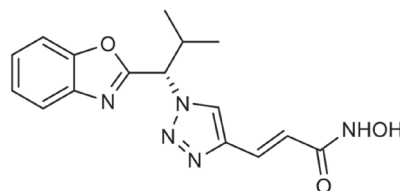
(11)

Marek et al.⁶⁸ reported a novel series by incorporating an alkoxy-amide linkage in hydroxamic acid-based compounds. Compound **17** exhibited the same effects contrasted to SAHA in a pan-HDAC cell-based assay and improved cytotoxic outcome against various cancer cell lines (A-2780, Cal-27, Kyse-510, and MDA-MB-231). Compound **12** exerted significant activity against HDAC enzyme and inhibited HDAC4 and 5 in nM concentrations.



(12)

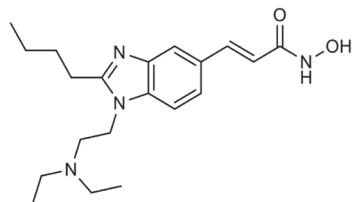
Hou et al.⁶⁹ described a potent chiral compound (NK-HDAC-51) that exhibited more potent activity than vorinostat in both enzyme- and cell-based assays due to its better physicochemical properties, e.g., Log-D, solubility, micromole stability of liver ($t_{1/2}$), stability of plasma ($t_{1/2}$), and apparent permeability.



(13)

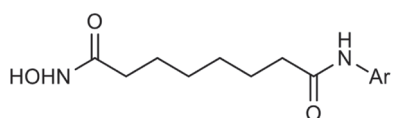
Wang et al.⁷⁰ outlined the synthesis of 3-(1,2-disubstituted-1*H*-benzimidazol-5-yl)-*N*-hydroxy-acryl-amides HDACIs. In

vivo studies against various tumor models (HCT-116, PC3, A-2780, MV411, and Ramos) showed that compound **14** is highly effective and has very good pharmacokinetics, safety, and pharmaceutical properties.



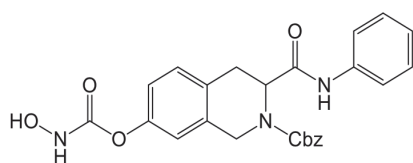
(14)

Chun et al.⁷¹ synthesized a series of compounds like **15** for anticancer activity and antiproliferative effects against MCF7, MDA-MB 231, MCF 7/Dox, MCF 7/Tam, SK-OV 3, LNCaP, and PC3 human cancer cell lines by the synthesis of suberoylanilide hydroxamate derivatives.⁷¹



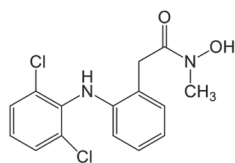
(15)

Zhang et al.⁸ reported a new series of 1,2,3,4-tetrahydroisoquinoline-3-carboxylic acid derivatives for the inhibition of HDACs. Compounds like **16** show potent activity and have better inhibitory activity than vorinostat.



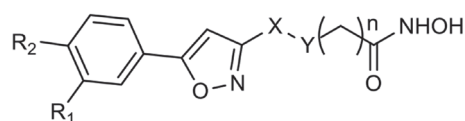
(16)

Koncic et al.⁷² carefully examined a number of hydroxamic acid derivatives of NSAIDs (**17**) and appraised their antioxidant, radical scavenging activity with regard to butylated hydroxyanisole.



(17)

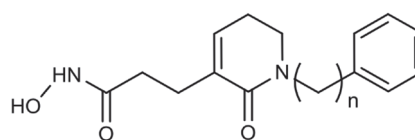
Kozikowski et al.⁷³ outlined a novel series of hydroxamate-based HDACIs synthesized by cycloaddition method. Compounds like **18** have greater potency against HDAC6 with an IC₅₀ value of 2 picomolar. Some compounds were found to be capable of preventing cell growth in pancreatic cancer approximately 10 times more effectively than vorinostat.



R1 = NHBoc or H
R2 = NHBoc or H
X = CO or CH2
Y = NH or O
n = 4 or 6

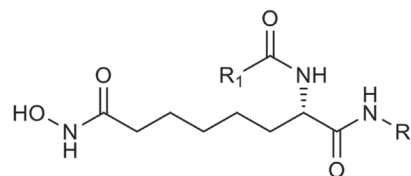
(18)

Kim et al.⁷⁴ reported that novel δ -lactam-based HDACIs that have various substituted benzyl, bi-aromatic cap groups were prepared through metathesis reaction. Compound **19** showed inhibitory activity against five different human cancer cell lines (PC3, AC-HN, NUGC3, HCT15, and MBA-MB-231).



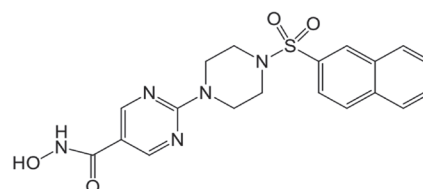
(19)

Kahnberg et al.⁷⁵ described various derivatives of 2-aminosuberic acid. Compound **31** has the ability to kill a range of tumor cells including MM96L melanoma cells, out of whole compounds. Compound **20** exhibits hyperacetylation of histones in both normal and cancerous cells, induces p-21 expression, and discriminates the survival of cancer cells to a nonproliferating phenotype.



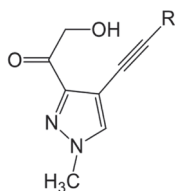
(20)

Angibaud et al.⁷⁶ described a series of novel pyrimidyl-5-hydroxamic acids for HDAC inhibition. Moreover, amino-2-pyrimidinylcan is used as a linker to provide enzymatic potency to HDACIs.



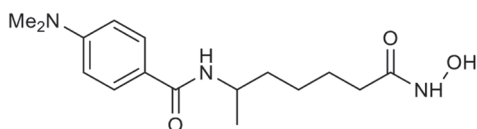
(21)

Mshvidobadze et al.⁷⁷ developed a variety of pyrazolohydroxamic acid molecules that showed greater efficiency against HDAC enzyme.



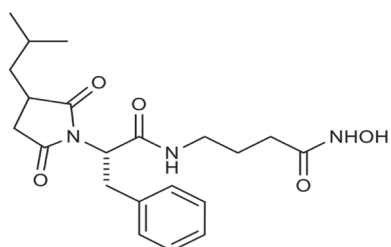
(22)

Van Ommeslaeghe et al.⁷⁸ reported potent amide type HDACs and molecular modeling confirms the flexibility of the linker chain of compound **23**, which is important for the orientation of the dimethyl-amino-benzoyl group in the enzyme.



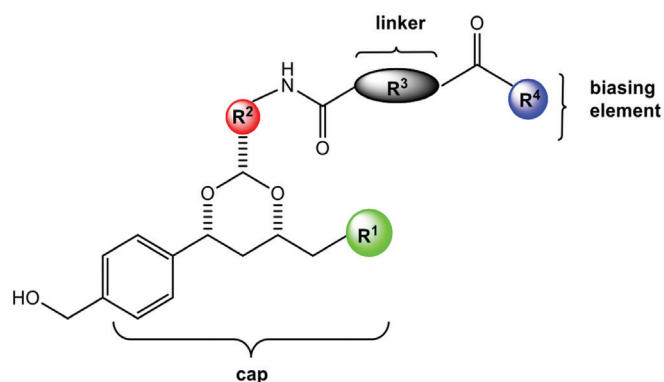
(23)

Curtin et al.⁷⁹ outlined the synthesis and evaluation of a series of succinimide hydroxamic acids, which were prepared and evaluated for HDAC inhibition and antiproliferation. Compound **24** was found to be more potent.



(24)

Sternson et al.⁸⁰ synthesized a series of potent compounds like **25** having 1,3-dioxane moiety that showed HDAC inhibitory activity.



(25)

CONCLUSIONS

Currently the management of cancer has been improved significantly, and although there are various medications for the treatment of cancer they still seem to be ineffective. Thus it is a major challenge for researchers to develop safe, effective agents

with an improved therapeutic index. HDACs, a new category of anticancer agents, exert innumerable biological effects, i.e., stimulation of cell differentiation, cell demise, cell-cycle arrest, and bringing on of autophagic cell death. Development of specific HDACs with an enhanced therapeutic index leads to successful target accomplishment that proceeds to increased efficacy. Additionally, recent clinical studies postulate that the inhibitor of HDAC enzyme responds to both hematological and solid tumor malignancies. A low therapeutic range is one of the major drawbacks of existing HDACs. Inhibitors of HDAC enzyme are used either in monotherapy or in combination therapy with different targeted agents. Combination therapy is more viably successful than monotherapy because it uses chemotherapeutic and biotherapeutic agents having lower toxicity and better clinical outcomes in tumors.

The present review highlights the structure–activity relationship of various HDACs synthesized across the globe, which will be helpful for designing new potential agents. Special attention was paid to the existing synthesized medicinal compounds over the past few years and their therapeutic application, which will be helpful for future advancement. Apart from cancer, HDACs are presently used in different remedial areas such as neurodegenerative disorders, cardiovascular disease, liver fibrosis, retinal degenerative disease, regulation of immune response, anti-inflammatory, conjunctivitis, and asthma. We have also tried to summarize the current developments in the structural scaffold of HDACs such as surface recognition site, linker region, and metal binding moiety. The recent summation by various research groups has been incorporated to understand the advancement of potential inhibitors.

ACKNOWLEDGEMENTS

The authors are thankful to the Vice-chancellor, Banasthali Vidyapith, for providing the necessary research facilities. The financial assistance provided by DST-CURIE, New Delhi, is duly acknowledged.

Conflict of interest: No conflict of interest was declared by the authors.

REFERENCES

1. Marks PA, Richon VM, Rifkind RA. Histone deacetylase inhibitors: inducers of differentiation or apoptosis of transformed cells. *J Natl Cancer Inst.* 2000;15:1210-1216.
2. Wang C, Henkes LM, Doughty LB, He M, Wang D, Meyer-Almes FJ, Cheng YQ. Thailandepsins: bacterial products with potent histone deacetylase inhibitory activities and broad-spectrum antiproliferative activities. *J Nat Prod.* 2011;74:2031-2038.
3. Mottamal M, Zheng S, Huang TL, Wang G. Histone deacetylase inhibitors in clinical studies as templates for new anticancer agents. *Molecules.* 2015;20:3898-3941.
4. Chen PJ, Huang C, Meng XM, Li J. Epigenetic modifications by histone deacetylases: Biological implications and therapeutic potential in liver fibrosis. *Biochimie.* 2015;116:61-69.

5. West AC, Johnstone RW. New and emerging HDAC inhibitors for cancer treatment. *J Clin Invest*. 2015;124:30-39.
6. Mai A, Massa S, Rotili D, Simeoni S, Ragno R, Botta G, Nebbioso A, Miceli M, Altucci L, Brosch G. Synthesis and biological properties of novel, uracil-containing histone deacetylase inhibitors. *J Med Chem*. 2006;49:6046-6056.
7. Paris M, Porcelloni M, Binaschi M, Fattori D. Histone deacetylase inhibitors: from bench to clinic. *J Med Chem*. 2008;51:1505-1529.
8. Zhang Y, Feng J, Liu C, Zhang L, Jiao J, Fang H, Su L, Zhang X, Zhang J, Li M, Wang B, Xu W. Design, synthesis and preliminary activity assay of 1,2,3,4-tetrahydroisoquinoline-3-carboxylic acid derivatives as novel Histone deacetylases (HDACs) inhibitors. *Bioorg Med Chem*. 2010;18:1761-1772.
9. Giannini G, Cabri W, Fattorusso C, Rodriguez M. Histone deacetylase inhibitors in the treatment of cancer: overview and perspectives. *Future Med Chem*. 2012;4:1439-1460.
10. Zhang Y, Li X, Hou J, Huang Y, Xu W. Design, synthesis, and antitumor evaluation of histone deacetylase inhibitors with L-phenylglycine scaffold. *Drug Des Devel Ther*. 2015;9:5553-5567.
11. Mehnert JM, Kelly WK. Histone deacetylase inhibitors: biology and mechanism of action. *Cancer J*. 2007;13:23-29.
12. Salvador LA, Luesch H. Discovery and mechanism of natural products as modulators of histone acetylation. *Curr Drug Targets*. 2012;13:1029-1047.
13. Kim B, Hong J. An overview of naturally occurring histone deacetylase inhibitors. *Curr Top Med Chem*. 2015;14:2759-2582.
14. Losson H, Schneckeburger M, Dicato M. Natural Compound Histone Deacetylase Inhibitors (HDACI): Synergy with Inflammatory Signaling Pathway Modulators and Clinical Applications in Cancer. *Molecules*. 2016;21:1608.
15. Yoshida M, Kijima M, Akita M, Beppu T. *J Biol Chem*. 1990;265:17174-17179.
16. Blumenschein GR Jr, Kies MS, Papadimitrakopoulou VA, Lu C, Kumar AJ, Ricker JL, Chiao JH, Chen C, Frankel SR. Phase II trial of the histone deacetylase inhibitor vorinostat (Zolinza, suberoylanilide hydroxamic acid, SAHA) in patients with recurrent and/or metastatic head and neck cancer. *Invest New Drugs*. 2008;26:81-87.
17. Finnin MS, Donigian JR, Cohen A. *Nature*. 1999;401:88-93.
18. Lane AA, Chabner BA. Histone deacetylase inhibitors in cancer therapy. *J Clin Oncol*. 2009;27:5459-5468.
19. Xu WS, Parmigiani RB, Marks PA. Histone deacetylase inhibitors: molecular mechanisms of action. *Oncogene*. 2007;26:5541-5552.
20. Atadja P. Development of the pan-DAC inhibitor panobinostat (LBH589): successes and challenges. *Cancer Lett*. 2009;280:233-241.
21. Muraoka M, Konishi M, Kikuchi-Yanoshita R, Tanaka K, Shitara N, Chong JM, Iwama T, Miyaki M. p300 gene alterations in colorectal and gastric carcinomas. *Oncogene*. 1996;12:1565-1569.
22. <http://www.fda.gov/NewsEvents/Newsroom/PressAnnouncements/ucm435296.html>
23. Tan J, Cang S, Ma Y, Petrillo RL, Liu D. Novel histone deacetylase inhibitors in clinical trials as anti-cancer agents. *J Hematol Oncol*. 2010;3:5.
24. He R, Chen Y, Chen Y, Ougolkov AV, Zhang JS, Savoy DN, Billadeau DD, Kozikowski AP. Synthesis and biological evaluation of triazol-4-ylphenyl-bearing histone deacetylase inhibitors as anticancer agents. *J Med Chem*. 2010;53:1347-1356.
25. Sholler GS, Currier EA, Dutta A, Slavik MA, Illenye SA, Mendonca MC, Dragon J, Roberts SS, Bond JP. PCI-24781 (abexinostat), a novel histone deacetylase inhibitor, induces reactive oxygen species-dependent apoptosis and is synergistic with bortezomib in neuroblastoma. *J Cancer Ther Res*. 2013;2:2-21.
26. Lopez G, Liu J, Ren W, Wei W, Wang S, Lahat G, Zhu QS, Bornmann WG, McConkey DJ, Pollock RE, Lev DC. Combining PCI-24781, a novel histone deacetylase inhibitor, with chemotherapy for the treatment of soft tissue sarcoma. *Clin Cancer Res*. 2009;15:3472-3483.
27. Plumb JA, Finn PW, Williams RJ, Bandara MJ, Romero MR, Watkins CJ, La Thangue NB, Brown R. Mol Pharmacodynamic response and inhibition of growth of human tumor xenografts by the novel histone deacetylase inhibitor PXD101. *Cancer Ther*. 2003;2:721-728.
28. Lai CJ, Bao R, Tao X, Wang J, Atoyan R, Qu H, Wang DG, Yin L, Samson M, Forrester J, Zifcak B, Xu GX, DellaRocca S, Zhai HX, Cai X, Munger WE, Keegan M, Pepicelli CV, Qian C. CUDC-101, a multitargeted inhibitor of histone deacetylase, epidermal growth factor receptor, and human epidermal growth factor receptor 2, exerts potent anticancer activity. *Cancer Res*. 2010;70:3647-3656.
29. Quintás-Cardama A, Kantarjian H, Estrov Z, Borthakur G, Cortes J, Verstovsek S. Therapy with the histone deacetylase inhibitor pracinostat for patients with myelofibrosis. *Leuk Res*. 2012;36:1124-1127.
30. Razak AR, Hotte SJ, Siu LL, Chen EX, Hirte HW, Powers J, Walsh W, Stayner LA, Laughlin A, Novotny-Diermayr V, Zhu J, Eisenhauer EA. Phase I clinical, pharmacokinetic and pharmacodynamic study of SB939, an oral histone deacetylase (HDAC) inhibitor, in patients with advanced solid tumours. *Br J Cancer*. 2011;104:756-762.
31. Zorzi AP, Bernstein M, Samson Y, Wall DA, Desai S, Nicksy D, Wainman N, Eisenhauer E, Baruchel S. A phase I study of histone deacetylase inhibitor, pracinostat (SB939), in pediatric patients with refractory solid tumors: IND203 a trial of the NCIC IND program/C17 pediatric phase I consortium. *Pediatr Blood Cancer*. 2013;60:1868-1874.
32. Mandl-Weber S, Meinel FG, Jankowsky R, Oduncu F, Schmidmaier R, Baumann P. The novel inhibitor of histone deacetylase resminostat (RAS2410) inhibits proliferation and induces apoptosis in multiple myeloma (MM) cells. *Br J Haematol*. 2010;149:518-528.
33. Walewski J, Paszkiewicz-Kozik E, Borsaru G, Moicean A, Warszevska A, Strobel A, Biggi A, Hauns B, Mais A, Henning SW. In Proceedings of the (52nd). ASH Annual Meeting and Exposition. Orlando; FL, USA; 2010:4-7.
34. Bitzer M, Ganten TM, Woerns MA, Siveke JT, Dollinger MM, Scheulen ME, Wege H, Giannini EG, Cillo U, Trevisani F. *J Clin Oncol*. 2013;31:15083-15088.
35. Arts J, King P, Mariën A, Floren W, Beliën A, Janssen L, Pilatte I, Roux B, Decrane L, Gilissen R, Hickson I, Vreys V, Cox E, Bol K, Talloen W, Goris I, Andries L, Du Jardin M, Janicot M, Page M, van Emelen K, Angibaud P. JNJ-26481585, a novel "second-generation" oral histone deacetylase inhibitor, shows broad-spectrum preclinical antitumoral activity. *Clin Cancer Res*. 2009;15:6841-6851.
36. Zabkiewicz J, Gilmour M, Hills R, Vyas P, Bone E, Davidson A, Burnett A, Knapper S. *Oncotarget*. 2016;7:16650-16662.
37. Moffat D, Patel S, Day F, Belfield A, Donald A, Rowlands M, Wibawa J, Brotherton D, Stimson L, Clark V, Owen J, Bawden L, Box G, Bone E, Mortenson P, Hardcastle A, van Meurs S, Eccles S, Raynaud F, Aherne W. Discovery of 2-(6-((6-fluoroquinolin-2-yl)methyl)amino)bicyclo[3.1.0]hex-3-yl)-N-hydroxypyrimidine-5-carboxamide (CHR-3996), a class I selective orally active histone deacetylase inhibitor. *J Med Chem*. 2010;53:8663-8678.

38. Banerji U, van Doorn L, Papadatos-Pastos D, Kristeleit R, Debnam P, Tall M, Stewart A, Raynaud F, Garrett MD, Toal M, Hooftman L, De Bono JS, Verweij J, Eskens FA. A phase I pharmacokinetic and pharmacodynamic study of CHR-3996, an oral class I selective histone deacetylase inhibitor in refractory solid tumors. *Clin Cancer Res*. 2012;18:2687-2694.
39. Moradei OM, Mallais TC, Frechette S, Paquin I, Tessier PE, Leit SM, Fournel M, Bonfils C, Trachy-Bourget MC, Liu J, Yan TP, Lu AH, Rahil J, Wang J, Lefebvre S, Li Z, Vaisburg AF, Besterman JM. Novel aminophenyl benzamide-type histone deacetylase inhibitors with enhanced potency and selectivity. *J Med Chem*. 2007;50:5543-5546.
40. Pili R, Salumbides B, Zhao M, Altiok S, Qian D, Zwiebel J, Carducci MA, Rudek MA. Phase I study of the histone deacetylase inhibitor entinostat in combination with 13-cis retinoic acid in patients with solid tumours. *Br J Cancer*. 2012;106:77-84.
41. Fournel M, Bonfils C, Hou Y, Yan PT, Trachy-Bourget MC, Kalita A, Liu J, Lu AH, Zhou NZ, Robert MF, Gillespie J, Wang JJ, Ste-Croix H, Rahil J, Lefebvre S, Moradei O, Delorme D, Macleod AR, Besterman JM, Li Z. MGCD0103, a novel isotype-selective histone deacetylase inhibitor, has broad spectrum antitumor activity in vitro and in vivo. *Mol Cancer Ther*. 2008;7:759-768.
42. Blum KA, Advani A, Fernandez L, Van Der Jagt R, Brandwein J, Kambhampati S, Kassis J, Davis M, Bonfils C, Dubay M, Dumouchel J, Drouin M, Lucas DM, Martell RE, Byrd JC. Phase II study of the histone deacetylase inhibitor MGCD0103 in patients with previously treated chronic lymphocytic leukaemia. *Br J Haematol*. 2008;147:507-514.
43. V El-Khoury V, Moussay E, Janji B, Palissot V, Aouali N, Brons NH, Van Moer K, Pierson S, Van Dyck E, Berchem G. The histone deacetylase inhibitor MGCD0103 induces apoptosis in B-cell chronic lymphocytic leukemia cells through a mitochondria-mediated caspase activation cascade. *Mol Cancer Ther*. 2010;9:1349-1360.
44. Garcia-Manero G, Assouline S, Cortes J, Estrov Z, Kantarjian H, Yang H, Newsome WM, Miller WH Jr, Rousseau C, Kalita A, Bonfils C, Dubay M, Patterson TA, Li Z, Besterman JM, Reid G, Laille E, Martell RE, Minden M. Phase 1 study of the oral isotype specific histone deacetylase inhibitor MGCD0103 in leukemia. *Blood*. 2008;112:981-989.
45. Guha M. HDAC inhibitors still need a home run, despite recent approval. *Nat Rev Drug Discov*. 2015;14:225-226.
46. Davie JR. Inhibition of histone deacetylase activity by butyrate. *J Nutr*. 2003;133(7 Suppl):2485-2493.
47. Bouzar AB, Boxus M, Defoiche J, Berchem G, Macallan D, Pettengell R, Willis F, Burny A, Lagneaux L, Bron D, Chatelain B, Chatelain C, Willems L. Valproate synergizes with purine nucleoside analogues to induce apoptosis of B-chronic lymphocytic leukaemia cells. *Br J Haematol*. 2009;144:41-52.
48. Stamatopoulos B, Meuleman N, De Bruyn C, Mineur P, Martiat P, Bron D, Lagneaux L. Antileukemic activity of valproic acid in chronic lymphocytic leukemia B cells defined by microarray analysis. *Leukemia*. 2009;23:2281-2289.
49. Mai A, Altucci L. Epi-drugs to fight cancer: from chemistry to cancer treatment, the road ahead. *Int J Biochem Cell Bio*. 2009;41:199-213.
50. Kijima M, Yoshida M, Sugita K, Horinouchi S, Beppu T. Trapoxin, an antitumor cyclic tetrapeptide, is an irreversible inhibitor of mammalian histone deacetylase. *J Biol Chem*. 1993;268:22429-22435.
51. Madsen AS, Kristensen HM, Lanz G, Olsen CA. The effect of various zinc binding groups on inhibition of histone deacetylases 1-11. *Chem Med Chem*. 2014;9:614-626.
52. Younes A, Oki Y, Bociek RG, Kuruvilla J, Fanale M, Neelapu S, Copeland A, Buglio D, Galal A, Besterman J, Li Z, Drouin M, Patterson T, Ward MR, Paulus JK, Ji Y, Medeiros LJ, Martell RE. Mocetinostat for relapsed classical Hodgkin's lymphoma: An open-label, single-arm, phase 2 trial. *Lancet Oncol*. 2011;12:1222-1228.
53. Bishton MJ, Harrison SJ, Martin BP, McLaughlin N, James C, Josefsson EC, Henley KJ, Kile BT, Prince HM, Johnstone RW. Deciphering the molecular and biologic processes that mediate histone deacetylase inhibitor-induced thrombocytopenia. *Blood*. 2011;117:3658-3668.
54. Galli M, Salmoiraghi S, Golay J, Gozzini A, Crippa C, Pescosta N, Rambaldi A. A phase II multiple dose clinical trial of histone deacetylase inhibitor ITF2357 in patients with relapsed or progressive multiple myeloma. *Ann Hematol*. 2010;89:185-190.
55. Su H, Altucci L, You Q. Competitive or noncompetitive, that's the question: research toward histone deacetylase inhibitors. *Mol Cancer Ther*. 2008;7:1007-1012.
56. Diedrich D, Hamacher A, Gertzen CG, Alves Avelar LA, Reiss GJ, Kurz T, Gohlke H, Kassack MU, Hansen FK, Rational design and diversity-oriented synthesis of peptoid-based selective HDAC6 inhibitors. *Chem Commun (Camb)*. 2016;52:3219-3222.
57. Senger J, Melesina J, Marek M, Romier C, Oehme I, Witt O, Sippl W, Jung M. Synthesis and Biological Investigation of Oxazole Hydroxamates as Highly Selective Histone Deacetylase 6 (HDAC6) Inhibitors. *J Med Chem*. 2016;59:1545-1555.
58. Zhang S, Huang W, Li X, Yang Z, Feng B. Synthesis, Biological Evaluation, and Computer-Aided Drug Designing of New Derivatives of Hyperactive Suberoylanilide Hydroxamic Acid Histone Deacetylase Inhibitors. *Chem Biol Drug Des*. 2015;86:795-804.
59. Li Y, Wang Y, Xie N, Xu M, Qian P, Zhao Y, Li S. Design, synthesis and antiproliferative activities of novel benzamides derivatives as HDAC inhibitors. *Eur J Med Chem*. 2015;100:270-275.
60. Chavan V, Mahajan SS. *Der Pharma Chemica*. 2015;7:199-204.
61. Zhang X, Kong Y, Zhang J, Su M, Zhou Y, Zang Y, Li J, Chen Y, Fang Y, Zhang X, Lu W. Design, synthesis and biological evaluation of colchicine derivatives as novel tubulin and histone deacetylase dual inhibitors. *Eur J Med Chem*. 2015;95:127-135.
62. Mendoza-Sanchez R, Cotnoir-White D, Kulpa J, Jutras I, Pottel J, Moitessier N, Mader S, Gleason JL. Design, synthesis and evaluation of antiestrogen and histone deacetylase inhibitor molecular hybrids. *Bioorg Med Chem*. 2015;23:7597-7606.
63. Fleming CL, Ashton TD, Gaur V, McGee SL, Pfeffer FM. Improved synthesis and structural reassignment of MC1568: a class IIa selective HDAC inhibitor. *J Med Chem*. 2014;57:1132-1135.
64. Cheng J, Qin J, Guo S, Qiu H, Zhong Y. Design, synthesis and evaluation of novel HDAC inhibitors as potential antitumor agents. *Bioorg Med Chem Lett*. 2014;24:4768-4772.
65. Feng T, Wang H, Su H, Lu H, Yu L, Zhang X, Sun H, You Q. Novel N-hydroxyfurylacrylamide-based histone deacetylase (HDAC) inhibitors with branched CAP group (Part 2). *Bioorg Med Chem*. 2013;21:5339-5354.
66. Ning C, Bi Y, He Y, Huang W, Liu L, Li Y, Zhang S, Liu X, Yu N. Design, synthesis and biological evaluation of di-substituted cinnamic hydroxamic acids bearing urea/thiourea unit as potent histone deacetylase inhibitors. *Bioorg Med Chem Lett*. 2013;23:6432-6435.
67. Guerrant W, Patil V, Canzoneri JC, Oyelere AK. Dual targeting of histone deacetylase and topoisomerase II with novel bifunctional inhibitors. *J Med Chem*. 2012;55:1465-1477.

68. Marek L, Hamacher A, Hansen FK, Kuna K, Gohlke H, Kassack MU, Kurz T. Histone deacetylase (HDAC) inhibitors with a novel connecting unit linker region reveal a selectivity profile for HDAC4 and HDAC5 with improved activity against chemoresistant cancer cells. *J Med Chem.* 2013;56:427-436.
69. Hou J, Li Z, Fang Q, Feng C, Zhang H, Guo W, Wang H, Gu G, Tian Y, Liu P, Liu R, Lin J, Shi YK, Yin Z, Shen J, Wang PG. Discovery and extensive in vitro evaluations of NK-HDAC-1: a chiral histone deacetylase inhibitor as a promising lead. *J Med Chem.* 2012;55:3066-3075.
70. Wang H, Yu N, Chen D, Lee KC, Lye PL, Chang JW, Deng W, Ng MC, Lu T, Khoo ML, Poulsen A, Sangthongpitag K, Wu X, Hu C, Goh KC, Wang X, Fang L, Goh KL, Khng HH, Goh SK, Yeo P, Liu X, Bonday Z, Wood JM, Dymock BW, Kantharaj E, Sun ET. Discovery of (2E)-3-{2-butyl-1-[2-(diethylamino)ethyl]-1H-benzimidazol-5-yl}-N-hydroxyacrylamide (SB939), an orally active histone deacetylase inhibitor with a superior preclinical profile. *Med Chem.* 2011;54:4694-4720.
71. Chun P, Won HK, Jungsu K, Kang JA, Hye JL, Young P, Mee YA, Hyung SK, Hyung RM. Synthesis and Importance of Bulky Aromatic Cap of Novel SAHA Analogs for HDAC Inhibition and Anticancer Activity. *Bull Korean Chem Soc.* 2011;32:1891-1896.
72. Koncic MZ, Rajic Z, Petric N, Zorc B. Antioxidant activity of NSAID hydroxamic acids. *Acta Pharm.* 2009;59:235-242.
73. Kozikowski AP, Tapadar S, Luchini DN, Kim KH, Billadeau DD. Use of the nitrile oxide cycloaddition (NOC) reaction for molecular probe generation: a new class of enzyme selective histone deacetylase inhibitors (HDACIs) showing picomolar activity at HDAC6. *J Med Chem.* 2008;51:4370-4373.
74. Kim HM, Hong SH, Kim MS, Lee CW, Kang JS, Lee K, Park SK, Han JW, Lee HY, Choi Y, Kwon HJ, Han G. Modification of cap group in delta-lactam-based histone deacetylase (HDAC) inhibitors. *Bioorg Med Chem Lett.* 2007;17:6234-6238.
75. Kahnberg P, Lucke AJ, Glenn MP, Boyle GM, Tyndall JD, Parsons PG, Fairlie DP. Design, synthesis, potency, and cytoselectivity of anticancer agents derived by parallel synthesis from alpha-aminosuberic acid. *J Med Chem.* 2006;49:7611-7622.
76. Angibaud P, Arts J, Van Emelen K, Poncelet V, Pilatte I, Roux B, Van Brandt S, Verdonck M, De Winter H, Ten Holte P, Marien A, Floren W, Janssens B, Van Dun J, Aerts A, Van Gompel J, Gaurrand S, Queguiner L, Argouillon JM, Van Hijfte L, Freyne E, Janicot M. Discovery of pyrimidyl-5-hydroxamic acids as new potent histone deacetylase inhibitors. *Eur J Med Chem.* 2005;40:597606.
77. Mshvidobadze EV, Vasilevskya SF, Elguero J. *Tetrahedron.* 2004;60:11875-11878.
78. Van Ommeslaeghe K, Elaut G, Brex V, Papeleu P, Iterbeke K, Geerlings P, Tourwé D, Rogiers V. Amide analogues of TSA: synthesis, binding mode analysis and HDAC inhibition. *Bioorg Med Chem Lett.* 2003;13:1861-1864.
79. Curtin ML, Garland RB, Heyman HR, Frey RR, Michaelides MR, Li J, Pease LJ, Glaser KB, Marcotte PA, Davidsen SK. Succinimide hydroxamic acids as potent inhibitors of histone deacetylase (HDAC). *Bioorg Med Chem Lett.* 2002;13:2919-2923.
80. Sternson SM, Wong JC, Grozinger CM, Schreiber SL. Synthesis of 7200 small molecules based on a substructural analysis of the histone deacetylase inhibitors trichostatin and trapoxin. *Org Lett.* 2001;3:4239-4242.



Two New Factors for the Evaluation of Scientific Performance: U and U'

Bilimsel Performansın Değerlendirilmesi İçin İki Yeni Faktör: U ve U'

Tayfun UZBAY*

Üsküdar University, Neuropsychopharmacology Application and Research Center, İstanbul, Turkey

ABSTRACT

Scientific performance of researchers that translates into academic improvement, tenure position in universities and project grants are commonly evaluated by using some bibliometric indicators. These indicators can be calculated through total number of papers and citations, impact factors of publishing journals, impact of each paper or impact of total papers. In addition, scientific impact of individuals is also determined by some indexes such as Hirsch (h) index. All of these measures and indexes have several limitations. Scientific projects and publications are mostly collaborative and all collaborators do not contribute to these projects and publications equally. Thus, it is difficult to understand and analyze an individual's performance by the outputs coming from collaborative studies. Here, a new practice for evaluating individual scientific performance is proposed. U and U' factors are able to detect a qualified article production capacity of the scientists producing from their research projects and studies objectively. Although these factors may not give an idea about their exact contributions and solutions on the specific scientific problems, U factors will assist a more objective evaluation for individual scientific performance or productivity of the scientists than other tools such as h factor and impact factor alone. Because h factor excludes certain articles of researchers, in this paper, I propose to use U factor instead of h for a more objective evaluation. Especially the U' factor may also be helpful for an objective selection in scientific awards, project grants and in appointing academic staff.

Key words: Bibliometric, grant, h index, impact factor, scientific performance, tenure

ÖZ

Araştırmacıların akademik gelişime dönüşen bilimsel performansı, üniversitelerde görev süreleri ve proje hibeleri, bazı bibliyometrik göstergeler kullanılarak değerlendirilmektedir. Bu göstergeler toplam makale sayısı ve atıflar, yayımlandıkları dergilerin etki faktörleri, her bir makalenin etkisi veya toplam makalelerin etkisi ile hesaplanabilir. Ayrıca bireylerin bilimsel etkileri de Hirsch (h) indeksi gibi bazı indeksler tarafından belirlenmektedir. Bu ölçümlerin ve indekslerin hepsinde çeşitli sınırlılıklar vardır. Bilimsel projeler ve yayınlar çoğunlukla fazla sayıda kişi ile iş birliğini gerektirir ve tüm ortak çalışanlar bu projelere ve yayınlara eşit ölçüde katkıda bulunmaz. Dolayısıyla, bir bireyin performansını kolaboratif çalışmalardan gelen çıktılarla anlamak ve analiz etmek zordur. Bu makalede bireysel bilimsel performansı değerlendirmek için yeni bir uygulama önerilmiştir. U ve U' faktörleri, bilimcilerin araştırma projelerinden ve çalışmalarından gelen çıktılarının ürün niteliğini ve nitelikli üretim kapasitesini objektif olarak tespit edebilmektedir. Bu faktörler, belirli bilimsel problemler üzerindeki kesin katkılar ve çözümler hakkında bir fikir veremese de, U faktörü, bilim insanlarının bireysel bilimsel performansı veya üretkenliği için, h faktörü ve etki faktörü gibi diğer araçlardan daha objektif bir değerlendirmeye yardımcı olacaktır. H faktörü, araştırmacıların bazı çalışmalarını göz ardı edebilmektedir ve bu makalede, daha objektif bir değerlendirme için h yerine U faktörü kullanımı önerilmektedir. U' faktörü de özellikle bilimsel ödüllerde, proje hibelerinde ve akademik personelin atanmasında objektif bir seçim için yararlı olabilir.

Anahtar kelimeler: Bibliyometrik, hibe proje teşviki/burs, h indeksi, etki faktörü, bilimsel performans, sabit kadro hakkı

INTRODUCTION

Beginning the new century, bibliometric analyses have increasingly turned to arithmetical methods using the parameters such as the impact factor of the scientific journals in which those publications appear first or corresponding author publications, and calculation at some specific index values. In 2005, Jorge E. Hirsch who is an Argentine American physicist proposed h-index for detecting scientific output of a researcher.¹

The h-index is an indicator which measures both the apparent scientific impact and the scientific productivity of a researcher. The index is based on the set of the scientist's most cited reports and the number of times that they have been cited in other people's scientific reports. An individual has index h if h of (his/her) N_p reports have at least h citations each. Hirsch suggested that the h-index provides a better prediction for the future achievement than the other indicators such as number

*Correspondence: E-mail: tuzbay@uskudar.edu.tr - tuzbay@yahoo.com, Phone: +90 216 400 22 22

Received: 10.09.2018, Accepted: 01.11.2018

©Turk J Pharm Sci, Published by Galenos Publishing House.

of papers, number of citations, and mean citations per paper.^{1,2} Other suggested bibliometric methods that also provide more importance to very highly cited scientific reports, such as Jin et al.'s³ AR index and Kosmulski's,⁴ H^2 index, probably suffer from the same weakness as total citation account does, because they will allocate the citations of highly cited reports equally to all co-authors without considering rank of names in the report. Egghe⁵ also introduced g-index which is defined as, "A researcher has index g, if g is the highest number that his or her top g publications received (together) at least g^2 citations.

These indexes are influenced by the citation database. Databases vary in respect to publication time span, subject, and variety of listed journals, may provide qualitatively and quantitatively different citation numbers for the similar articles.⁶ For example, although Scopus is one of the largest citation database, it reflects only those scientific reports available after 1995. Thus, Thompson Reuters Web of Science, another popular database, may provide more precise evaluation of lifetime performance. Mazloumian⁷ evaluated citation info of almost 150.000 scientists from the Web of Science database and they suggested that the h value is a well predictor for the future citations of both published and future papers. Many databases frequently express both of h-index and impact factor of individuals for general assessments.

Scientific projects and publications are mostly collaborative and all collaborators do not contribute to these projects and publications equally. However, scientific impact of individuals is determined by making metrics such as the total publications, citations and various remarks or indexes such as h, A, C and P indexes that are unidirectional and insufficient measurements.⁸ A collaboration effect on scientific output has been subjected to various studies.⁹⁻¹¹ Total numbers of publications, citations or bibliometric techniques based on indexes such as h-index may not provide objective and relevant results every time, especially about evaluation of individual performance. Because h-index and some other similar indexes exclude a part of articles of the researchers, we can sometimes reach inflated or fractional results regarding individual performances.

In this study, it was aimed that h-index is improved through considering the impact factor of scientist which is a value obtained from dividing total citations to total publications. Thus, here, a new evaluation practice, U and U' factors, is proposed for a more objective evaluation of scientist's individual productivity and performance.

Method and Formulation

What is U factor?

U factor is a value simply obtained from multiplication of the Hirsch index (h) with the impact factor (if). Impact factor for an individual scientist is calculated by dividing total citations to total publications without taking into consideration the place of name in the article and impact of the published journal. For example, a scientist has 1000 citations for a total of 100 articles and his/her h-index is 20. What is his/her factor?

$$U = if \times h$$

$$if = \frac{1000}{100} = 10$$

$$h = 20$$

$$U = 20 \times 10 = 200$$

What is U' factor?

U' factor needs a more complex calculation and it gives us a very objective evaluation for individual productivity and performance of scientists, because it highlights specific own effort of the scientist within the total activity. For U' factor, firstly, general U value of the scientist is calculated as described above. Then, U_s value indicating the scientist's specific contribution by his/her publications is calculated. For that purpose, the articles in which the scientist is the first name or is corresponding author are taken into consideration. Number of citations is counted exactly for these articles and the obtained value is divided into total number of articles in which the scientist's is the first name or is corresponding author for calculating if_s value. Then, the scientist's specific h-index including only the articles in which the author is the first name or is corresponding author, is calculated as h_s . Then, U_s value is obtained by multiplying if_s with h_s . When we divided U_s by U ; U' is obtained.

A sample calculation for U'

There is a scientist who has a total of 100 articles and 1000 citations. He/she is the first author in 20 and corresponding author in 30 of total articles. Thus, he/she has 50 articles for U' calculation. In addition, the scientist has 500 citations obtained from these articles. Let's assume, his/her h_s index is 12 according to these specific articles. What is the U' factor for this scientist?

First, we calculate general U as mentioned above and U is found as 200.

$$U = h \times if = 20 \times 10 = 200$$

$$if_s = \frac{500}{50} = 10$$

$$h_s = 12$$

$$U_s = if_s \times h_s = 10 \times 12 = 120$$

$$U' = \frac{U_s}{U} = \frac{120}{200} = 0.6$$

U' is an indicator of scientist's own contribution or significant contribution among his/him total publications. As the U' value grows and closes to 1, it is understood that the scientist's own contribution in total publications is significant. As the U' value becomes smaller, it is understood that the scientist's own contribution in total publications is insignificant. In this example, because U' is found as 0.6, the scientist's own contribution to the total articles can be accepted as qualified. Table 1 presents a proposed model for the level of the scientist's own or specific contribution according to U and U' .

Table 1. Scientific performance levels according to and *

U	U'	Scientific level
<100	<0.25	Low
100-200	0.25-0.50	Moderate
201-400	0.51-0.75	Qualified
>400	>0.75	Outstanding

*In this table, and are independent from each other (values do not reflect every time , vice versa). is a more available indicator of scientists' own contribution within their total activity. We can use as a more available indicator of researchers' general scientific effort.

DISCUSSION AND CONCLUSION

Academic researchers transfer their discoveries, new ideas and experimental observations to the scientific community by refereed printed papers in academic journals. Only biomedical sciences generate more than a million new scientific articles each year. These publications are the basic source for measuring the outputs of an individual scientist. The specific publications are also the expressions of intellectual discoveries expressed explicitly aiming to convey new ideas or information for further knowledge. Bibliometric indicators have been widely used to measure the performance of the scientific community in general and in particular, to assess the productivity of a scientist or an academic journal.¹² While impact factor and annual total citation number are two of the most commonly used evaluative tools, they are also undoubtedly less sophisticated than other field-normalized approaches advanced by bibliometric applicators.¹³

Within all of the indices, Hirsch's h-index is undoubtedly the most known index. It has been used in most popular databases such as ISI Web of Science, Scopus and Google Scholar Academic. It is designed to develop on generally used metrics and it reflects the cumulative impact of an individual's effort. It is determined from the distribution of citations received by a researcher's publications. A researcher has Hirsch index h if h of his/her N_p publications have, at least, h citations each.¹⁴ For example, a researcher who has an h-index of 10 must have published ten articles that each have at least ten citations. The h-index is becoming a reference instrument for career evaluation, and it has been considered by some institutions in allocation, promotion and funding choices.^{12,15}

Because there are alterations in citation behavior in different subject areas, the impact factor alone should only be used to compare journals or scientists working on the similar subject.¹⁶ H-index has also several limitations. This index is a promising general assessment of the quality of a young scientist's effort.^{17,18} Because the h-index cannot exceed the amount of underlying papers, we can even describe $h=0$ for fully inactive scientists. Sensitivity to performance changes of h-index is low. It can never decrease and is only weakly sensitive to the number of citations. This is the reason for the development of most of the other type of indices. Because h-index is size-dependent, the use of h-index as an only factor for the evaluation of the scientific occupation of a researcher is not adequate.¹⁹ In addition, in comparison with the cumulative number of citations, the h-index

is not critically inflated by a small number of highly cited articles. Furthermore, the h-index considers scientific impact as well as productivity, and it is hardly influenced by self-citation. It could identify outstanding and successful scientists and could facilitate academic improvement in divisions, universities, and other academic frames.¹⁴ Similar to mean citations per publication, the h-index shows a positive correlation with time. Furthermore, like other indexes, the h-index does not consider the background of citations, for example, those citations with a negative background that show inadequate or limited published article will have the effect of increasing the ranking of scientists when citation indices are used.²⁰ Thus, U factor presenting in our study may enable more objective and effective evaluation for individual scientific performance as compared to individual impact and h factors since it combines both impact and h. Indeed, U factor obtained by multiplying h value and impact may be a new and useful metric in the scientometrics and seems to eliminate some limitations generating from impact factor and h-index alone. Multiplying of h-index with the impact factor of individual provides a correction in h-index and allows a more objective evaluation of scientists' performance.

One of the most important problems in evaluation of individual scientific performance is the papers with multiple names. This kind of studies are generally multidisciplinary. However, we can also see many articles with numerous names in a sole scientific area especially in life sciences and medicine. Some of them is also a gift authorship which is defined as lack of significant contribution of the author to the manuscript or study. They are best opportunistic and worse scientific misconducts.²¹⁻²³ An important question is that how we can detect a significant individual scientific performance and his/her specific contribution to any scientist who has highly cited articles with multiple names?

Any scientist could have too many articles and could have a very high citation number too. Therefore, he/she could also have very high impact factor and high degree in h-index. However, this high impact value and high h-index do not show that this scientist is always qualified or a senior scientist. Thus, rank of the name in the article becomes an important determinant. Being first name or a corresponding author in the article indicates a significant contribution to the study. Thus, the number of the articles of a scientist in which his/her name appears as first name or corresponding author within the total articles and citations for these articles within the total citations are noteworthy indicators for the individual's own specific effort in the total articles and citations. U' directly gives us an objective opinion about the scientist's own specific effort in the related scientific zone. The most important benefit of U' in evaluation of individual scientific performance is sorting out of the publications regarding gift, honorary or guest authorship. If the scientist's U' is much smaller than 1, he/she will have so much gift or guest authorship in his/her articles.

While U can be used as an individual indicator like h or the similar factors, U' can mainly be used for detecting the scientists' outstanding scientific activity within the total and

together with U , for instance, it may be useful for an objective evaluation in competitive statements such as award, grant and tenure position in universities. If a scientist has U' that is closer to 1 or more than 1, that means he/she has a significant direct contribution to the studies turning into publication in the same extent. A U' value too much lower than 1 indicates that the scientist has not a direct relation or contribution to the studies that result in publication. This statement could also imply too much gift, honorary or guest authorship. A scientist who has a very low U' value, even if he/she has a high citation count and a high h index, cannot be accepted as outstanding or senior researcher in the scientific community.

Evaluation of U' will help a more equal selection in the competitive statements of the science i.e. award, grant allocation or tenure positions. However, the main problem for U' evaluation is that there is a possibility for detecting a high U' value in the individuals who have low publication and citation counts. This problem can be overcome by making comparison of the individuals who have an acceptable threshold value. The threshold value can be detected according to an acceptable U value obtained from a suitable h index and impact factor. For example, according to property of competition, a borderline value can be defined and the individuals who have a lower borderline value are not included in the evaluation.

Currently, an apparent problem is that there is not a software regarding practical calculation of these values provided by any database. Thus, calculation seems to be a bit difficult and time-consuming. However, a freely available software simply presents a solution for this problem and will make the calculation easier.

In conclusion, here, new practical indexes for assessment of individual scientific performance have been presented. These indexes may be useful for selection in competitive scientific statements and they seem to be more effective than h-index or impact alone. Thus, we have used successfully this method for evaluating the performance of the scientists from pharmaceutical sciences during detection of science awards and grants of Turkish Pharmacists' Association, Pharmacy Academy since 2007. We observed that U and U' factors are practical, equitable and more effective than h for individual evaluation of scientific performance.

ACKNOWLEDGEMENTS

Author would like to thank to Dr. Serhat Özekes and Dr. Ahmet Can Timuçin for their valuable comments for the manuscript. Turn-it-in program was used for checking plagiarism (9%) in this manuscript.

Conflict of Interest: No conflict of interest was declared by the authors.

REFERENCES

- Hirsch JE. An index to quantify an individual's scientific research output. *Proc Natl Acad Sci USA*. 2005;102:16569-16572.

- Hirsch JE. Does the H index have predictive power? *Proc Natl Acad Sci USA*. 2007;104:19193-19198.
- Jin B, Liang L, Rousseau R, Egghe L. The R- and AR- indices: Complementing the h-index. *Chin Sci Bull*. 2007;52:855-863.
- Kosmulski M. A new Hirsch-type index saves time and works equally well as the original h-index. *ISSI Newsletter*. 2006;2:4-6.
- Egghe L. Theory and practice of the g-index. *Scientometrics*. 2006;69:131-152.
- Kulkarni AV, Aziz B, Shams I, Busse JW. Comparisons of citations in Web of Science, Scopus, and Google Scholar for articles published in general medical journals. *JAMA*. 2009;302:1092-1096.
- Mazloumian A. Predicting scholars' scientific impact. *PLoS One*. 2012;7:e49246.
- Stallings J, Vance E, Yang J, Vannier MW, Liang J, Pang L, Dai L, Ye I, Wang G. Determining scientific impact using a collaboration index. *Proc Natl Acad Sci USA*. 2013;110:9680-9685.
- Foulkes W, Neylon N. Redefining authorship. Relative contribution should be given after each author's name. *BMJ*. 1996;312:1423.
- Campbell P. Policy on papers' contributors. *Nature*. 1999;399:393.
- Ball P. A longer paper gathers more citations. *Nature*. 2008;455:274-275.
- Hadagali GS, Kumbar BD, Gourikeremath GN, Hiremath R. g-index as an improvement of the h-index: A comparative study of prominent Indian scientists. *Int J Inf Dissem Tec*. 2016;(Suppl 1):42-48.
- Hutchins BI, Yuan X, Anderson JM, Santangelo GM. Relative citation ratio (RCR): A new metric that uses citation rates to measure influence at the article level. *PLOS Biol*. 2016;14:e1002541.
- Ball P. Achievement index climbs the ranks. *Nature*. 2007;448:737.
- Garcia-Perez MA. A multidimensional extension to Hirsch's h-index. *Scientometrics*. 2009;81:779-785.
- Jones T, Huggett S, Kamalski J. Finding a way through the scientific literature: Indexes and measures. *World Neurosurg*. 2011;76:36-38.
- Bornmann L, Daniel HD. Does the h-index for ranking of scientists really work? *Scientometrics*. 2005;65:391-392.
- Bornmann L, Daniel HD. What do we know about the h-index? *J Am Soc Inf Sci Tec*. 2007;58:1381-1385.
- Costas R, Bordons M. The h-index: Advantages, limitations and its relation with other bibliometric indicators at the micro level. *J Informetr*. 2007;1:193-203.
- O'Leary JD, Crawford MW. Bibliographic characteristics of the research output of pediatric anesthesiologists in Canada. *Can J Anaesth*. 2010;57:573-577.
- Gasparyan AY, Ayvazyan L, Kitas GD. Authorship problems in scholarly journals: Considerations for authors, peer reviewers and editors. *Rheumatol Int*. 2013;33:277-284.
- Rajasekaran S, Shan RL, Finnoff JT. Honorary authorship: frequency and associated factors in physical medicine and rehabilitation research articles. *Arch Phys Med Rehabil* 2014;95:418-428.
- Harvey LA. Gift, honorary or guest authorship. *Spinal Cord*. 2018;56:91.